

GENETIC AND EPIGENETIC PROFILES OF ELDERLY AML

ACUTE MYELOID LEUKEMIA IN THE ELDERLY IS CHARACTERIZED BY A DISTINCT
GENETIC AND EPIGENETIC LANDSCAPE

D i s s e r t a t i o n

zur Erlangung des akademischen Grades

d o c t o r r e r u m n a t u r a l i u m

(Dr. rer. nat.)

im Fach Biologie

eingereicht an der

Lebenswissenschaftlichen Fakultät
der Humboldt-Universität zu Berlin

von

M.Sc., Diplm., Patricia Alexandra, Santos Silva

Präsidentin der Humboldt-Universität zu Berlin

Prof. Dr.-Ing. Dr. Sabine Kunst

Dekan der Lebenswissenschaftlichen Fakultät
der Humboldt-Universität zu Berlin

Prof. Dr. Bernhard Grimm

Gutachter/innen

1. Prof. Dr. rer. nat. Ana Pombo
2. Prof. Dr. rer. nat. Nils Blüthgen
3. Prof. Dr. med. Claudia Baldus

Tag der mündlichen Prüfung: 29th May 2019

A word cloud visualization of biological and clinical terms. The most prominent words are "AML", "patients", "genes", "DNA", "molecular", "mutations", "elderly", "cohort", "network", "distinct", "high", "mutual", "epigenetic", "pathway", "ICBP", "months", "repair", "modules", "ASXL1", "RNA", "heterogeneity", "sequencing", "altered", "target", "tumor", "flow", "frequency", "poor", "coverage", "PANC", "candidate", "proteins", "immunity", "sequence", "second", "years", "alterations", "regulators", "showed outcome", "patient", "RUNX1", "BHLA2", "non", "variable", "included", "addition", "median", "survival", "splicing", "mutation", "younger", "SRSF", "investigation", "identified", "LDMTSA", "module", "IT2".

HUMBOLDT-UNIVERSITÄT ZU BERLIN

*We stumble on a mystery and embrace it.
We investigate and we doubt, but it would be
ignorance to believe the inexplicable is impossible.
In the end, our reward is a story worth telling.
One that not only contributes to knowledge but also transforms us.*

Patricia Silva

TABLE OF CONTENTS

LIST OF FIGURES	VI
LIST OF TABLES	VIII
DEDICATION.....	1
ACKNOWLEDGEMENTS.....	2
AUTHORSHIP DECLARATION	3
CONTRIBUTIONS	4
ABSTRACT [ENGLISH]	5
ABSTRACT [GERMAN]	6
KEY POINTS	8
TERMS AND ABBREVIATIONS	9
CHAPTER 1. INTRODUCTION.....	12
1.1 Hematological diseases.....	13
1.1.1 Normal hematopoiesis	13
1.1.2 Hematopoietic disorders	15
1.1.3 Aging of hematopoietic stem cells.....	17
1.2 Acute Myeloid Leukemia	19
1.2.1 AML diagnosis	21
1.2.2 AML classifications	22
1.2.3 AML prognostic factors	23
1.2.4 AML treatments	26
1.3 Genetic groups of AML.....	29
1.4 Epigenetic patterns in AML.....	35
1.5 Elderly AML specificities.....	40
1.5.1 Survival of elderly AML patients.....	40
1.5.2 Molecular characteristics of elderly AML	42
CHAPTER 2. AIM OF THE PROJECT	43
CHAPTER 3. PATIENTS AND METHODS	45
3.1 Elderly AML cohort characteristics.....	46
3.2 Mutations in protein coding sequences of 555 genes	48
3.3 Sequence data analyses, variant classification and confirmations.....	51
3.4 Functional categorization of mutated genes	52
3.5 Correlation studies of mutated genes	52
3.6 Statistical analysis of overall survival	52
3.7 DNA methylation profiling	54

3.8 Survival predictions from TCGA cohort gene expression profiles.....	57
CHAPTER 4. RESULTS.....	58
4.1 Mutation profiles of the SAL elderly AML	59
4.1.1 Frequently mutated epigenetic regulators	65
4.1.2 High rate of mutations in splicing proteins	67
4.2 Genetic alterations associated with elderly AML	69
4.3 Genetic heterogeneity in the SAL elderly AML	71
4.4 Protein networks and pathways of SAL elderly AML	73
4.4.1 Molecular patterns of mutations in mRNA processing and DNA repair proteins.....	73
4.5 Specific DNA methylation pattern of the elderly AML	78
4.5.1 Genomic locations of elderly AML differential methylation.....	82
4.5.2 Differentially methylated genes in elderly AML	87
4.6 Robust epigenetic patterns of AML	92
4.7 Epigenetic heterogeneity in the SAL elderly AML	94
CHAPTER 5. DISCUSSION	97
5.1 Genetic patterns of elderly AML.....	99
5.1.1 Molecular alterations correlated to age	99
5.1.2 Factors for elderly AML poor prognosis.....	101
5.1.3 Genomic classifications of elderly patients	103
5.1.4 Functional interactions of protein targets.....	104
5.1.5 Mutational progression into elderly AML.....	105
5.2 Epigenetic pattern of elderly AML	107
5.2.1 Pathways involved in elderly AML epigenetics	108
5.2.2 Regions, genes and prognosis predictions of elderly AML	109
5.3 Interconnected genetic and epigenetics.....	113
5.3.1 DNA instability features of elderly AML	113
5.3.2 Methylation profiles within SAL elderly AML	114
5.3.3 Specific targets in elderly AML	115
CHAPTER 6. CONCLUSION	117
REFERENCES.....	118
APPENDIX A	127
Table of detailed clinical data for the 93 patients of SAL elderly AML.....	128
APPENDIX B	129
Table of information from the genetic alterations in the SAL elderly AML	129
APPENDIX C	130
Table of DMRs of hierarchical cluster of elderly (vs cluster of young)	130

LIST OF FIGURES

Figure 1.1.1 The normal hematopoiesis and the leukemic stem cell model.	14
Figure 1.2.1 Progress in defining the molecular landscape of AML.	20
Figure 1.3.1 Organization of mutations into categories of related genes.	30
Figure 1.3.2 Molecular classes of AML and concurrent gene mutations in adult patients.	31
Figure 1.3.3 Different overall survival of molecularly classified groups of AML.	32
Figure 1.3.4 Types of epigenetic regulators mutated in AML that change or read epigenetic marks in DNA or histones.	33
Figure 1.4.1 Epigenetically defined classification of AML.	37
Figure 1.5.1 Survival of patients with AML in a population study according to their age at the time of diagnosis.	41
Figure 3.1.1 Distribution of patients' age at diagnosis in the SAL elderly AML.	46
Figure 3.2.1 Quality controls of mapping and coverage of the target sequencing of the SAL elderly AML samples.	49
Figure 3.7.1 Representation of quality controls used for the integration of SAL and TCGA epigenetic data.	55
Figure 4.1.1 Frequencies of mutations in the SAL elderly AML for each gene.	59
Figure 4.1.2 Frequencies of mutations in the SAL elderly AML for each patient.	60
Figure 4.1.3 Variant allele frequencies of mutations in the SAL elderly AML.	61
Figure 4.1.4 Rate of mutation of AML samples in the TCGA cohort and SAL cohort.	62
Figure 4.1.5 Survival analysis of AML patients in the TCGA cohort and in SAL cohort.	63
Figure 4.1.6 Recurrently mutated genes in the SAL elderly AML.	64
Figure 4.1.7 Mutations in epigenetic regulators in elderly AML.	65
Figure 4.1.8 Epigenetic regulators mutated in TCGA elderly and TCGA young AML groups.	66
Figure 4.1.9 Frequency of mutations in splicing factors.	67
Figure 4.2.1 Mutation rates in the SAL elderly AML compared to mutation rates reported in two other cohorts.	70
Figure 4.3.1 Mutations correlated to SAL elderly AML groups that were defined by WBC counts of prognostic relevance.	72
Figure 4.4.1 Reactome functional interaction network of altered proteins.	74
Figure 4.4.2 Overall survival of the groups defined by the Reactome functional interaction network analysis in the SAL elderly AML.	76
Figure 4.4.3 Overall survival of the groups defined by the Reactome functional interaction network analysis in the TCGA cohort.	77
Figure 4.5.1 Methylation profiles of AML patients (TCGA cohort and SAL elderly).	78
Figure 4.5.2 Differential methylation patterns of the elderly in comparison to young.	80

<i>Figure 4.5.3 Enrichment of biological terms for genes associated with the differential methylation signature in the elderly.....</i>	<i>81</i>
<i>Figure 4.5.4 Distribution of DMRs of the cluster of elderly AML across chromosomes.</i>	<i>83</i>
<i>Figure 4.5.5 Distinct methylation profiles of elderly in the KIAA1447/ACTG1/FSCN2 region.....</i>	<i>85</i>
<i>Figure 4.5.6 Overall survival of patient groups defined by high vs low RNA expression levels for age genes that are associated with DMRs.</i>	<i>89</i>
<i>Figure 4.6.1 Methylation profiles of Group C and complex karyotype AML samples and uniqueness of patients with IDH mutations.....</i>	<i>93</i>
<i>Figure 4.7.1 Methylation profiles of SAL elderly AML patients.</i>	<i>94</i>
<i>Figure 4.7.2 Specific differential methylation signature of epigenetic regulators mutated in the SAL elderly AML.....</i>	<i>95</i>
<i>Figure 4.7.3 Specific signature of differential methylation for mutated genes in the SAL elderly AML.....</i>	<i>96</i>

LIST OF TABLES

<i>Table 1.2.1 WHO 2016 classifications of AML</i>	23
<i>Table 1.2.2 ELN 2017 risk stratification by genetics characteristics</i>	26
<i>Table 1.4.1 Prognostic genes regulated by DNA methylation</i>	38
<i>Table 3.1.1 Characteristics of elderly AML cohort</i>	47
<i>Table 3.2.1 Mutated genes selected for the targeted NGS design</i>	50
<i>Table 4.1.1 Description of the clinical characteristics of patients with mutations in splicing components</i>	68
<i>Table 4.4.1 Characteristics of the groups defined by the Reactome functional interaction network analysis in the SAL elderly AML</i>	75
<i>Table 4.4.2 Characteristics of SAL elderly AML cohort compared to the characteristics of the TCGA cohort</i>	77
<i>Table 4.5.1 HyperMRs of the cluster of elderly AML concentrated in chr17 q25.3</i>	84
<i>Table 4.5.2 Genes in DMRs of the cluster of elderly AML which are related to age, cancer and AML pathogenesis or survival</i>	88

DEDICATION

I am dedicating this thesis firstly to my beloved husband, António Nascimento, who always gave me his unwavering support and positivism.

Then to my parents (Luis and Adelina Silva) and my brother (André Silva) who were essential through the years to get here. My parents especially, for they are my heroes and that will always mean everything to me. They gave me more than you can ask from any parent.

Also to my supervisor, Claudia Baldus, for I was very fortunate to have found her. I am grateful to her for providing the right balance of leadership and freedom, paramount to the realization of this work.

ACKNOWLEDGMENTS

I personally have to thank all the people that were direct and indirectly responsible for this achievement.

To all members of the lab, a big thank you for your everyday support and helpful suggestions. I will be forever thankful to all of you for providing the best environment to work in. I want to thank Liliana Mochmann for providing more than scientific discussions, for the friendship that made my life happier.

Finally, in the name of this project and all that were involved, I thank our financial supporters.

This study was supported by research funding from Else Kröner-Fresenius-Stiftung (2013A153), the German Cancer Consortium (Deutsches Konsortium für Translationale Krebsforschung DKTK, Heidelberg, Germany), the Deutsche Krebshilfe (Mildred Scheel Stiftungsprofessur CDB).

AUTHORSHIP DECLARATION

The findings I present in this publication were obtained and written by me and were previously published in the *Leukemia* journal (NPG®) where I am the first author¹, namely: Silva, P. *et al.* Acute myeloid leukemia in the elderly is characterized by a distinct genetic and epigenetic landscape. *Leukemia* **31**, 1640–1644 (2017). Therefore most chapters and pictures were adapted from my previous manuscript, some were extended and some were added new. Statements from my previous abstract in *Blood* journal and respective oral presentation in the American Society of Hematology meeting 2015² might also be present, namely from: Silva, P. *et al.* Acute Myeloid Leukemia in the Elderly Is Characterized By a Distinct Genetic Landscape. *Blood* **126**, (2015).

A research like ours surely had to be a joint effort. We all know collaborations between researchers and fellow scientists are essential to achieve important knowledge in such an interdisciplinary area as translational medicine. Therefore, although I was involved in all the parts of the project from design to experiments (where I prepared libraries, implemented strategies/workflows, performed computational and statistical analysis and confirmed mutations) I cannot forget others. The physicians that treated patients, collected samples and information and the technicians that treated the samples and isolated gDNA. So I would like to leave a more detailed account of contributions from the several collaborators to this work (in the next chapter).

I hereby declare that I completed the doctoral thesis independently based on the stated resources and aids. I have not applied for a doctoral degree elsewhere and do not have a corresponding doctoral degree. I have not submitted the doctoral thesis, or parts of it, to another academic institution and the thesis has not been accepted or rejected. I declare that I have acknowledged the Doctoral Degree Regulations which underlie the procedure of the Faculty of Mathematics and Natural Sciences of Humboldt-Universität zu Berlin, as amended on 05th May 2015. Furthermore, I declare that no collaboration with commercial doctoral degree supervisors took place, and that the principles of Humboldt-Universität zu Berlin for ensuring good academic practice were abided by.

29th of May 2019, Berlin, Germany

Patricia Silva

CONTRIBUTIONS

- P Silva¹, M Neumann^{1,2,3} and CD Baldus^{1,2,3} designed the study and interpreted the data;
- J Ortiz-Tanchez¹ and K Isaakidis¹ did some of the sample processing and DNA extractions;
- M Neumann^{1,2,3} and J Hecht^{11,12} designed NGS gene panel;
- P Silva¹ and C Schlee¹ prepared NGS libraries;
- A Graf⁷, S Krebs⁷, H Blum⁷ and PA Greif^{2,3,4} performed sequencing;
- M Neumann^{1,2,3}, S Vosberg^{2,3,4} and PA Greif^{2,3,4} pre-processed sequencing data;
- MP Schroeder¹ pre-processed Illumina BeadChip arrays;
- P Silva¹ and MP Schroeder¹ run DMR algorithm and its statistical analysis;
- P Silva¹ examined pre-processed data and performed final processing on NGS sequencing and Illumina BeadChip array data;
- P Silva¹ designed and performed statistical analyses for all processed data;
- P Silva¹, K Isaakidis¹ and T Hartung¹ confirmed mutations;
- S Türkmen^{5,6} and C Thiede^{2,3,9} were involved in clinical diagnostics;
- G Ehninger^{2,3,9}, C Röllig^{2,3,9}, C Müller-Tidow⁸, H Serve^{2,3,10}, WE Berdel¹³, M Neumann^{1,2,3}, LR Fransecky¹ and CD Baldus^{1,2,3} were involved in patient care and provided clinical and follow-up data;
- G Ehninger^{2,3,9}, C Röllig^{2,3,9}, C Müller-Tidow⁸, H Serve^{2,3,10} and WE Berdel¹³ are primary investigators of the SAL registry;
- P Silva¹ implemented outcome analyses of the clinical data;
- P Silva¹ and CD Baldus^{1,2,3} wrote the manuscript in Leukemia and the abstract in Blood Journal.

Authors Affiliation:

1Department of Hematology and Oncology, Charité University Hospital, Berlin, Germany;

2German Cancer Consortium (DKTK), Heidelberg, Germany;

3German Cancer Research Center (DKFZ), Heidelberg, Germany;

4Department of Internal Medicine 3, Ludwig Maximilians University, Munich, Germany;

5Labor Berlin Charité Vivantes GmbH, Berlin, Germany; 6Institute of Medical Genetics and Human Genetics, Charité University Medicine, Campus Virchow-Klinikum, Berlin, Germany;

7Laboratory for Functional Genome Analysis, Gene Center, Ludwig Maximilians University, Munich, Germany;

8Medizinische Klinik V, Universitätsklinikum Heidelberg, Heidelberg, Germany;

9Department of Internal Medicine I, University Hospital Carl-Gustav- Carus, Dresden, Germany;

10Department of Medicine II, Hematology/Oncology, University Hospital Frankfurt, Frankfurt am Main, Germany;

11Centre for Genomic Regulation (CRG), The Barcelona Institute of Science and Technology, Barcelona, Spain;

12Universitat Pompeu Fabra (UPF), Barcelona, Spain;

13Department of Medicine A, University Hospital Münster, Münster, Germany;

ABSTRACT [English]

Despite advances in the characterization of molecular alterations in younger acute myeloid leukemia (AML) patients, comprehensive studies in elderly AML are lacking. Thus, we investigated genetic and epigenetic alterations and probed for specific signatures to understand the unfavorable outcomes of elderly AML. We studied 93 AML patients (65 to 90 years old), enrolled in the Study Alliance Leukemia (SAL) registry (SAL elderly AML). To capture a broad spectrum of alterations, we sequenced 555 genes on an Illumina HiSeq2000 platform and investigated DNA methylation profiles using the Illumina 450K array.

Overall, we detected 814 molecular alterations in 281 genes, with a median of 7 genes mutated per patient. Particularly high mutation frequencies were identified for *DNMT3A* (33%), *TET2* (24%), *SRSF2* (23%) and *ASXL1* (21%). We observed frequent alterations in epigenetic regulators (85%) and in splicing factors (38%). Notably, SAL elderly AML patients with mutations in *DNMT3A* or DNA repair genes (in absence of mutations in *NPM1* or splicing factors) had an inferior survival of only 9 months (compared to 17 months for the remaining patients).

In addition, for the analysis of elderly AML DNA methylation, we integrated the SAL cohort with TCGA methylation data for comparisons of methylation levels to younger patients. A distinct DNA methylation profile was observed in older AML patients, which correlated with the presence of mutations in *IDH1/2*, *RUNX1* and *ASXL1* and epigenetic similarities with TP53/Complex samples. The differential methylated regions of elderly AML (compared to younger AML samples) were shown to overlap genes from several pathways that are hallmarks of both age and cancer. Subdivisions of elderly AML showed that *IDH1/2* or *DNMT3A/NPM1/FLT3* mutated samples had diverging epigenetic signatures.

In conclusion, we unraveled distinct patterns of genetic alterations and correlated specific epigenetic profiles of elderly AML to high rate mutated epigenetic regulators. This molecular categorization underscored the distinct biology and the need for specific therapeutic approaches in elderly AML.

ABSTRACT [German]

Die molekulare Charakterisierung von genetischen Veränderungen der Akuten Myeloischen Leukämie (AML) wurde vor allem bei jungen Patienten in den letzten Jahren vorangebracht, hingegen fehlen eingehende Analysen für die AML bei älteren Patienten. Entsprechend ergab sich hieraus die Rationale, genetische und epigenetische Alterationen bei älteren AML Patienten zu untersuchen, um spezifische Signaturen zu identifizieren, die möglicherweise die schlechteren Behandlungsergebnisse bei älteren AML Patienten erklären. Hierzu untersuchten wir 93 AML Patienten (Alter: 65 bis 90 Jahre) aus dem Study Alliance Leukemia (SAL) Register (SAL elderly AML). Um ein breites Spektrum von Alterationen abzudecken, wurden 555 Gene auf der Illumina HiSeq2000 Plattform sequenziert und DNA Methylierungsprofile mittels dem Illumina 450K Array untersucht.

Insgesamt wurden 814 molekulare Alterationen in 281 Genen detektiert (im Median 7 mutierte Gene pro Patient). Besonders hohe Mutationsfrequenzen wurden in den Genen *DNMT3A* (33%), *TET2* (24%), *SRSF2* (23%) und *ASXL1* (21%) notiert. Alterationen in epigenetischen Regulatoren (85%) und in Genen, die in Splicing involviert sind (38%), wurden gehäuft beobachtet. Beachtenswerter Weise wiesen ältere AML Patienten mit Mutationen in *DNMT3A* oder DNA Reparaturgenen eine geringere Lebenserwartung von nur 9 Monaten auf (im Vergleich zu 17 Monaten in der restlichen Kohorte).

Darüber hinaus integrierten wir die Methylierungsdaten aus der SAL Kohorte mit denen der TCGA Kohorte, umso die Methylierungsmuster von älteren mit denen von jüngeren Patienten zu vergleichen. Es konnte ein distinktes Methylierungsprofil in den DNA Proben von älteren AML Patienten nachgewiesen werden, welches mit Mutationen in *IDH1/2*, *RUNX1* und *ASXL1* korrelierte. Die im Vergleich zu jüngeren AML Patienten unterschiedlich methylierten Regionen bei älteren AML Patienten überlappten mit Genen verschiedener Signalwege, die Hallmarks von Alterungsprozessen und Krebs entsprechen. Weitere Analysen zeigten zudem divergente epigenetische Signaturen zwischen Proben mit *IDH1/2* Mutationen und *DNMT3A/NPM1/FLT3* mutierten Proben bei älteren AML Patienten.

Zusammenfassend konnten wir für die Kohorte älterer AML Patienten distinkte genetische Alterationen nachweisen und mit spezifischen Profilen von Mutationen in epigenetischen Regulatoren korrelieren. Diese molekulare Kategorisierung unterstreicht distinkte biologische Mechanismen in älteren AML Patienten und die

Notwendigkeit von spezifischen Therapieansätzen für diese Kohorte mit ungünstiger Prognose.

KEY POINTS

- Elderly AML is a distinct entity with a high frequency of mutations in spliceosome components, epigenetic regulators and DNA repair factors.
- Enrichment of mutations in the DNA repair model postulates treatment resistance and poor outcome in about ¼ of patients.
- Elderly AML has aberrant DNA methylation profiles associated with molecular alterations in *IDH1/2*, *ASXL1* and *RUNX1*.
- The epigenetic patterns of elderly AML related these disease to methylation patterns of poor prognosis involving changes in genes known to be involved in age and cancer/AML processes.
- High frequency of mutations in *IDH1/2* and *DNMT3A* observed in the SAL elderly AML translated into opposite patterns of methylation and drive distinct clusters.
- Elderly AML is in need of different therapeutic approaches to address its molecular specificities and resistance mechanisms.

TERMS AND ABBREVIATIONS

Abbreviation	Full term
2-HG	D-2-hydroxyglutarate
AKT	AKT Serine/Threonine kinase
ALL	Acute lymphoblastic leukemia
alloSCT	Allogenic stem cell transplantation
AML	Acute myeloid leukemia
APL	Acute promyelocytic leukemia
Ara-C	Cytarabine
ATM	ATM Serine/Threonine kinase
ATR	ATR Serine/Threonine kinase
ATRA	All-Trans-Retinoic acid
Aza	Azacitidine
b	Bases, unit (kb=Kilo bases, Mb=Mega base)
biCEBPA	Biallelic mutated CEBPA
BM	Bone marrow
bp	Base pair, unit
BSC	Best supportive care
CBF	Core-binding factor
CDC42	Cell Division Cycle 42
CHIP	Clonal hematopoiesis of indeterminate potential
CHK	Checkpoint kinase
chr	Chromosome
CLL	Chronic lymphoblastic leukemia
CML	Chronic myeloid leukemia
CN-AML	Cytogenetically normal AML
CNS	Central nervous system
COSMIC	Catalogue of somatic mutations in cancer
CpGs	Cytosine-phosphate-guanine sequential nucleotides
CTCF	CCCTC-Binding Factor
DMRs	Differentially methylated regions
DNA-PK	DNA dependent protein kinase catalytic subunit, signaling pathway
DOT1L	DOT1 Like histone lysine methyltransferase
ECOG	Eastern Cooperative Oncology Group
EFS	Event-free survival
ELN	European LeukemiaNet
EMA	European Medicines Agency
ERRBS	Enhanced reduced representation bisulfite sequencing
FAB	French-American-British
FDA	Food and drugs administration
FDR	False discovery ratio
FGFR	Fibroblast growth factor receptor
FI	Functional interaction
FISH	Fluorescence in situ hybridization
GO	Gene Ontology

Gene Symbol	Gene name
ABL1	ABL Proto-Oncogene 1, Non-Receptor Tyrosine Kinase
ACTG1	Actin Gamma 1
APC	APC, WNT Signaling Pathway Regulator
APOB	Apolipoprotein B
ARID1A	AT-Rich Interaction Domain 1A
ASXL1	Additional sex combs-like 1
ATG16L1	Autophagy Related 16 Like 1
ATG5/7	Autophagy Related 5 or 7
ATM	Ataxia telangiectasia mutated
ATR	Ataxia telangiectasia and Rad3 related
BAIAP2	BAI1 Associated Protein 2
BCOR	BCL6 Corepressor
BCORL1	BCL6 Corepressor Like 1
BCR	BCR, RhoGEF And GTPase Activating Protein
BRCA2	Breast cancer 2
C7orf13	Long Intergenic Non-Protein Coding RNA 1006
CBFB	Core-Binding Factor Subunit Beta
CBL	Cbl Proto-Oncogene
CD34	Hematopoietic Progenitor Cell Antigen CD34
CEBPA	CCAAT/enhancer-binding protein-alpha
CHK	Checkpoint Kinase
CHMP6	Charged Multivesicular Body Protein 6
CLU	Clusterin
CREBBP[KAT3A]	CREB binding protein
DAB2IP	DAB2 Interacting Protein
DDX5	DEAD-Box Helicase 5
DEK	DEK Proto-Oncogene
DNA-PK	DNA-dependent protein kinase
DNMT3A	DNA Methyltransferase 3 Alpha
DSC2	Desmocollin 2
EP300	E1A Binding Protein P300
ERCC2	ERCC Excision Repair 2, TFIIH Core Complex Helicase Subunit
ESR1	Estrogen Receptor 1
EZH2	Enhancer of Zeste 2
FAM127A	Retrotransposon Gag Like 8C
FAM127B	Retrotransposon Gag Like 8A
FAM92A1	Family With Sequence Similarity 92 Member A
FANCC	FA Complementation Group C
FASN	Fatty Acid Synthase
FAT1/2/3	FAT Atypical Cadherin 1, 2 or 3
FLT3	Fms-Like Tyrosine Kinase 3
FSCN2	Fascin Actin-Bundling Protein 2, Retinal
GATA2	GATA Binding Protein 2

HDAC	Histone deacetylase complex	GNAS	GNAS Complex Locus
HELP	HpaII tiny fragment enrichment by ligation-mediated PCR	HIVEP3	Human Immunodeficiency Virus Type I Enhancer Binding Protein 3
HOXL	HOX-Like subclass homeobox genes	HOXB3/4/5	Homeobox B3, B4 or B5
HSCs	Hematopoietic stem cells	IDH1/2	Isocitrate Dehydrogenase 1 or 2
HSPCs	Hematopoietic stem and progenitor cells	IGFBP3	Insulin-Like Growth Factor Binding Protein 3
HyperMRs	Hypermethylated regions	JAG1	Jagged 1
HypoMRs	Hypomethylated regions	JAK2	Janus Kinase 2
INDEL	Insertions and deletions	KIAA1447[BAHCC1]	BAH Domain And Coiled-Coil Containing 1
inv(*)	Inversions, notation	KRAS	KRAS Proto-Oncogene, GTPase
ITD	Internal tandem duplication	MECOM[EVI1]	MDS1 And EVI1 Complex Locus
JAK-STAT	Janus kinase/signal transducers and activators of transcription	MEIS1	Meis Homeobox 1
KI	Knockin, of a gene	MGMT	O-6-Methylguanine-DNA Methyltransferase
LDH	Lactate dehydrogenase	MIR155HG	MIR155 Host Gene
LOH	Loss of heterozygosity	MLL[KMT2A]	Mixed-Lineage Leukemia
LSC	Leukemic stem cell	MLLT3	MLLT3, Super Elongation Complex Subunit
MAF	Minor allele frequency	MTOR	Mechanistic Target Of Rapamycin Kinase
MDS	Myelodysplastic syndromes	MYH11	Myosin Heavy Chain 11
mon	months	MYST3[KAT6A]	Lysine Acetyltransferase 6A
MPNs	Myeloproliferative neoplasms	NEXN	Nexilin F-Actin Binding Protein
mTORC1	Mammalian target of rapamycin complex 1	NHLRC1	NHL Repeat Containing E3 Ubiquitin Protein Ligase 1
NGS	Next generation sequencing	NPM1	Nucleophosmin
NKL	NK-like homeobox genes	NRAS	NRAS Proto-Oncogene, GTPase
no.	numbers	NSD1[KMT3B]	Nuclear Receptor Binding SET Domain Protein 1
NOTCH	Notch, for signaling pathway	NUP214	Nucleoporin 214
NPM1c	c-terminal mutation of Nucleophosmin	PARP1	Poly(ADP-ribose) Polymerase 1
OS	overall survival	PDE4DIP	Phosphodiesterase 4D Interacting Protein
PARP	Poly(ADP-ribose) polymerase	PHF6	PHD Finger Protein 6
PB	Peripheral blood	PIK3C2B	Phosphatidylinositol-4-Phosphate 3-Kinase Catalytic Subunit Type 2 Beta
PCA	Principal component analysis	PIK3CA	Phosphatidylinositol-4,5-Bisphosphate 3-Kinase Catalytic Subunit Alpha
PCR	Polymerase chain reaction	PIK3R1	Phosphoinositide-3-Kinase Regulatory Subunit 1
PI3K	Phosphatidylinositol-4,5-bisphosphate 3-kinase	PML	Promyelocytic Leukemia
RAS	RAS family, signaling pathway	PPM1D	Protein Phosphatase, Mg ²⁺ /Mn ²⁺ Dependent 1D
SAL	Study Alliance Leukemia	RAD21	RAD21 Cohesin Complex Component
sAML	Secondary AML	RAD23A	RAD23 Homolog A, Nucleotide Excision Repair Protein
SEER	Surveillance, Epidemiology, and End Results	RAD51	RAD51 Recombinase
SNP	Single-nucleotide polymorphism	RAD52	RAD52 Homolog, DNA Repair Protein
SNV	Single-nucleotide variation	RARA	Retinoic Acid Receptor Alpha
Src	Proto-oncogene tyrosine-protein kinase Src	RHOC	Ras Homolog Family Member C
t(*;*)	Translocations, notation	RPTOR[RAPTOR]	Regulatory Associated Protein Of MTOR Complex 1
t-AML	Therapy-related AML	RUNX1	Runt Related Transcription Factor 1
TCGA	The Cancer Genome Atlas	RUNX1T1	RUNX1 Translocation Partner 1
TKD	Tyrosine kinase domain	SCRN1	Secernin 1
TNF	Tumor necrosis factor	SF3B1	Splicing Factor 3b Subunit 1
TSG	Tumor suppressor genes	SMC1A	Structural Maintenance Of Chromosomes 1A

TSS	Transcription Start Site	SMC3	Structural Maintenance Of Chromosomes 3
VAF	Variant allele frequency	SOCS2	Suppressor Of Cytokine Signaling 2
WBC	White blood cells	SRSF2	Serine And Arginine Rich Splicing Factor 2
WHO	World Health Organization	TEKT2	Tektin 2
WNT	WNT, for signaling pathway	TET2	Ten-eleven-translocated 2
y	Years	TNF	Tumor Necrosis Factor
α-KG	α-Ketoglutarate	TP53/63/73	Tumor Protein 53, 63 or 73
		TTC12	Tetratricopeptide Repeat Domain 12
		U2AF1	U2 Small Nuclear RNA Auxiliary Factor 1
		VWA8	Von Willebrand Factor A Domain Containing 8
		WT1	Wilms Tumor 1
		XRCC3	X-Ray Repair Cross Complementing 3
		ZRSR2	Zinc Finger CCCH-Type, RNA Binding Motif And Serine/Arginine Rich 2

Note: An alternative name for a gene is given inside “[]”. A “/” corresponds to a pair of different genes. An “-” separates two genes involved in a fusion. The “*” denotes the possibility of several chromosome parts.

CHAPTER 1. INTRODUCTION

1.1 Hematological diseases

“Only if we understand how hematopoietic stem cells age, we can begin exploring opportunities to prevent, delay, or even reverse aspects of the aging process.”³

The current indicators show the population of the developing world is expected to continue aging as our lifespan is increasing. Therefore, we need to understand and revert the decline of our tissue regenerative capacities to prevent further deterioration of the quality of life of the elderly. If we cannot prevent the aging-associated tissue attrition the frequency of diseases associated with age will carry on rising. Blood disorders are now counted amongst the classes of diseases markedly increased by age, which was not anticipated since the blood system is constantly renewed with several billion cells being produced every day. However, we continuously find more and more explanations for why hematological diseases are so very age-dependent.

1.1.1 Normal hematopoiesis

Blood cells are continuously regenerated by hematopoietic stem cells (HSCs) residing in the bone marrow (BM) of adult mammals, the process is denominated hematopoiesis. These are rare cells (0.01–0.2% of the total BM mononuclear cells in humans) that seldom divide. When they do divide they undergo asymmetrical divisions assuring one of the daughter cells is a new HSC (self-renewal)^{4,5} and so keep the number of HSCs stable.

For the normal functioning of the immune system relative amounts of the blood cells from the lymphoid, erythroid and myeloid lineages need to be produced and kept in balance. Therefore, hematopoiesis has to be very tightly regulated.

HSCs give rise to progenitor cells (HSPCs) that become increasingly lineage-restricted and ultimately differentiate into all lineages of mature blood cells (Figure 1.1.1A).

The hierarchy by which the HSCs became committed to a terminally differentiated blood cell has been under assessment in the latest years since the possibility of analysing mutations, gene expression, proliferation and differentiation at a single-cell level have come to challenge the classical model of hematopoiesis^{6,7,8,9}.

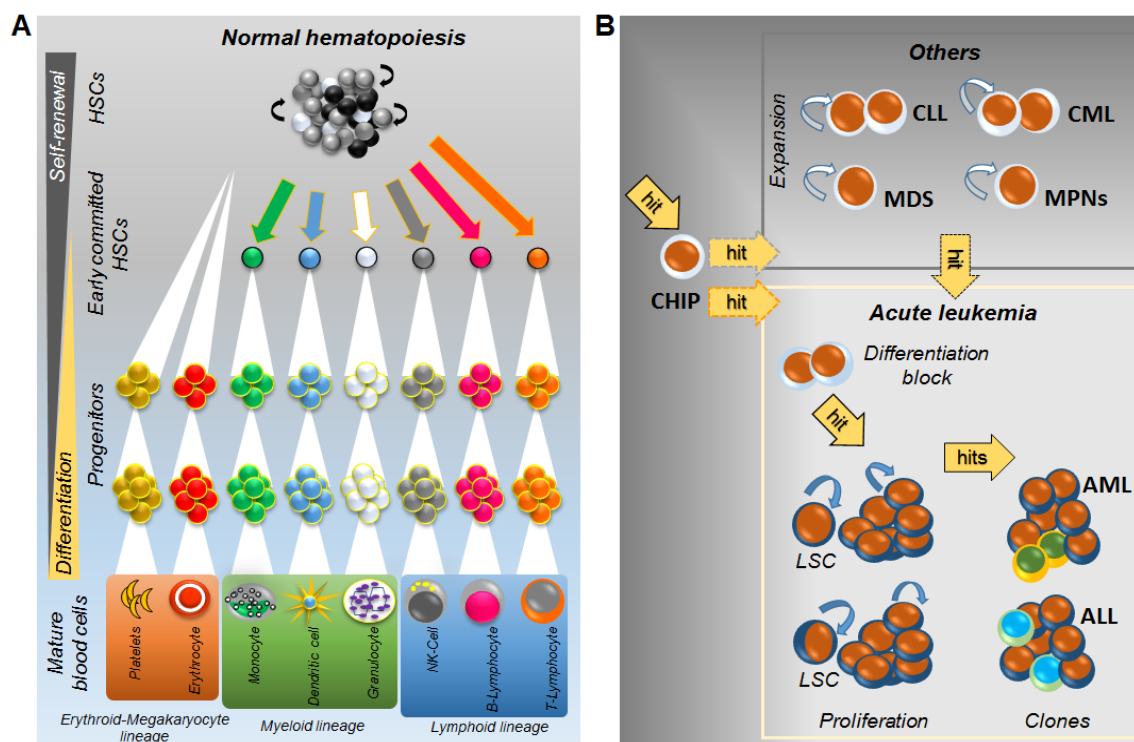


Figure 1.1.1 The normal hematopoiesis and the leukemic stem cell model.

(A) In normal hematopoiesis, rarely dividing hematopoietic stem cells (HSCs) with unlimited self-renewal capacity (indicated by curved arrows) give rise to progenitors (HSPCs). The pool of undifferentiated HSPCs comprises a continuum of transitory cell stages that lack hierarchical structures and discrete lineage-specific progenitor stages. In turn, these intensely proliferative progenitors have progressive states in which self-renewal capacities are decreasing until they ultimately differentiate to all the mature cells of the peripheral blood. (B) The formation of a leukemic stem cell (LSC) in myeloid leukemia may result from mutations in cells in different stages of the hematopoietic hierarchy. Hematologic malignancies are driven by combinations of genetic lesions, the 1st somatic mutation giving rise a pre-leukemic clone: clonal hematopoiesis of indeterminate potential (CHIP), or myelodysplastic syndromes (MDS), or myeloproliferative neoplasms (MPNs). In a pre-leukemic disease phase, cells are genetically unstable, increasing the possibility of further mutations that give rise to the LSCs, developing a chronic or acute disease: acute myeloid leukemia (AML) or acute lymphoblastic leukemia (ALL), chronic myeloid leukemia (CML) or chronic lymphocytic leukemia (CLL). These self-renewing LSCs clonally expand, facilitating the acquisition of additional mutations and development of different leukemic clones. Design by Patricia Silva.

In the classical view, there were bifurcations in commitment steps from multipotent progenitor cells to oligopotent (mixed lineages progenitors) to unipotent (single lineage progenitors). This is currently seen as an early commitment of progenitors with a linear continuum of transitions to the final specification and not requiring several steps, as was previously implied^{6,7,9}. Therefore, the existing HSPCs are a heterogeneous pool of cells with long-term durable self-renewal capacities, made of subpopulations of cells already primed for a specific differentiation program^{6,8}. This view is being reinforced by the fact the oligopotent progenitors of mixed lineages differentiation potentials were so far not found in the context of hematopoiesis in the

adult bone marrow, but there is evidence they are present in the fetal liver⁷. These new facts delineated a shift in the hierarchy of blood progenitor classes from in utero to adulthood⁷. This readjustment anticipates the existence of high age-plasticity of hematopoiesis.

1.1.2 Hematopoietic disorders

When the hematopoietic process fails and a proliferation of immature bone marrow-derived cells (blasts) occurs that constitutes a hematological disorder (Figure 1.1.1B). These could be pre-leukemic diseases characterized by ineffective hematopoiesis that present phenotypes of cytopenia (lack of certain lineages of mature blood cells).

Nowadays, these are commonly denominated myelodysplastic syndromes (MDS) and myeloproliferative neoplasms (MPNs) and said to evolve from a clonal hematopoiesis of indeterminate potential (CHIP), a newly recognized entity.

The CHIP condition despite possibly being phenotype free (without cytopenia) is defined by the occurrence of molecular alterations in leukemia-associated genes. These are mutations that can be found in the peripheral blood of a small proportion of healthy individuals^{10,11}. The pre-leukemic clones in CHIP are cells predisposed to subsequent acquisition of additional genomic alterations. Evolution into an MDS/MPNs is due to further events involving genetic aberrations that do not induce malignant transformations but result in a clonal expansion of mutant progenitors and consequently an increased probability of progression into a leukemic disease.

Therefore, these pre-leukemias can develop into acute leukemia or constitute a chronic form. The most common types of leukemia are: lymphoid leukemias, such as acute lymphoblastic leukemia (ALL) and chronic lymphocytic leukemia (CLL) products of expanded progenitors primed for a lymphoid lineage; or myeloid leukemias, including acute myeloid leukemia (AML) and chronic myeloid leukemia (CML) products of myeloid primed progenitors.

The main model for the development of a full-blown leukemia is the “two-hit hypothesis”¹². It suggests that the malignant transformation of a progenitor cell to a leukemic stem cell (LSC) that maintains leukemia requires at least two mutations. One of the mutations should guarantee a differentiation blockade and another should ensue uncontrolled proliferation and apoptosis evasion (these are usually referred to as the initiation mutations)^{12,13}. It is a simplistic model, it says nothing about the contribution

of epigenetic mechanisms for a fully transformed phenotype and does not have a class for the many mutations found in epigenetic regulators.

In leukemia, it is based mainly on several observations showing that one mutation is usually not enough for leukemic transformations *in vitro* or in mouse models. Recently, the hierarchy of mutations has been studied in several of the leukemic diseases, to identify disease initiation events that are thought to occur early in disease progression. Several early lesions have been identified, for example: DNA methyltransferase 3A (*DNMT3A*) mutations that are found in AML with normal karyotype (CN-AML)^{13,14}; *PML-RARA* fusion found in acute promyelocytic leukemia; ten-eleven-translocated 2 (*TET2*) or isocitrate dehydrogenase 2 (*IDH2*)¹⁵ mutations, as well as core-binding factor (CBF) or mixed-lineage leukemia (*MLL[KMT2A]*)¹⁶ translocations found in 2 other AML types and *ETV6-RUNX1* fusion found in childhood B-ALL¹⁷.

Upon transformation, tumor cells will further acquire multiple genomic or chromosomal aberrations (cooperating mutations)¹³, due to their genomic instability. The environmental pressures¹⁸, a tumor is subjected to, result in the natural selection of some clones in detriment of others. Therefore, leukemias are dynamic systems constantly subjected to Darwinian evolution during malignant progression. In leukemia, genomic analyses at the single-cell level are describing clonal compositions, showing which multiple coexisting clones are present at the time of diagnosis^{19,20}.

Many previous studies had already distinguished the first mutations from the latest clones to arise. These used cytogenetic, molecular and sequencing data obtained from bulk material by estimating variant allele frequencies (VAFs) of the events. Now studies using single-cell genomic analyses are inferring the order of lesions and they found good correlations to the data acquired from the bulks^{20,21}.

Generally, in AML samples at the time of diagnosis, several initiating mutations have been found in a major clone (that are called driver mutations) but also several later mutations that are not in all the blasts (which were termed passenger mutations). Unlike solid cancers the number of these mutations in hematological disorders looks to be limited, with some recognizable patterns, these observations are giving the field hope to advance treatment options using drugs to target cells with these specific mutations.

1.1.3 Aging of hematopoietic stem cells

Since the HSCs are needed for a lifelong generation of mature blood cells, the adult small population of HSCs needs to be properly maintained during aging for a functional hematopoiesis. The normal HSCs reside in a specialized microenvironment in the bone marrow (called niche) surrounded by supporting stromal cells that provide microenvironmental factors for protection and tight regulation over HSCs survival and function. To guard against internal stresses related to divisions (like telomere erosion) HSCs are in a notorious quiescent state, it has been shown the most primitive of all HSC may undergo only 4 to 5 divisions in the lifetime of a mouse²². The burden of proliferation being left for more committed progenitors, HSPCs.

Notwithstanding all guards, human hematopoiesis has shown several phenotypes of age, with older HSCs increasing in frequency, becoming less quiescent⁵, exhibiting myeloid-biased differentiation potential compared with young HSC and mobilizing away from the niche⁴. On the molecular level, mouse aged HSCs were observed to lose polarity of proteins like Cdc42, Scribble and Tubulin (in the cytoplasm) and H4K16ac (in the nucleus)²³, whereas human aged HSCs show increased expression of genes involved in myeloid differentiation and lower expression of genes responsible for lymphopoiesis⁵.

The notion of continued self-renewal capacities of HSCs had been notoriously hard to reconcile with the aging process. HSCs being tissue-specific stem cells have restricted self-renewal potential and suffer a functional decline with age, what is usually termed of stem cell exhaustion^{3,24}. The fact was revealed several times in the hematopoietic system, as transplantation studies showed that HSCs isolated from younger donors have superior powers in repopulating ablated bone marrows²⁵. It is believed that for each division an HSC loses some of its stem cell potential and the pool of progenitors with reduced potential increases to compensate³.

The mechanisms underlying dysfunction of aging HSCs could be cell-intrinsic and cell-extrinsic mechanisms. Most of the phenotypes of HSC associated with age have been attributed to cell-intrinsic mechanisms, although cell-intrinsic changes may also be due to changes that occur in the bone marrow microenvironment. Especially since its shown that malignant myeloid progenitor cells are supported by an altered microenvironment with mesenchymal stromal cells displaying disturbed signaling pathways²⁶ that could contribute to disease development²⁷ (including adhesion molecules and metabolic pathways, as well as endocytosis).

However, the most immediate possibility is the occurrence of molecular alterations in the aging HSCs, leading to clonal expansions of dysfunctional progenitors in the human HSPCs pool. The progenitor's contribution to the blood lineages is then skewed to myeloid progeny⁵. The conjecture is that the aged hematopoietic system has clonal hematopoiesis (CHIP) and might then be predisposed to develop myeloid malignancies as a result.

Our understanding of these clonal events took a forward leap in 2012 and 2014 when several reports proved that clonal hematopoiesis is a frequent event in healthy elderly people^{10,11,28,29}.

In one of these studies from a population of 17,182 persons 10% of the individuals older than 70 years of age carried somatic mutations, the most common mutated genes being *DNMT3A*, *TET2*, and *ASXL1*¹⁰. This was reproduced in another study where more than 2% of the 2,728 individuals had mutations in the blood¹¹, most of the mutations being associated with advanced age. The vast majority of those mutations (83%) occurred in 19 genes associated with leukemia and lymphoma, nine were recurrently mutated (*DNMT3A*, *TET2*, *JAK2*, *ASXL1*, *TP53*, *GNAS*, *PPM1D*, *BCORL1*, and *SF3B1*)¹¹.

In both cases, these accumulations do not appear to be random because they were found in specific loci known to be involved in hematological diseases, which could discourage the view of the accumulation of these mutations in the HSPCs being due to DNA damage. Still, the increased mutation loads must indicate persistent DNA damage in these aging cells upon suffering repeated insults.

These studies were transforming. The field became aware that age-related clonal hematopoiesis is a common condition, associated with an increased risk of developing hematologic cancer and increased risk of cardiovascular disease^{10,11,29}.

This led to the use of the term “pre-leukemic mutation” for these mutations. They are to be considered part of the evolution to leukemia in patients that suffered from CHIP. A very important fact if we are to understand the specificity of elderly AML since these are the patients that likely suffered from CHIP.

1.2 Acute Myeloid Leukemia

“Acute myeloid leukemia (AML) is the most common form of acute leukemia among adults, and it accounts for the largest number of annual deaths from leukemias in the United States. An estimated 21,380 people will be diagnosed with and 10,590 patients will die of AML in 2017.”³⁰

This statement was based in the last cancer statistics of 2017 published every year by the American Cancer Society using the Surveillance, Epidemiology, and End Results program (SEER) as a source for long-term population-based incidence data³¹. It reflects the importance of AML within the blood cancers and the need for treatment options in leukemia, as estimations still predict about 50% of patients with AML will die of the disease.

AML is a hematologic malignancy resulting from an oncogenic transformation and blocked differentiation of cells in a myeloid lineage. These immature cells proliferate in the bone marrow, peripheral blood and other tissues. The major cause of the disease symptoms are these accumulations of blasts in the bone marrow for they result in the impairment of normal hematopoiesis. As a result, the anemia causes fatigue and shortness of breath, the neutropenia/leukopenia causes increased susceptibility to infections and the thrombocytopenia (lack of platelets) causes bruises and bleedings. In turn, the invasion of the tissues by blasts can cause specific symptoms depending on the affected organ (like headaches, slurred speech and confusion, belly swelling). The most pressing ones are caused by lack of oxygen in the tissues because blasts clog vessels, making it difficult for erythrocytes to reach them (leukostasis).

Diagnosis of the acute form of a blood disorder traditionally required the presence of 30% of blast cells in the bone marrow³². This is now a more relaxed criterion, with the arbitrary number of 20% blasts proposed to be enough for diagnosis of AML, if certain morphologic and cytogenetic features are present in the blood smears or peripheral blood and prior treatment has been excluded³³. Current recommendations suggest this is possible when some known cytogenetic abnormalities are detected³³. Namely, if in presence of a number of balanced chromosomal rearrangements and their resulting chimeric fusion genes, which are designated as “recurrent genetic abnormalities”, for example t(15;17), t(8;21), inv(16),

or t(16;16) or in a complex karyotype (with 3 or more abnormalities). Reflecting that these are genetic alterations that are recognized to be pathogenic in AML.

Classically, the classification of AML was based more on the morphology of the leukemic blasts and associated dysplasia, surface and intracellular protein expression, and specific chromosomal abnormalities³⁴. Nowadays, we know AML as a broad entity and its pathogenesis is highly heterogeneous, involving several combinations of cytogenetic abnormalities, genetic mutations and epigenetic anomalies that were identified over the years (Figure 1.2.1).

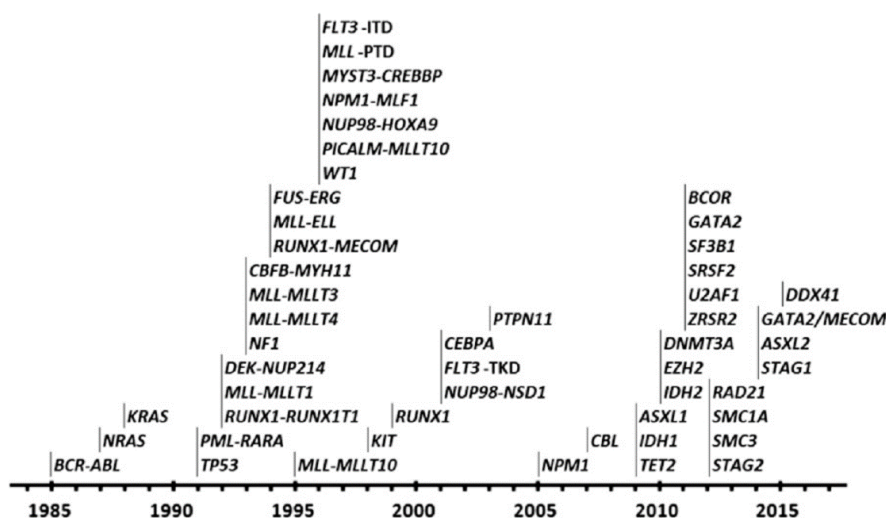


Figure 1.2.1 Progress in defining the molecular landscape of AML.

Timeline of the identification of leukemic fusion genes and mutations underlying the pathogenesis of AML. Adapted from Grimwade *et al.* 2016³⁵.

As the knowledge of the molecular pathogenesis of AML advanced, several classifications dividing AML entities by cytogenetic aberrations and different diagnostic/prognostic molecular markers have been established³⁶. Cytogenetic and molecular cytogenetic studies have long ago found recurrent balanced and unbalanced translocations and inversions that constitute separate molecular classes in AML and were associated with distinct outcomes³⁶. However, up to now nearly 50% of AML samples still present a normal karyotype and many of these genomes lack structural abnormalities, even when assessed with high-density comparative genomic hybridization or single-nucleotide polymorphism (SNP) arrays³⁷. Therefore, several studies started using target sequencing and found recurrent somatic mutations. Currently, the emerging high throughput sequencing techniques are providing extensive molecular data on AML. These recent updates are characterizing novel AML subgroups based on patterns of somatic mutations^{1,37,38,39}.

The leukemic field expects that grouping AML into genetically defined subtypes could provide insights into new treatment designs or at least outcome predictions. The big amount of research effort being applied to that objective in recent years has reflected the importance of this goal. In the duration of our study, several other studies have tried to get at this objective using large cohorts of AML to categorize AML patients^{34,37,38,40}.

1.2.1 AML diagnosis

The diagnosis of AML requires a trained hematologist for the analysis of the morphology of the cells present in blood and marrow smears. They are required to count 200 leukocytes in a blood smear and 500 nucleated cells in marrow aspirate smears³⁶ and report the percentage of cells with blast morphology found.

Apart from these, specific lineage markers are used to help define an immunophenotype for the disease. So, flow cytometric assessments of the expression of cell-surface and cytoplasmic markers are important. These markers should establish the amounts of myeloid progenitors (using CD34, CD117, CD33, CD13, and HLA-DR) and of several lineages: granulocytic (using CD65 and cytoplasmic myeloperoxidase), monocytic (using CD14, CD36 and CD64), megakaryocytic (using CD41 and CD61) and erythroid (using CD235a and CD36)³⁶.

Furthermore, for a suspected AML, the diagnostic workup has to include conventional cytogenetic tests³⁶. Many patients with AML will have cytogenetic aberrations which can be detected through karyotyping or fluorescent in situ hybridization (FISH). Therefore rapid testing of common rearrangements should be done for they are useful for the recommendation of suitable therapies, like *PML-RARA*, *CBFB-MYH11*, *RUNX1-RUNX1T1*, *BCR-ABL1*. Additionally, rearrangements involving genes encoding epigenetic regulators (*MLL[KMT2A]*, *CREBBP[KAT3A]* and *NSD1[KMT3B]*) or nuclear pore complex components (*NUP214*, *NUP98*) although less frequent can be found.

Recently, molecular testing has also entered clinical practice, mostly using reverse transcriptase–polymerase chain reaction (RT-PCR) for the detection of some of the recurrent rearrangements (*RUNX1-RUNX1T1*, *CBFB-MYH11*, *MLLT3-MLL*, *DEK-NUP214*) but also some mutations with prognosis predictions, like: alterations of nucleophosmin (*NPM1*) that change tryptophan residues in the protein C-terminus (*NPM1c*), biallelic mutations of CCAAT/enhancer-binding protein-alpha (*biCEBPA*) and Fms-Like Tyrosine Kinase 3 (*FLT3*) internal tandem duplications (*FLT3-ITD*).

The most recent recommendations indicate that confirmation of AML should further include tests of mutations in the tyrosine kinase domain of FLT3 (*FLT3*-TKD, codons D835 and I836), *RUNX1*, *TP53* and *ASXL1*³⁶. Sequencing all these genes will be more feasible by applying gene panel next generation sequencing (NGS) techniques and will soon become the norm, due to the decreasing costs of the NGS.

1.2.2 AML classifications

The first classifications of leukemia proposed were based in morphological features, for instance, the French-American-British (FAB) co-operative group³² classification, but their power for clinical outcome prediction was very limited. The identification of leukemia-associated chromosomal translocations and inversions paved the way to the World Health Organization (WHO) classification of myeloid neoplasms and acute leukemia in 2001⁴¹ and for its revision in 2008⁴². These classifications of AML were mostly cytogenetic based. They were used to guide the care of patients with AML for many years, for they allowed the division of patients into groups with favorable, intermediates, or adverse prognosis.

Since then, the advances in NGS provided molecular knowledge that led to the WHO updated classification³³ in 2016.

This publication greatly illustrated how, despite the increased knowledge, it remains a struggle to describe the morphological heterogeneity of the AML disease and the AML related diseases. Therefore, the disease was divided into many groups of general morphologic characteristics and these had to be further divided into subgroups with more specific phenotypes and genetic alterations (Table 1.2.1).

Table 1.2.1 WHO 2016 classifications of AML

AML and related precursor neoplasms and acute leukemia of ambiguous lineage classified as by WHO in 2016. Adapted simplification from Arber *et al.*³³ and Döhner *et al.*³⁶.

AML and related neoplasms	
AML with recurrent genetic abnormalities	
○	AML with t(8;21)(q22;q22.1); <i>RUNX1-RUNX1T1</i>
○	AML with inv(16)(p13.1q22) or t(16;16)(p13.1;q22); <i>CBFB-MYH11</i>
○	Acute promyelocytic leukemia with <i>PML-RARA</i>
○	AML with t(9;11)(p21.3;q23.3); <i>MLLT3-MLL[KMT2A]</i>
○	AML with t(6;9)(p23;q34.1); <i>DEK-NUP214</i>
○	AML with inv(3)(q21.3q26.2) or t(3;3)(q21.3;q26.2); <i>GATA2, MECOM[EVI1]</i>
○	AML (megakaryoblastic) with t(1;22)(p13.3;q13.3); <i>RBM15-MKL1</i>
○	Provisional entity: AML with <i>BCR-ABL1</i>
○	AML with mutated <i>NPM1</i>
○	AML with biallelic mutations of <i>CEBPA</i>
○	Provisional entity: AML with mutated <i>RUNX1</i>
AML with myelodysplasia-related changes	
Therapy-related myeloid neoplasms	
AML, NOS	
○	AML with minimal differentiation
○	AML without maturation
○	AML with maturation
○	Acute myelomonocytic leukemia
○	Acute monoblastic/monocytic leukemia
○	Pure erythroid leukemia
○	Acute megakaryoblastic leukemia
○	Acute basophilic leukemia
○	Acute panmyelosis with myelofibrosis
Myeloid sarcoma	
Myeloid proliferations related to Down syndrome	
○	Transient abnormal myelopoiesis
○	Myeloid leukemia associated with Down syndrome
Blastic plasmacytoid dendritic cell neoplasm	
Acute leukemias of ambiguous lineage	
Acute undifferentiated leukemia	
MPAL with t(9;22)(q34.1;q11.2); <i>BCR-ABL1</i>	
MPAL with t(v;11q23.3); <i>MLL[KMT2A]</i> rearranged	
MPAL, B/myeloid, NOS	
MPAL, T/myeloid, NOS	

1.2.3 AML prognostic factors

Typically, there are several considerations to have when trying to predict a patient resistance to treatment or outcome, mainly because not only the disease factors but also the patient previous and current health state are relevant. Even so, the presence of certain genetic lesions are the most important factors accounting for good or bad outcomes³⁶.

Foreseeably, research into predictive markers based on the genetic characteristics of the disease has been one of the most important fields of leukemia for many years. However, until now predictive models for live expectancy have only reached 75-80% accuracy³⁶, with contributions from demographic, clinical and treatment variables being hard to model.

According to current knowledge, prognostic factors have been divided into patient-related factors or AML-related factors⁴³.

The most important prognostic factor patient-related is increasing age at the time of diagnosis, which has been shown to be an independent predictor of poor outcome^{44,45,46} and suggests the effect of unknown age-related factors⁴⁷. Other patient-related factors have been associated to differences in outcomes such as coexisting medical conditions (especially comorbidities) and poor performance status (a measure of patient fitness from the impact of cancer on patients daily living abilities, ECOG score, graded 0-healthy to 5-death). These factors complicate the application of intensive induction chemotherapies and are correlated to increased treatment-related early death⁴³.

The majority of prognostic factors known are related to the disease itself. One of these factors is white blood cells count (WBC), which when higher than $100 \times 10^9/L$ is considered hyperleukocytosis and connected to increased mortality during chemotherapy.

Others are splenomegaly and elevated serum lactate dehydrogenase (LDH), although these appear to provide poor prognosis only in certain cohorts⁴³.

Furthermore, the AML diagnosed according to the disease history has consistently proved to be of prognostic value. AML can be classified into 3 distinct categories based on clinical ontogeny: secondary AML (sAML) represents the transformation of an antecedent diagnosis of MDS/MPNs; therapy-related AML (t-AML) that develops as a complication in patients with prior exposure to cytotoxic therapies; and *de novo* AML that refers to the absence of any identified hematological disorder or prior exposure to therapy.

The two classes sAML and t-AML have demonstrated poor prognosis predictions, mostly due to increased resistance to current standard chemotherapy leading to low median overall survival probabilities^{43,48}. However, the spectrum of genetic lesions of these two classes is different from the *de novo* AML, having shown genetic aberrations typical of the MDSs (like single nucleotide variations, SNVs, in splicing factors) and low frequencies of cytogenetic characteristics of favorable prognosis (like CBF rearrangements)⁴⁹. Therefore, the sAML and t-AML ontogenies are connected to genetic abnormalities that are powerful prognostic factors and might be the responsible factors that confer these particular poor prognoses^{49,50}.

Since the presence of specific genetic abnormalities still has the most power to predict survival probabilities, genetically based predictors are the most informative

disease-related factors. So far, the prediction of inferior outcomes in a clinical setting has depended on the evaluation of common cytogenetic lesions and 3 molecular genetic markers (*NPM1c* and *biCEBPA* mutations and *FLT3*-ITD). These were factors included in the European LeukemiaNet (ELN) recommendations of 2010⁴⁷ that became clinical practice. The 2010 ELN recommendations were done by a panel of international experts, which endeavored to standardize the reports of genetic abnormalities and its correlations to clinical outcomes. They stratified patients into 4 risk categories according to their molecular genetic data (favorable, intermediate-I, intermediate-II and adverse)⁴⁷.

The amount of research data accumulated in the last 5 years was calling for a revision of this system. To start with, the 2 groups intermediate-I and II were impossible to distinguish in older patients, which actually are the major group of patients. Additionally, several studies had shown previously unknown genetic markers associated with poor prognosis. As a result, last year the ELN published their update of the recommendations for the groups based on this new data on treatment outcomes³⁶.

Therefore, the most significant changes were the merging into 3 risk categories (favorable, intermediate and adverse). Typically, patients with favorable risk cytogenetic profiles present balanced structural rearrangements (fusions *PML-RARA*, *RUNX1-RUNX1T1*, *MYH11-CBFB*), and normal karyotype with *biCEBPA* or mutated *NPM1*. Conversely, patients with unfavorable-risk cytogenetic profiles display imbalanced abnormalities (fusions like *DEK-NUP214* or *BCR-ABL1*, rearrangements of *KMT2A*, *MECOM* or *GATA2*, deletion of 5q, abnormal 3q, monosomy of chromosome 7), or three or more complex abnormalities (complex karyotype). This group now includes the poor outcomes of patients with *RUNX1*, *ASXL1* or *TP53* mutations (originating Table 1.2.2).

Table 1.2.2 ELN 2017 risk stratification by genetics characteristics.Table with the new ELN risk categories simplified from the reported in Bullinger *et al.*⁵¹.

Risk Category	Genetic Lesion
Favorable	<ul style="list-style-type: none"> ○ t(8;21)(q22;q22.1); <i>RUNX1-RUNX1T1</i> ○ inv(16)(p13.1q22) or t(16;16)(p13.1;q22); <i>CBFB-MYH11</i> ○ Mutated <i>NPM1</i> without <i>FLT3</i>-ITD or with <i>FLT3</i>-ITD^{low} ○ Biallelic mutated <i>CEBPA</i>
Intermediate	<ul style="list-style-type: none"> ○ Mutated <i>NPM1</i> and <i>FLT3</i>-ITD^{high} ○ Wild-type <i>NPM1</i> without <i>FLT3</i>-ITD or with <i>FLT3</i>-ITD^{low} (if without adverse-risk gene mutations) ○ t(9;11)(p21.3;q23.3); <i>MLL T3-MLL[KMT2A]</i> (takes precedence over adverse-risk mutations) ○ Cytogenetic abnormalities not classified as favorable or adverse
Adverse	<ul style="list-style-type: none"> ○ t(6;9)(p23;q34.1); <i>DEK-NUP214</i> ○ t(v;11q23.3); <i>MLL[KMT2A]</i> rearranged ○ t(9;22)(q34.1;q11.2); <i>BCR-ABL1</i> ○ inv(3)(q21.3q26.2) or t(3;3)(q21.3;q26.2); <i>GATA2, MECOM[EV11]</i> ○ -5 or del(5q); -7; -17/abn(17p) ○ Complex karyotype^Δ, monosomal karyotype* ○ Wild-type <i>NPM1</i> and <i>FLT3</i>-ITD^{high} ○ Mutated <i>RUNX1</i> (if without favorable-risk AML gene mutations) ○ Mutated <i>ASXL1</i> (if without favorable-risk AML gene mutations) ○ Mutated <i>TP53</i>

FLT3-ITD^{low}: low allelic ratio (<0.5); *FLT3*-ITD^{high}: high allelic ratio (≥0.5); semi quantitative assessment of *FLT3*-ITD allelic ratio (using DNA fragment analysis) is determined as the ratio of the area under the curve “*FLT3*-ITD” divided by the area under the curve “*FLT3*-wild-type”; recent studies indicate that acute myeloid leukemia (AML) with *NPM1* mutation and *FLT3*-ITD low allelic ratio may also have a more favorable prognosis, and patients should not routinely be assigned to allogeneic hematopoietic cell transplantation.

^ΔThree or more unrelated chromosome abnormalities in the absence of one of the WHO-designated recurring translocations or inversions (ie, t(8;21), inv(16) or t(16;16), t(9;11), t(v;11)(v;q23.3), t(6;9), inv(3) or t(3;3), AML with *BCR-ABL1*).

*Defined by the presence of one single monosomy (excluding loss of X or Y) in association with at least one additional monosomy or a structural chromosome abnormality (excluding core-binding factor AML).

These risk-groups are expected to change soon, for they are predicated on patients being treated with the conventional chemotherapies. They could soon become obsolete due to the good results of new therapies that are being directed to certain molecular alterations.

1.2.4 AML treatments

Since 1970, when it was recognized the activity of cytarabine (Ara-C) and anthracyclines against blasts, major progress has been made in the treatment of patients with AML⁵². The recommendation is, as soon as the diagnostic workup of a patient has been completed with an AML diagnosis, intensive chemotherapy should start, provided he/she can tolerate it³⁶. The standard induction therapy currently used consists of 7 days of cytarabine (100-200 mg/m² continuous IV) and 3 days of an anthracycline (daunorubicin, at least 60 mg/m², idarubicin, 10-12 mg/m², or mitoxantrone, 10-12 mg/m²), this treatment is commonly denominated “7+3”. This regime as yield an average 35 to 40% long-term cures in young patients with AML (meaning patients 60 years old or younger)⁴³.

The major accomplishments in AML therapy in the recent past are due to advances in the understanding of AML heterogeneity since improvements have been obtained only from matching particular treatments to specific subgroups of AML⁵². For instance, regimens that have resulted in cure rates 80% to 90%, like treatments with All-Trans-Retinoic Acid (ATRA) and arsenic trioxide⁵² in acute promyelocytic leukemia (APL), that target its PML-RARA and eliminated the need for chemotherapy^{53,54}. The same is happening for treatments using fludarabine, high-dose cytarabine, anthracyclines⁵⁵ or gemtuzumab ozogamicin^{56,57} in patients with the CBF type of AML⁵².

More recently, genetic studies have provided insights into other molecular targets, for example, *FLT3*-ITD that had consistently been associated with poor prognosis mostly due to a high relapse rate⁵⁸. The molecular characterization of this target has led to the development of a novel therapy soon to be integrated into clinical practice. It consists in the addition of Midostaurin (multi-targeted kinase inhibitor) to standard chemotherapy, which has shown to significantly prolong overall and event-free survival (OS and EFS) among patients with *FLT3* mutations⁵⁹ and is now approved for treatment of this group of patients.

Other targeted therapeutic approaches have promised improvements in patient outcomes, including epigenetic directed treatment approaches with hypomethylating agents^{60,61}. The first of this class to be applied were azacitidine (Aza) and decitabine (5-aza-2-deoxycytidine), licensed by the Food and drugs administration (FDA) for their demethylation activities (to use in MDS)⁶² and registered by the European Medicines Agency (EMA; for use in elderly AML patients aged 65 years and older)^{63,64}. These agents promote a broad epigenomic reprogramming, which has been shown to reverse the hypermethylations at promoters of tumor suppressor genes (TSG) and allow for normal differentiation. Interest in these therapies for AML has been increasing due to reports that several enzymes with special roles in the epigenetic regulation of gene expression and initiation of chromatin remodeling are affected by somatic mutations in AML. Since the epigenetic alterations in AML are not only responsible for silencing of TSGs, but also for several transcription activations, it has been very difficult to identify which subset of AML may benefit most from such broadly hypomethylating therapies.

More directed therapies are underway, for instances specifically targeting DNA methyltransferases (DNMTs) which one of the protein families affected by mutations. The mammalian DNMTs are DNMT1, DNMT3A and DNMT3B, which together with accessory proteins, like DNMT3L, are responsible for the acquisition of methylation

patterns during gametogenesis, embryogenesis and somatic tissue development. The DNMTs affected in AML are mostly DNMT3A, with the highest frequency of genetic alterations³⁷, and DNMT3B for which overexpression in samples represents lower survival probability⁶⁵. At least DNMT3A is an essential DNA methylation regulator thought to have a severe impact on DNA methylation patterns⁶⁶. Despite that, specific DNMT3A inhibitors have so far not been applied and combinations of these with the histone deacetylase complex (HDACs) inhibitors are still under evaluation⁶⁷.

In contrast, specific inhibitors of mutant isocitrate dehydrogenases (IDHs) were developed much faster^{68,69,70}. IDHs are enzymes involved in metabolism, by catalyzing the conversion of isocitrate to α -ketoglutarate (α -KG) in the tricarboxylic acid cycle (TCA cycle), for which point mutations were found in AML (in the genes *IDH1* or *IDH2*)^{1,71,72}. The latest developments of IDH inhibitors have led to the approval of Enasidenib (AG-221)⁷³, by the FDA⁷⁴, for the treatment of relapsed and refractory *IDH2* mutated AML patients. For the corresponding *IDH1* mutated group of patients other IDH inhibitors are already in clinical trial. Specifically, Ivosidenib (AG-120) has shown good results inducing remissions in relapsed or refractory AML patients and was a well-tolerated treatment⁷⁵.

All the new treatments in AML being developed are expected to increase patients' survival and promise a bright future to the field. A future that was not within sight during the last decades, when progress was only due to improvements in best supportive care and in stem cell transplantation techniques. This is now a foreseeable future due to hard work in the analysis of the mechanisms by which certain genetic and epigenetic aberrations drive AML.

1.3 Genetic groups of AML

“The recent quantum leap in sequencing technology, aided by a dramatic reduction in sequencing costs, has allowed for the generation of previously unparalleled amounts of information annotating mutational landscapes and their evolution across multiple cancers. As befits the first cancer genome sequenced, nowhere is this more apparent than in AML.”³⁵

Most of the genetic alterations that initiate AML were only discovered after 2008 when the first whole cancer genome sequence and its matching normal tissue was published⁷⁶. The study, done by Ley *et al.*⁷⁶, reported the sequencing of a CN-AML sample. They found this patient had non-synonymous somatic mutations that could be relevant for AML pathogenesis and would not have been sequenced otherwise, for they were unforeseen⁷⁶. This demonstrated broad NGS approaches were required if we were to discover new recurrent somatic mutations to identify candidate genes for treatment development.

The first comprehensive NGS study genetically characterized 200 AML patients with a *de novo* AML disease using a whole-exome sequencing approach. It was performed by the consortium The Cancer Genome Atlas³⁷ (TCGA) in 2013. The study reported, 154 genes had more than 1 non-synonymous somatic mutation and an additional 1,623 genes had a validated coding mutation in one sample. They observed 23 genes to be significantly mutated, including genes that were established as being relevant to AML pathogenesis (e.g., *DNMT3A*, *FLT3*, *NPM1*, *IDH1*, *IDH2*, and *CEBPA*), along with genes that have only recently been implicated in AML pathogenesis (*U2AF1*, *EZH2*, *SMC1A*, and *SMC3*).

The genes frequently mutated in AML were grouped into nine larger sets or pathways (Figure 1.3.1): transcription factor fusions, the *NPM1* gene, tumor suppressor genes, DNA methylation-related genes/epigenetic regulators, signaling genes, chromatin-modifying genes, myeloid transcription factor genes, cohesion complex genes, and spliceosome complex genes/splicing factors³⁷.

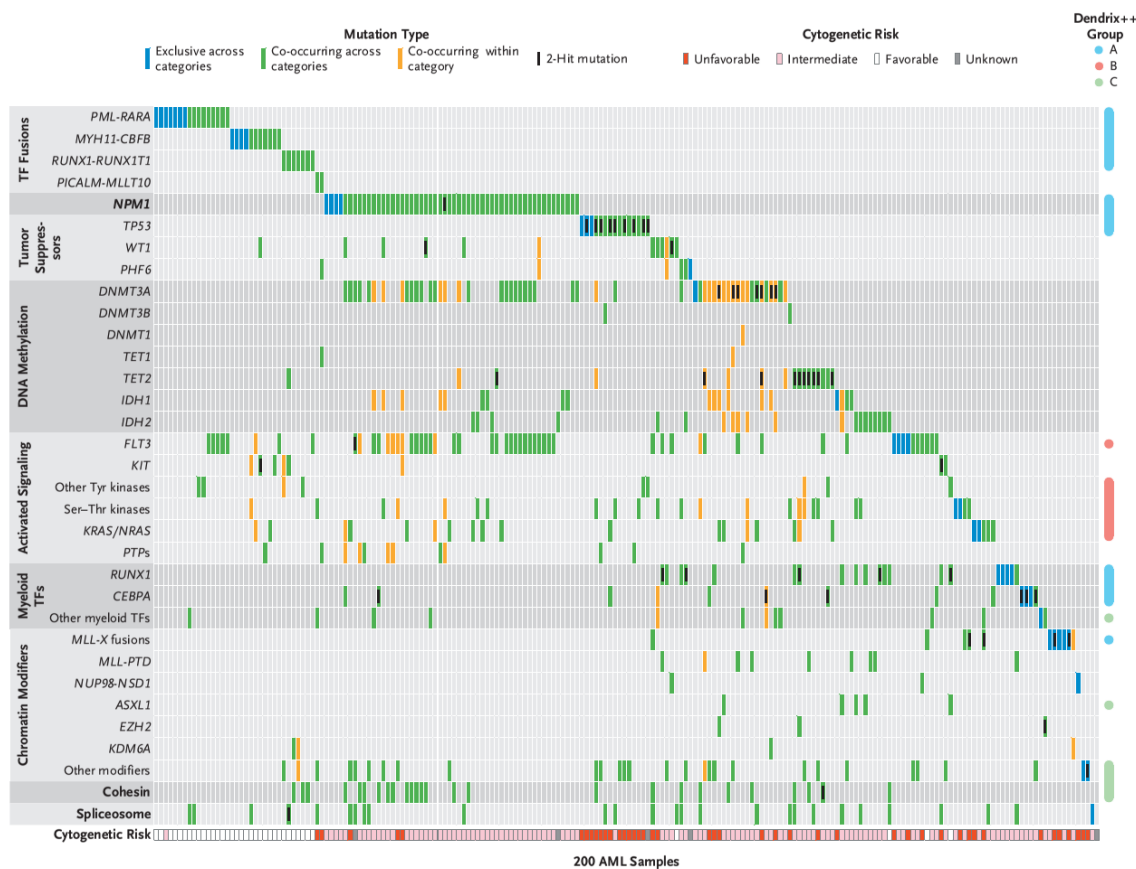


Figure 1.3.1 Organization of mutations into categories of related genes.

“Shown are somatic, nonsynonymous mutations in individual genes and sets of genes, grouped into nine categories, including one single-gene category, as labeled on the left. Of the 200 samples evaluated, 199 (>99%) had at least one mutation in one of the listed genes or sets. Blue boxes indicate mutations that are exclusive across all categories; green boxes, mutations that co-occur in the same sample across different categories; and orange boxes, mutations that co-occur in the same sample in the same category. Computational analysis with the use of the Dendrix++ algorithm identified three significant, mutually exclusive groups of genes, annotated on the right as groups A, B, and C. The cytogenetic risk for each patient is shown at the bottom of the chart. Ser–Thr denotes serine–threonine, TF transcription factor, and Tyr tyrosine.” Adapted from TCGA study of 2013³⁷.

These gene sets were used to examine patterns of mutual exclusivity and co-occurrence of mutations within and between groups. In this analysis, TCGA identified combinations of mutations in samples that occur in non-random patterns. The most prominent relation was the significant co-occurrence between mutations in *FLT3*, *DNMT3A*, and *NPM1*, which they considered to constitute a new AML group³⁷.

At present, several studies (including ours) have applied target re-sequencing techniques and confirmed several genes to be frequently mutated, with patterns of co-occurrence or mutual exclusivity quite similar to the discovered by TCGA^{1,37,39,51}.

One of the latest studies investigated 111 genes by NGS studying 1,540 AML patients³⁹. They found 76 genes mutated with the large majority of patients having at least 2 driver mutations. The co-mutational patterns they found resulted in a genetic-

based classification of 11 non-overlapping AML classes, some of them newly recognized classes (Figure 1.3.2). These classes were primarily made of the different known fusion genes or the presence of some class defining mutations: *NPM1*; *biCEBPA*; *TP53*/chromosomal aneuploidies; chromatin and RNA-splicing regulators; *IDH2*^{R172} alterations. Other samples were segregated into groups without driver mutations, without class defining mutations or included in a group for the rare fusions³⁹.

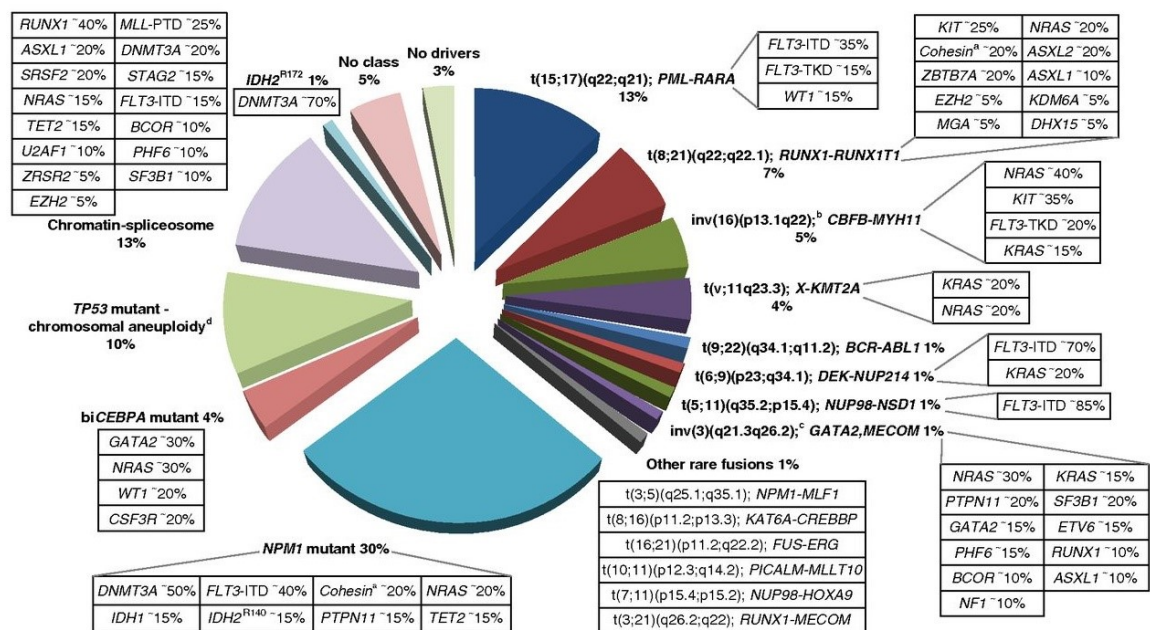


Figure 1.3.2 Molecular classes of AML and concurrent gene mutations in adult patients.

"For each AML class denoted in the pie chart, frequent co-occurring mutations are shown in the respective boxes. Data on the frequency of genetic lesions are compiled from the databases of the British Medical Research Council (MRC), the German-Austrian AML Study Group (AML SG), and from selected studies.

^a, indicates cohesion genes including *RAD21* (~10%), *SMC1A* (~5%), and *SMC3* (~5%); ^b, *inv(16)(p13.1;q22)* or *t(16;16)(p13.1;q22)*; *CBFB-MYH11*; ^c, *inv(3)(q21.3q26.2)* or *t(3;3)(q21.3;q26.2)*; *GATA2*, *MECOM(EVI1)*; and ^d, *TP53* mutations are found in ~45%, and complex karyotypes in ~70% of this class". The structure of the pie chart is adapted from Grimwade *et al.*³⁵ generated by Adam Ivey (King's College London, London, United Kingdom) and presented in Döhner *et al.*³⁶, with the data from Papaemmanuil *et al.*³⁹.

The statistical power of profiling 1,540 patients gave them the opportunity to attribute different survival probabilities to several of these groups, by separating patients with gene fusions from others³⁹.

They found class defining gene fusions had different probabilities of survival between them, which was expected. They further report, individual mutational patterns in absence of gene fusions could also have a distinct prognosis and small classes of

groups defined by the presence or absence of drivers can also be discriminated (Figure 1.3.3)³⁹.

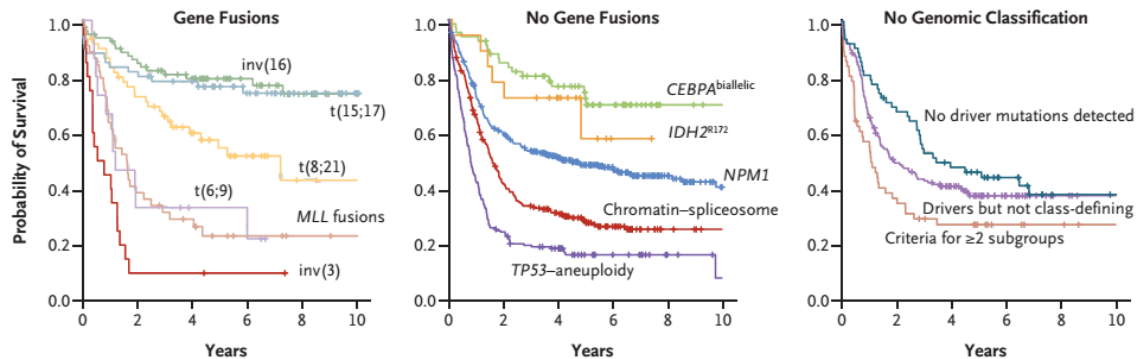


Figure 1.3.3 Different overall survival of molecularly classified groups of AML.

The panels show Kaplan–Meier curves for overall survival among patients in the 11 genomically defined subgroups and patients who did not have a straightforward classification. Adapted from Papaemmanuil *et al.*³⁹.

All data gathered with the new genetic analysis of AML cohorts brought the field close to understanding the complex molecular patterns of the disease. Since underneath the heterogeneity certain genetic alterations make up specific subsets of AML we can now set to understand what drives the disease in each case. Furthermore, studies can dedicate to mapping tumor dynamic progressions, using its multiple driver mutations and coexisting competing clones that mark disease evolution over time⁵¹.

However, studying the time dimension has still not been enough. Ever since chromosomal translocations and fusions were discovered pathologic in AML, it was suspected that the disease complexity does not end at the genetic level. Many of them affected chromatin modulators as *MLL*[*KMT2A*], *CBP*[*KAT3A*], and *NSD1*[*KMT3B*], but still, that was only a small fraction of AML.

Nowadays, we know that chromatin is affected in most of the AML samples. The whole genome or exome sequencing of AML and the massive parallel sequencing studies led to the identification of mutations in many genes that affect the epigenetic landscape. These modulators of transcription include a broad spectrum of regulators of DNA-methylation or demethylation and modifiers of histone acetylation or methylation (Figure 1.3.4). Recurrent mutations in AML and MDS were found in DNA methyltransferases (*DNMT1/3A*), isocitrate dehydrogenases (*IDH1/IDH2*), methylcytosine dioxygenases of the ten-eleven-translocated family (*TET1/2*), human homologs of the *Drosophila* polycomb complex such as Enhancer of Zeste 2 (*EZH2*) and additional sex-combs like genes (*ASXL1/2*). Moreover, there are a number of examples of epigenome modulators that are not directly mutated but have been

indirectly implicated in AML pathogenesis, like the histone methyltransferase DOT1L that interacts with the MLLTs which in turn are usually MLL-fusion partners.

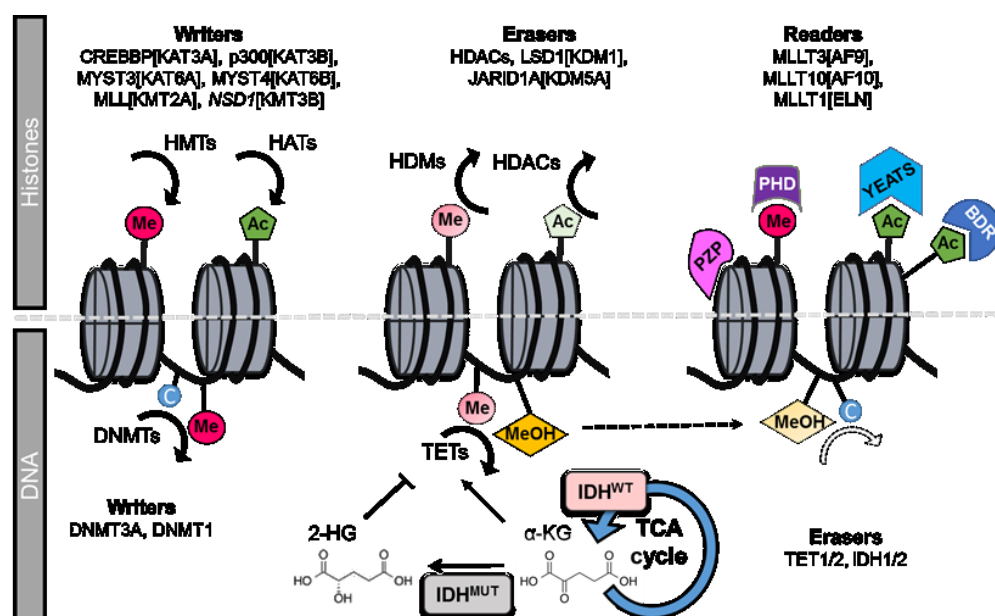


Figure 1.3.4 Types of epigenetic regulators mutated in AML that change or read epigenetic marks in DNA or histones.

Epigenetic “writers” such as histone methyltransferases (HMTs), and histone acetyltransferases (HATs), deposit methylation and/or acetylation on histones, as do DNA methyltransferases on DNA. These epigenetic marks may be removed by epigenetic “erasers,” including histone demethylases (HDMs) and histone deacetylase complexes (HDACs). Removal of methylation from DNA is a stepwise process that involves many intervening enzymes directly and indirectly affected by mutations in AML (TETs and IDHs). Epigenetic “readers” are highly specialized proteins that specifically bind to distinct epigenetic marks to convey this information to downstream effectors. Abbreviations of molecules and domains: alpha-ketoglutarate (α -KG); 2-hydroxyglutarate (2-HG); bromodomains (BRDs); plant homeodomain (PHD); PHD-zinc finger-PHD (PZP). In brackets are alternative gene names/symbols. Design by Patricia Silva.

DNMT: Mutations in *DNMT3A* are observed in 12–22% of AML in most cohorts and usually are heterozygous mutations. Approximately 60% of all *DNMT3A* mutated AML patients harbor a missense mutation in the arginine 822 residue that diminishes its methyltransferase activity while reducing its binding affinity to DNA. These mutations have a dominant negative function over the wild-type DNMT3A protein⁷⁷. The majority of the remaining mutations of *DNMT3A* are nonsense or frame-shift mutations in the protein-coding region that led to premature truncations of the protein.

TET: The ten-eleven translocation (TET) family of proteins regulates DNA methylation through the conversion of 5-methylcytosine to 5-hydroxymethylcytosine, which constitutes a step in a complex reaction for removal of DNA methylation⁷⁸. The 5-hydroxymethylcytosine is thought to block the binding of proteins that mediate

transcriptional silencing by recognizing methylated DNA and therefore it present in sites of active transcription. Currently, the higher mutation frequency is in *TET2*, with around 14% up to 22% in some cohorts. Most of these mutations are insertions or deletions, but point-mutations also have been found. *TET2*-mutations constitute loss-of-function leading to decreased 5-hydroxymethylcytosine sites. This results in aberrant hypermethylation and therefore decreased expression of key differentiating enzymes and inhibition of normal cellular differentiation^{79,80}.

***IDH*:** AML samples were found to have frequent point mutations in *IDH1* Arg132 (R132) and *IDH2* Arg172 or Arg140 (R172 or R140)^{1,37,38,39}. *IDH1* and *IDH2* mutations are found at a frequency of about 10% each and more common in CN-AML. It was proposed that these mutations in the *IDH* genes constitute a gain-of-function. These confer an enzymatic activity to the protein that converts α -KG producing a new oncometabolite D-2-hydroxyglutarate (2-HG), found increased in mutant *IDH* cells⁷¹. This metabolite is an inhibitor of several α -KG-dependent deoxygenase reactions, for it is a cofactor for proteins of the TET family and the JumonjiC domain histone demethylases (erasers of DNA and histone methylation). One of these enzymes is TET2. By inhibiting TET2 the molecular alterations in *IDH* give rise to the strong hypermethylation phenotypes found in *IDH* mutant AML patients^{1,37}, which results in undifferentiated states. On the other hand, by inhibiting the JumonjiC type enzymes it deregulates histone methylation. Accordingly, a general increase in certain histone methylation marks has revealed closed DNA conformation in *IDH1*-KI mouse cells⁸⁰ and *IDH* mutation induce CNS-derived⁷¹.

1.4 Epigenetic patterns in AML

“DNA methylation and its influence on gene expression are key in understanding cancer pathogenesis. Even though it is becoming clear that DNA methylation strongly interacts with other components of the epigenetic machinery such as histone modifications, aberrant DNA methylation can still be regarded as a crucial hallmark of cancer by itself.”⁸¹

Biology has evolved a great deal in grasping the rules of gene expression by recognizing that the process involves several dimensions of regulation. The first reports described heritable DNA methylation, histone modifications and micro RNA variability. Nowadays, epigenetics refers to all heritable changes in gene expression that are not due to any alteration in the DNA sequence, this includes DNA methylation, chromatin remodeling (by histone modifications or binding of certain proteins to DNA, like the insulator binding CTCF) and the activities of non-coding RNAs. The interplay between these epigenetic components has not been completely determined, but a complex picture of gene expression control has emerged. Since the correct distribution of DNA methylation is essential for every tissue differentiation and homeostasis⁸² deregulations of epigenetic processes are connected to oncogenesis. DNA methylation is nowadays recognized as a mechanism by which cells acquire cancer hallmark capabilities⁸³ (of undifferentiating and self-renewal), playing important roles in initiation, progression and maintenance of malignant phenotypes.

Since the patterns of aberrant gene expression in AML are not well explained by the classifications based on mutational patterns the role of DNA methylations has been under examination. The quantification of 5-cytosine methylation (5-methylcytosine, m⁵C) in the cytosine-phosphate-guanine sequential nucleotides (CpGs) based in genome-wide techniques has provided valuable information about observed gene expression patterns in several cancers including colon, lung and breast cancer⁸⁴ and was expected to do the same for AML.

Genome-wide analysis of DNA methylation suggested that aberrant DNA methylation in cancer occurs at defined genomic locations, termed cancer-specific differentially methylated regions (DMRs)⁸⁴. Genome-wide studies indicated that cancer cells have global DNA hypomethylation when compared to their respective tissues,

with regions of hypermethylation associated with CpG-islands at promoter sites^{84,85}, creating patterns that could even guide us into better clinical classifications of tumors⁸⁶.

Standing in contrast to these solid tumors, AML has a more complex picture of epigenetic regulation. The earliest analyses of DNA methylation in AML found aberrant DNA methylation in the promoters of some genes, for the available data covered only 14,000 promoters^{87,88}. Later, a crucial analysis of multidimensional data in AML integrated genetic and epigenetic patterns of 344 AML samples and defined 16 subclasses of patients according to their DNA methylation profiles using 50,000 CpGs accessed by HELP (HpaII tiny fragment enrichment by ligation-mediated PCR)⁸⁹. These 16 groups of patients presented unique methylation patterns when compared to normal bone marrow CD34⁺ cells. Unexpectedly most groups were largely hypermethylated and only a minority hypomethylated, additionally many promoter regions were actually hypomethylated⁸⁹.

This diversity of epigenetic changes in AML adds complexity to the already complex genetic heterogeneity. The only common epigenetic signature of these AML samples consisted of 45 genes differentially methylated (mostly hypermethylated in relation to the normal bone marrow CD34⁺ cells) and that was obtained considering only 70% of patients⁸⁹. Other studies, that profiled the methylation status of more patients and more genes, also found only small sets of genes had methylation patterns deregulated across samples^{37,90}.

In contrast, most studies find groups of patients that are reflective of the presence of specific cytogenetic and genetic aberrations in samples. Namely, there were different groups for the fusions *PML-RARA*, *CBFB-MYH11*, *RUNX1-RUNX1T1* (*AML1-ETO*) and then for the mutations of *CEBPA* double mutants and *NPM1* and *CEBPA* silenced in one study⁸⁹; and in another study for *MLL* translocations vs *IDH* mutated samples⁹⁰.

More recently the epigenetic landscapes of AML have been analysed by TCGA, using the genome-wide DNA methylation BeadChip from Illumina® covering 99% of RefSeq genes with over 450,000 CpGs. In this study TCGA determined significant changes in methylation at 160,516 CpGs loci when the 192 patients were compared to CD34⁺CD38⁻ cells from healthy donors, confirming hypermethylations were the majority of changes (67%) while hypomethylations were only present in a minority of places (33%)³⁷. In this case, groups of samples with specific genetic lesions were still present but not so clearly defined³⁷, with the strongest methylation signatures being obtained using regions of the genome with low amounts of CpGs. This brought back

the questions about which CpGs might be more important for regulation of gene expression.

The latest study followed indications that the defining DMRs in leukemia might not be the typical hypermethylations in gene promoters and instead be correlated to regulatory elements outside of promoters⁹¹. These would possibly be in regulatory DNA sequences, which in vertebrates often have little or no methylation, like enhancers⁹². They used a new technique not centered on promoters and denominated enhanced reduced representation bisulfite sequencing (ERRBS), that allowed for the widest probing of the methylation status so far (about 951,000 CpGs). Using this dataset they found that despite the methylation heterogeneity of samples some genetic lesions could still be correlated to specific DNA methylation profiles (Figure 1.4.1)⁹¹.

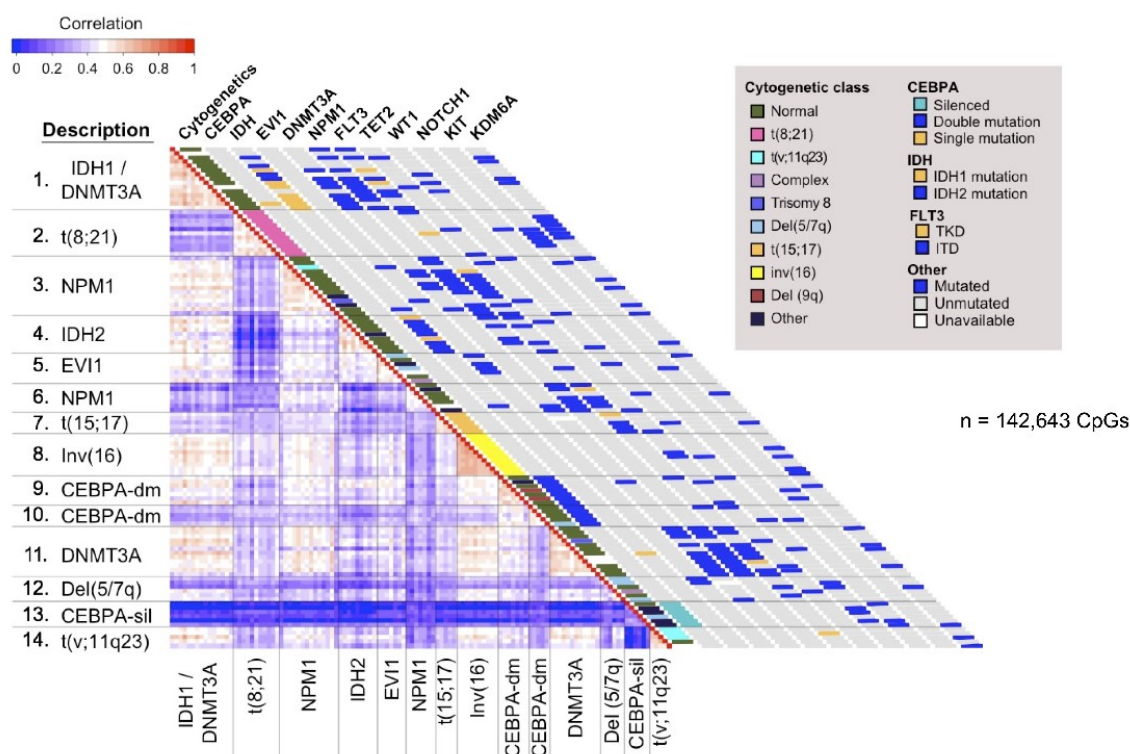


Figure 1.4.1 Epigenetically defined classification of AML.

“Representation of hierarchical clustering results based on ERRBS data using a correlation matrix heatmap. ERRBS defines AML subtypes with distinct molecular and cytogenetic characteristics. Groups were defined using a hierarchical clustering approach and labeled according to their dominant distinguishing molecular and cytogenetic features. The lower triangular heatmap represents the correlation between the most divergent CpGs represented in all samples. Cytogenetic and specific molecular features are represented in the diagonal bars on the right.” Adapted from Glass et al.⁹¹.

Additionally, the epigenetic identity of genetically similar samples was best captured by using gene CpGs in gene neighborhoods (between 2kb and 50kb away

from the transcription start site or transcription end site) rather than promoters, or by CpGs in shores in opposition to CpGs islands if using only CpGs in promoters⁹¹.

These high-throughput DNA methylation data in AML were not only mere curiosities, due to its dynamic nature it provides potential targets for therapy. Knowing that AML is populated with DNA hypermethylation provided bases for the application of hypomethylating agents in clinical settings, although their mechanisms of action are not well defined since they indiscriminately remove methyl groups from DNA⁶². Therefore, targeting specific genes with expression affected by different DNA methylation marks would possibly be more effective.

Many studies have found that DNA methylation could predict clinical outcome in AML patients and therefore indicated aberrant DNA methylation can serve as a biomarker for risk stratification (Table 1.4.1).

Table 1.4.1 Prognostic genes regulated by DNA methylation.

Genes with differential DNA methylation that were identified by genome-wide detection methods applied to large cohorts of AML patients. Adapted from Li *et al.* 2017⁹³.

Reference	Method	AML group	Prognostic genes regulated by DNA methylation
Figueroa <i>et al.</i>⁸⁹	HELP	344 <i>de novo</i> AML, median Age 48y (range:15-77)	<i>BLR1</i> [<i>CXCR5</i>], <i>BTBD3</i> , <i>E2F1</i> , <i>FAM110A</i> , <i>FAM30A</i> , <i>GALNT5</i> , <i>KIAA1305</i> , <i>LCK</i> , <i>LMCD1</i> , <i>PRMT7</i> , <i>SLC7A6OS</i> , <i>SMG6</i> , <i>SRR</i> , <i>USP50</i> , <i>VWF</i> , <i>ZFP161</i>
Li <i>et al.</i>⁹⁴	ERRBS	138 Paired AML (diagnosis and relapse), mean Age 50.5±14y	<i>CCDC85C</i> , <i>CHL1</i> , <i>ELAVL2</i> , <i>FAM115A</i> , <i>FAM196A</i> , <i>GPR146</i> , <i>GPR6</i> , <i>HEL Z2</i> , <i>ID4</i> , <i>IL2RA</i> , <i>KCNG3</i> , <i>LOC254559</i> , <i>LOC284801</i> , <i>NPAS2</i> , <i>PCDHAC2</i> , <i>PROB1</i> , <i>SHISA6</i> , <i>SLC18A3</i> , <i>SOCS2</i> , <i>TRIM67</i> , <i>ZFP42</i>
Marcucci <i>et al.</i>⁹⁵	MethylCap-seq	134 CN-AML training (Age range ≥60y) + 355 CN-AML validated (Age range 17-83y)	<i>AATK</i> , <i>ACAP3</i> , <i>ADCK2</i> , <i>ADCY6</i> , <i>AGPAT9</i> , <i>AHCY</i> , <i>ALOX15B</i> , <i>ANXA6</i> , <i>APBB1</i> , <i>APOD</i> , <i>AQP11</i> , <i>ARHGAP27</i> , <i>AXL</i> , <i>BRF1</i> , <i>C15orf62</i> , <i>C17orf77</i> , <i>C8orf51</i> , <i>CABLES1</i> , <i>CARD11</i> , <i>CD34*</i> , <i>CHMP7</i> , <i>CISH</i> , <i>CLDN15</i> , <i>CLEC3B</i> , <i>DDIT4</i> , <i>DHCR24</i> , <i>DHRS12</i> , <i>EGFL7</i> , <i>ETS1</i> , <i>EVC</i> , <i>F2RL1*</i> , <i>FAM92A1*</i> , <i>FCHO1</i> , <i>FKBP4</i> , <i>FLVCR1</i> , <i>FLVCR1-AS1</i> , <i>FZD6</i> , <i>GAL3ST3</i> , <i>GCNT2</i> , <i>GIT1</i> , <i>GPR56</i> , <i>H1FO</i> , <i>HCN2</i> , <i>HIVEP3</i> , <i>IQSEC1</i> , <i>KCNK6</i> , <i>KDM2B</i> , <i>KLHL3</i> , <i>KNCN</i> , <i>LOC646627</i> , <i>MDFI</i> , <i>ME3</i> , <i>MEOX1</i> , <i>MIR126</i> , <i>MIR155HG*</i> , <i>MVD</i> , <i>NAV1</i> , <i>NBL1</i> , <i>NLRP1</i> , <i>PLK3</i> , <i>PMM1</i> , <i>PRKCZ</i> , <i>PRKG2</i> , <i>RAB36</i> , <i>RGS3</i> , <i>RHOC*</i> , <i>RHPN1</i> , <i>SCARF1</i> , <i>SCRN1*</i> , <i>SH3TC1</i> , <i>SPRY1</i> , <i>SRC</i> , <i>TBL2</i> , <i>TCEA3</i> , <i>TENC1</i> , <i>UBXN6</i> , <i>VWA8*</i> , <i>WDR16</i> , <i>WDR86</i> , <i>WRAP53</i> , <i>ZNF623</i> , <i>ZNF70</i>
*Seven genes (<i>CD34</i> , <i>RHOC</i> , <i>SCRN1</i> , <i>F2RL1</i> , <i>FAM92A1</i> , <i>MIR155HG</i> , and <i>VWA8</i>) had not only DNA methylation regions (DMRs) but also expression levels that were associated with outcome.			

Unfortunately, even when analysing many CpGs, studies usually did not find many genes with DNA methylation signatures associated with prognosis. Only 16, 22 and 82 different genes were found to be correlated to survival, by the studies of Figueroa *et al.*⁸⁹, Li *et al.*⁹⁴ and Marcucci *et al.*⁹⁵ respectively. There was no overlap between them, which is understandable because the cohorts used have very different compositions in terms of AML genetic and clinical factors. The impossibility of comparison is made worse by the fact that these investigations were done using

different techniques. In addition, these predictive signatures were still not reproduced by independent studies.

Therefore, to establish DNA methylation levels that could be used as prognostic indicators has so far been challenging. However, the possibility of clarifying the driving forces of gene expression alterations from the DNA methylation changes in AML is still very attractive and is the subject of continuous study. Establishing the prognostic value of individual DNA methylation sites as biomarkers, especially on the context of specific cytogenetic subgroups, is a very appealing prospect since it could lead to new therapeutic strategies.

1.5 Elderly AML specificities

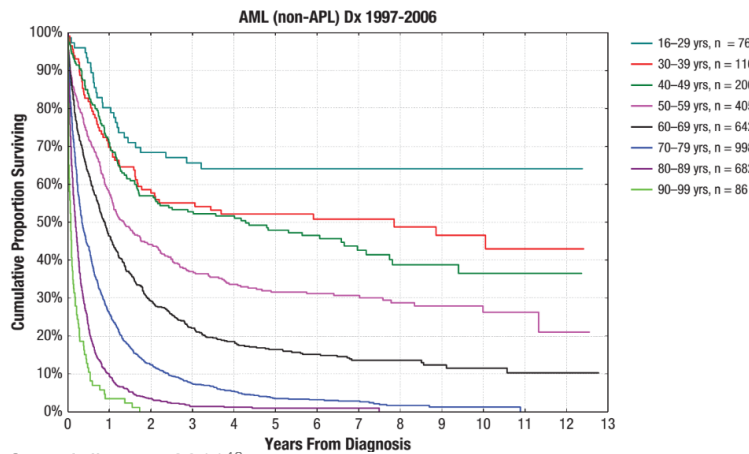
“First, how does the hematopoietic system change with age, how does this lead to a spectrum of hematological conditions, and would it be possible to pharmacologically intervene in this process? Second, if hematological disease presents in an elderly patient, should this be treated differently than if it had occurred in a young patient?”⁹³

These are pertinent questions for which answers have so far eluded hematologists. They are of utmost importance because AML is primarily a disease of the elderly population with the incidence rising with age. According to the SEER population statistics, only 1.9 of 100,000 people under 65 years old develop AML, a number rising to 19.1 for the elderly population of 65 years and older (between 2009 and 2013)⁹⁶. Expectedly, the median age of patients with AML at the time of diagnosis is around 71 years old (indicated by the compulsory reports of population-based studies like the Swedish AML registry with about 3,363 adult AMLs)^{46,45,97}.

1.5.1 Survival of elderly AML patients

Overall, elderly patients with AML have a poor survival probability, as studies show that survival to AML decreases with advanced age (Figure 1.5.1)^{46,45,98}.

Although the goal of curing AML can only be reached using intensive chemotherapies, the therapy choices for older patients also include less intensive chemotherapy or supportive care. This depends on the doctors' perception of the patient's condition (performance status, ECOG score, co-morbidities, and tolerance to intensive chemotherapy). These patients are many times considered *unfit* for the intensive chemotherapy for fear of the high rates of early death in initial treatment. For instance, patients older than 75 years with an ECOG performance score of 3 (*“capable of only limited self-care; confined to bed or chair more than 50% of waking hours”*) or higher have a 30-day mortality rate of more than 50%⁴⁴.



from Juliusson 2011⁴⁶.

Figure 1.5.1 Survival of patients with AML in a population study according to their age at the time of diagnosis.

Kaplan-Meier curves for all the patients diagnosed with AML (non-acute promyelocytic leukemia) between 1997 and 2006, treated and untreated (n=3205). Divisions were done by decades. With data used was from the compulsory Swedish registry of AML with a median follow-up of 6.2 years. Adapted

As a result, in the US 60% of AML patients 65 years or older have not received therapy 3 months after diagnosis⁹⁹. The lack of viable options leads clinicians in Europe to widely use the less intensive approaches in patients over 65 years old, like decitabine or azacitidine, for although the effectiveness of these hypomethylating agents is not well established, they are promising^{100,101}. They remain a viable option, having in mind that even with intensive chemotherapy only 50% of patients older than 60 years achieve complete remissions and 50% of those would have relapsed within 2 years¹⁰².

Advances in therapy in the elderly patients have been compromised by extrapolation of results from clinical trials that mostly use young patients (frequently younger than 60 years). Elderly patients tend to be excluded from clinical trials for many reasons. The selection bias is frequently due to strict criteria for entering trials with intent-to-treat and by the drop out due to the impossibility of many of this patients to begin treatments, to complete them, or to go through consolidation phases¹⁰³.

Therefore, we know little about how and why treatments *work* or *not work* in the elderly group of AML patients. Higher rates of resistance to intensive chemotherapy treatment regimens and high rates of relapse have been observed in the older patients when compared to younger AML patients. Response rates were observed to decrease with age (as well as the median overall survival) even when there were no protocol-directed differences in dosing of patients⁴⁴. Moreover, in a recent study, the treatment response of patients 57-59 years old to a full-dose chemotherapy proved to be no different from 60-63 year's patients receiving an attenuated-dose therapy¹⁰⁴. Therefore it is regularly concluded that age is an important independent determinant of therapy-response in AML.

1.5.2 Molecular characteristics of elderly AML

These facts have been attributed to several disease characteristics displayed by elderly AML when compared to young AML patients, like the fact that older patients are more likely to have adverse cytogenetics^{105,106}. Nevertheless, elderly AML patients irrespective of their cytogenetic group show an inferior outcome compared to younger patients with the same risk alterations^{106,107}.

In an effort to examine the phenotype of this disease a study analysed the status of oncogenic pathways in elderly AML in comparison to younger AML¹⁰⁸. They found older patients had a higher probability of RAS, Src, and tumor necrosis factor (TNF) pathway activation¹⁰⁸.

All of these data underscored the biological differences between AML in younger and older patients. Evidences that led us to postulate that elderly AML is a different entity for which a targeted treatment is needed and should be properly investigated. As it remained an open question if additional molecular alterations have important contributes to the poor prognosis of AML in the elderly patients this was one focus of our project¹.

Meanwhile, attending to these indications in last two years some studies that sequenced genes known to be frequently mutated in AML have made a point in dividing their cohorts into young and elderly patients to look at frequencies of genetic alterations^{34, 38,40}.

In general, it is now established the commonly mutated genes in older patients with AML included *RUNX1*, *TET2*, *IDH2*, *ASXL1*, *SRSF2*, *TP53*, *BCOR* and *SF3B1* while *WT1* mutations were more frequent in the younger patients^{1,34,38,40}.

Since the genetic profiles might explain some of the poor prognosis of elderly AML the origin of this very specific profiles should provide important information for new treatment design.

As age-related changes of the diseased hematopoietic system are found they must be the result of the aged state of the HSCs. Therefore we should explore the possible effects of age on the progenitor cells that give rise to the elderly AML.

CHAPTER 2. AIM OF THE PROJECT

Many studies of AML pathogenesis in elderly people led us to raise the hypothesis that, **AML in the elderly is not just AML in an older person**. Is the landscape of molecular alterations in AML different in older patients with a higher load of pre-existing alterations? Which pathogenic processes are more affected in elderly AML than in younger patients? Do specific genetic and epigenetic features contribute to the poor prognosis and treatment resistance of elderly cohorts?

Though complex patterns of molecular alterations had been characterized in some younger cohorts, comprehensive and integrated studies (genetic and epigenetic) in older cohorts were lacking. We aimed to find the **genetic alterations and global epigenetic changes** in elderly AML that differed from AML in younger patients. We expected both profiles were necessary to define the specificity of elderly AML.

1. We first concentrated on obtaining a picture of the **relevant molecular alterations** in this tumor entity:

- ✓ Exploring recurrent genetic alterations known in AML in a large number of patients with elderly AML using targeted NGS.
- ✓ Probing for unknown events, analysing a broad set of candidate genes by an extended NGS panel of 555 genes.
- ✓ Describing global genome methylation patterns for elderly AML using an array that covers over 450,000 methylation sites.

2. We aimed to define **elderly AML** comparing its genetic and epigenetic patterns to profiles of younger AML cohorts.

3. We next wanted to determine the **pathways/cellular processes** that are more affected in elderly AML than in younger AML cells (both by mutations and/or epigenetic alterations).

4. We postulated the **interconnection of genetic and epigenetic profiles** would allow the division of elderly AML patients in epigenetically defined subgroups associated with specific genetic alterations.

5. We meant to explore possible genetic/epigenetic **factors responsible for the poor survival** of elderly AML and therefore reasons for the age factor.

We expected the knowledge of this distinct genomic/epigenomic entity and its complexity to lay a foundation for future development of **smarter therapeutic regimes**.

CHAPTER 3. PATIENTS AND METHODS

3.1 Elderly AML cohort characteristics

The cohort studied was composed of 93 AML patients enrolled in the Study Alliance Leukemia (SAL) registry between 2005 and 2014. All patients provided written informed consent in compliance with the Declaration of Helsinki. This cohort consisted of patients 65 years and older at the time of AML diagnosis (Figure 3.1.1), chosen using only this criteria and the availability of sufficient material in quality and quantity as well as clinical information¹. Clinical data are summarized in Table 3.1.1, showing our cohort had a composition within expected, due to similarities to reports of AML in general population⁹⁷, where 75% were diagnosed with *de novo* AML, 19% sAML and 5% therapy-related AML (further detailed in Appendix A).

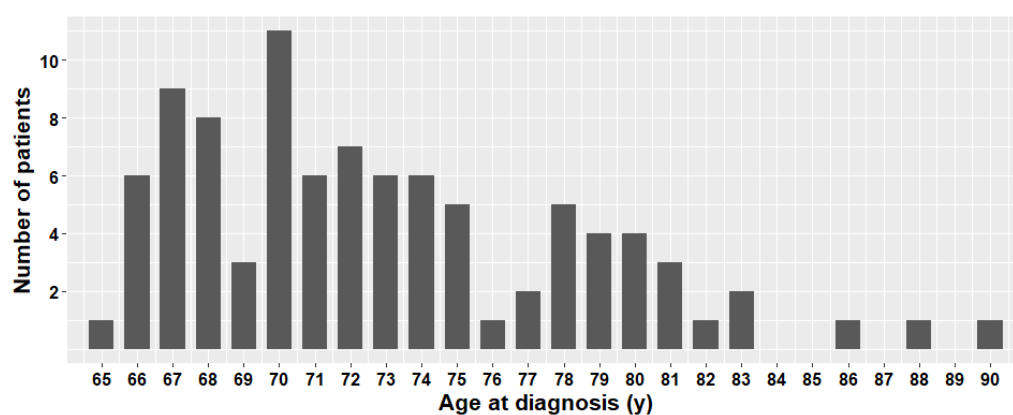


Figure 3.1.1 Distribution of patients' age at diagnosis in the SAL elderly AML.

The plot shows the number of samples present in the SAL cohort for each specific patient age, in intervals of 1 year, calculated from the date of birth.

Table 3.1.1 Characteristics of elderly AML cohort.

Summary of characteristics of patients: *de novo* AML (no previous leukemic related diagnosis), secondary AML (sAML, with a previous diagnosis of myelodysplastic syndrome or myeloproliferative neoplasm), or therapy-related AML (t-AML, patients with prior exposure to cytotoxic therapy and/or radiotherapy). The cytogenetic groups were defined as: cytogenetically normal (CN, no detected cytogenetic abnormalities), core binding factor (CBF, includes t(8;21) or inv(16)/t(16;16)), Complex (3 or more cytogenetic abnormalities), or other (1 or 2 cytogenetic abnormalities). Treatments of patients were divided according to the application of standard intensive chemotherapy or not (the latter consisted of palliative or best supportive care, which includes treatment with hypomethylating agents). Several abbreviations were used: *FLT3* internal tandem duplications (*FLT3*-ITD), mutations in nucleophosmin altering tryptophan residues in the C-terminus of the protein (*NPM1c*), white blood cell counts (WBC), Lactate dehydrogenase (LDH), bone marrow (BM), months (mon) and years (y). As presented in Silva *et al.* 2017¹.

Clinical characteristics, n=93	
Age at diagnosis (y), median (ranges)	72 (65-90)
Sex (Male), no. (%)	47 (50.5)
<i>de novo</i> AML, no. (%)	70 (75)
sAML, no. (%)	18 (19)
t-AML, no. (%)	5 (5)
LDH (U/L), median (ranges)	406 (138-4219)
WBC (/nL), median (ranges)	14.8 (0.9-210)
BM Blasts, % (ranges)	75 (25-99)
Cytogenetic, n=75	
CN, no. (%)	28 (37)
CBF, no. (%)	5 (6.7)
Complex, no. (%)	12 (16)
Other, no. (%)	30 (40)
Molecular data	
<i>FLT3</i> -ITD, no./ total no.(%)	15/70 (21)
<i>NPM1c</i> , no./ total no.(%)	15/69 (22)
Treatment, n=90	
Palliative or best supportive care, no. (%)	19 (21)
Intensive chemotherapy, no. (%)	71 (79)
[no. stem cell transplantation]	[10]
Survival, n=92	
Median survival time (mon)	15
Follow up time (mon), median (ranges)	7.4 (0.1-92)

3.2 Mutations in protein coding sequences of 555 genes

We obtained sequence data from target enrichment coupled NGS of 555 genes (Table 3.2.1).

DNA was extracted, using the AllPrep DNA/RNA kit (©QIAGEN, N.V.), after a Ficoll isolation (Ficoll-Paque™ PLUS, GE Healthcare, USA) for enrichment of the fraction of blast cells from the bone marrow aspirates of 93 patients (or from peripheral blood mononuclear cells, n=1) obtained prior to treatment.

For the exome capture, SureSelect^{XT} custom 0.5Mb-2.9Mb was used to prepare a library from sonicated DNA with lengths of 300-400bp (SureSelect®, Agilent Technologies, USA) according to manufacturer's protocol, using 1µg to 3µg of DNA as starting material according to availability. During this preparation, DNA samples were analysed using an Agilent DNA 1000 chip run on an Agilent Bioanalyzer 2100 (G2938B, Agilent Technologies, USA) to assess sizes of DNA fragments obtained after sonication procedure (average lengths of 280bp). Similar electropherogram summaries were made for the final libraries of captured fragments of all samples in order to assure fragment sizes averaging between 300-330bp. For confirmation of specific capture of the targets in the DNA libraries (obtained for each patient), two simultaneous qPCR reactions were performed. A positive control verifying the presence of exon 23 of *DNMT3A* (labeled probe FAM and BHQ1) and a negative control verifying the non-hybridization of the gDNA of the non-target *GATA4* using a set of primers that span the promotor (labeled probe Joe and TAMRA). The DNA amount of the samples was then quantified using Quantus™ Fluorometer (Promega Corporation, USA) to guarantee the normalized amount of 16 patients per pool (10nmol/L of each patient sample).

The captured targets were subjected to massively parallel sequencing using Illumina HiSeq2000 with 2x100bp paired-end reads (functional genome analysis gene center, Muenchen), using 1 pool per sequencing lane. Sequenced reads were aligned using a BWA to the GRCh37/hg19 reference genome. From the 25±10 million reads per sample retrieved about 91.8±8.2% of reads mapped to the genome, about 99.5±0.4% of mapped reads had high-quality scores ($Q \geq 20$, Figure 3.2.1). After removal of PCR duplicates, we obtained a median target coverage of 408±164 reads and then considered only targets sequenced with the minimal 30x coverage (98.4±1.8% of all targets, Figure 3.2.1). Non-synonymous single nucleotide variants, small insertions or deletions in the coding sequence and affecting splice sites were detected with VarScan2 and Pindel according to standard quality assurances.

Mutations were considered if alterations were present at a variant allele frequency (VAF) higher than 20%, which was further adjusted for the genes in the X chromosome and therefore denominated adjusted VAF.

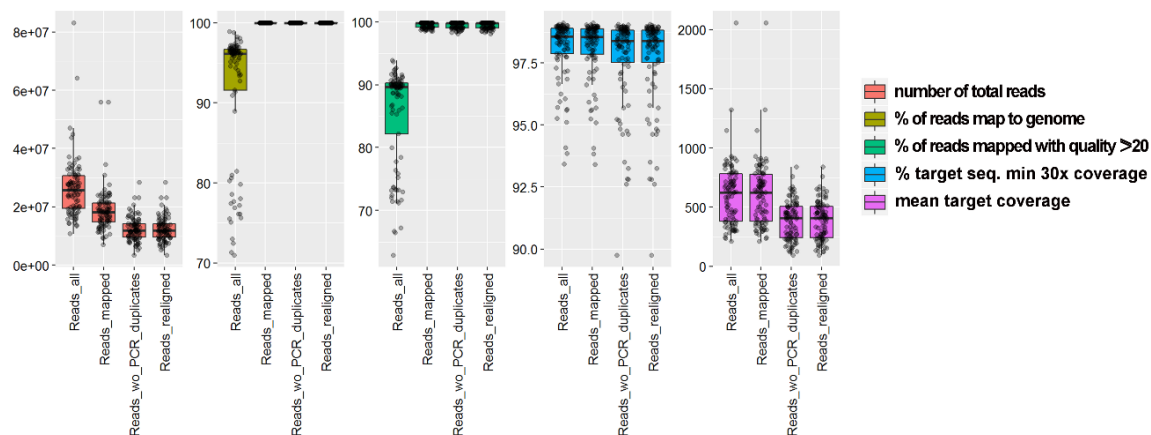


Figure 3.2.1 Quality controls of mapping and coverage of the target sequencing of the SAL elderly AML samples.

The plots show results of the application of the BWA algorithm, used for alignment of NGS reads to the genome. In the horizontal axis are the points at which data was collected during the mapping process (before and after alignment, after removal of PCR duplicates and the final trimmed/realigned fragments). In the vertical axis are the numbers of reads or the % of reads obtained for each of the 93 samples, according to the analysis reported in the legend. Abbreviations in legend and axis were seq. for sequences, min for minimum, wo for without and 30x for 30 times.

Table 3.2.1 Mutated genes selected for the targeted NGS design.

List of the 555 genes previously correlated to leukemia or other cancer types and developmental diseases. Listed in alphabetic order.

ABI1	BUB1B	CARD11	EZH2	HIP1	LCP1	NBN	PIM1	SEPT5	TIRAP
ABL1	CCDC6	CARS	EZR	HIPK1	LHFP	NCKIPSD	PLAG1	SEPT6	TLX1
ABL2	CCNB1IP1	CASC5	FAM46C	HIST1H4I	LIFR	NCOA1	PML	SEPT9	TLX3
ACACA	CCND1	CBFA2T3	FANCA	HLF	LMNA	NCOA2	PMS1	SET	TMPRSS2
ACER1	CCND2	CBFB	FANCC	HMGA1	LMO1	NCOA4	PMS2	SETD2	TNFAIP3
ACSL3	CCND3	CBL	FANCD2	HMGA2	LMO2	NDRG1	POM121	SF3B1	TNFRSF14
ACSL6	CCNE1	CBLB	FANCD2OS	HNF1A	LPP	NEBL	POU2AF1	SFPQ	TNFRSF17
ACTN4	CCNL1	CBLC	FANCE	HNRNP2B1	LRIG3	NF1	POU5F1	SH3GL1	TNRC18
AFF1	CD274	DAB2IP	FANCF	HOOK3	LYL1	NF2	PPARG	SH3GL1	TOP1
AFF3	CD74	DACH1	FANCG	HOXA11	MAF	NFE2L2	PPARGC1A	SIRT1	TP53
AFF4	CD79A	DAXX	FAS	HOXA13	MAFB	NFIB	PPP2R1A	SIRT3	TPM3
AKAP9	CD79B	DCP1A	FAT1	HOXA9	MALT1	NFKB2	PRCC	SLC34A2	TPM4
AKT1	CDC42EP1	DCPS	FAT2	HOXC11	MAML2	NIN	PRDM1	SLC45A3	TPR
AKT2	CDC73	DDB2	FAT3	HOXC13	MAP2K4	NKX2-1	PRDM16	SLCO1B3	TRDMT1
ALDH2	CDH1	DDIT3	FBXO11	HOXD11	MAPRE1	NONO	PRF1	SMAD4	TRIM24
ALK	CDH11	DDX10	FBXW7	HOXD13	MDM2	NOTCH1	PRG4	SMAP1	TRIM27
AMER1	CDK12	DDX5	FCGR2B	HRAS	MDM4	NOTCH2	PRKAR1A	SMARCA4	TRIM33
APC	CDK4	DDX6	FCRL4	HSP90AA1	MSD2	NPM1	PRKCZ	SMARCB1	TRIP11
APOB	CDK6	DEK	FEV	HSP90AB1	MED12	NR4A3	PRRX1	SMO	TSC1
ARHGAP26	CDKN2A	DICER1	FGFR1	HSPB2	MEN1	NRAS	PSIP1	SNX29	TSC2
ARHGEF12	CDKN2C	DLL1	FGFR1OP	IDH1	MET	NRIP3	PTCH1	SOC3	TSHR
ARHGEF17	CDX2	DNM2	FGFR2	IDH2	MITF	NSD1	PTEN	SORBS2	TTL
ARID1A	CEBPA	DNMT1	FGFR3	IGF1R	MKL1	NTRK1	PTPN11	SOX2	U2AF1
ARID2	CEBPD	DNMT3A	FH	IGFBP7	MLF1	NTRK3	PTPRT	SPECC1	UBE4A
ARNT	CELA3B	DNMT3B	FHIT	IKZF1	MLH1	NUMA1	RABEP1	SRGAP3	UCP2
ASPSCR1	CHCHD7	DUX4	FIP1L1	IL2	MLL	NUP214	RAD21	SRSF2	UCP3
ASXL1	CHEK2	E2F1	FLCN	IL21R	MLL2	NUP98	RAD51B	SRSF3	USP6
ATF1	CHIC2	EBF1	FLI1	IL6ST	MLL3	NUTM1	RAF1	SS18	VAV1
ATIC	CHN1	ECT2L	FLNA	IL7R	MLLT1	NUTM2A	RALGDS	SS18L1	VHL
ATM	CIC	EED	FLT3	ING1	MLLT10	OLIG2	RANBP17	SSX1	VTI1A
ATRX	CIITA	EEFSEC	FBNP1	IRF4	MLLT11	OMD	RANBP2	SSX2	WAS
AUTS2	CLP1	EGFR	FOXO2	ITK	MLLT3	P2RY8	RAP1GDS1	SSX4	WHSC1
BAALC	CLTC	EIF4A2	FOXO1	JAK1	MLLT4	PAFAH1B2	RARA	STIL	WHSC1L1
BAP1	CLTCL1	ELF4	FOXO3	JAK2	MLLT6	PALB2	RB1	STK11	WIF1
BCL10	CNBP	ELK4	FOXO4	JAK3	MN1	PATZ1	RBM15	STRN3	WLS
BCL11A	CNOT	ELL	FOXO1	JARID2	MNX1	PAX3	RCSD1	SUFU	WRN
BCL11B	CNR2	ELN	FRYL	JAZF1	MPL	PAX5	RECQL4	SUZ12	WT1
BCL2	COL1A1	EML4	FSTL3	JUN	MSH2	PAX7	REL	SYK	WWTR1
BCL3	COX6C	EP300	FUBP1	KDM5A	MSH6	PAX8	RET	TAF15	XPA
BCL6	CREB1	EPOR	FUS	KDM5C	MSI2	PBRM1	RHOH	TAL1	XPC
BCL7A	CREB3L1	EPS15	GAS7	KDM6A	MSN	PBX1	RMI2	TAL2	XPO1
BCL9	CREB3L2	ERBB2	GATA1	KDR	MTCP1	PCM1	RNF213	TCEA1	YWHAE
BCOR	CREBBP	ERC1	GATA2	KDSR	MTOR	PCSK7	ROS1	TCF12	ZBTB16
BCORL1	CRLF2	ERCC2	GATA3	KIAA0284	MUC1	PDCCD1LG2	RPL22	TCF3	ZFYVE19
BCR	CRTC1	ERCC3	GMPS	KIAA1549	MUTYH	PDE4DIP	RPN1	TCF7	ZMPSTE24
BECN1	CRTC3	ERCC4	GNA11	KIF3B	MYB	PDGFB	RUNX1	TCF7L2	ZMYM2
BIRC3	CRYAB	ERCC5	GNAQ	KIF5B	MYC	PDGFRA	RUNX1T1	TCL1A	ZNF276
BLM	CTNNB1	ERG	GNAS	KIT	MYCL	PDGFRB	SBDS	TCL6	ZNF331
BMPR1A	CXCR7	ETV1	GOLGA5	KL	MYCN	PER1	SCD	TET1	ZNF384
BRAF	CYLD	ETV4	GOPC	KLF6	MYD88	PHF13	SDC4	TET2	ZNF521
BRCA1	C15orf65	ETV5	GPC3	KLK2	MYH11	PHF6	SDHAF2	TFE3	ZRSR2
BRCA2	C20orf112	ETV6	GPHN	KRAS	MYH9	PHOX2B	SDHB	TFEB	
BRD3	C2CD3	EVI1	H3F3B	KTN1	MYO1F	PICALM	SDHC	TFG	
BRD4	C2orf44	EWSR1	HERC1	LAMC3	MYST3	PIK3C2B	SDHD	TFPT	
BRIP1	CAMTA1	EXT1	HERPUD1	LASP1	MYST4	PIK3CA	SEPT11	TFRC	
BTG1	CANT1	EXT2	HEY1	LCK	NACA	PIK3R1	SEPT2	THRAP3	

3.3 Sequence data analyses, variant classification and confirmations

Variants were functionally annotated using Ensemble¹⁰⁹. To differentiate known and putative leukemia driver mutations from known germline polymorphisms, all variants listed in the National Center for Biotechnology Information Short Genetic Variations database (dbSNP, version 138)¹¹⁰ were eliminated. We also eliminated variants with SNP annotation from version 142 that were not reported in the catalogue of somatic mutations in cancer (COSMIC)¹¹¹. We then included variations in positions confirmed to have somatic mutations from all TCGA cohorts¹¹² with a non-tumor control sample (Acute Myeloid Leukemia, Ovarian serous cystadenocarcinoma, Rectum adenocarcinoma, Colon adenocarcinoma) and variants that were labeled pathogenic. Finally, all variants presented have a minor allele frequency (MAF) <0.01 according to the 1,000 genomes project¹¹³.

Artifacts of the sequencing procedure were analysed by submitting to the same NGS procedures 9 DNA samples from the bone marrow of healthy donors and 5 DNA samples collected from AML patients in remission. For bone marrow samples of healthy donors, mononuclear cells were isolated using Ficoll (Ficoll-Paque™ PLUS, GE Healthcare, USA) and CD34⁺ cells were then sequestered using CD34 Microbead Kit (MACS® Miltenyi Biotec, Germany), according to the manufacturer's instructions. Using the same protocol for DNA extraction, library preparation and analytical pipelines the data from these samples were retrieved. In this way, several molecular alterations deemed to be assay specific artifacts due to their recurrent presence in this samples (and high frequencies in the cohort samples >50%) were recognize and eliminated.

All remaining positions were manually curated in the Integrative genomics viewer^{114,115} to guaranty provenience from trustable mapping. Genes that bear many fragments with noise or unknown mutations that were exclusively found in the tips of fragments were either investigated or straightly removed, depending on the quality of the mapping in the region.

Furthermore, we did several assessments of false discovery rate (FDR) by parallel techniques: using PCR followed by Sanger sequencing, routine diagnosis data and whole-exome data. We designed primer pairs for PCR amplification and sequenced 85 reactions with a Sanger technique (LGC Genomics GmbH) to check several uncertain mutations (either known or unknown). For example, we confirmed some mutations that are rare (*ASXL1* p.Gly646TrpfsTer12 and p.Ser689Ter, *APOB* p.Ser2429Leu, *DAB2IP* p.Thr11Ile; *EP300* p.Asn2209_Gln2213del, *ERCC2* p.Val476Ile and p.Gln662Ter; *FAT2* p.Asp1294Asn; *FAT3* p.Ile3265Thr; *MYST3*

p.Arg256Gln; *NSD1* p.Tyr1971Cys; *TET2* p.Arg544Ter, p.Arg1359Ser and p.Tyr1649Cys) and others unknown (*APC* p.Val569Met and p.Gln1303Lys, *APOB* p.Pro2620Ser, *BRCA2* p.Asp635Glu and p.Gln1595Pro, *FAT1* p.Ala4190Thr and p.Val4532Ile; *MYST3* p.Pro1003Ala; *NSD1* p.His390Gln; *TET2* p.Gln1652Ter, p.Gln1526Ter, p.Gly1391Val and p.Asn1387Ser). We also used Sanger sequencing to access the frequency of *NPM1c*, a known mutation in a place suspected to have suffered from bad coverage. In this case, 19 *NPM1c* were detected by sequencing 92 samples (Appendix A).

These refined filtering criteria had previously allowed us to keep true positive calls in a confidence of at least 95%¹¹⁶. After these methodologies, we were confident of having removed germline and unreliable mutations to keep FDR between 4-7%.

Finally, results were analysed with R software and Gitools¹¹⁷. Mutation data was deposited in NCBI's Sequence Read Archive (SRP089816).

3.4 Functional categorization of mutated genes

A protein functional interaction network was constructed with the Cytoscape 3.2.1¹¹⁸, using the Reactome FIViz app¹¹⁹ for gene set/mutation analysis to obtain a subnetwork of proteins affected (using genes mutated more than once and without linkers). The sub-network created was further clustered with a spectral partition based network clustering algorithm¹²⁰ into sub-networks (modules). Pathway and GO term enrichment analysis of the modules included modules with two or more genes, using FDR<0.05, on the several sources of pathway annotation available (KEEG, CellMap, Reactome, NCI PID, Panther, and BioCarta).

3.5 Correlation studies of mutated genes

Correlations between molecular alterations and/or other molecularly/clinically defined groups were calculated using Pearson correlation and significance was determined with Fisher exact tests or Mann-Whitney U test (for dichotomous and continuous variables respectively). The mutual exclusivity for gene pairs was analysed with CoMEt exact test¹²¹ in R. Larger sets of genes patterns were analysed with Gitools¹¹⁷ using the MutEx algorithm with 10,000 permutations.

3.6 Statistical analysis of overall survival

Overall survival (OS) analysis was performed in R using the survival package, with event defined as death by any cause or time censored at last follow-up. Differences between groups were tested with unadjusted Kaplan-Meier curves using

log-rank tests. Hazard ratios were estimated from Cox proportional hazard regression, used to evaluate the independent effects of covariates. Univariate, covariate and multivariate analysis were evaluated for Cox proportionality.

3.7 DNA methylation profiling

For DNA methylation assessment we used the Infinium® HumanMethylation450 BeadChip platform (Illumina Inc, CA, USA), reported to have high coverage (with 99% of RefSeq genes covered across gene regions and 96% of CpG islands that include shelves and shores). The array was performed on the 80 DNA samples from the SAL cohort with sufficient material available. A bisulfite-converted DNA was amplified, fragmented and hybridized to the probes of the microarray according to the manufacturer's protocol. For analysis of the Infinium® HumanMethylation450 BeadChip data we used the IDAT files with result values of 273 samples together (194 of the TCGA and 79 of SAL), or the 80 SAL samples only in R software, which were homogenized using the `dasen` function (`wateRmelon` package^{122,123}). The DNA methylation fraction at each CpG is represented by the index of DNA methylation fraction, beta-values (β), calculated as $\beta = M/(M + U + \alpha)$, where M and U are methylated and unmethylated signal intensities and α is an arbitrary offset to account for measurements of low values. The dbSNP-related CpGs with MAF>0.01 were filtered out and the beta values of methylation in sex-related positions CpGs were removed.

Density profiles of the beta and M-values (β -logit2 transformed) samples were reviewed (Figure 3.7.1A-D). Principal components of all methylation values were analysed to guarantee the removal of batch effects and outliers (PCA, Figure 3.7.1E).

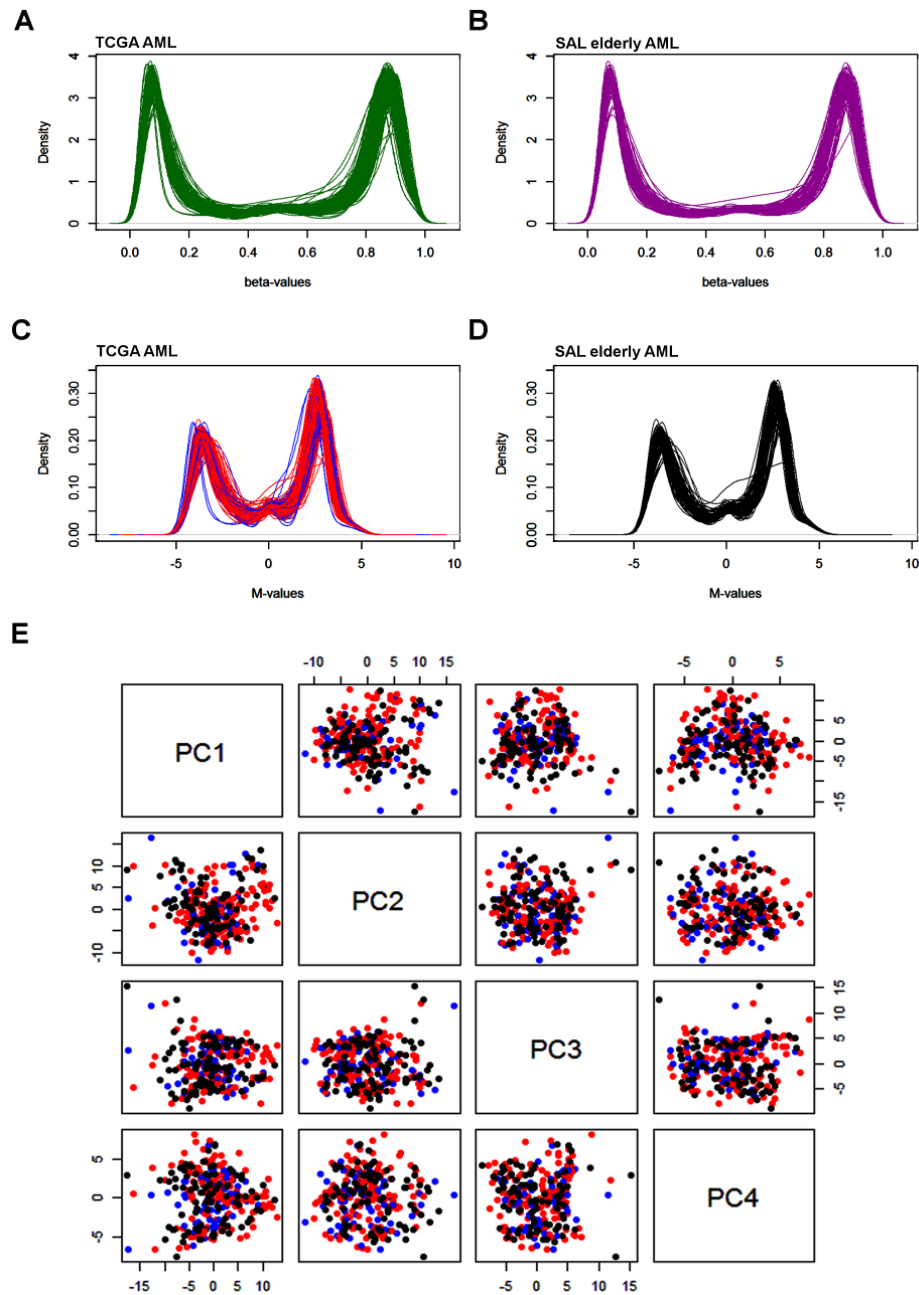


Figure 3.7.1 Representation of quality controls used for the integration of SAL and TCGA epigenetic data.

(A-D) Density plots that compare the distribution of methylation data from the TCGA and from the SAL cohorts. The first 2 graphics show β -values of the TCGA cohort (A, in green) and SAL cohort (B, in purple). The next 2 are representations of the corresponding M-values from the patients of TCGA cohort (C): young patients (less than 65y, in red) and elderly patients (65y or older, in blue) and from the SAL elderly cohort (D, 65y or older, in black). (E) Principal component plots for the first 4 components (which represent a good proportion of the variation). The plots show the homogeneity of the methylation data after application of the dasen function. Batch effects could not be perceived either for TCGA young cohort (less than 65y, in red), for TCGA elderly patients (65y or older, in blue) or for the SAL elderly cohort (in black).

Several unsupervised hierarchical clustering of the samples with M-values were done, using an average linkage of the Euclidian distance performed in Gtools¹¹⁷. Annotations of CpGs localized at promoters were done according to the Illumina manifest, as was the division of high-dense and low-dense CpGs regions (PHANTOM annotation) and the relative position of CpGs to CG islands (shelves and shores). A *t*-test was used to analyse the distribution of ages in the methylation groups defined by hierarchical clustering.

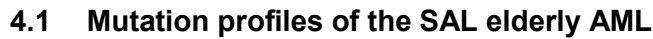
To determine differentially methylated regions (DMRs), we used R to apply 1000 permutations with the Bumphunter¹²⁴ algorithm and considered significant regions of $p\text{Area} < 0.05$, family-wise error rate $< 10\%$ and > 2 CpGs differently methylated. The functional significance was extracted from the resulting cis-regulatory regions and genes which are proximal (within 5kb upstream and 1kb downstream) and distal (up to 1000kb) extracted from the entire genome GRCh37/hg19 by the Genomic Regions Enrichment of Annotations Tool v 3.0.0 (GREAT)¹²⁵. These gene lists were analysed also using DAVID 6.7^{126,127} and results were considered significant for EASE scores with $\text{FDR} < 10\%$ and enrichment score of the respective cluster ≥ 1.3 . Specific genes/regions were plotted in R using the heatmapByChromosome function from the methyAnalysis package. Calculation of the overlap of DMRs with genes, gene promoters and transcription start sites (TSS) were reported as analysed in EpiExplorer¹²⁸. Positions of DMRs across the genome were plotted using the function plotKaryotype from the R package karyoploteR¹²⁹.

Array data was deposited and is accessible through NCBI's Gene Expression Omnibus (GSE86409).

3.8 Survival predictions from TCGA cohort gene expression profiles

We used the gene expression data from the TCGA cohort corresponding to the AML patients used in methylation. The TCGA RNA-seq dataset was used as processed by Pancan12¹³⁰, n=173, which is a log2-RSEM transformed and mean ranked matrix of 17,262 genes. The data were imported in R and for each gene a group of patients with gene expression lower than mean and another with equal or higher than mean was defined. The overall survival analysis performed was done following the implemented in the R package 'survival', with survival times given by time from diagnosis to the event (death from any cause) or censored at last follow-up. Differences between these groups were tested with unadjusted Kaplan-Meier curves using log-rank tests.

CHAPTER 4. RESULTS



A median number of 7 genes were mutated per patient (ranging 1 to 23 mutations per sample, Figure 4.1.2), most samples with at least one insertion or deletion and more than one SNV. We could not make comparisons of the rates of mutation in each patient to the reported average of 13 genes mutated per patient in the TCGA cohort. Therefore, we judged the median number of 7 genes mutated per patient to be reasonable, since our selection of 555 genes was biased for genes known to be mutated in AML and we had a cut off at VAF of 20%.

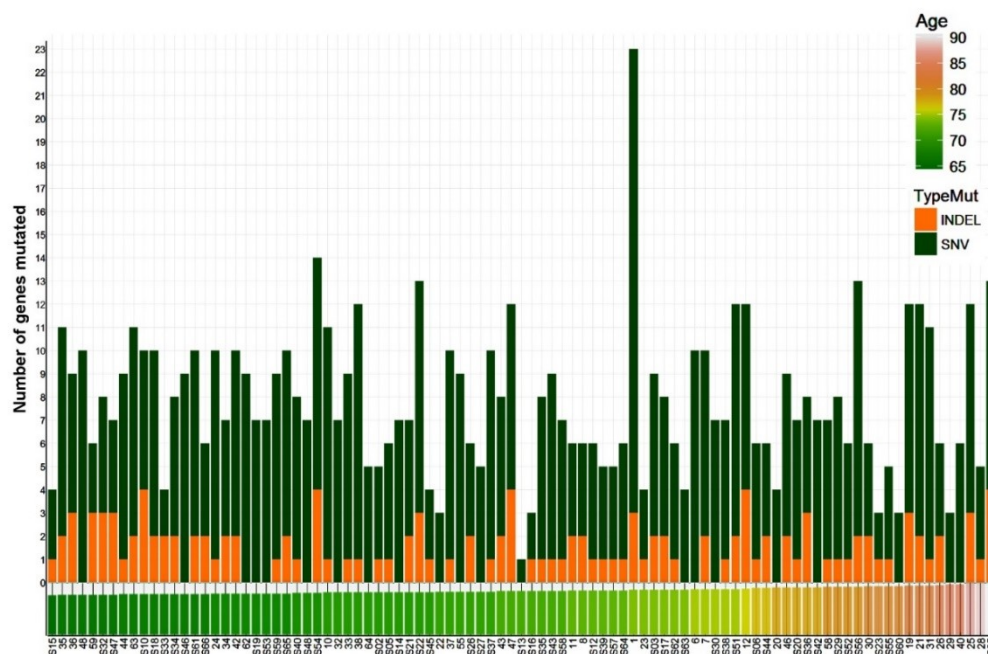


Figure 4.1.2 Frequencies of mutations in the SAL elderly AML for each patient.

The bar graph represents the number of genes mutated in each patient, organized by increasing patient age and annotated for the type of mutation found insertion or deletion (INDEL) or single nucleotide variation (SNV). The age of the patients at diagnosis is depicted by the heatmap code (in legend).

All patients had at least one mutation likely belonging to a major clone (in at least 37% of the tumor sample, as assessed by adjusted VAF), with exception of the patient with only 1 mutation (Figure 4.1.3A).

Furthermore, most of the altered genes displayed mutations of a possible founding clone, meaning adjusted VAF higher than the 37% (Figure 4.1.3B). The vast majority of the genes frequently mutated even showed a median adjusted VAF higher than the 37%. All of the genes with 3 or more mutations detected had at least one mutation belonging to a major clone, even if they seem to have a tendency for mutations with low VAF (for example *PDE4DIP*, see Figure 4.1.3B).

younger and older patients have different survival probabilities within the SAL cohort and within the TCGA cohort (Figure 4.1.5).

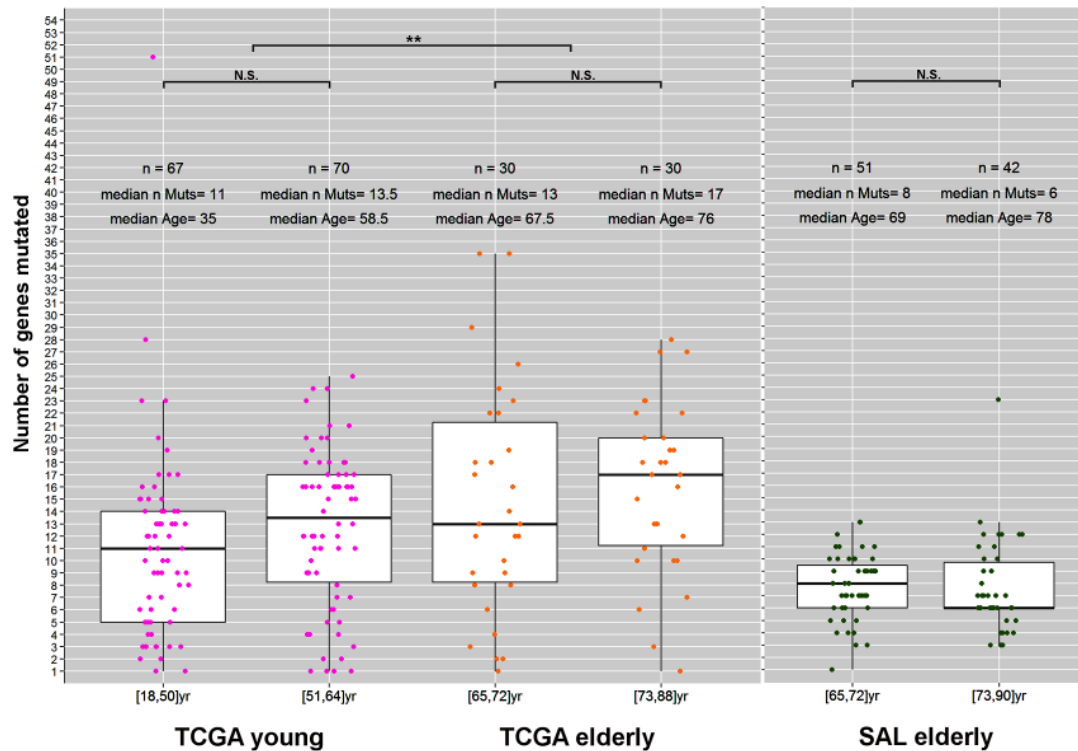


Figure 4.1.4 Rate of mutation of AML samples in the TCGA cohort and SAL cohort.

The boxplots show the number of genes mutated per sample found in TCGA cohort and in the SAL elderly cohort (including subdivisions of these into smaller age groups). The comparison depicts the increased number of genes with mutations from young patients (<65 years) to elderly (≥ 65 years), but not in further subdivisions of these TCGA groups (yr, years). The same was observed for the same subdivision of the SAL elderly cohort. Differences between groups were conducted with t-test analyses and are represented as N.S. non-significant and $**p \leq 0.01$. These were only accessed within each cohort due to the differences in the platforms of whole-exome of TCGA and our panel of exon sequencing.

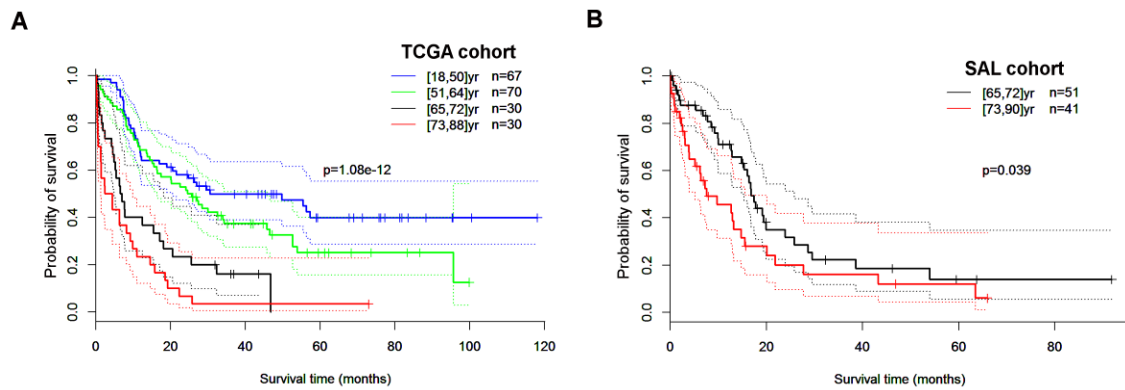


Figure 4.1.5 Survival analysis of AML patients in the TCGA cohort and in SAL cohort.

Kaplan-Meier curves show estimations of the overall survival of TCGA cohort (A) and of the SAL elderly cohort (B). The graphs show the differential outcome for the subdivisions of young (<65 years, yr) and elderly patients (≥65 years) into smaller age groups according to the median ages of 50y in young and 72y in elderly. Statistics were calculated with the log-rank test and the dotted lines mark the 95% confidence bounds of each curve.

In general, thirty-one genes were frequently mutated in the SAL elderly AML, as they were mutated in more than 5% of patients (Figure 4.1.6). The most frequently mutated genes were: *DNMT3A* 33.3%, *TET2* 25.8%, *SRSF2* 22.6%, *ASXL1* 21.5%, *RUNX1* and *IDH1* 17.2%, *NPM1* 16.1%, *IDH2* 10.8% (Figure 4.1.6).

Of note, we identified novel non-recurrent aberrations in previously reported cancer driver genes encoding proteins of the PI3K/mTOR pathway (PIK3CA, PIK3C2B, MTOR) and DNA damage proteins (BRCA2, ERCC2, FANCC).

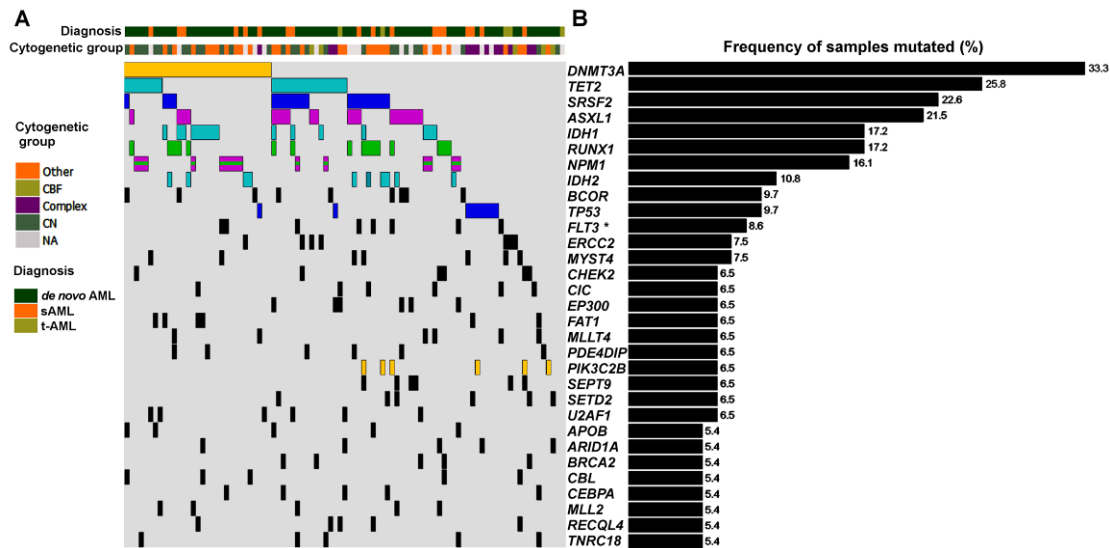


Figure 4.1.6 Recurrently mutated genes in the SAL elderly AML.

(A) Representation of mutations in genes (mutated in 5 or more samples) with patients represented in vertical and classified by cytotenetic groups. Classification of complex was defined for samples with 3 or more cytotenetic abnormalities (n=12, Complex), core binding factor included samples with t(8;21) or inv(16)/t(16;16) (n=5, CBF), samples with no cytotenetic abnormalities were designated cytotenetically normal (n=28, CN), others were samples with 1 or 2 cytotenetic abnormalities (n=30, other) and some were not available (n=18, NA). (B) The frequency of mutations in the genes was given in bars depicting the percentage of samples in the cohort with a mutation in the gene. Reporting NGS results only, not accounting for the *NPM1c* found only by Sanger sequencing and *FLT3 ** refers to SNV not *FLT3*-ITD from the clinical data (in Table 3.1.1). Different colors mark pairs of genes with mutual exclusion: *NPM1* vs *ASXL1* (p=0.01, pink) and *NPM1* vs *RUNX1* (p=0.02, green), *IDH1* vs *IDH2* vs *TET2* (p=0.003, light blue), *DNMT3A* vs *PIK3C2B* (p=0.04, yellow), *SRSF2* vs *TP53* (p=0.04, blue). Adapted from Silva *et al.* 2017¹.

4.1.1 Frequently mutated epigenetic regulators

The frequency of mutations in epigenetic regulators was particularly high in the SAL elderly AML and affected 85% of patients (Figure 4.1.7). These mutations affected 30 genes that encode proteins belonging to several epigenetic protein families.

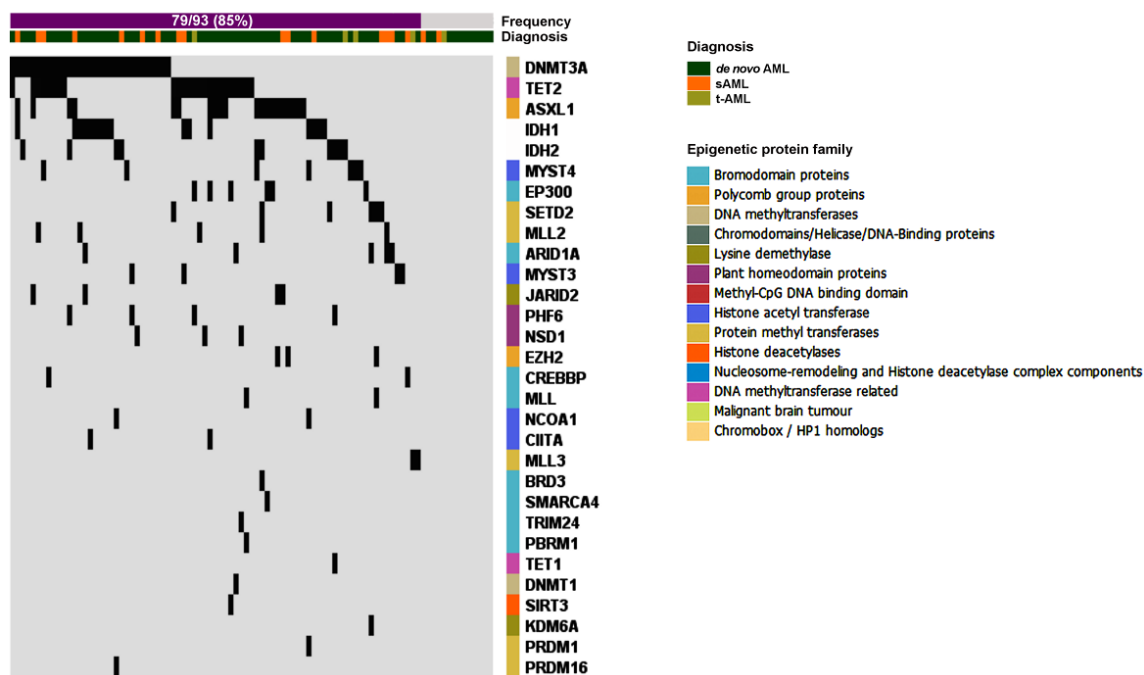


Figure 4.1.7 Mutations in epigenetic regulators in elderly AML.

Depiction of mutations found in epigenetic regulators with patients represented in vertical and genes classified into their protein families (sorted by co-exclusivity patterns). Patients were labeled with information collected at diagnosis as *de novo* AML (n=70), sAML (n=18) and t-AML (n=5). The frequency of patients with at least one of these genes mutated (in the bar) was calculated with the number of mutated/total number of patients (%). As presented in Silva *et al.* 2017¹.

Frequencies of mutations in *DNMT3A*, *TET2*, *ASXL1*, and *IDH1* were higher in the SAL elderly AML than previously reported for the general AML population^{35,37,38,39,131}. In agreement with this result, in the TCGA young group (18 to 64 years old) we found 51% of samples with at least one mutation in an epigenetic regulator, while in the TCGA elderly group (65 to 88 years old) these mutations were present in 67% of samples (Figure 4.1.8).

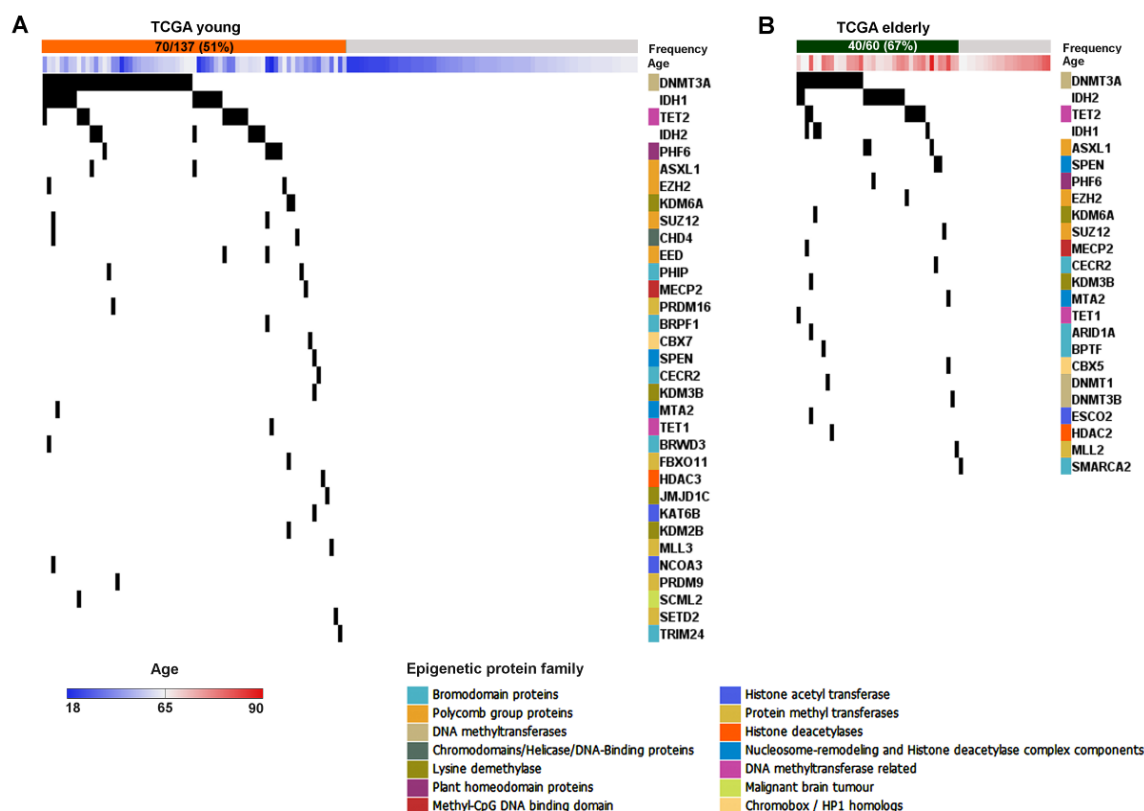


Figure 4.1.8 Epigenetic regulators mutated in TCGA elderly and TCGA young AML groups.

Representation of somatic mutations in 33 epigenetic regulators present in the TCGA young AML patients (A, n=137, <65 years) and 24 epigenetic regulators present in the TCGA elderly AML patients (B, n=60, patients ≥65 years). The frequency of patients with at least one of these genes mutated (in the bar) was calculated with the number of mutated/total number of patients (%). Genes were classified into their protein family and patients' ages were represented in heatmap code (in legend). As presented in Silva *et al.* 2017¹.

DNMT3A had the highest mutation frequency in our elderly AML cohort (33.3%) and has been previously reported to be mutated in 23-28% in other cohorts^{37,39}. In addition, the incidence of *ASXL1* mutation with 21.5% (20/93) was much higher than the reported 3-6%^{37,39,132}. A high rate of molecular alterations was observed for *IDH1/2* with a combined frequency of 28.0% (26/93). Of the 26 *IDH* mutations, 57.7% were *IDH1* R132 (15/26), 30.8% were *IDH2* R140 (8/26) and 8.3% were *IDH2* R172 (2/26). As expected molecular alterations in *IDH1* and *IDH2* were mutually exclusive and mutually exclusive with *TET2* (p=0.003, Figure 4.1.6). *TET2* mutations also showed a high mutation rate of 24% in elderly AML patients compared to the reported rate of 8-10% in other cohorts^{37,39}.

4.1.2 High rate of mutations in splicing proteins

We found frequent alterations in five genes of splicing factors including *SRSF2*, *U2AF1*, *SF3B1*, *ZRSR2*, and *DDX5*, affecting 38% of the AML elderly patients (Figure 4.1.9A). These are in a mutually exclusive manner ($p=0.015$), consistent with previous reports suggesting that these mutations elicit similar phenotypes^{133,134}. Although most of these molecular alterations have been reported in MDS^{133,135}, in AML they have been reported only at low rates¹³³ (Figure 4.1.9B).

Strikingly, 22.6% of the SAL elderly AML patients (21/93) harbored *SRSF2* mutations (all alterations in residue P95), higher than the 8.3% or 10% recently reported in age unselected cohorts^{38,39}. Thus, elderly AML had a distinct pattern of molecular alterations in splicing factors when compared to other AML entities such as *de novo* AML or sAML (Figure 4.1.9B), being present in patients with no clinical history of MDS.

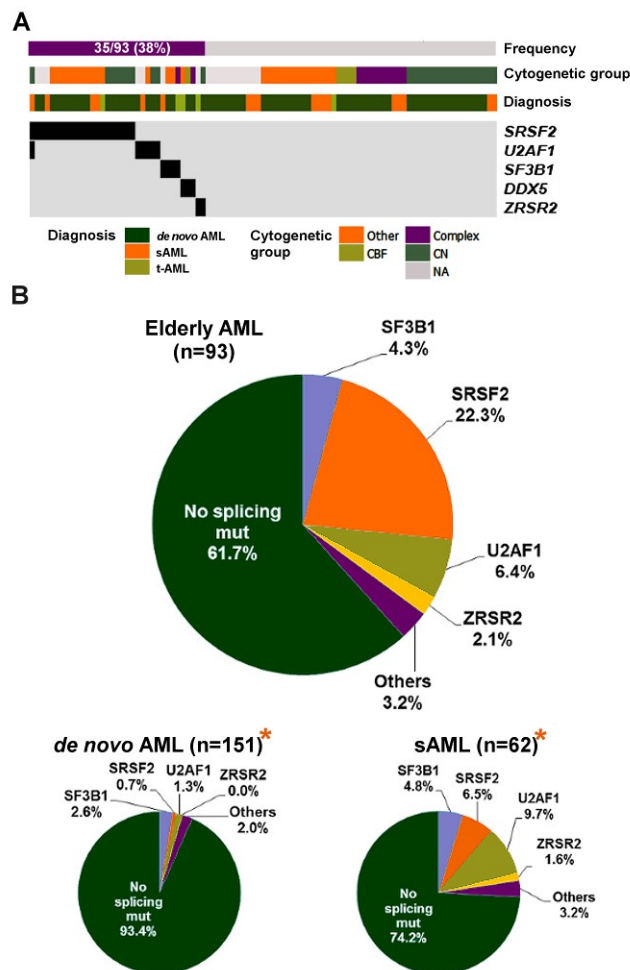


Figure 4.1.9 Frequency of mutations in splicing factors.

(A) Illustration of mutations found in splicing factors with patients represented in vertical and genes in horizontal sorted by co-exclusivity ($p=0.015$). Patients were labeled with information collected at diagnosis as *de novo* AML ($n=70$), sAML ($n=18$) and t-AML ($n=5$). The cytogenetic groups were defined as: cytogenetically normal (CN), core binding factor (CBF), Complex (3 or more cytogenetic abnormalities), or other (1 or 2 cytogenetic abnormalities). The frequency of patients with at least one of these genes mutated (in the bar) was calculated with the number of mutated/total number of patients (%). Fisher exact tests (two-sided) were performed to compare cytogenetic and diagnostic characteristics of groups with and without mutations in splicing factors: no significant difference was observed for the characteristics. (B) Pie charts compare the percentage of alterations on splicing factors in elderly AML to other reported AML entities (*de novo* AML and sAML to a myelodysplastic syndrome, * data from Yoshida *et al.* 2011¹³³). As presented in Silva *et al.* 2017¹.

The patients with these mutations did not present significant enrichments in particular patient diagnostic, cytogenetic or phenotypic characteristic that we could determine (Table 4.1.1).

Table 4.1.1 Description of the clinical characteristics of patients with mutations in splicing components.

The table reports the p-values from the Fisher tests (two-sided) performed for each characteristic between the two groups of patients (with and without mutations in splicing components). We classified patients using cytogenetic and diagnostic characteristic, as well as with the available data on the presence of at least one type of myelodysplastic features (megakaryocytic, granulocytic or erythroid dysplasia), which was termed as dysplasia, Dys. Patients were divided as: *de novo* AML, secondary AML (sAML), or therapy-related AML (t-AML). The cytogenetic groups were defined as: cytogenetically normal (CN, no detected cytogenetic abnormalities), core binding factor (CBF, includes t(8;21) or inv(16)/t(16;16)), Complex (3 or more cytogenetic abnormalities), or other (1 or 2 cytogenetic abnormalities).

Group	Mutations in splicing regulators	No mutations in splicing regulators	All	P-value
Diagnosis				
n	35	58	93	
<i>de novo</i> AML, no. (%)	25 (71)	45 (78)	70 (75)	0.72
sAML, no. (%)	6 (17)	12 (21)	18 (19)	0.79
t-AML, no. (%)	4 (11)	1 (1.7)	5 (5)	0.06
Cytogenetic				
CN, no. (%)	10 (36)	18 (38)	28 (37)	0.90
CBF, no. (%)	1 (3.6)	4 (8.5)	5 (6.7)	0.64
Complex, no. (%)	2 (7.1)	10 (21)	12 (16)	0.19
Others, no. (%)	15 (54)	15 (32)	30 (40)	0.09
Dysplasia				
n	17	32	49	
Dys, no. (%)	10 (59)	19 (59)	29 (59)	1.00
No Dys, no. (%)	7 (41)	13 (41)	20 (41)	

4.2 Genetic alterations associated with elderly AML

Overall, several gene mutations appeared to have an age dependency in SAL elderly AML due to high or low frequencies when compared to AML reports for age unselected cohorts³⁷. The associations between age and genetic alterations were made clear not only in our cohort but also in two other studies from Metzeler and colleagues³⁸ and Eisfeld and colleagues³⁴.

Therefore, we compared the frequency of mutations in the SAL elderly cohort (median age of patients was 72 years old) with the other 4 younger groups of patients from these 2 reports (Figure 4.2.1). Several tendencies for increased or decreased frequency of mutations with the groups' age became apparent in this analysis. Known mutations with strong correlations to WHO defined AML groups with adverse prognosis have higher frequencies with increasing age (*RUNX1*, *TP53* and *ASXL1*). In contrast, mutations that are correlated to WHO defined groups of favorable prognosis were less frequent in the older groups of patients (*NPM1* and *CEBPA*).

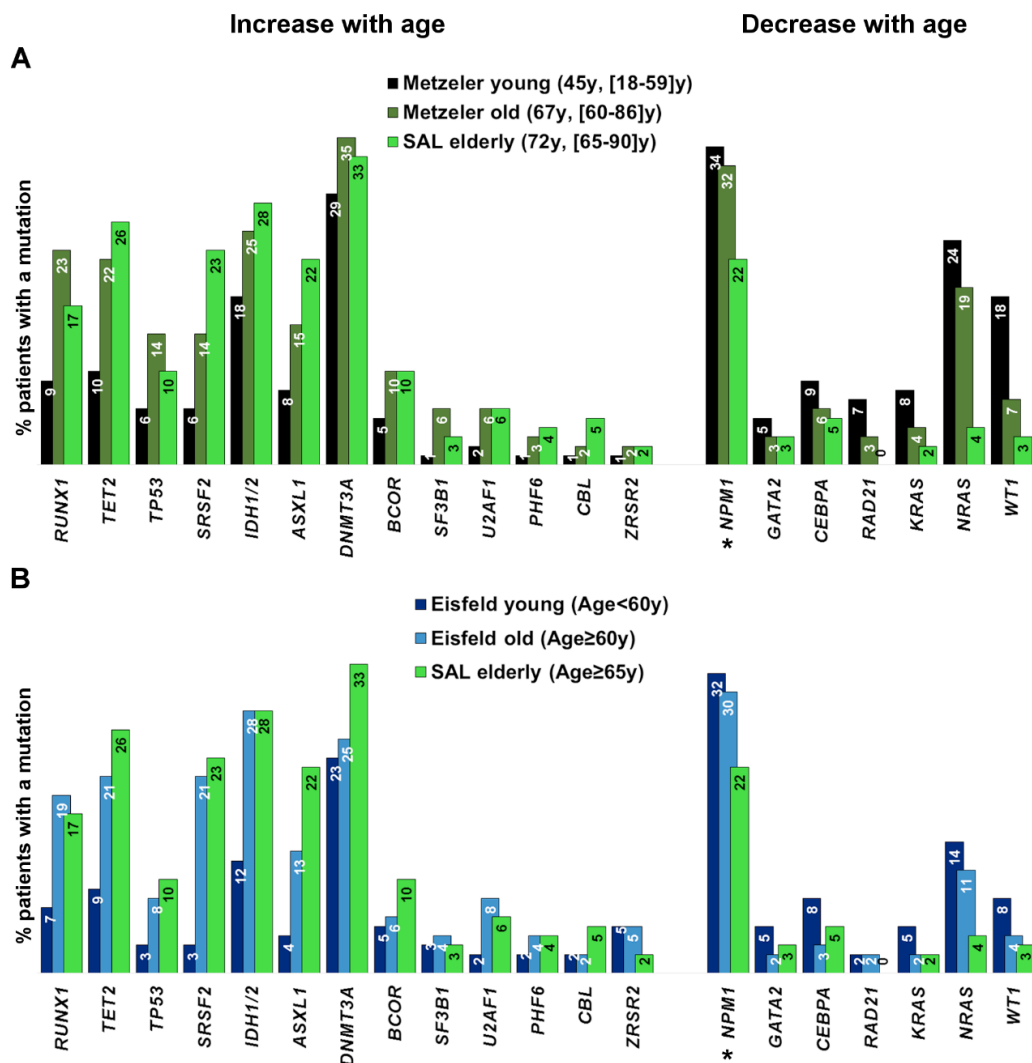


Figure 4.2.1 Mutation rates in the SAL elderly AML compared to mutation rates reported in two other cohorts.

Graphic representation of frequencies of mutations in genes, which have previously been associated with age. The frequencies obtained by gene panel approaches reported by (A) Metzeler *et al.*³⁸ (black and dark green, n=376 and n=288 respectively) and by (B) Eisfeld *et al.*³⁴ (dark and light blue, n=1080 and n=523 respectively) were compared to the obtained for the SAL cohort (light green, n=93). The legend shows the age restriction of each cohort with median and range of the ages in parenthesis when available. * In the SAL elderly AML *NPM1* rate is stated as the combined estimation of frequency of 22% (from correlation to Sanger results and retrieval from NGS detections with low coverage). Adapted in part from Silva *et al.* 2017¹.

4.3 Genetic heterogeneity in the SAL elderly AML

In the SAL elderly AML cohort, several combinations of genetic alterations originated genetically heterogeneous groups, similar to the ones found in age unselected AML cohorts.

Different mutational profiles were noticeable as the occurrence of several mutations does not appear to be random (Figure 4.1.6A). For instance, in spite of the general increase of mutations in epigenetic regulators and splicing factors, groups of patients with distinctive mutational patterns can be described. This could be seen by the co-exclusivity of patients with mutations in *IDH1* vs *IDH2* vs *TET2* ($p=0.003$) and *SRSF2* vs *TP53* ($p=0.04$). In the same way, in spite of the many *ASXL1* (21.5%) and *RUNX1* (17.2%) mutations, these were not present in patients with *NPM1* mutations. Furthermore, mutations in *TP53* were related to samples of complex karyotype, with 7 co-occurrences out of the 9 *TP53* mutated patients and out of the 12 complex karyotype samples (Pearson's correlation 0.63 ± 0.08).

To further study genetic particularities of subgroups of elderly AML we obtained the survival data of several groups within the cohort. The expectation was that groups of patients with alterations in genes used to classify patients as adverse prognosis in other cohorts would also show poor survival in elderly AML. However poor prognosis within the elderly cohort could only be obtained for the group of patients with complex karyotype vs all others (log-rank $p=5.27\times10^{-6}$) or *TP53* mutated vs all others (log-rank $p=1.2\times10^{-3}$). The other genes (and combinations) that have prognostic implications in other cohorts did not have differential survival probabilities in the SAL elderly AML. The mutations in *ASXL1* and *RUNX1* or even *DNMT3A/NPM1* combinations would be expected to be prognostic predictors in our cohort and were not. This was curious because the cohort had a relatively good median survival of 15 months (considering the patient's ages) and 79% of patients were treated with intensive chemotherapy regimens (Table 3.1.1).

On the other hand, the prognostic value of white blood cell count was still seen within the SAL elderly cohort. High WBC counts were indicators of poor prognosis for patients with values 35/nL or higher (Figure 4.3.1A). These groups with different WBC counts, the smoldering group ($WBC<35/nL$) or proliferative group ($WBC\geq35/nL$) correlated to specific molecular marker contexts. Namely, *NPM1* and *FLT3* mutations (odds 0.069 ± 0.001 and odds 0.23 ± 0.06 , respectively) were almost specific of the proliferating group, as *IDH1* (odds 11.3 ± 1.6) mutated samples were of the smoldering group (Figure 4.3.1B).

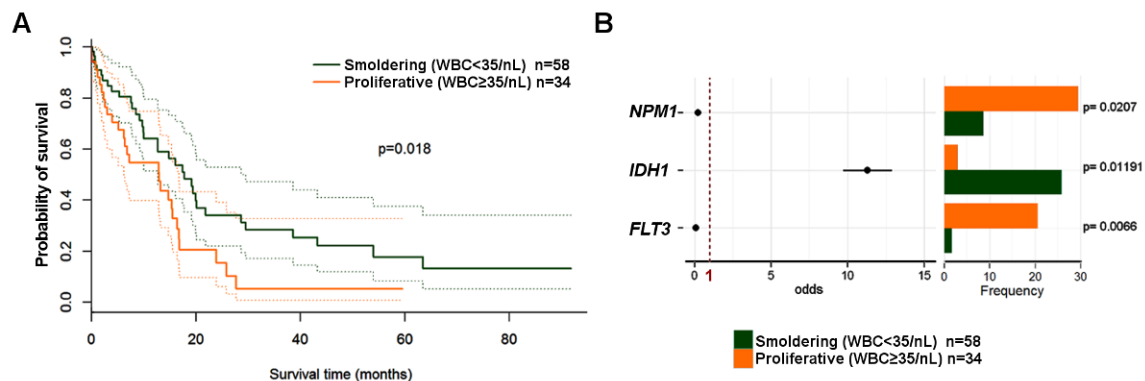


Figure 4.3.1 Mutations correlated to SAL elderly AML groups that were defined by WBC counts of prognostic relevance.

(A) Kaplan-Meier curves display the estimation of the overall survival for the division of the SAL elderly AML cohort into 2 groups, classified according to WBC counts at diagnosis into smoldering (lower than 35/nL) or proliferative (35/nL and higher). A significant difference between overall survivals was calculated with the log-rank test and dotted lines mark the 95% confidence bounds. (B) The odds ratio represents the skewness of mutation frequency in the SAL elderly groups smoldering versus proliferative (with odds 1 marked with dotted line). The corresponding frequency of mutations in each gene is plotted in horizontal bars, representing the % of mutated samples of each group. The p-values were calculated for the proportions of each gene in groups with Fisher exact tests corrected for the 281 genes mutated.

4.4 Protein networks and pathways of SAL elderly AML

To describe this complex molecular heterogeneity, we constructed a Reactome functional interaction (FI) network with the 139 genes that were mutated in more than one patient in the cohort. The network clustering algorithm identified highly interacting groups of proteins, establishing 8 different sub-networks (modules, Figure 4.4.1A). The four most prominent modules included 72 altered proteins and nearly every sample of the cohort (90 of 93). Module 1 was composed of NPM1 and mRNA processing proteins (RNA splicing and transport proteins), while Module 2 was composed of DNMT3A and DNA repair proteins. In turn, Module 3 was comprised of RUNX1, ASXL1 and other transcription factors (included prominent pathways NOTCH and WNT signaling), while Module 4 was formed by known oncogenes like FLT3 and KRAS/NRAS (mainly proteins with kinase activity, which included FGFR signaling molecules and the PI3K-AKT signaling pathway). Other modules were small and included BCOR, FAT proteins, and components of the mTOR signaling pathway.

4.4.1 Molecular patterns of mutations in mRNA processing and DNA repair proteins

Alterations in NPM1/mRNA processing (Module 1) and in DNMT3A/DNA repair proteins (Module 2) were spread across the cohort ($p=0.004$) and affected the majority of the patients 86% (80/93). Furthermore, alterations were mutually exclusive within each module: NPM1/mRNA processing ($p=0.011$) and DNMT3A/DNA repair proteins ($p=0.052$).

In addition, alterations in the two modules classified patients into four groups (Figure 4.4.1B): patients with mutations only in NPM1/mRNA processing proteins (Group A), patients with mutations in both the modules (Group B), patients with mutations only in DNMT3A/DNA repair proteins (Group C), and patients lacking any mutation in these modules (Group D). Patients of Group C ($n=25$) showed an inferior outcome, with a median OS of only 9 months, compared to patients with other mutation patterns (non-Group C, $n=67$, median OS 17 months, Figure 4.4.1C).

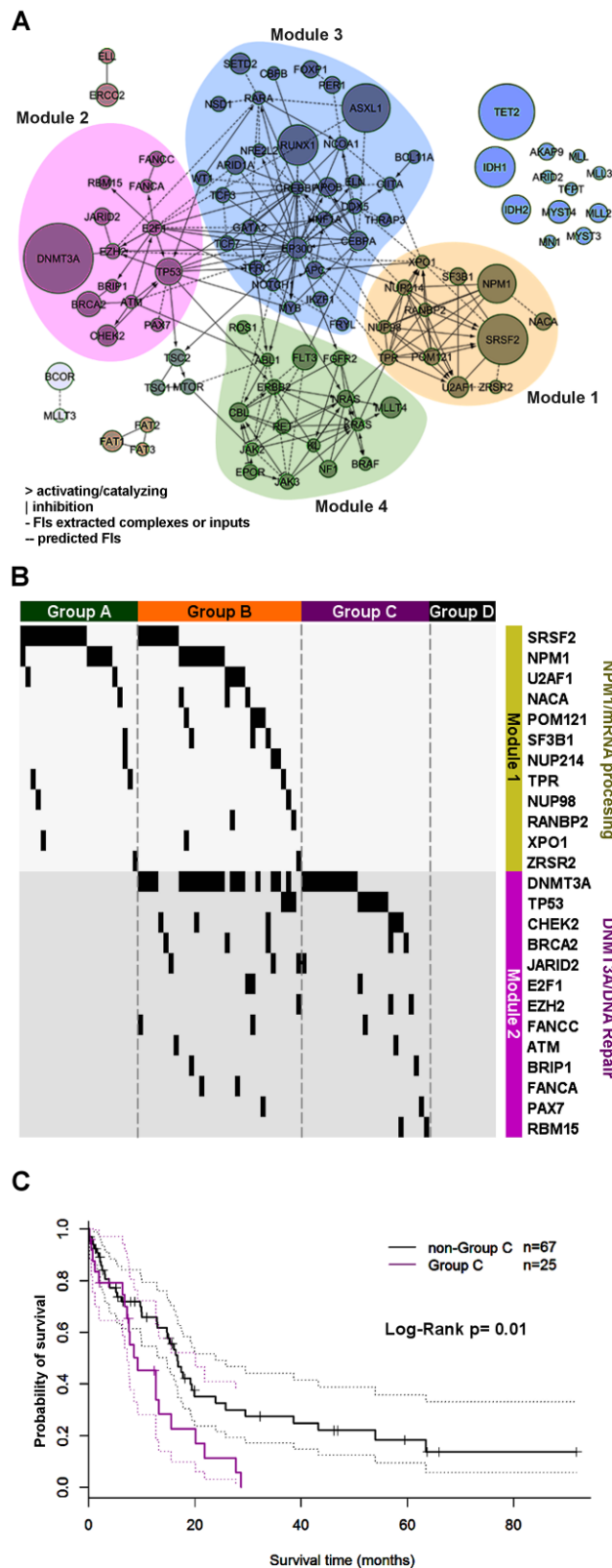


Figure 4.4.1 Reactome functional interaction network of altered proteins.

(A) Pathways affected by mutations were analysed with a FI network of proteins that clustered into 8 modules with 82 proteins. The 4 major modules were labeled as Module 1 (light green), Module 2 (pink), Module 3 (blue) and Module 4 (green). Some of the proteins that did not cluster in the FI network are also represented (light blue). The nature of the interactions is in the legend. (B) Representation of the division of the 93 AML into groups of samples with mutations in Module 1, in both Modules 1 and 2, only Module 2, or none of these modules (respectively Group A-D). (C) Kaplan-Meier estimation of the overall survival ($n=92$) showed the poor outcome of patients in Group C (log-rank test). Dotted lines mark the 95% confidence bounds. As presented in Silva *et al.* 2017¹.

This was a tendency denoted in the survival curves of the four groups (Figure 4.4.2A). Apart from the genetic characteristics, Group C did not show enrichment of cytogenetic or clinical characteristics that could define it and be correlated to survival (Table 4.4.1).

Table 4.4.1 Characteristics of the groups defined by the Reactome functional interaction network analysis in the SAL elderly AML.

The table shows the clinical and molecular characteristics for the subgroups A, B, C, D within the Modules 1 and 2 (see Figure 4.4.1). The cytogenetic groups were defined as: cytogenetically normal (CN), core binding factor (CBF), complex (3 or more cytogenetic abnormalities), or other. Diagnosis were grouped by: *de novo* AML, secondary AML (sAML), or therapy-related AML (t-AML). Treatment regimens included standard intensive chemotherapy (induction treatment with 7+3 and high dose Ara-C consolidation), allogeneic stem cell transplantation (alloSCT), palliative (low dose Ara-C or hypomethylating agents) or best supportive care (BSC). The response was evaluated for patients receiving intensive induction chemotherapy, and relapses are shown for patients that had achieved a remission. Abbreviations used: white blood cell counts (WBC), Lactate dehydrogenase (LDH), bone marrow (BM). * The p-values were calculated by Fisher tests for the comparison of patients in Group C vs the remaining patients. As presented in Silva *et al.* 2017¹.

Group	A	B	C	D	All	P value*
Clinical characteristic						
n	23	32	25	13	93	
Age at diagnosis (y), median (ranges)	72 (66-86)	70 (65-90)	74 (66-88)	72 (69-80)	72 (65-90)	0.38
WBC (/nL), median (ranges)	26.2 (0.91-189.0)	14.9 (1.30-127.5)	10.2 (0.86-209.6)	14.7 (1.00-160.8)	14.8 (0.9-210)	0.56
LDH (U/L), median (ranges)	412 (138-3340)	402 (144-2015)	388 (161-4219)	516 (169-1482)	406 (138-4219)	0.97
BM Blasts, % (ranges)	82 (30-99)	74 (45-95)	74 (25-99)	72 (25-99)	75 (25-99)	0.19
Diagnosis						
<i>de novo</i> AML, no. (%)	18 (78)	23 (72)	18 (72)	11 (85)	70 (75)	0.79
sAML, no. (%)	3 (13)	7 (22)	7 (28)	1 (8)	18 (19)	0.24
t-AML, no. (%)	2 (8.7)	2 (6.2)	0 (0)	1 (8)	5 (5)	0.32
Cytogenetic						
n	16	26	21	11	75	
CN, no. (%)	5 (31)	13 (50)	7 (33)	3 (27)	28 (37)	0.79
CBF, no. (%)	0 (0)	0 (0)	2 (9.5)	3 (27)	5 (6.7)	0.62
Complex, no. (%)	0 (0)	5 (19)	5 (24)	2 (18)	12 (16)	0.30
Others, no. (%)	11 (69)	8 (31)	7 (33)	4 (36)	30 (40)	0.67
Treatment						
n	21	31	25	13	90	
BSC or Palliative, no. (%)	4 (19)	7 (23)	7 (28)	1 (7.7)	19 (21)	0.39
Intensive Chemotherapy	17 (81)	24 (77)	18 (72)	12 (92)	71 (79)	
[no. alloSCT]	[2]	[6]	[1]	[2]	[11]	
Response to induction						
n	17	23	18	12	70	
Refractory, no. (%)	6 (35)	7 (30)	8 (44)	3 (25)	24 (34)	0.39
Remission, no. (%)	11 (65)	16 (70)	10 (56)	9 (75)	46 (66)	
[no. relapses]	[8]	[10]	[8]	[5]	[31]	0.46

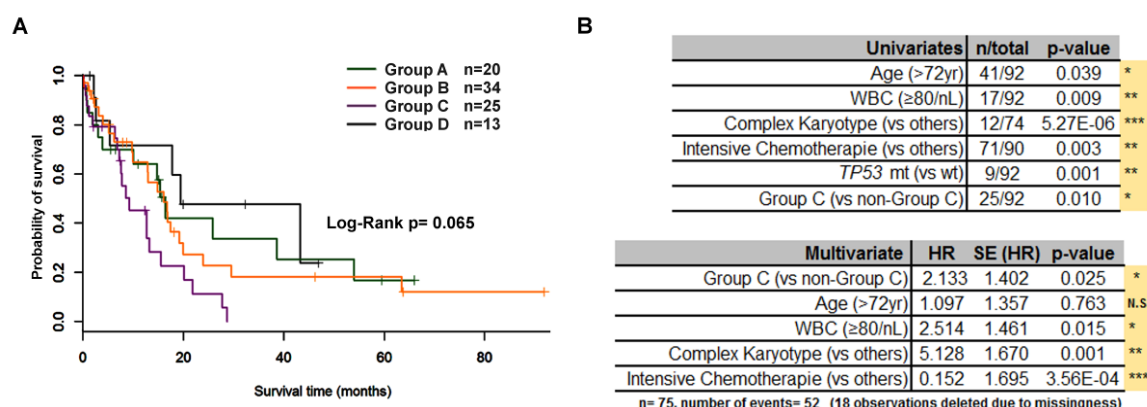


Figure 4.4.2 Overall survival of the groups defined by the Reactome functional interaction network analysis in the SAL elderly AML.

(A) The Kaplan-Meier displays the estimation of the overall survival for the division of the SAL cohort into Group A, B, C and D using Modules 1 and 2 (see Figure 4.4.1; $n=92$). (B) The first table reports on all the factors with a significant effect on overall survival probability for the elderly AML cohort (univariates log-rank tests with $p \leq 0.05$). The second displays a multivariate analysis for all independent factors found for the SAL elderly AML (*TP53* mutations were not independent of complex karyotype). Hazard ratios (HR) were calculated with Cox's proportional hazard model. SE denotes standard error, N.S. is non-significant, * $p \leq 0.05$, ** $p \leq 0.01$, *** $p \leq 0.001$ and WBC denotes white blood cell count. As presented in Silva *et al.* 2017¹.

The prognostic significance of Group C was maintained when the analysis was restricted to patients that received intensive chemotherapy and in a multivariate analysis, the mutation profile of Group C was of independent adverse prognostic relevance (Figure 4.4.2B).

Importantly, using the TCGA cohort the prognostic significance of Group C could be confirmed (Figure 4.4.3), despite the difficulties of group division posed by the undetected *SRSF2* mutations³⁹ and some clinical differences of the cohorts (Table 4.4.2).

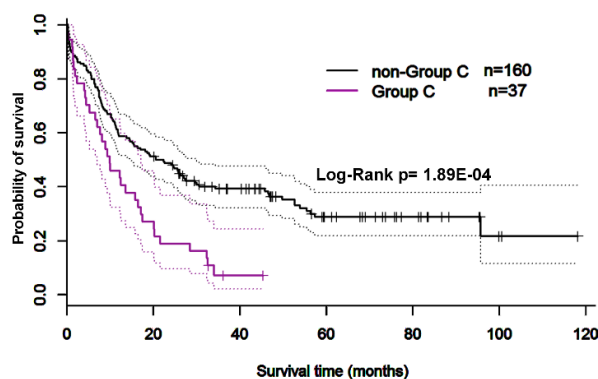


Figure 4.4.3 Overall survival of the groups defined by the Reactome functional interaction network analysis in the TCGA cohort.

Kaplan-Meier displays the estimation of the overall survival for the division of the TCGA cohort ($n=197$)³⁷ that showed the poor outcome of patients in Group C (log-rank test). Despite the age difference between our cohort (65 to 90 years) and the TCGA cohort (18 to 88 years) major clinical features and treatment characteristics were comparable. In both cohorts, the majority of patients were treated with standard intensive

chemotherapy resulting in a similar median survival time. To note, more patients went on to alloSCT in the TCGA cohort, as these included a younger patient population. Dotted lines mark the 95% confidence bounds. As presented in Silva *et al.* 2017¹.

Table 4.4.2 Characteristics of SAL elderly AML cohort compared to the characteristics of the TCGA cohort.

Summary of the characteristics of patients: de novo AML, secondary AML (sAML), or therapy-related AML

	SAL cohort n=93	TCGA cohort n=200
Clinical characteristics		
Age at diagnosis (y), median (ranges)	72 (65-90)	57 (18-88)
Sex (Male), no. (%)	47 (50.5)	108 (54)
de novo AML, no. (%)	70 (75)	200 (100)
sAML, no. (%)	18 (19)	0 (0)
t-AML, no. (%)	5 (5)	0 (0)
LDH (U/L), median (ranges)	406 (138-4219)	NA
WBC (/nL), median (ranges)	14.8 (0.9-210)	16.2 (0.4-298)
BM Blasts, % (ranges)	75 (25-99)	73 (30-100)
Cytogenetic		
CN, no. (%)	28 (37)	92 (47)
CBF, no. (%)	5 (6.7)	12 (6.2)
Complex, no. (%)	12 (16)	24 (12)
Other, no. (%)	30 (40)	46 (24)
PML-RARA, no. (%)	0 (0)	18 (9.2)
BCR-ABL1, no. (%)	0 (0)	3 (1.5)
Molecular data		
FLT3-ITD, no./total no. (%)	15/70 (21)	NA
NPM1c, no./total no. (%)	19/92 (21)	NA
Treatment		
Palliative or Best Supportive Care, no. (%)	19 (21)	38 (19)
Intensive Chemotherapy, no. (%)	71 (79)	161 (81)
[no. alloSCT]	[11]	[78]
Survival		
Median survival time (mon)	15	17
Follow up time (mon), median (ranges)	7.4 (0.1-92)	47 (20-118)

(t-AML). The cytogenetic groups were defined as: cytogenetically normal (CN), core binding factor (CBF, includes t(8;21) or inv(16)/t(16;16)), Complex (3 or more cytogenetic abnormalities), or other (1 or 2 cytogenetic abnormalities). Treatments included standard intensive chemotherapy or not (the latter consisted of palliative or best supportive care, which includes treatment with hypomethylating agents and a low dose of Ara-C). Several abbreviations were used: FLT3 internal tandem duplications (FLT3-ITD), mutations in nucleophosmin altering tryptophan residues in the C-terminus of the protein (NPM1c), white blood cell counts (WBC), Lactate dehydrogenase (LDH), bone marrow (BM), allogeneic stem cell transplants (alloSCT), months (mon) and years (y).

4.5 Specific DNA methylation pattern of the elderly AML

First, we explored whether age and the high frequency of alterations in epigenetic regulators affected global DNA methylation. Thus, we combined the methylation data of the available TCGA cohort (n=194) and our SAL elderly AML cohort (n=79), performed unsupervised clustering and integrated somatic mutation information. In an unsupervised exploration, we found differential methylation in CpGs located in promoters that resulted in the separation of patients into two clusters with different age ranges (Figure 4.5.1). One cluster constituted mostly by elderly patients (n=118, median age of 70 years, ranging 27-90, 62% of the SAL cohort) and another cluster with younger patients (n=155, median age of 57 years, ranging 18-82, 38% of the SAL cohort).

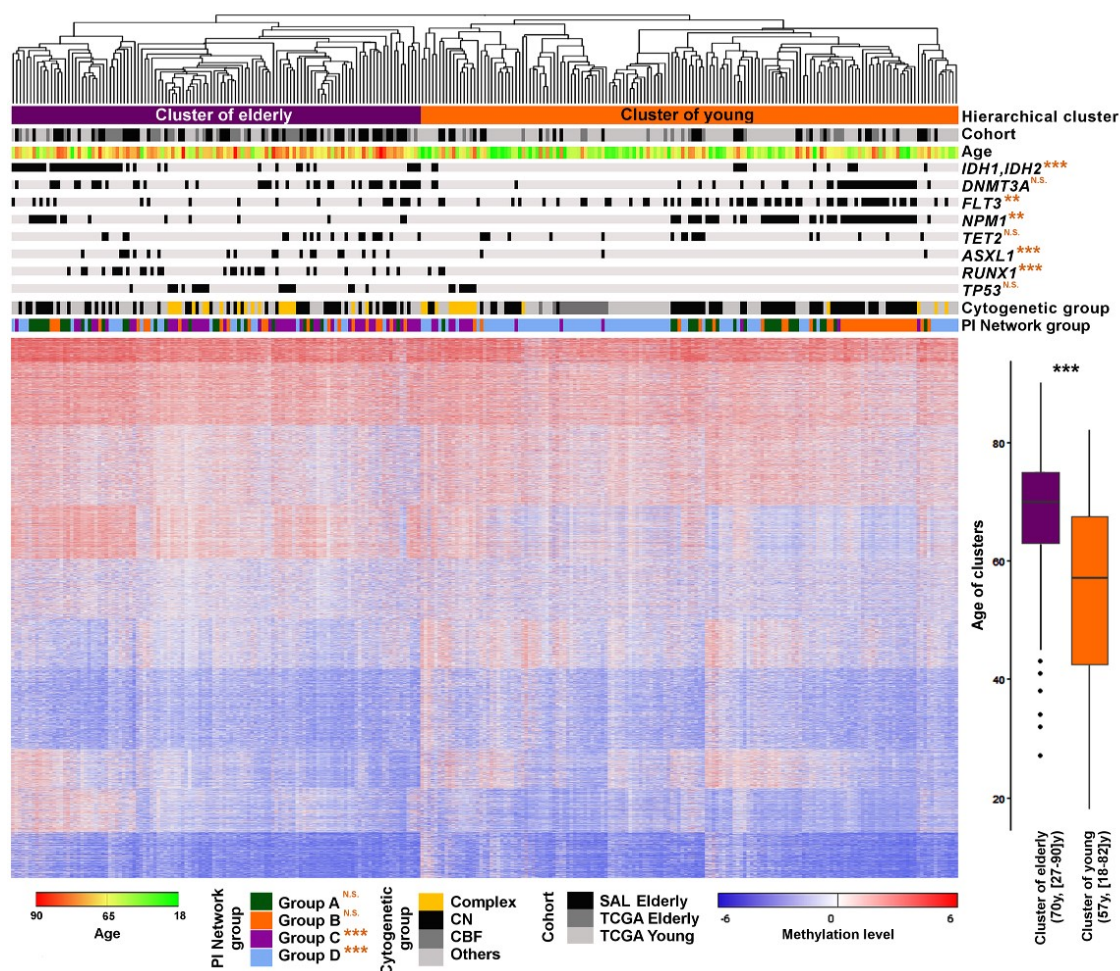


Figure 4.5.1 Methylation profiles of AML patients (TCGA cohort and SAL elderly).

The representation displays the methylation profiles of AML patients (TCGA and SAL cohorts combined), showing differential methylation patterns of elderly and young AML patients. (Caption continues in the next page)

Analysis of DNA methylation values in the 5,238 most variable CpGs in promoter regions (in the horizontal axis), scaled from unmethylated (-6, blue) to fully methylated (6, red). The depiction shows the unsupervised hierarchical clustering of 273 AML samples (in the vertical axis) with mutation information: 194 patients from the TCGA cohort (136 young of 18–64 years and 58 elderly of 65–88 years) and 79 patients from the SAL elderly cohort (65–90 years). Age of patients at the time of diagnosis is represented in the heatmap code (see legend). Samples considered part of the two hierarchical clusters were labeled as cluster of the elderly (n=118, purple) and cluster of the young (n=155, orange), due to the significantly different median age of the patients (70 years and 57 years, respectively, *** $P \leq 0.001$ obtained by t-test, boxplot in the right, median and range of ages are annotated). Patients were classified in cytogenetic groups: cytogenetically normal (CN), core-binding factor (CBF), complex (3 or more cytogenetic abnormalities) or others. *FLT3* included both SNVs and *FLT3*-ITDs available and *NPM1* included both mutations identified by NGS and Sanger sequencing. Adjusted Fisher exact tests for skewness of mutations between the cluster of the elderly and cluster of the young is specified on the right of each gene, or of the legend in case of the groups found using the protein functional interaction network (PI network, NS denotes non-significant, * $P \leq 0.05$, ** $P \leq 0.01$ and *** $P \leq 0.001$). Adapted from Silva *et al.* 2017¹.

Of note, these two epigenetic clusters were markedly different in genetic alterations (Figure 4.5.1), as most of the samples with mutations in *IDH1/2* (79%), *ASXL1* (86%), *RUNX1* (90%), *TP53* (72%) and co-mutated for *IDH/DNMT3A* (73%) were in the cluster of the elderly. In contrast, the cluster of young patients was enriched for *DNMT3A/NPM1/FLT3* triple mutated samples (88% of these triple mutated samples were in this cluster).

Comparing the cluster of the elderly with the cluster of the young, we identified many differentially methylated regions (n=1,641), while using categorical age groups elderly (TCGA+SAL, ≥ 65 years) vs young (TCGA, < 65 years) 4.6x fewer regions were identified (n=356, Figure 4.5.2A). Hypomethylated regions in the cluster of the elderly (hypoMRs, n=662) were almost all in genes (83%) and more than half overlapped promoters, while the hypermethylated regions (hyperMRs, n=979) although mostly overlapping genes were less associated to promoter regions or transcription start sites (Figure 4.5.2B, complete lists of regions are in Appendix C).

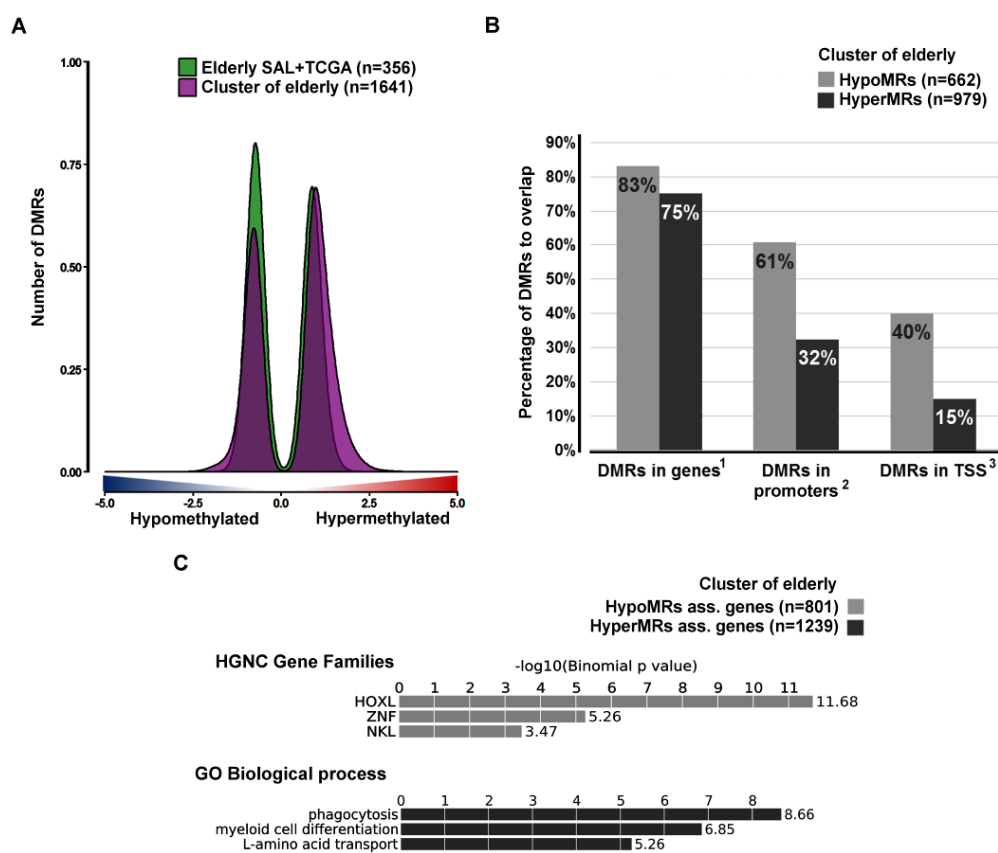


Figure 4.5.2 Differential methylation patterns of the elderly in comparison to young.

(A) The density graph reports the significant differential methylated regions (DMRs) between the first level hierarchical clusters from the unsupervised analysis (cluster of elderly vs cluster of young), or between the chronological age groups (elderly TCGA and SAL ≥ 65 y vs young TCGA < 65 years). These regions were obtained from the 104,675 most variant CpGs (n is the total number of DMRs). (B) The bar graph shows the percentage of DMRs between the hierarchical clusters associated with specific gene regulatory features. DMRs were classified into hypermethylated (hyperMRs, $n=979$) or hypomethylated (hypoMRs, $n=662$) according to their ratio of methylation in the cluster of elderly/cluster of young (n is the total number of DMRs hypomethylated and hypermethylated). The associations of DMRs to 3 gene regulatory features were examined: ¹DMRs with at least 1b overlapping a gene; ²DMRs within 1kb of a gene promoter; ³DMRs with at least 1b overlapping to a transcription start site (TSS). Associations calculated in EpiExplorer¹²⁸. (C) The graph is a representation of enrichments in gene families and biological processes of genes associated (ass.) to the DMRs, for the genes associated to hyperMRs ($n=1,239$) and for the genes associated to hypoMRs ($n=801$) connected to the cluster of the elderly. Associations to genes and enrichments were calculated by GREAT¹²⁵. Adapted from Silva *et al.* 2017¹.

Hypomethylated regions ($n=662$) in the cluster of the elderly were associated with genes ($n=801$) responsible for morphogenesis (HOXL and NKL gene families), while hypermethylated regions ($n=979$) were related to genes ($n=1,239$) associated with phagocytosis, myeloid differentiation and amino acid transport (Figure 4.5.2C and detailed in Figure 4.5.3).

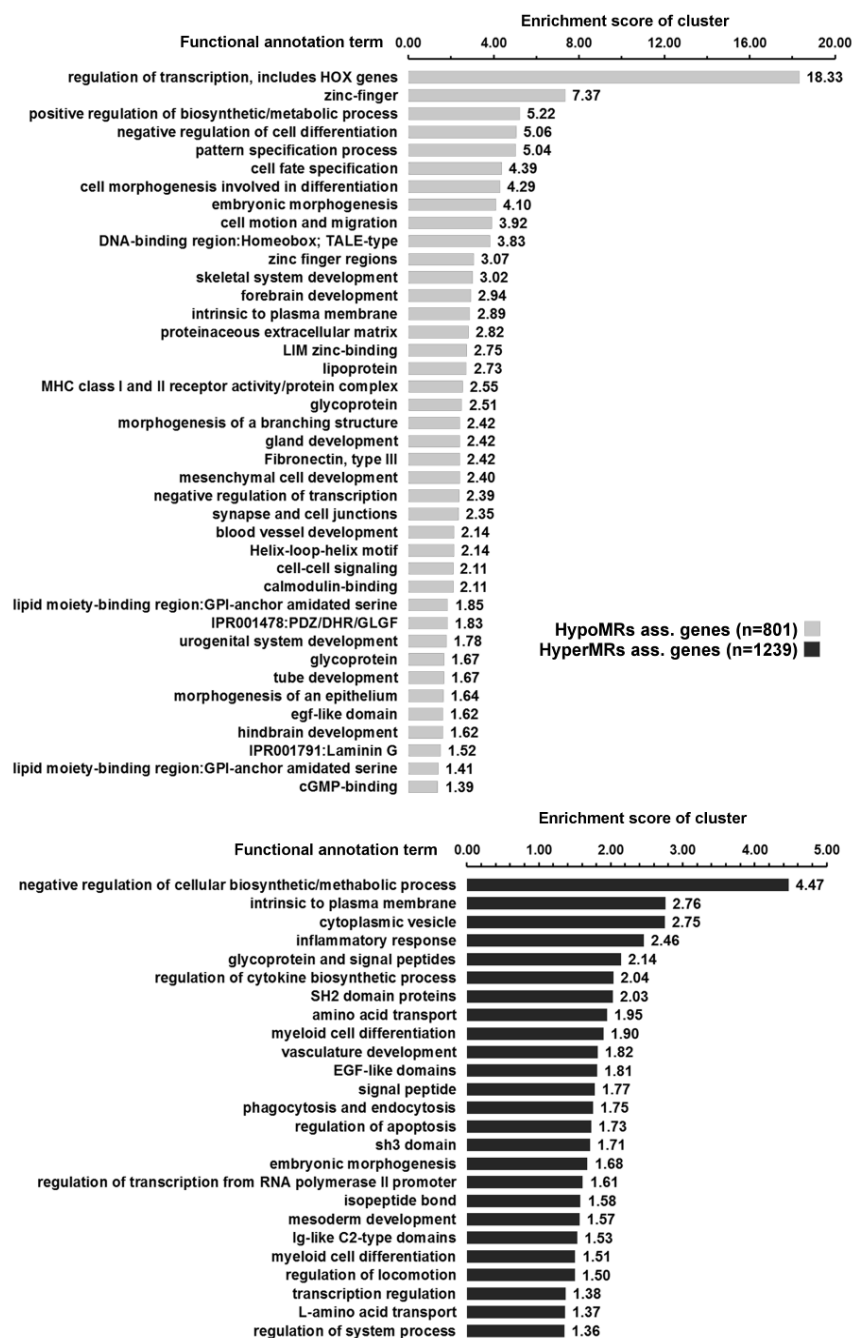


Figure 4.5.3 Enrichment of biological terms for genes associated with the differential methylation signature in the elderly.

Biological terms enriched in the list of genes associated with the DMRs from the comparison of the first level hierarchical clusters of the unsupervised analysis (cluster of elderly vs cluster of young). Regions were classified as hypermethylated (hyperMRs) or hypomethylated (hypoMRs) in relation to the cluster of the elderly AML. DMRs' associations to genes were calculated in GREAT¹²⁵ (n was the number of ass. genes). Enrichment scores of each functional annotation cluster were calculated using DAVID (EASE scores with FDR<10%)^{126,127}. As presented in Silva *et al.* 2017¹.

4.5.1 Genomic locations of elderly AML differential methylation

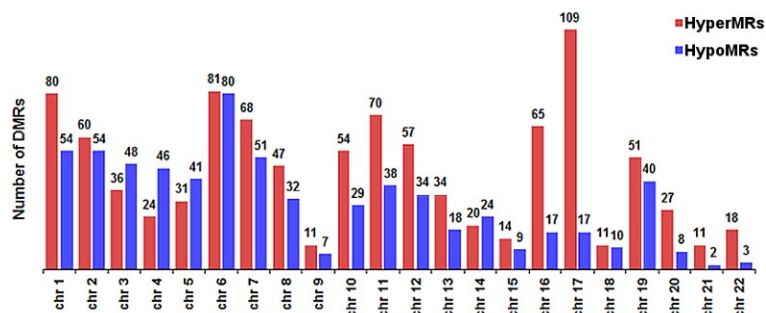
We were attentive to the importance of defining genomic regions where the methylation levels are unique. Large epigenetic changes that occur in specific regions of the genome might be of additional significance.

So, we analysed particular patterns in the distribution of the elderly AML DMRs across genomic positions. We made two main observations: 1) most chromosomes had comparable amounts of hyperMRs and hypoMRs, except for chromosomes 16 and 17 where the number of hypermethylations in samples of cluster of elderly AML was clearly high (Figure 4.5.4A) and 2) there was a tendency of the hyperMRs to be located in the tips of chromosomes (Figure 4.5.4B).

The higher methylation levels of the samples from the cluster of the elderly were more striking in chromosome 17. This was the chromosome with the highest number of hyperMRs (109 of the 979, 11%) and many of these regions were located in the q25.3 band (Figure 4.5.4B, box). This was an unusual concentration of hypermethylation on the tip of chr17 in which 35 hyperMRs (35/109, 32%, Table 4.5.1) were concentrated in about 2.4Mb (highest density area in the blue box of Figure 4.5.4B).

Within this area, there were 2 major regions strongly hypermethylated, the regions related to neighboring genes *ACTG1/KIAA1447* and to *RPTOR/CHMP6*. These were the 4 genes that had the highest number of hypermethylated regions from the cluster of elderly associated to them. There were 9 hyperMRs per each pair of genes (*ACTG1/KIAA1447* and *RPTOR/CHMP6*) and each of these regions related at least to 3CpGs.

A



B

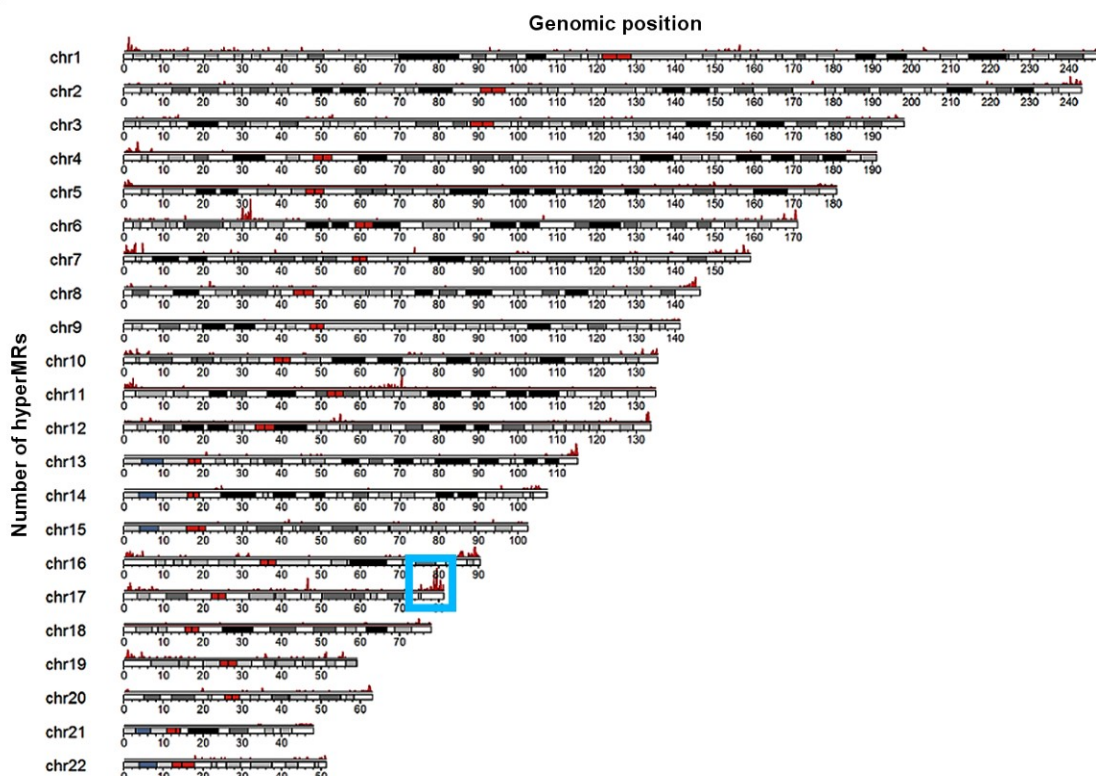


Figure 4.5.4 Distribution of DMRs of the cluster of elderly AML across chromosomes.

(A) The bar graph reports the number of DMRs from the cluster of elderly vs cluster of young in each chromosome (comparison of hierarchical clusters in Figure 4.5.1). These were classified as hypermethylated (hyperMRs, in red) or hypomethylated (hypoMRs, in blue) according to the methylation level in the cluster of elderly AML. (B) The graph shows the hyperMRs plotted according to their genomic position from the start of the short arm to the end of the long arm (oriented left to right) of chromosomes 1 to 22. The density plots represent the number of hyperMRs calculated by partitioning the genome in 0.2Mb regions. Chromosome 17q25.3 band was highlighted with a blue box. The scale of genomic regions is given in Mb. Red region of chromosome ideograms marks the centromeres.

Table 4.5.1 HyperMRs of the cluster of elderly AML concentrated in chr17 q25.3.

The table shows genomic positions of 35 regions obtained with the bumphunter algorithm as hypermethylated in the cluster of elderly (Figure 4.5.1) and the genes correlated to each region. These are spanning the region chr17:77901030-80292252 (using assembly hg19). Each gene association was calculated by GREAT¹²⁵ with the predefined association rule: Basal + extension: 5kb upstream, 1kb downstream, 1Mb maximum extension and curated regulatory domains included. The distance of each gene to the region CpGs is given in parentheses.

Chr	Start	End	Genes correlated (distance to gene in bases)
chr17	77901030	77901317	CBX4 (-87946), TBC1D16 (+108473)
chr17	78058704	78058778	GAA (-16762), CCDC40 (+48306)
chr17	78190755	78190983	SLC26A11 (-3360), SGSH (+3330)
chr17	78560478	78560916	CHMP6 (-404944), RPTOR (+41629)
chr17	78735268	78735596	CHMP6 (-230209), RPTOR (+216364)
chr17	78748077	78748494	CHMP6 (-217355), RPTOR (+229218)
chr17	78753273	78754372	CHMP6 (-211818), RPTOR (+234755)
chr17	78755379	78755442	CHMP6 (-210230), RPTOR (+236343)
chr17	78829626	78829930	CHMP6 (-135863), RPTOR (+310710)
chr17	78851149	78851262	CHMP6 (-114435), RPTOR (+332138)
chr17	78854232	78854418	CHMP6 (-111316), RPTOR (+335257)
chr17	78865263	78866235	CHMP6 (-99892), RPTOR (+346681)
chr17	79004850	79006166	BAIAP2 (-3454)
chr17	79109729	79109910	AATK (+29997), BAIAP2 (+100858)
chr17	79128918	79129078	AATK (+10819), BAIAP2 (+120036)
chr17	79228937	79229385	C17orf89 (+16122), SLC38A10 (+39944)
chr17	79282893	79283959	SLC38A10 (-14321), TMEM105 (+21048)
chr17	79297435	79297618	SLC38A10 (-28422), TMEM105 (+6947)
chr17	79374327	79374741	KIAA1447 (+994)
chr17	79377272	79378207	KIAA1447 (+4200), ACTG1 (+102067)
chr17	79380400	79380706	KIAA1447 (+7013), ACTG1 (+99254)
chr17	79419796	79420424	KIAA1447 (+46570), ACTG1 (+59697)
chr17	79425877	79426432	KIAA1447 (+52615), ACTG1 (+53652)
chr17	79428036	79428750	ACTG1 (+51414), KIAA1447 (+54853)
chr17	79429330	79429729	ACTG1 (+50277), KIAA1447 (+55990)
chr17	79432709	79433150	ACTG1 (+46877), KIAA1447 (+59390)
chr17	79442037	79442206	ACTG1 (+37685), KIAA1447 (+68582)
chr17	79484960	79485709	FSCN2 (-10223), ACTG1 (-5528)
chr17	79799358	79799549	PPP1R27 (-6545), P4HB (+19116)
chr17	80159399	80159595	FASN (-103289), SLC16A3 (-32066)
chr17	80190129	80190154	SLC16A3 (-1421)
chr17	80196719	80197538	SLC16A3 (+5566), CSNK1D (+34478)
chr17	80266884	80267030	CSNK1D (-35350), CD7 (+8521)
chr17	80273242	80273685	CSNK1D (-41857), CD7 (+2014)
chr17	80292079	80292252	SECTM1 (-292)

When examined in detail different CpGs across this 2.4Mb region have different factors that correlate with their methylation levels. Some CpGs seem strongly affected by mutations and other clearly more related to patients' age. As an example of this, we show the regions of the 3 adjacent genes *KIAA1447*, *ACTG1* and *FSCN2* (Figure 4.5.5). Some CpGs were clearly different between the 2 hierarchical clusters (examples in boxes A and B), while others were particularly hypomethylated in *DNMT3A/NPM1/FLT3* mutated samples (example in box C) and/or very strongly hypermethylated in the *IDH1/2* mutated patients (example in box D).

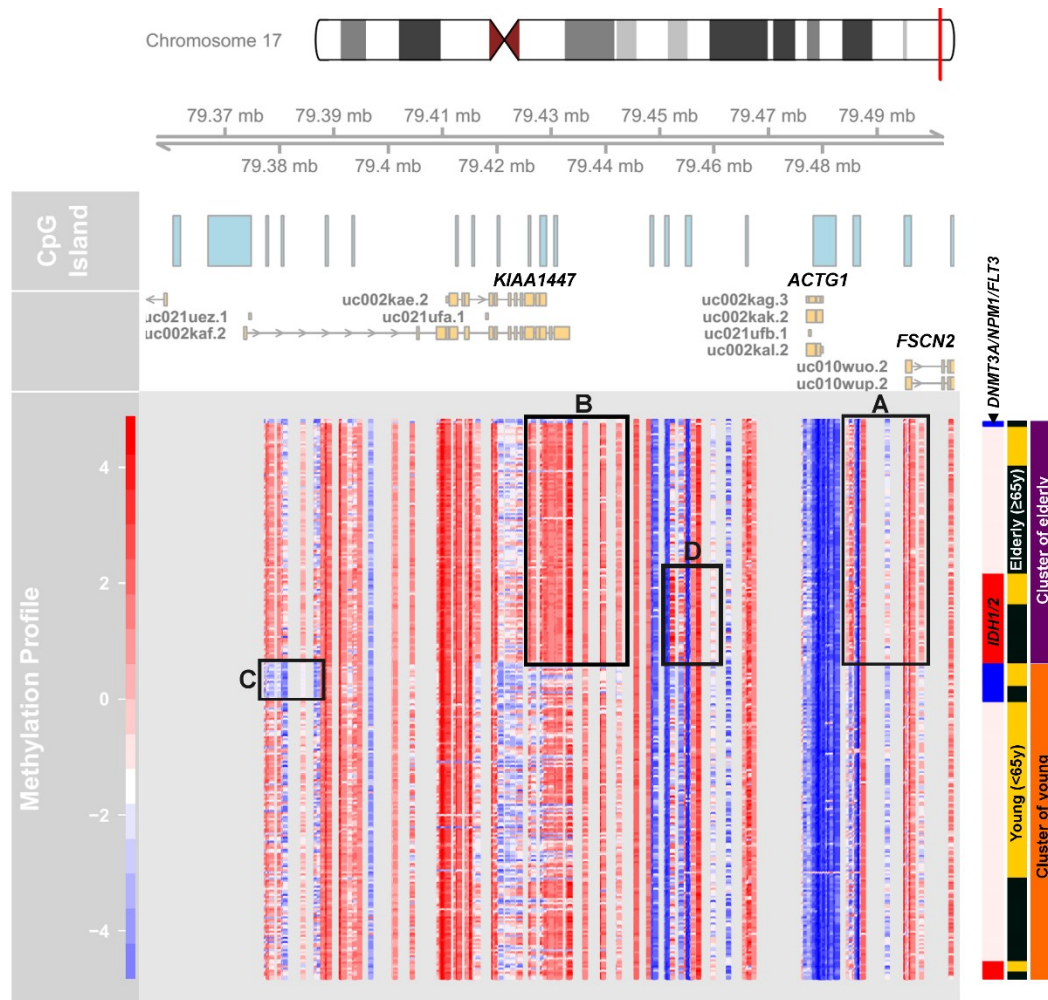


Figure 4.5.5 Distinct methylation profiles of elderly in the KIAA1447/ACTG1/FSCN2 region.

DNA-methylation from the CpGs in the tip of the long arm of chromosome 17 using beta-values scaled from unmethylated (-5, blue) to fully methylated (5, red). In the depiction the 273 AML samples from the two cohorts (TCGA and SAL) are in horizontal and positions of CpGs according to GRCh37/hg19 are in vertical. The CpG islands of the genomic region are marked with blue boxes. Patients are annotated according to the group of the 1st division of hierarchical clustering (cluster of elderly, purple annotation, or young, orange annotation, Figure 4.5.1), age group according to patient chronological age (elderly for ≥65 years old, black annotated, or young for <65 years old, yellow annotation) and mutation information for 2 relevant high rate mutated groups (*IDH1/2*, red annotation, and triple mutated *DNMT3A/NPM1/FLT3*, blue annotation).

The particular hypermethylation pattern of the tip of chr17 overlapped several genes that were part of endocytosis and phagocytosis processes (see gene enrichment in Figure 4.5.3), with emphasis on functions in actin organization. The *ACTG1* codes for the gamma-actin in the cellular cytoskeletons and is one of the genes in the biological process enrichment phagocytosis of the hyperMRs¹³⁶. Gamma-actin is also important for cell adhesion, being involved with the cadherins/protocadherins and catenins for the regulation of adherens junctions¹³⁶ (families of proteins for which we

found many other DMRs). The third gene *FSCN2* (Fascin Actin-Bundling Protein 2, Retinal) codes a protein with an actin-binding function which is expressed only in retina and blood¹³⁶.

Interestingly, in their study Bullinger and colleagues in 2010¹³⁷ connected the hypermethylation in this region of the chr17 long arm overlapping the neighboring genes *KIAA1447* and *ACTG1* to poor survival in AML (these confirmations are marked with * in Table 4.5.2B, next chapter). Not much is known about *KIAA1447*, an alias of *BAHCC1* (BAH Domain And Coiled-Coil Containing 1). This is a gene encoding a protein with a chromatin binding domain, interacting with the chromatin silencing complex for transcription regulation¹³⁶.

Furthermore, *BAIAP2* is the gene that encodes BAI1 Associated Protein 2, a protein that functions as an insulin receptor tyrosine kinase substrate in the brain¹³⁶. It interacts with CDC42, being necessary for the CDC42-mediated reorganization of the actin cytoskeleton and whose RNAi phenotype is a reduction of endocytosis. Moreover, *CHMP6* is also involved in endocytosis and is in this genomic region¹³⁶. CHMP6 is a probable core component of the endosomal sorting required for transport complex III which is involved in multivesicular bodies formation and sorting of endosomal cargo proteins¹³⁶.

Besides *BAIAP2*, in this region were two other genes of proteins involved in metabolism, namely in insulin response, *RPTOR* and *FASN*. The gene *RPTOR* codes for the protein Regulatory Associated Protein Of MTOR Complex 1¹³⁶. RPTOR or RAPTOR is involved in the control of the mammalian target of rapamycin complex 1 (mTORC1) activity which regulates cell growth, survival, and autophagy/longevity in response to nutrient and hormonal signals¹³⁶. A DMR overlapping *RPTOR* was found in the most recent paper reporting DMRs with correlations to survival probability (using this TCGA methylation data)¹³⁸. They advanced this gene to have one of the 8 DMRs signature that could be used as a prognostic marker and have a crucial role in AML.

In turn, *FASN* codes for the Fatty acid synthase, which main function is to catalyze the synthesis of palmitate from acetyl-CoA and malonyl-CoA and is a downstream responder in the insulin signaling pathway¹³⁶.

4.5.2 Differentially methylated genes in elderly AML

The gene expression of particular genes has proved to be very relevant for age phenotypes, for cancer development and more specifically for AML. Therefore, we wanted to report the levels of DNA-methylation that could affect specific genes known to be involved in these phenotypes.

Additionally, we looked at the DMRs found for the cluster of elderly to identify regions/genes with DNA-methylation levels that were previously correlated to survival in AML. These genes could constitute candidates for further use as predictors of poor survival of AML patients. We also wanted to highlight which of these genes could have expression levels correlated to survival in AML. To access this we obtained the Kaplan-Meier curves of the patients with low versus high gene expression, using the RNA-seq data of the TCGA cohort. Hence, we examined the survival of the groups of patients with lower than mean expression value vs the group of higher than mean expression value for the individual genes of interest.

Our results from the application of these methods are reported in Table 4.5.2 A-C, showing the genes we identified as differentially methylated in the cluster of elderly AML in our dataset (n=2040) that are also known to be involved in specific phenotypes.

Table 4.5.2 Genes in DMRs of the cluster of elderly AML which are related to age, cancer and AML pathogenesis or survival.

The tables show the genes correlated to regions of hypo and hypermethylation in the cluster of the elderly that are involved in age and cancer (A) or AML (B and C). (A) The genes overlapping age-related genes¹³⁹ and oncogenes or tumor suppressor genes (TSG) according to the 20/20 rule¹⁴⁰. (B) The genes overlapping genes that are correlated to DMR signatures of AML samples (CD34⁺_vs_AML⁸⁸: AML compared with normal bone marrow CD34⁺ cells and Ctr_vs_AML¹³⁷: AML compared to blood from healthy donors). (C) The genes overlapping genes correlated to DNA methylation regions with prognosis value previously reported in 3 papers: Marcucci *et al.*⁹⁵, Li *et al.*⁹⁴ and Figueroa *et al.*⁸⁹. Bold marks the genes for which the cluster of elderly showed both hypo and hypermethylated regions. Blue marks genes that were reported in the respective study to be hyper and hypomethylated depending on the AML group that was compared and not in the overall AML. Green and red mark the genes we could confirm to be of prognosis value in the TCGA samples with the appropriate correlation to the DNA methylation alteration. Green marks the bad prognosis for the low expression of the gene, while red marks the bad prognosis for the high expression of the gene. The * marks genes that are part of a big region of hypermethylation on chr17 shown in Figure 4.5.5.

A hypoMRs hyperMRs		B hypoMRs hyperMRs		C hypoMRs hyperMRs	
Age Genes (21/307)		CD34⁺_vs_AML (6/30)		Marcucci <i>et al.</i> (22/82)	
CTF1	TP63	(1/8)	(6/25)	CABLES1	ALOX15B
HOXC4	BCL2	SEPT9	DIO3	CD34	IQSEC1
PON1	POLD1		ASCL2	CLDN15	PRKCZ
NRG1	FGF23		CDH13	DDIT4	AATK
TP73	SNCG		PTK6	GAL3ST3	GCNT2
IGFBP3	GSTP1		RUNX3	KLHL3	
TFAP2A	STAT3		SEPT9	MDF1	
SOCS2	RAD52	Ctrl_vs_AML (8/16)		ME3	
PIK3R1	TFDP1	PITX2	FSCN2*	PRKG2	
NCOR2	NCOR2	ESR1	GYPC	WDR16	
ESR1	TNF	CDH1	KIAA1447*	APBB1	
TSG (11/71)			RASSF1	ETS1	
BAP1	ARID1A		SNX9	F2RL1	
CDH1	ASXL1			H1FO	
GATA3	CEBPA			HIVEP3	
PIK3R1	CREBBP			KDM2B	
WT1	PRDM1			SCRN1	
	SMAD2			AATK	
Oncogenes (5/54)				GCNT2	
GATA2	BCL2			Li <i>et al.</i> (7/16)	
	DNMT3A			ID4	TRIM67
	FGFR3			ZFP42	GPR146
	U2AF1			CHL1	
				PCDHAC2	
				SOCS2	
				GPR146	
				Figueroa <i>et al.</i> (1/22)	
					LCK

4.5.2.1 Age genes

At least 21 genes (Table 4.5.2A) of the genes in the proximity of these DMRs have been previously correlated to age and are present in the GenAge database¹³⁹ (n=307). Some are involved in biologic processes that are hallmarks of aging like DNA damage repair/senescence (*Rad52*, *TP63*, *TP73*) or nutrient sensing/Insulin and IGF-1-signaling pathways (*IGFBP3*, *PIK3R1*, *SOCS2*). Not present in the GenAge database but also a hallmark of aging were the autophagy genes (for example *ATG16L1*, *ATG5* and *ATG7*).

We further found the expression levels of 3 of these genes could be correlated to survival (Figure 4.5.6), with poor survival attributed to high *SOCS2* expression (p=0.01), high *ESR1* expression (p=5.6x10⁻⁴) and to low *TNF* expression (p=0.04).

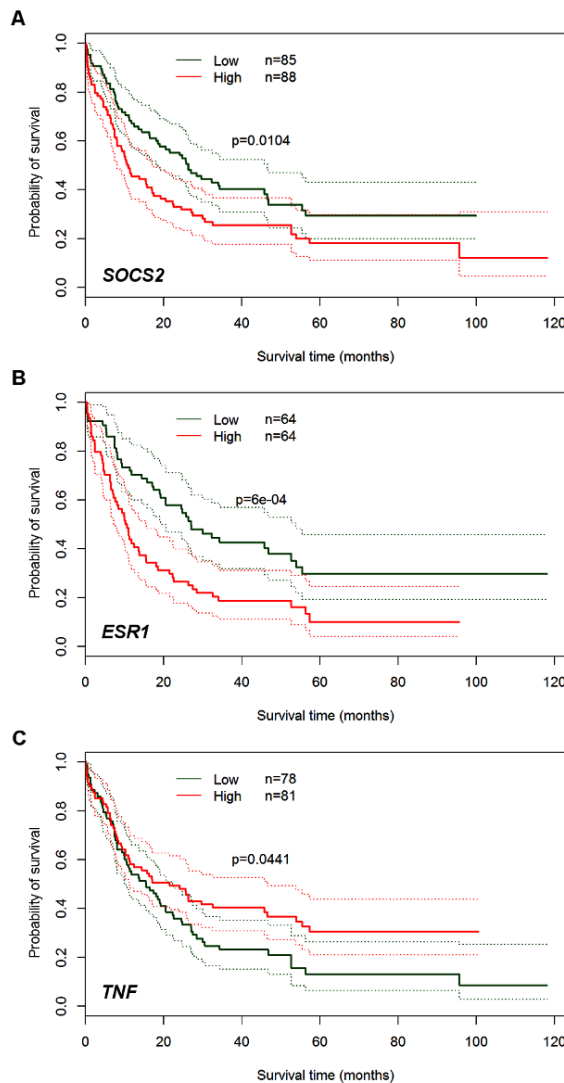


Figure 4.5.6 Overall survival of patient groups defined by high vs low RNA expression levels for age genes that are associated with DMRs.

Kaplan-Meier curves display the estimation of the overall survival for the division of the TCGA cohort into two groups with High (value \geq mean) versus Low expression (value<mean) of the genes: *SOCS2* (A), *ESR1* (B) or *TNF* (C), using the expression levels from RNA-seq. The significance of the difference between overall survivals was calculated with the log-rank test. Dotted lines mark the 95% confidence bounds.

4.5.2.2 Cancer genes

Additionally, several genes correlated to hypoMR and hyperMRs of the cluster of the elderly are associated with cancer (Table 4.5.1A). We categorized them using the classification of Vogelstein *et al.*¹⁴⁰ that classified cancer related genes into oncogenes and TSGs using the “20/20 rule” whereby “a driver mutation can be described as oncogenic if at least 20 of its mutations are recurrent as well as being missense” and “a tumor suppressor gene would subsequently require a threshold of 20 mutations that all resulted in an inactivating effect.”¹⁴⁰ Importantly, one known oncogene (*GATA2*) was related to a hypoMR and six TSGs had related hyperMRs, most of them are known for being molecularly altered in AML (*ARID1A*, *ASXL1*, *CEBPA*, *CREBBP*).

4.5.2.3 AML genes

There were also several genes particularly associated to AML related to hyperMRs and hypoMRs of the cluster of elderly (Table 4.5.2B), as determined by matching our list to 2 lists of differentially methylated genes in AML samples when compared to healthy controls. In both studies, the Alvarez *et al.*⁸⁸ and the Bullinger *et al.*¹³⁷, the number of genes that are related to CpGs exclusively hypermethylated or hypomethylated across all AML samples of corresponding cohorts was very limited (30 of 807 genes and 16 of 80 genes, respectively). Therefore, it was remarkable that 14 of these 43 genes (since 3 genes have both hyper and hypomethylated CpGs) connected to AML pathology were also in the DMRs of the hierarchical cluster of the elderly.

4.5.2.4 Genes related to prognosis predictions in AML

The cluster of the elderly also contained a good number of hypoMRs (n=25, Table 4.5.2C) associated to genes previously reported to have differential DNA-methylation with prognosis correlation (n=120, complete list Table 1.4.1 in section 1.4). Furthermore, we could confirm the poor survival of the patients with high expression levels of *F2RL1* (p=0.04), *HIVEP3* (p=0.02) and *SOCS2* (p=0.01) in the TCGA RNA-seq data, which was consistent with the results in the cohorts of these studies.

While the majority of DMRs found for the cluster of elderly resulted from the higher methylation values found for this group (hyperMRs) not many of these genes were previously mentioned as predictors of survival. Even from the ones that were,

none of them could be confirmed to have prognostic prediction using the TCGA RNA-seq data.

4.6 Robust epigenetic patterns of AML

Since CpG island shores are variable between tissues and very disease-specific we performed unsupervised clustering using the most variable CpGs in island shores (both N-shores and S-shores, Figure 4.6.1). There were several patients with similar methylation profiles that were defined by genetic alterations. There was a first cluster-defined group with 3 samples that have methylation patterns different from all other samples. The next group division (of hierarchical clustering) clearly distinguished *IDH1/2* mutated samples from all others (n=31). After a few more samples were clustered into groups, one of the next group separations divided most of the remaining patients into two groups (dark grey, n=87, and light grey, n=146).

Like in the promoters profile, there was enrichment of elderly patients to the smaller group (dark grey: median age 70y, ranging 41-90y) when compared to the patients in the other group (light grey: median age 57.5y, ranging 21-82y, Welch's t-test Bonferroni corrected $p = 1.54 \times 10^{-9}$). The latter group, with younger patients, contained most of the triple mutated *DNMT3A/NPM1/FLT3* samples (green) and a CBF defined cluster (yellow). Whereas the group of the elderly patients contained samples with complex karyotype/*TP53* (blue) and most of the samples classified as group C using the protein FI network classification.

This group highlighted once more the similarities between the elderly AML samples and samples that are typically known for DNA instability. This resembled what was apparent in the genetic profiles, this time similarities are seen on the epigenetic level.

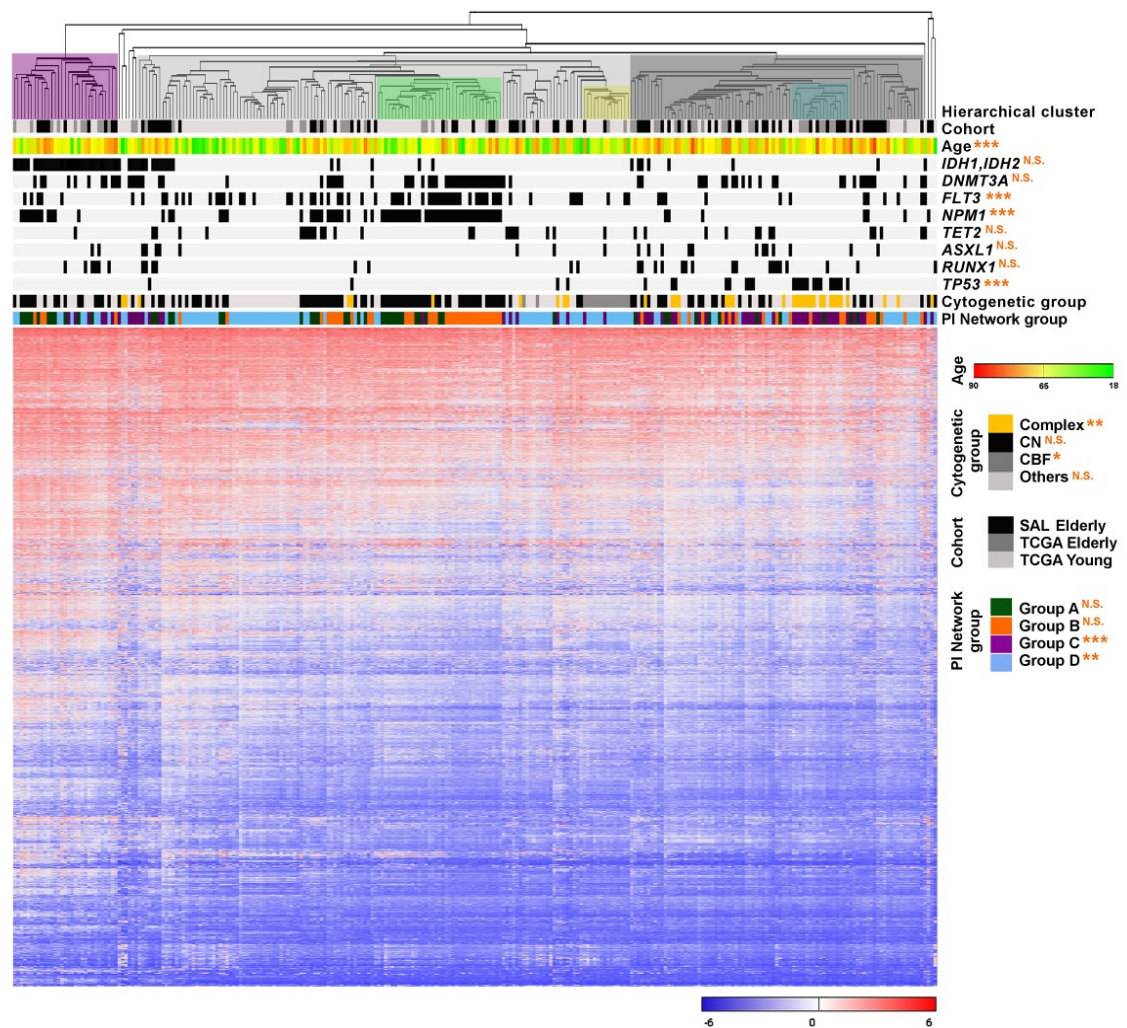


Figure 4.6.1 Methylation profiles of Group C and complex karyotype AML samples and uniqueness of patients with *IDH* mutations.

Analysis of DNA-methylation values in the 6369 most variable CpGs in promoter regions that are in N-shores or S-shores of the CpG islands (in the horizontal axis), scaled from unmethylated (-6, blue) to fully methylated (6, red). Depiction of the unsupervised hierarchical clustering of 274 AML samples (in the vertical axis) with mutation information for high rate mutated genes: 194 patients from the TCGA cohort (136 young of 18-64 years and 58 elderly of 65-88 years) and 80 patients from the SAL cohort (all elderly of 65-90 years). Age of patients at the time of diagnosis was represented as a heatmap code (in the legend). Samples considered part of hierarchical clusters of importance were highlighted. Patients are represented in vertical and classified in cytogenetic groups: cytogenetically normal (CN, no detected cytogenetic abnormalities), core binding factor (CBF, includes t(8;21) or inv(16)/t(16;16)), complex (3 or more cytogenetic abnormalities), or others. *FLT3* included both SNVs and *FLT3*-ITDs available. Adjusted Fisher exact test for skewness of mutations between the cluster in dark grey and the cluster in light grey is specified on the right of each gene, or patient characteristic, or of the legend in case of the groups found using the protein functional interaction network (PI network, N.S. denotes non-significant, * $p \leq 0.05$, ** $p \leq 0.01$ and *** $p \leq 0.001$).

4.7 Epigenetic heterogeneity in the SAL elderly AML

In the next step, we dissected the methylome of the SAL elderly AML samples using unsupervised hierarchical clustering (Figure 4.7.1) and identified two discernible clusters (cluster 1 and 2), recapitulating the patterns of the combined cohort. Cluster 1 constituted of *IDH1/2* mutant samples and cluster 2 constituted of triple mutated samples *DNMT3A/NPM1/FLT3*. Additionally, a small cluster of samples with *TET2* mutations was observed in this elderly AML cohort (cluster 3).

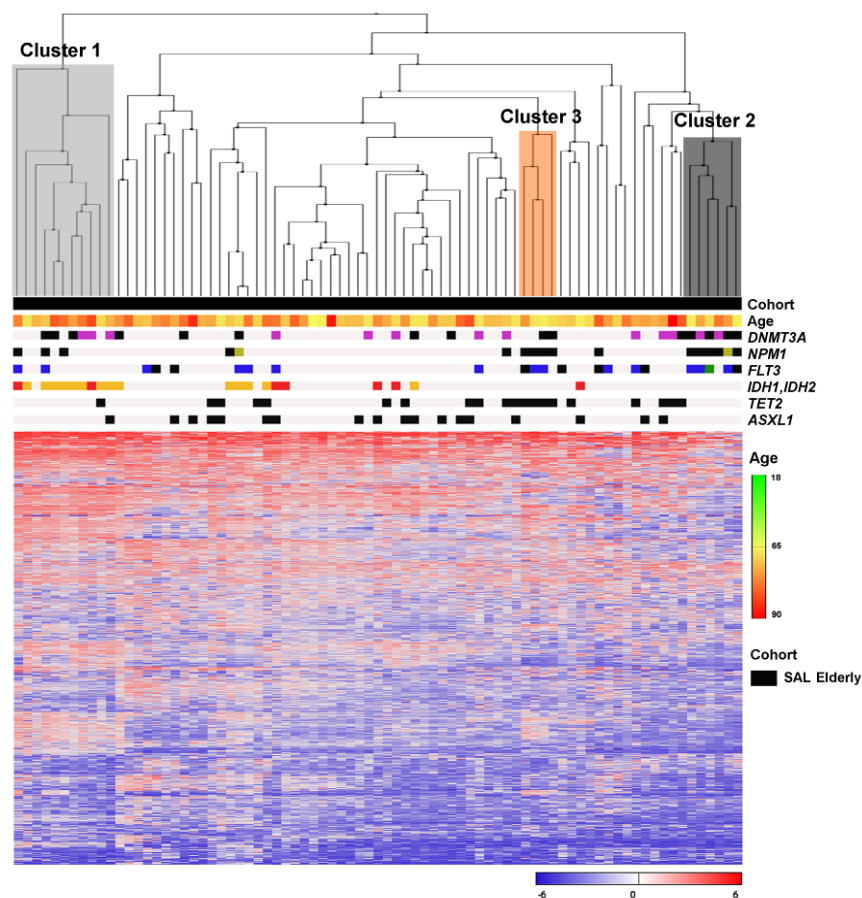


Figure 4.7.1 Methylation profiles of SAL elderly AML patients.

Analysis of DNA methylation values from the 1,000 most variable CpGs of high-dense CpG regions (according to Illumina PHANTOM annotation) using scaled hues from unmethylated (-6, blue) to fully methylated (6, red). Depiction of the unsupervised hierarchical clustering of 79 elderly AML samples integrated with mutation information (for some high rate mutated genes). The different colors represented are: *DNMT3A* R882 mutations (pink), *IDH1* mutations (orange) and *IDH2* mutations (red). Mutational data derived by PCR were included: *NPM1c* mutation status (light green), *FLT3*-ITD (blue) and concomitant *FLT3* SNV with *FLT3*-ITD (green). Samples considered part of specific clusters were shaded and clusters labeled 1 to 3. Age of patients at the time of diagnosis was depicted as a heatmap code (in the legend). Adapted from Silva *et al.* 2017¹.

We obtained DMRs in two-group comparisons (cluster vs non-cluster samples and mutated vs wild-type samples). This analysis showed definite patterns of differential methylation (Figure 4.7.2A). Cluster 1 (and *IDH1/2*) showed about 230

DMRs, almost all hypermethylated, associated with genes enriched for biosynthetic/metabolic processes and myeloid cell differentiation (Figure 4.7.2B). For cluster 2 (*DNMT3A/NPM1/FLT3*) and for *DNMT3A* we found regions were exclusively hypomethylated, particularly affecting Homeobox genes (*HOXB3*, *HOXB4*, *HOXB5*, *MEIS1*, Figure 4.7.2).

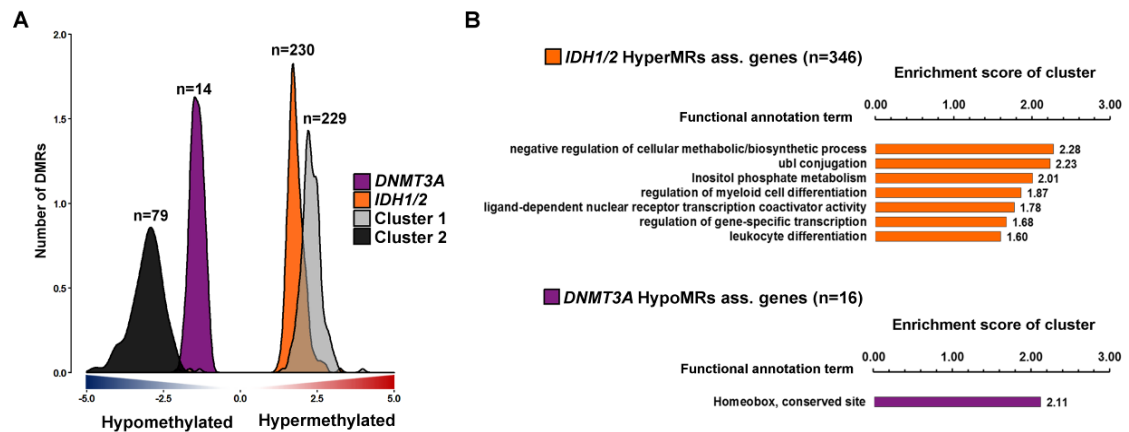


Figure 4.7.2 Specific differential methylation signature of epigenetic regulators mutated in the SAL elderly AML.

(A) The density of differential methylated regions (DMRs) plotted for mutational status groups of mutant *IDH1/2* or *DNMT3A* (versus its wildtype samples) and for methylation cluster 1 or 2 from the unsupervised analysis (against non-cluster samples). The numbers of DMRs with at least 3 CpGs differentially methylated were obtained from the most variable 104,852 CpGs and classified into hypermethylated regions (hyperMRs) or hypomethylated regions (hypoMRs), according to their ratio of methylation in the test group (n is the total number of DMRs). (B) Biological terms found enriched in the list of genes associated with *IDH1/2* hyperMRs and *DNMT3A* hypoMRs are enumerated (n ass. genes was the number of associated genes). Associations were obtained using GREAT¹²⁵ and enrichments score for each functional annotation cluster were calculated using DAVID (EASE scores with FDR<10%)^{126,127}. As presented in Silva *et al.* 2017¹.

However, *NPM1* mutated or *FLT3* mutated samples by themselves did not share this clear tendency, having only slightly more regions classified as hypomethylated than classified as hypermethylated (Figure 4.7.3A). Like in traditional cancer DMRs, for both of these the hypermethylations were more correlated to gene promoters than the hypomethylations (Figure 4.7.3C).

In comparison, *DNMT3A* mutations despite being present in many samples with *IDH1/2* mutations do not show any hypermethylated regions. Furthermore, hypomethylated regions in *DNMT3A* mutated samples were distinctly covering extended regions of the genome, being bigger than the average other DMRs, mostly due to larger numbers of CpGs changed by region (with the average of 10 CpGs changed in each region, Figure 4.7.3B).

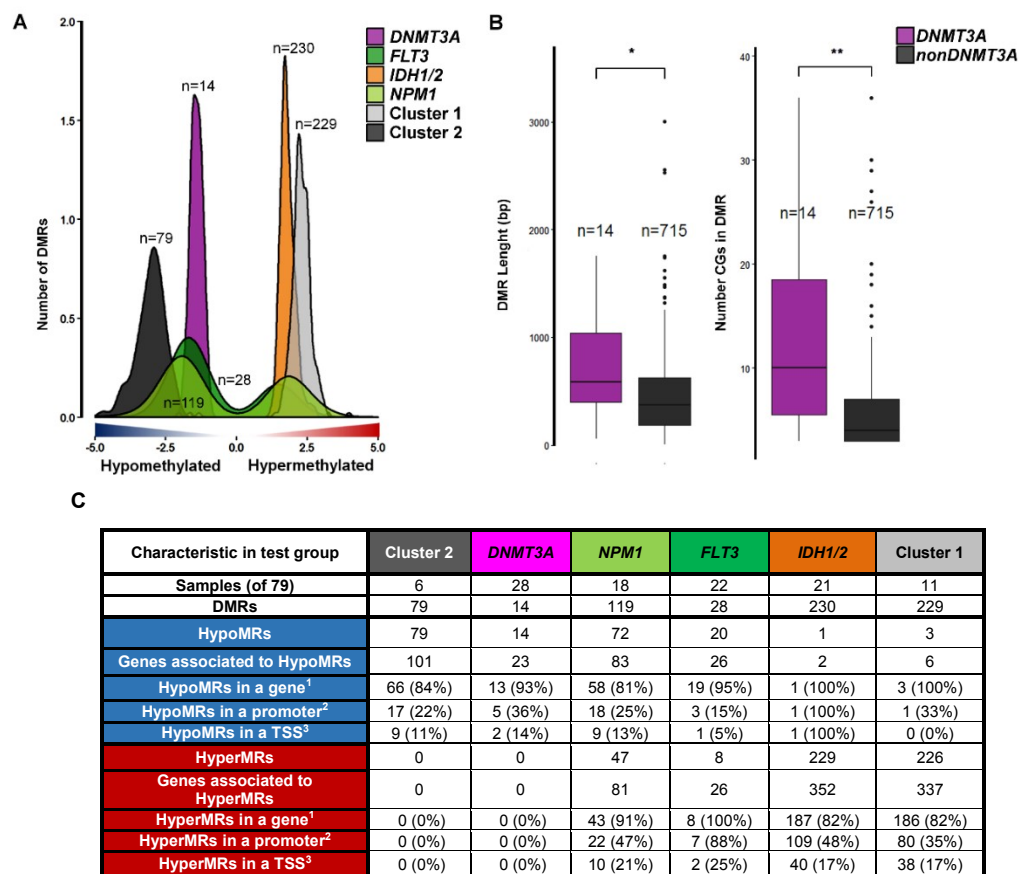


Figure 4.7.3 Specific signature of differential methylation for mutated genes in the SAL elderly AML.

(A) The density of the significant differential methylated regions (DMRs) for groups of mutant versus its wildtype samples (for *IDH1/2*, *NPM1*, *FLT3* and *DNMT3A* mutations) and for the methylation clusters against non-cluster samples. DMRs were classified into hypermethylated DMRs (hyperMRs) or hypomethylated DMRs (hypoMRs) according to this methylation ratio. (B) Length of the DMRs and number of CGs they contained, for the DMRs of *DNMT3A* mutants vs all the DMRs found for all other groups tested (*nonDNMT3A*: *IDH1/2*, *NPM1*, *FLT3*, *TET2*, *ASXL1*, *RUNX1*, *SRSF2*, and clusters 1,2,3). n: the total number of DMRs for each comparison group; * $p \leq 0.05$; ** $p \leq 0.01$. (C) The table reports differently methylated regions in specific groups of the SAL elderly AML. DMRs relate the number of highly significant DMRs (with at least 3 CGs changed) for high rate mutated genes or clusters from the unsupervised analysis. The DMRs and the genes found to be associated with these regions were classified according to each state of differential methylation (hypoMRs or hyperMRs). The number of DMRs associated to specific regulatory features are stated with the percentage they represent: 1- DMRs with at least 1b overlapping a gene; 2- DMRs within 1kb of a gene promoter; 3- DMRs with at least one 1b overlapping to a transcription start site (TSS). Associations were calculated by EpiExplorer¹²⁸.

CHAPTER 5. DISCUSSION

Since the advent of NGS, we have recognized that AML has a large heterogeneity in molecular alterations that make it a highly complex disease, but its patterns are resolvable for the number of mutations found in AML (average 13 Tier1 mutations) is not as high as in most of the other cancers¹⁴¹. The recent NGS studies suggest the development of an AML involves the acquisition of somatic mutations in a stepwise manner, due to the accumulation of mutations in stem cell progenitors responsible for continuous blood production. This dynamic of the disease would explain why AML is more frequently found in the elderly population.

Among the molecular alterations found in AML many occur in epigenetic regulators, with a high prevalence of mutations found for example in *IDH1*, *IDH2*, *DNMT3A* and *TET2*, which underscored possible roles of the epigenome in the pathogenesis of AML. The initial observations that epigenetic mechanisms are dysregulated in AML lead to the analysis of the unclear relationships between patterns of mutations and epigenetic phenotypes^{37,79,66}. Nowadays these patterns can be comprehensively explored since both can be obtained with whole genome/exome coverage.

At the time of our study the molecular analysis of AML, genomic and epigenomic landscapes, referred either to selected groups of patients, like cytogenetically normal (CN⁶⁶), *de novo* or secondary AML (sAML⁴⁹), young patients (<60 years old⁷⁹), or to unselected cohorts like the one with 200 samples sequenced by TCGA³⁷. Despite the exponential increase of studies in genetic or epigenetic classifications of AML patients in the last 2 years, both patterns had not been addressed together specifically in the elderly patients (using either global or non-global approaches), until our study¹.

Therefore, we aimed to unravel the genetic and epigenetic patterns of the elderly AML that could provide more detailed evidence into its specific pathogenesis. We described many specificities found in the SAL elderly cohort and our procedures allowed us to point to known and new molecular alterations of biological relevance or prognostic value that can be used as druggable targets.

5.1 Genetic patterns of elderly AML

In our comprehensive approach, we analysed a large set of candidate cancer genes (555) by targeted NGS and established several particularities of the elderly AML genetic profiles.

With this extended panel sequencing, we found 281 genes mutated, which was about 5x more genes than included in the panel Illumina has set up as the myeloid sequencing panel (54 genes). Since the elderly patients of TCGA (≥ 65 years old) showed that the median mutations per patient was high (when compared to the younger patients) panels like this would have proved insufficient to evaluate AML in the elderly population.

5.1.1 Molecular alterations correlated to age

The number of mutations observed per patient did not directly correlate with the age neither in the SAL elderly nor in the TCGA elderly, even though the increased age related to decreased survival probability. Instead, the increase in the median number of mutations per patient could only be seen between TCGA young and TCGA elderly group of patients. Both facts were consistent with young and elderly AML being distinct groups of AML.

This also indicated that specific genetic alterations and patterns in elderly AML would have to be analysed for only they might provide novel insights for the dismal prognosis of these patients.

With our approach, we obtained **extensive information** that was not captured as a whole in other studies investigating elderly AML. While others describe increased frequencies of certain mutations in older patients^{131,142,143}, we were able to extend this mutational pattern by exploring phenotypic interactions between functional groups of proteins. The most prominent characteristics of the genetic patterns of elderly AML to emerge were: (i) that almost all elderly patients had at least one mutation in an epigenetic regulator (85%), (ii) the large percentage of patients with mutations in splicing regulators (38%) and (iii) the presence of mutations in several proteins involved in DNA repair.

The high coverage of targets obtained in the many **epigenetic regulators** we targeted could be partially responsible for the high amounts of alterations detected in the SAL elderly cohort. Since these many of targets had only been found by the TCGA study, and because it was done using a whole-exome approach they have less coverage, there were difficulties in effecting comparisons. Hence we looked for further confirmation, which was then obtained by analysis of the young vs elderly patients in the TCGA cohort. Furthermore, the increased frequency of mutations in epigenetic factors was not completely unforeseen, since many of these mutations had previously been correlated with increasing age of AML patients^{28, 131,142,144}.

Still, the amount of these mutations that could be identified was prominent for together they are present in the majority of patients. One example of this was the unexpectedly **high amount of *IDH1* mutations** (17%), a fact for which age could be blamed since no other explanation could be retrieved. To our knowledge this has not been confirmed in other cohorts, usually, *IDH2* is the enzyme with more mutations (between the two) and the one that has been correlated to older AML patients^{145,146,147}. Another example was the **high frequency of mutations in *ASXL1*** (22%) that was previously found at 6% in a young AML cohort¹³² and at 11% in *de novo* AML¹⁴⁸. The latter study correlated *ASXL1* mutations to age for their occurrence in 6% of young patients (<60y) and in 18% of older patients (≥60y)¹⁴⁸. Similarly, in a cohort with CN-AML patients, *ASXL1* mutations were present in 3% of the young patients (≤60y) and 16% in the older patients (>60y)¹⁴². A further example was the 26% of the SAL elderly AML patients with a *TET2* mutation. This is considered a **high frequency of *TET2* mutations** because these have been reported in age unselected cohorts of *de novo* AML at 8%³⁷ and 13%¹³¹. This second study also concluded these were closely associated with older age as they were present in 7% of the young patients (≤60y) and 24% in the older patients (>60y)¹³¹. Furthermore, new studies that applied the most recent targeted NGS analysis (which we used for comparison in results section 4.2) have also confirmed the substantially increased incidence of these mutations with age^{34,38}.

It was striking to find a high frequency of mutations in **spliceosome components**. We found unusual the number of mutations in *SRSF2* (23%) since at the time there was no comparable value. After our first report² other studies have found that the frequency of mutations in *SRSF2* reported by the early studies (~1%) was much lower than the ones found by panel NGS nowadays (6% or 10%)^{38,39}. Additionally, Eisfeld and colleagues³⁴ have reported a similar value (~21%) when looking at their group of older patients (≥60y). We believed this was explained by the low coverage of previous studies, which is believed to be due to the high CG content of the region with the most frequent mutation (Proline 95), this was also the assumption made by Papaemmanuil and colleagues³⁹ (when comparing to TCGA).

Furthermore, using our extensive target list, we identified several mutations in genes related to **DNA repair** that were not restricted to *TP53*. These genes included other DNA damage response and surveillance proteins such as BLM, BRIP1, XPC, ERCC2, ERCC3, ERCC4, ERCC5, BRCA2, FANCA, FANCC, FANCD2OS, FANCF, ATM, CHEK2, NBN, MSH6 and MLH1 (many of these mutations have been found in other tumor types). Furthermore, *TP53* was frequently mutated in SAL elderly AML (10%), a reasonable

expectation since an age association for this gene could be found in the TCGA cohort (increasing from 4% in TCGA young to 18% in TCGA elderly).

5.1.2 Factors for elderly AML poor prognosis

In the elderly AML, there are typically high frequencies of cytogenetic patterns of poor prognosis, which might help explain the dismal outcomes of these patients. The SAL elderly AML had rates of **CN-AML** not very different from younger cohorts. In turn, **CBF** samples or balanced abnormalities (of favorable prognosis) were not as frequent as in young, but high frequencies of **complex karyotypes** and **unbalanced rearrangements** (of unfavorable prognosis) were seen. Several papers^{34,40} published a bit before and right after our report¹ confirmed the congruence of this SAL elderly AML cytogenetic distribution. This includes the comparable amount of CN, the increase in complex karyotype and the low amount of CBF found in older patients that were later corroborated by Eisfeld and co-workers³⁴.

Since **cytogenetic characteristics** have been insufficient to explain elderly AML poor prognosis^{106,107} we had postulated that **specific genetic alterations** could correlate to the poor prognosis of these patients.

We found the main factor of elderly AML poor prognostic could be related to the frequency of mutations in specific genes, since we identified a high frequency of mutations in genes known as **poor prognostic predictors**: *DNMT3A*, *SRSF2*, *IDH1/2*, *RUNX1*, *TET2*, *ASXL1*, *TP53*, *BCOR* and noted the low frequency of mutations in genes typically correlated with **favorable outcomes**, *NPM1* and *CEBPA*.

We described this by comparing SAL elderly values to two particular studies, Metzeler and colleagues³⁸ and Eisfeld and colleagues³⁴. Although both sequenced using different NGS panels with smaller sets of genes, limiting some comparisons, they included many samples. We compared our resulting frequencies to both these studies keeping in mind each one has its own peculiarities in relation to ours. In the study of Metzeler and colleagues³⁸ only 68 genes were sequenced but 31 of them only in known hotspots. In the study by Eisfeld and colleagues³⁴, the samples were restricted to *de novo* AML and only 79 genes were sequenced using an NGS procedure.

There were several other **technical considerations** that advised for caution in these comparisons. Many of the genes sequenced in ours and these 2 studies do not have high mutation frequencies and do not allow proper analysis of the differential amount of mutations. Hence, there were low frequencies (which were in agreement with one or both this studies) that we included in results but we did not stress for fear these might be resulting of unknown selection bias due to the small number of patients in the SAL elderly AML, like *KRAS*, *NRAS*, *ZRSR2*, *GATA2*, *RAD21*, and *WT1*. Furthermore, some

mutations were not completely ascertained in SAL elderly AML and were not used, like *FTL3*-ITD. These eluded our attempts of determination using the Pindel algorithm and manual curations were not clear. We were confined to use the data provided by the diagnostic testing, obtained for 70 of the 93 patients. Similar problems do not allow the comparisons of the frequency of mutations in *MLL* since *MLL*-PTD is the most frequent mutation. Some new algorithms and changes to Pindel have been developed meanwhile^{39,149,150} and they might make it possible to include large mutations like these in a future analysis.

We mostly found tendencies of increasing or decreasing frequency of mutations with patients' age that have now been observed in other cohorts, except for the mutations in *NPM1*. There was an appreciable **low amount of *NPM1* mutations** found in the SAL elderly (16%) by using our strict criteria of considering only mutations in areas where the coverage was 30x and VAFs higher than 20% obtained by NGS. Other studies have found *NPM1* mutations much more frequent, age unselected cohorts having about 30% to 34% of mutations in *NPM1*^{38,34}. Since the tetranucleotide insertions (known as *NPM1c*) are prone to be missed due to the low coverage on this small insertion position, we did a manual evaluation of all samples and retrieved 2 mutations that were missed due to the low amount of fragments mapped to the region. The evaluation of *NPM1c* amplified by PCR and Sanger sequenced reclaimed another 2 mutations, that were not even visible in NGS, bringing our maximum number to 20 mutations (20/93=22%). Therefore, the low number of *NPM1c* mutations remains unexplained and a correlation of this gene with age is not established by others. Then again, it seems plausible this frequency would be low in elderly AML because these mutations do not usually co-occur with mutations in *ASXL1* and *RUNX1*, which are both increased in the SAL elderly AML.

The survival prognosis for patients with mutations in single genes (or combinations) that are **well-established survival factors** in non-elderly specific cohorts did not provide survival predictions in SAL elderly AML, except for the two strongest poor prognostic factors **complex cytogenetic** and the ***TP53* mutated**. On the one hand, our low power for these predictions might be a reason for this fact. On the other hand, other studies have also observed the **loss of several predictions in the older cohorts**, when using factors that have been seen in age unselected cohorts and in young cohorts. In their study, Tsai⁴⁰ and collaborators lacked the survival prediction of the double-mutation in *CEBPA*, the *RUNX1* and the *IDH2* mutations when using only the older patients. Their elderly retained only the good prognosis of *NPM1* mutated/*FLT3*-ITD wild-type vs other subtypes and the bad prognosis of *DNMT3A* and of *TP53* mutated. In contrast, in the study of Metzeler *et al.*³⁸ the bad prognosis of *DNMT3A* mutations was only observed in the young group and

the good prognosis of *NPM1* mutations was only seen in the older group. As a result, the combinations of mutations in *NPM1/DNMT3A* only had predictive value in the group of young patients. Additionally, the poor survival prediction of *RUNX1* mutations was also not observable in their group of older patients, while the good prediction of *biCEBPA* and the bad prediction of *TP53* mutated were observed independently of the age group³⁸. Therefore, it was not unthinkable that only the stronger prognostic factor seen in both these studies (*TP53* mutated) would show significant impact in survival probabilities in the SAL cohort.

A prognostic factor not lost in SAL elderly AML was the **WBC count**, which was a poor prognosis predictor at values as low as 35/nL, even when hyperleukocytosis is only deliberated for values superior to 100/nL. When using the WBC levels to divide the SAL elderly into two groups with different survival probability it revealed a correlation of $WBC \geq 35/nL$ to the presence of *NPM1* or/and *FLT3* mutations in samples and $WBC < 35/nL$ to the presence of *IDH1* mutations. This exposed the diverse nature of the two groups, possibly reflecting a higher proliferation rate of the disease with *NPM1* or/and *FLT3* mutations than with the *IDH1* mutated. A difference that would be reflected on the low survival probability of the high WBC group ($WBC \geq 35/nL$). This opposition between samples with mutations in *IDH1* vs *NPM1/FLT3* highlighted the heterogeneities that could be found amongst the SAL elderly AML.

5.1.3 Genomic classifications of elderly patients

We had indications elderly AML had **specific genetic patterns** due to the increased frequency of mutation in elderly AML, but the heterogeneity of the SAL elderly AML was not entirely different from younger cohorts. Elderly AML patients had known patterns of co-occurrence and mutual exclusions of specific mutations. The mutations in epigenetic regulators (both *IDHs* vs *TET2*) still mainly appeared once per patient and co-occurrence of mutations in splicing components was also nearly null. Elderly AML could also be divided into groups of **patients bearing similar genetic profiles** and these groups were quite relatable to the ones found in younger cohorts.

Using the new genetic-based classification of AML, proposed by Papaemmanuil and co-workers³⁹, we observed that the majority of our elderly AML patients fell into their class of **“AML with mutated chromatin/splicing regulators”** (instead of to class “*NPM1* mutated”). There were 34.4% of our patients that belonged to this class, with co-occurring mutations in *SRSF2*, *SF3B1*, *U2AF1*, *ZRSR2*, *ASXL1*, *BCOR*, *MLL*, *EZH2*, *PHF6* and *RUNX1* ($p=0.006$). Consistent with our results, in their study³⁹ this class (only 18% of their cohort) was correlated with older age but not with sAML samples. The prominence of these mutations was news at the time, but have now been confirmed in the mutational oncoprints

of several elderly cohorts^{34,38,151}. For a time most of these mutations were referred to as “secondary AML mutations” but according to our analysis (and in those studies also), the clinical definition of sAML does not reproduce the biological entity where these are present.

As previously mentioned, ***TP53*/aneuploidies** were also found in high frequency in elderly AML and this was the other genetically defined group that had been correlated to age³⁹. These particular mutational patterns are said to develop due to DNA instability of the stem cell progenitors since they are related to impairments of DNA repair. This characteristic of this AML class is pointed as the reason these clones are particularly difficult to eradicate.

In opposition, the ***biCEBPA* group** was not detected in SAL elderly AML and was 4% in the age unselected cohort used by Papaemmanuil and co-workers³⁹ to establish the genomic classification. In the SAL elderly cohort, *CEBPA* mutations were present but there was not homozygous and were present in different patients. This could be coincidental because the number of *biCEBPA* was expected to be low, any accidental bias in the SAL cohort could be responsible.

If the **general increase of mutations in elderly AML** was a product of random occurrences the many patterns of genetic classifications that are emerging in the younger cohorts would not have been present in elderly AML, which was not the case. This analysis pointed to the redundancy of mutations within the similar molecular functions and the possible molecular synergy among specific mutations, which was worth exploring.

5.1.4 Functional interactions of protein targets

Having identified 281 mutated genes in elderly AML we used clustering algorithms to group the genes into modules based on protein-protein interactions. This methodology enabled us to unravel pathway information using the functional relation between the proteins affected by mutations.

This exploration gave new insights, as it separated proteins into **groups with different functional properties**. These sub-networks identified molecular signatures of patients, with different overall survival probabilities, based on their mutational patterns in 2 of these sub-networks: NPM1/mRNA processing proteins or DNMT3A/DNA repair proteins.

The close relation of **DNMT3A and DNA repair proteins** that brought them into the same functional interaction module suggests a possible interaction of DNMT3A in DNA repair mechanisms. This possible functional role of DNMT3A in DNA repair has been recently explored by Guryanova and co-workers¹⁵², who showed impairment of DNA damage sensing mechanisms in *DNMT3A* mutated cells was a possible explanation for the treatment resistance observed in AML.

In contrast, the patients with ***NPM1* mutation and/or splicing regulators** seem to be less resistant to treatment in SAL elderly AML. A fact that is in line with the reports of favorable treatment response of elderly patients with *NPM1* mutations in groups of patients more than 60 or 70 years old (higher complete remission rates and longer overall survivals)^{38,103}, as we have mentioned. This was the only favorable prognostic factor found to be stronger in the elderly than in younger patients, has been validated in several other cohorts and found to be of special importance in the elderly AML^{38,153,154}. We speculated that because we had a good detection of *SRSF2* mutations (and a high number in elderly AML) the patterns of these groups became clear in the SAL elderly AML, despite our low statistical power.

We expected this biological characteristic to be **robust** and the result **reproducible**. In the TCGA cohort, we could replicate the main result by determining the bad prognosis of samples with *DNMT3A*/DNA repair mutations lacking mutations *NPM1*/mRNA processing proteins. This was attainable despite their low number of *SRSF2* (0.5%) and regardless of the composition of the cohort being restricted to *de novo* AML. Furthermore, the disparity of the survival probability of patients with mutations in DNA repair and *NPM1*/mRNA processing can also be evaluated by observing the decreasing survival probability of the 3 different genetic classes: “*NPM1* mutated” vs “chromatin/splicing regulators mutated” vs “*TP53*/aneuploidy” (see Figure 1.3.3) in the cohort from Papaemmanuil and co-workers³⁹.

5.1.5 Mutational progression into elderly AML

Last, we took notice that elderly AML mutation rates appeared to **reflect pre-existent alterations**, bearing high mutation rates in the chromatin, epigenetic and splicing regulators most of them **found in CHIP**. Since the genes, *DNMT3A*, *TET2*, *SRSF2*, *ASXL1*, *SF3B1*, *IDH1/2*, and *TP53* had increased frequencies of mutation in elderly AML and have previously been related to clonal hematopoiesis in the healthy elderly population^{10,11}. Moreover, these somatic mutations (in *IDH1*, *IDH2*, *TP53*, *DNMT3A*, *TET2* and spliceosome genes) were recently confirmed to be part of the **pre-malignant mutational landscape**, being present years before the development of AML and significantly increasing the risk of developing the disease¹⁵⁵. Also of note, not all genes formerly detected to be mutated in CHIP presented with an increased mutation rate in elderly AML (for example *GNAS* and *JAK2*). The **lack of enrichment of mutations in *JAK2*** in the elderly AML was especially surprising since this is a frequent mutation in CHIP (as frequent as *IDH2*, *TP53* or *ASXL1*, depending on the study). Although, in these studies, the mutations in this particular gene failed to show a trend to increase with age, while *TET2*, *ASXL1* and *SF3B1* were predominantly found in the oldest individuals with CHIP¹¹.

The presence of mutated epigenetic regulators in CHIP and elderly AML indicates the epigenetic changes might be preceding AML driver mutations in proliferative genes and contributing to the development of hematopoietic diseases.

Finally, in the elderly AML, some mutations in *DNMT3A*, *TET2*, *TP53*, and *RUNX1* had very high VAFs which denoted that in many blasts these were homozygous mutations (marked as LOH). This could be an indication that these mutations had **occurred very early** in the elderly AML development. In this case, it is important to highlight that *RUNX1* mutations are typically found in MDS but not usually found in CHIP¹¹.

All of this leaves unanswered questions about the course of development of elderly AML, for it can either evolve from undiagnosed MDS or develop directly from CHIP. But it definitely pointed to a correlation of the elderly AML disease to the increased epigenetic variability of HSC with age.

5.2 Epigenetic pattern of elderly AML

Since in general the methylomes are impacted by age¹⁵⁶ it was important to address the specificity of the elderly AML methylome, for this changes could contribute to the heterogeneity of the disease.

Thus, we compared the epigenetic profiles of elderly AML with a group of younger patients. We combined the methylation profiles of our cohort with the TCGA cohort methylation profiles, providing power for the comparisons between the two age groups. Due to the robustness of the Illumina 450K assay and the available normalization algorithms we experienced **no difficulties in integrating the data** we obtained for SAL elderly AML with the TCGA data.

We segregated patients into a group of elderly AML (≥ 65 years) and a group of young AML (< 65 years) and used these to determine DMRs. Elderly AML revealed a low number of DMRs showing no strong bias for hypermethylation vs hypomethylation, exposing the **moderate effects of the categorical age** in the AML epigenetic pattern. The elderly vs young AML had several DMRs located -5kb to 1kb distance from gene promoters. Elderly patients had lower levels of DNA methylation in 244 genes, from which 12 were related to cellular carbohydrate metabolic processes (GO:0044262), and had higher levels of DNA methylation in 91 genes, from which 17 were functionally related to biological adhesion (GO:0022610). Furthermore, both these DMRs have many genes annotated to regulation of metabolic process (GO:0019222).

Although these biological functions have been related to aging²⁴ in our analysis of the DMRs of the elderly AML **we did not find the age-related CpGs** referenced in other reports^{157,158,159}. These age-related CpGs were CpGs with clear correlations between DNA methylation levels and donors age that others found using data from whole blood samples^{157,158,159}. In fact, it was shown that age-related CpGs suffer an almost linear hyper- or hypomethylation that allowed the construction of models using them to estimate chronological age¹⁵⁹. We particularly did not find the three CpGs from the model in Weidner *et al.*¹⁶⁰ that demonstrated these were enough to estimate biological age in blood.

Upon further analysis, we found that several of our unsupervised hierarchical clustering of these epigenetic profiles resulted in the separation of patients into two groups with strong statistical differences in age. This showed that the elderly AML patients have **distinctive epigenetic patterns associated with age**, which was a strong feature in the analysis of the CpGs in promoters. The group of patients with the majority of elderly samples, formed in this manner, was denominated cluster of elderly and used to probe the differences between these AML diseases. The analyses showed that epigenetic patterns of AML **decoupled from age according to patterns** related to genetic characteristics.

We observed the specific age-related signature of DNA methylation at promoters was significantly correlated to several mutations, being positively correlated with mutations *IDH1/2*, *RUNX1* and *ASXL1*, as samples with these mutations were almost exclusively in the cluster of the elderly.

These previous observations were in line with the report of Lin and Wagner¹⁵⁷. They did a systematic examination of age-associated DNA methylation patterns of 25 cancers using TCGA data¹⁵⁷. The results clearly indicated that epigenetic patterns of the **categorical age were abrogated in cancers tissues**. They found AML, in particular, lacked any CpG methylation levels with a good correlation to patients' age¹⁵⁷. They further report that CpGs hypermethylated upon aging in non-malignant tissues were coherently modified in a non-stochastic manner in AML depending on mutations¹⁵⁷. Higher **age-predictions were associated with mutations** in *RUNX1*, *WT1*, and *IDH2*, and younger age-predictions were predicted in *TET2*, *TP53*, mutations and *PML-RARA* fusions¹⁵⁷.

Knowing this, we used the cluster of the elderly as the **epigenetically defined group of elderly AML** for further explorations. We noticed the cluster of the elderly AML had more hyperMRs than hypoMRs, but in general, in the whole blood of older age healthy donors, the number of hypomethylated CpGs supplants hypermethylated CpGs¹⁵⁷. Furthermore, the hyperMRs of the cluster of elderly had no clear relation to promoters but the hypoMRs were enriched in promoter regions (with 61% of the hypoMRs while in the 450K assay only 20% of the CpGs are annotated to promoters). While for whole blood age-related hypermethylations were the ones significantly enriched in gene promoter regions, whereas hypomethylations occurred rather outside of gene promoters¹⁵⁷.

5.2.1 Pathways involved in elderly AML epigenetics

The combined cohort revealed a specific elderly AML epigenetic signature (quite dissimilar from young AML) that was not just driven by physiologic changes in age-associated CpGs. In turn, genes potentially affected by differential methylation between the elderly and the young were enriched in **cellular components connected to age** (for example extracellular matrix and cytoplasmic vesicles components) and in **genes connected to AML phenotypes** (mainly *HOX* genes and myeloid differentiation regulators).

This distinction of the DNA methylation changes that are attributed to age or attributed to cancer is not clear because of the **overlap between age-associated CpGs and cancer-associated CpGs**¹⁶¹. After an effort to dissect this effects Wang *et al.*¹⁶¹ concluded: "*Genes only differentially methylated in aging⁽ⁱ⁾ were mainly enriched in Golgi vesicle transport and regulation of cellular metabolic process. Genes only differentially methylated in cancer⁽ⁱⁱ⁾ were enriched in immune response, defense response and*

response to wounding. While overlapped⁽ⁱⁱⁱ⁾ genes were primarily involved in cell-cell signaling, cell adhesion and neuron differentiation, etc.”¹⁶¹. Our analysis found many gene enrichments with biological/cellular functions related to the ones in their report: (i) regulation of biosynthetic/metabolic process and cytoplasmic vesicle (aging); (ii) inflammatory response, phagocytosis and endocytosis (cancer); (iii) cell-cell signaling, synapse and cell junctions, forebrain and hindbrain development (overlapped).

The genes related to the DMRs in our list could be responsible for elderly AML specific phenotypes **if their expression is altered in the elderly** vs the young patients.

However, none of them were reported in the work of Lin and Wagner¹⁵⁷, which had a very **short list of genes** (n=11) **differently expressed** between two age groups (elderly when compared to the young), obtained by using the RNA-seq from the original TCGA cohort. Ten of them were higher expressed in the older group (*C7orf13*, *CLU*, *DSC2*, *FAM127A*, *FAM127B*, *JAG1*, *LOC644538*, *NHLRC1*, *TEKT2*, and *TTC12*) and only *NEXN* (Nexilin F-Actin Binding Protein) was less expressed. Interestingly from those 10, only the gene *C7orf13*[*MY040*] was present, but in our list of genes with hyperMRs in the elderly. This RNA gene from the class of non-coding RNAs has recognized involvement in the regulation of endocytosis¹³⁶. The phenotype of low expression of *C7orf13* (achieved by siRNA in HeLa cells) is decreased transferrin endocytosis and decreased endosome-nucleus distance (endosomes clustered in the perinuclear region)¹⁶². We observed that for many genes with marked high methylation levels in the elderly AML this was a phenotype attributed to their low expression.

In addition, another study dissected the **age-specific biology of AML** by analysing the gene expression of gene-sets that constitute signatures of specific pathways¹⁰⁸. Applying this methodology, Rao *et al.*¹⁰⁸ determined older patients with AML had a **lower probability** of E2F and PI3K pathway activation but a **higher probability** of RAS, TNF, Src, and epigenetic stem-cell signature pathway activation¹⁰⁸. These were not the pathways found to be especially enriched in our lists of genes with DMRs for the elderly AML (compared to younger AML). Contrary to the Rao *et al.*¹⁰⁸ study, our result found *TNF* to be hypermethylated in the elderly AML samples, which indicates the probability was for low activation of the TNF pathway in this samples.

These **lack of direct correlations** were an indication the relation between gene expression and DNA methylation is not easily deducted in AML, a fact that is a well-known problem, usually attributed to the high complexity of gene regulation processes.

5.2.2 Regions, genes and prognosis predictions of elderly AML

We thought the distribution of DMRs across chromosomes could hold some information about the epigenetic difference between elderly and younger samples. We

found most regions with very high methylation levels in samples of elderly patients (hyperMRs) were **localized at the ends of chromosomes**. This result was thought-provoking since we could not find a good explanation for the observation, two hypothesis could be put forward.

The first idea was, the tips of chromosomes in the elderly AML could be protected by **shorter telomeres** and therefore be different in elderly patients when compared to young. This could be due to telomere shortening in the aged progenitor cells¹⁶³ that give rise to the elderly AML. The telomeres have been found to be involved in loops with genes located up to 10Mb from the tips of chromosomes of human myoblasts and fibroblasts¹⁶⁴. This 3D conformation of DNA is modified when the telomere changes in length, affecting the expression of genes in the region¹⁶⁴. Since the position of the hyperMRs in chromosome tips was mostly within these 10Mb regions this could indicate we were picking up on different DNA conformations as a result of telomeres shortening.

Another possibility was, that the elderly AML blasts have compromised **boundaries of subtelomeric regions**, which again could be coming from aged progenitor cells that give rise to the elderly AML. A fact with no precedent, as the existence of a boundary to the subtelomeric regions was only recently postulated in *S. pombe*¹⁶⁴, where it was found to protect the genes in the tip of chromosomes from a heterochromatin spread, which results in gene silencing¹⁶⁴. Since our hyperMRs regions were not restricted to subtelomeric regions (telomere-adjacent regions of approximately 500Kb¹⁶⁵), but they seem to be mostly concentrated in the immediate proximity of subtelomeric regions, this would be a plausible reason.

Taking a further look at the hyperMRs in the elderly AML group there was a region within chromosome 17 that called to attention. Not only for its **uncommonly big size** but also because it overlapped several genes associated to **cellular processes of metabolism, endocytosis and cell adhesion**, many of these proteins being associated to the organization of the actin cytoskeleton. This was remarkable for these were the 3 processes that were strongly implicated in **stroma-leukemia interaction**²⁶. They were found to be deregulated in both the transcriptional and the DNA methylation signatures of the mesenchymal stromal cells from the BM of AML patients (when compared to the BM of healthy people)²⁶. Since there have been indications that interactions between HSC and stroma in the niches can influence HSCs^{5,27} it is conceivable that elderly AML blasts are more affected by the environment of the abnormal niche.

Also noteworthy, the hypermethyations in *RPTOR* (regulator of mTOR) and *BAIAP2* (regulator of CDC42) implicate mTOR pathway and cell polarity in the distinction of elderly AML for young AML. Both mechanisms have been highlighted as **cell-intrinsic**

mechanisms that contribute to the phenotypes of aged HSCs³. This indicated that the altered region of chromosome 17 could be reflecting the origin of elderly AML from HSCs affected by age.

We inspected the list of regions with differential methylation levels in elderly AML for genes with **known associations to age and/or cancer**. Therefore, we searched the literature for corroborations that specific genes could be implicated in AML pathophysiology and/or specific age phenotypes. Lastly, we observed if certain levels of DNA methylation were associated with genes that have previously been **correlated to poor survival in AML**. We detected some DMRs are consistent with other reports which could introduce particular genes as good candidates for further study. However, the majority of DMRs of the elderly AML were not cited in literature or were contrary to expectations.

We found **some candidate genes** in genes that are **related to age**. Due to the lack of correlation of DNA methylation levels to the age of patients with AML (that we have discussed) we expected not many of the genes that distinguish the elderly AML epigenetic profile for the younger AML would have been related to age. We found 7% of the genes in the GenAge database were genes related to DMRs of the elderly cluster (vs the young cluster).

We thought the **differential methylation in *ESR1*** (which encodes the estrogen receptor 1) might be significant since this has been related to age and cancer. It was hypermethylated in the BM of AML patients vs healthy people¹³⁷ and was the first shown to become hypermethylated in colon with increasing age¹⁶⁶. As we already mentioned, to label genes as age or cancer related is not easy since it is not a trivial distinction. Horvath *et al.* summed-up cancer vs age DNA methylation changes in this concise sentence: *“Important cancer-related genes become hypermethylated during aging, including those encoding the estrogen receptor, insulin growth factor, and E-cadherin, and key developmental genes”*¹⁵⁸. Therefore *ESR1* was already a known overlap of DNA methylation changes related to age and cancer.

In the study of Bullinger *et al.*¹³⁷ (where *ESR1* was also found hypermethylated in AML) the high levels of *ESR1* methylation among AML patients were found to be a strong poor prognosis predictor¹³⁷. On the contrary, our analysis determined that *ESR1* had a region before the gene coding region with low methylation levels in the elderly group of patients (that accordingly had lower survival probability) and TCGA patients with higher expression of this receptor were the ones with the unfavorable prognosis. The discrepancy is of unclear significance and would merit further investigation.

Therefore, from our age and cancer list, we would emphasize the **differential methylation of a region in SOCS2** (which was lower in elderly patients) that was accompanied by the corroboration that **high expression of the gene constitutes a poor prognosis** predictor in the TCGA AML cohort. SOCS2 expresses a protein connected to the insulin signaling pathway and is a feedback inhibitor of the JAK-STAT cascade¹³⁶. Both pathways are very connected to leukemic diseases, namely AML and ALL. High SOCS2 expression was shown to be part of the molecular signature of the most primitive HSCs and was linked to AML subsets of unfavorable outcome^{94,167}. This was consistent with our results making this **one of the candidates with more potential** for exploration as a prognosis marker.

We could find several genes that other studies found to have **epigenetic marks characteristic of AML** when compared to healthy samples. We should highlight among these were *KIAA1447* and *FSCN2*, genes in the highly methylated region of the tip of chromosome 17. The corroboration with the study of Bullinger *et al.* offered us a substantial suggestion that the many hypermethylations in this region might be **physiologically relevant for AML phenotypes**.

Many **survival markers** have been suggested in AML, several of these were based in DNA methylation levels defining AML groups with poor survival (see Table 1.4.1). While these studies could not confirm each other's biomarkers of poor survival prognosis, many of these genes were found in our DMR lists. The biggest commonality was with the Marccuci *et al.*⁹⁵ study, through 22 genes with epigenetic marks. Most importantly this overlap included 3 (*CD34*, *SCRN1*, *F2RL1*) of the 7 genes score (*CD34*, *RHOC*, *SCRN1*, *F2RL1*, *FAM92A1*, *MIR155HG*, and *VWA8*) identified in their study. Notably, in their study⁹⁵, all 7 had both promoter low methylation and high gene expression associated with low overall survival⁹⁵.

Therefore, we found several genes with suggested involvement in the elderly AML pathogenesis that could be developed into prognostic markers in AML. The low DNA methylation levels of ***F2RL1*, *HIVEP3* and *SOCS2*** were **particularly interesting** because, besides having been found by others, we could confirm their high gene expression was associated with low overall survival in the TCGA cohort.

Collectively the results of the DMR analysis showed many genes could be valuable biomarkers of elderly AML. The prediction value of these differential DNA methylation levels will have to be further evaluated in other cohorts. **Confirmation studies are needed** in order to design potential therapies using these targets to specify treatment strategies to elderly patients.

5.3 Interconnected genetic and epigenetics

We also examined the possible **roles of genetic alterations in the general epigenetic patterns** of AML by observing the integrated genetic and epigenetic profiles.

We found the **cluster defining genetic lesions** in our unsupervised clustering of epigenetic levels in promoters were **similar** to the descriptions in the TCGA report³⁷. Most notably, similar groups were perceived using the genomic regions annotated as CpC-sparse regions. In both cases there were groups with similar lesions bearing defined epigenetic profiles, *IDH1/2* mutated, CBF samples, or co-mutated *DNMT3A/NPM1/FLT3*. In our analysis, these groups were possibly more pronounced due to the added samples.

Furthermore, the correlation between genetic lesions and DNA methylation defined groups as seen in Glass *et al.*⁹¹ was **partially comparable to our findings**. Unsupervised clustering of DNA methylation levels in the SAL elderly and TCGA cohorts showed some **analogous molecular groups**. For example, the triple mutated *DNMT3A/NPM1/FLT3* group they termed *DNMT3A* and the CBF they termed *Inv(16)*. But we could not confirm the existence of an epigenetic group with *NPM1/FLT3* (they termed *NPM1*) and there was no segregation of *IDH1* vs *IDH2* mutations into the 2 different groups (that they termed *IDH1/DNMT3A* and *IDH2*). Instead, the integrated cohorts (SAL elderly and TCGA) demonstrated the existence of an epigenetic profile that defined a group with ***IDH1/2* mutations combined**. Additionally, we found **other epigenetic groups** like the one with **complex samples**, not found in Glass *et al.*⁹¹. They missed this possibly due to the composition of their cohort that only included 3% of complex samples while our integrated cohorts (SAL elderly and TCGA) had about 13%. Not surprisingly, they did not report a good separation of young and elderly epigenetic profiles since they had only 12% of patients 60 years or older. Hence, comparisons are limited since some of the differences between the epigenetic classifications found using these cohorts might be due to their fundamentally different age composition.

5.3.1 DNA instability features of elderly AML

Notably, with this extended dataset the epigenetic profiles of the samples from elderly AML patients could be associated to mutations in *IDH1/2* or *TP53* or *IDH1/DNMT3A* and connected to Group C. This indicated that elderly samples were epigenetically comparable to samples with genetic profiles **suggestive of low DNA stability**. Not only because of the mutations in *DNMT3A* and DNA repair proteins (that we previously mentioned connected to group C) but also because of the many *IDH1* mutations. The latter

were recently shown to affect the expression of ATM and create a situation of low DNA stability through this defect in DNA damage repair⁸⁰.

Moreover, the **shores of CpG islands** have revealed good correlations to gene expression in many cancer types. In AML they have produced tight patterns of methylation that were defined by specific genetic alterations as was seen by Glass *et al.*⁹¹ using a new whole-genome approach. Therefore, we decided to analyse the epigenetic profiles of CpG in island shores using the 450,000 CpGs we had available. The profiles revealed similar conclusions to the analysis of promoters but **showed more clearly the epigenetic similarities** of the elderly samples with the samples of complex/*TP53* group, independently of *IDH* mutations.

In addition, some proteins connected to DNA repair were differently affected in the cluster of the elderly, with hypermethylated regions associated to *RAD52*, *RAD23A*, *XRCC3*, *TP63* and *MGMT* and a hypomethylated region related to *TP73*.

All these epigenetic observations matched the assumption drawn from the genetic identity of the elderly AML samples that had already pointed to the **similarities of these samples to samples with impaired DNA repair**. These conjectures highlighted another possible reason for the resistance to treatment and consequently the bad prognosis perceived in the elderly AML.

5.3.2 Methylation profiles within SAL elderly AML

In other AML cohorts distinct methylation patterns have been described for different molecular and cytogenetic groups (including for samples with mutations in *NPM1*, *CEBPA*, *IDH1/2*, *DNMT3A* or *RUNX1*)^{89,168}, therefore we expected **distinct epigenetic signatures** to exist in the SAL elderly AML. Upon dissection of the DNA methylation profiles of elderly AML we found distinct signatures of samples with **mutations in epigenetic regulators** *IDH1/2* and *DNMT3A*.

These two signatures, with **divergent methylation patterns**, revealed distinct biological functions over-represented among the genes aberrantly methylated. While *DNMT3A* mutations were only associated to differential methylation on members of the HOX family⁶⁶, patients with mutations in *IDHs* had a **stronger signature**, with DMRs localized in genes of transcription factors that are important in differentiation of the myeloid lineage⁷⁹, but also in genes of other biosynthetic and metabolic processes. The restricted amount of DMRs found for samples with *DNMT3A* mutations could be due to effects of the alternation of commutations in *IDH1/2* or in *NPM1/FLT3*. Whereas the signature of *IDH1/2* mutations was stronger **despite the split between samples** with or without *DNMT3A* mutations.

Last of all, in the case of *NPM1* and/or *FLT3* mutated samples (vs the respective non-mutated) several DMRs could be found, even though these proteins are not known for being direct influencers of DNA methylation. No inferences were made from this for the cause is unclear since the large majority of these samples also bear mutations in *DNMT3A*.

We concluded, DNA methylation profiles for samples with specific mutations that have been described in younger cohorts using other techniques like HELP^{79,89} and ERRBS⁹¹, but also the 450K array⁶⁶, were **comparable to the findings in the SAL elderly AML**. The presence of *DNMT3A* mutations had been previously connected to hypomethylations in HOX genes⁶⁶, while the *IDH* mutations were previously correlated to many hypermethylations⁷⁹.

5.3.3 Specific targets in elderly AML

Finally, we would like to remark, these genetic and methylation analyses underscored the **interconnection of regulatory mechanisms in elderly AML**. Due to the unresponsiveness of elderly AML to intense chemotherapy, these profiles hold important information for the design of more attractive treatment regimens for this group of patients.

(i) Based on the high frequency of mutations in epigenetic regulators in the elderly AML, the use **hypomethylating agents**^{101,169} need to be explored more sophisticatedly. This will include studies testing combinational therapies that are currently under assessment^{170,171}. On the other hand, patients within the major genetic subgroup, with mutations in chromatin and splicing regulators, should be correlated to treatment response, since these mutations are also observed in MDS where azacitidine and decitabine treatments (demethylation agents) have shown promising results^{172,173}.

(ii) Due to the high prevalence of mutations in *IDH1/2* and their very particular epigenetic signature, the use of specific **IDH inhibitors**^{69,174,175} is of high relevance specifically for elderly AML. This is now possible since the recent approval of Enasidenib⁷³.

(iii) As several differentiation pathways were strongly affected by hypermethylation, elderly AML patients may benefit from **differentiation therapy**. Interestingly, all-trans-retinoic acid was shown to induce myeloid differentiation in *IDH* mutated AML¹⁷⁶ and might still be an alternative in the elderly.

(iv) Since the elderly samples were genetically and epigenetically correlated to DNA instability perhaps treatment of elderly AML should be adapted accordingly. The possibilities of obtaining synthetic lethality by **targeting DNA damage response pathways** that are underway should be applied to elderly AML (PARP, ATR, ATM, CHK or DNA-PK inhibitors)¹⁷⁷. The poly(ADP-ribose) polymerase (PARP) inhibitor olaparib has

already shown therapeutic benefits in BRCA-mutant ovarian and breast cancer¹⁷⁸ and induction of apoptosis of AML *in vitro*¹⁷⁹.

Until enough data about specific treatments that would benefit elderly AML can be defined studies like ours should be taken into account since it at least they imply that **not all elderly patients with AML should be treated equal**. While some elderly patients share genetic and epigenetic profiles with younger patients (and would clearly benefit from treatments applied to younger patients), most patients show an elderly AML with genetic and epigenetic reasons for treatment resistance and would **need a different approach**. Therefore, a first step would be to use studies like ours to insert patients into specific groups, defined by **integrated genetic and epigenetic data**, and allow patients not be excluded from treatment only on the bases of age and fitness.

Further advances in treatment will surely be accomplished by confirming and finding additional evidence of the **heterogeneity** and the **specificity** of elderly AML.

CHAPTER 6. CONCLUSION

The main aim of this study was to develop a feasible approach to find the specificity of AML in the elderly that might be contributing to its distinct poor prognosis. We investigated genetic alterations and global epigenetic changes in elderly AML and found both these rigorous determinations were necessary to define a specific molecular profile for elderly AML.

We concluded, elderly AML is a specific entity that harbors specific characteristic genetic and epigenetic patterns, which likely contribute to the treatment resistance in this disease entity.

We found a high frequency of genetic alterations in spliceosome components, epigenetic regulators and in DNA repair factors, the latter being associated with poor prognosis. The molecular categorization of elderly AML into groups according to mutation patterns in DNMT3A/DNA repair or NPM1/RNA processing proteins underscored its distinct biology.

Epigenetic landscapes also separated elderly AML into a particular leukemic group with distinct DNA methylation levels in many gene promoter regions. In general, the disease showed epigenetic similarities to samples of high DNA instability, like samples with complex karyotypes and the samples of a major epigenetic subgroup formed by *IDH1/2* (and/or *DNMT3A* mutants). Methylation levels of regions correlated to elderly AML showed dependencies not only on age but also on two particular genetic groups (*IDH1/2* or *DNMT3A/NPM1/FLT3*). At least an extended region on the tip of the long arm of chromosome 17 could be particularly correlated to poor survival probability.

The CpGs with particular methylation levels for the elderly AML entity overlapped genes known to be involved in age, cancer and particularly AML pathogenesis. Several of them showed potential to be developed into epigenetic-based prognosis markers.

After this last 2 years, with our data and data gathered by others, the field can consider a new view of elderly AML. Agreeing that age is a determinant of elderly AML biology and treatment response because it is connected to specific genetic and epigenetic profiles with its own complexity.

We hope our characterization of genetic and epigenetic patterns of the specific elderly AML group may guide the future development of new strategies to adapt treatments of this unfavorable AML entity.

REFERENCES

1. Silva, P. *et al.* Acute myeloid leukemia in the elderly is characterized by a distinct genetic and epigenetic landscape. *Leukemia* **31**, 1640–1644 (2017).
2. Silva, P. *et al.* Acute myeloid leukemia in the elderly is characterized by a distinct genetic and epigenetic landscape. *Blood* **126**, (2015).
3. De Haan, G. & Lazare, S. S. Aging of hematopoietic stem cells. *Blood* **131**, 479–487 (2018).
4. Busch, K. *et al.* Fundamental properties of unperturbed haematopoiesis from stem cells in vivo. *Nature* **518**, 542–546 (2015).
5. Pang, W. W. *et al.* Human bone marrow hematopoietic stem cells are increased in frequency and myeloid-biased with age. *Proc. Natl. Acad. Sci.* **108**, 20012–20017 (2011).
6. Wilson, N. K. *et al.* Combined Single-Cell Functional and Gene Expression Analysis Resolves Heterogeneity within Stem Cell Populations. *Cell Stem Cell* **16**, 712–724 (2015).
7. Notta, F. *et al.* Distinct routes of lineage development reshape the human blood hierarchy across ontogeny. *Science* **351**, aab2116 (2016).
8. Sonia Nestorowa,* Fiona K. Hamey,* Blanca Pijuan Sala, Evangelia Diamanti, Mairi Shepherd, Elisa Laurenti, Nicola K. Wilson, David G. Kent, and B. G. & Ottgens. A single-cell resolution map of mouse hematopoietic stem and progenitor cell differentiation. *Blood J.* **128**, (2016).
9. Paul, F. *et al.* Transcriptional Heterogeneity and Lineage Commitment in Myeloid Progenitors. *Cell* **163**, 1663–1677 (2015).
10. Jaiswal, S. *et al.* Age-Related Clonal Hematopoiesis Associated with Adverse Outcomes. *N Engl J Med December* **25**, 2488–2498 (2014).
11. Xie, M. *et al.* Age-related mutations associated with clonal hematopoietic expansion and malignancies. *Nat. Med.* **20**, 1472–1478 (2014).
12. Kelly, L. M. & Gilliland, D. G. Genetics of myeloid leukemias. *Annu. Rev. Genomics Hum. Genet.* **3**, 179–198 (2002).
13. Welch, J. S. *et al.* The Origin and Evolution of Mutations in Acute Myeloid Leukemia. *Cell* **150**, 264–278 (2012).
14. Shlush, L. I. *et al.* Identification of pre-leukaemic haematopoietic stem cells in acute leukaemia. *Nature* **506**, 328–333 (2014).
15. Corces-Zimmerman, M. R., Hong, W.-J., Weissman, I. L., Medeiros, B. C. & Majeti, R. Preleukemic mutations in human acute myeloid leukemia affect epigenetic regulators and persist in remission. *Proc. Natl. Acad. Sci.* **111**, 2548–2553 (2014).
16. Moriya, K. *et al.* Development of a multi-step leukemogenesis model of mll-rearranged leukemia using humanized mice. *PLoS One* **7**, (2012).
17. Greaves, M. F. & Wiemels, J. Origins of chromosome translocations in childhood leukaemia. *Nat. Rev. Cancer* **3**, 639–649 (2003).
18. Nowell, P. C. The clonal evolution of tumor cell populations. *Science* **194**, 23–8 (1976).
19. Anderson, K. *et al.* Genetic variegation of clonal architecture and propagating cells in leukaemia. *Nature* **469**, 356–361 (2011).
20. Hirsch, P. *et al.* Genetic hierarchy and temporal variegation in the clonal history of acute myeloid

- leukaemia. *Nat. Commun.* **7**, 12475 (2016).
21. Jan, M. *et al.* Clonal evolution of preleukemic hematopoietic stem cells precedes human acute myeloid leukemia. *Sci. Transl. Med.* **4**, (2012).
 22. Bernitz, J. M., Kim, H. S., MacArthur, B., Sieburg, H. & Moore, K. Hematopoietic Stem Cells Count and Remember Self-Renewal Divisions. *Cell* **167**, 1296–1309.e10 (2016).
 23. Florian, M. C. *et al.* Cdc42 activity regulates hematopoietic stem cell aging and rejuvenation. *Cell Stem Cell* **10**, 520–530 (2012).
 24. López-Otín, C., Blasco, M. A., Partridge, L., Serrano, M. & Kroemer, G. The hallmarks of aging. *Cell* **153**, (2013).
 25. Dykstra, B., Olthof, S., Schreuder, J., Ritsema, M. & de Haan, G. Clonal analysis reveals multiple functional defects of aged murine hematopoietic stem cells. *J. Exp. Med.* **208**, 2691–2703 (2011).
 26. von der Heide, E. K. *et al.* Molecular alterations in bone marrow mesenchymal stromal cells derived from acute myeloid leukemia patients. *Leukemia* **31**, 1069–1078 (2016).
 27. Zambetti, N. A. *et al.* Mesenchymal Inflammation Drives Genotoxic Stress in Hematopoietic Stem Cells and Predicts Disease Evolution in Human Pre-leukemia. *Cell Stem Cell* **19**, 613–627 (2016).
 28. Busque, L. *et al.* Recurrent somatic TET2 mutations in normal elderly individuals with clonal hematopoiesis. *Nat. Genet.* **44**, 1179–81 (2012).
 29. Genovese, G. *et al.* Clonal Hematopoiesis and Blood-Cancer Risk Inferred from Blood DNA Sequence. *N. Engl. J. Med.* **371**, 2477–2487 (2014).
 30. O'Donnell, M. R. *et al.* Acute Myeloid Leukemia, Version 3.2017, NCCN Clinical Practice Guidelines in Oncology. *J. Natl. Compr. Canc. Netw.* **15**, 926–957 (2017).
 31. Siegel, R. L., Miller, K. D. & Jemal, A. Cancer statistics, 2017. *CA. Cancer J. Clin.* **67**, 7–30 (2017).
 32. Bennett, J. M. *et al.* Proposals for the Classification of the Acute Leukaemias French- American-British (FAB) Co- operative Group. *Br. J. Haematol.* **33**, 451–458 (1976).
 33. Arber, D. A. *et al.* The 2016 revision to the World Health Organization classification of myeloid neoplasms and acute leukemia. *Blood* **127**, 2391–2405 (2016).
 34. Eisfeld, A.-K. *et al.* The mutational oncoprint of recurrent cytogenetic abnormalities in adult patients with de novo acute myeloid leukemia. *Leukemia* **31**, 2211–2218 (2017).
 35. Grimwade, D., Ivey, A. & Huntly, B. J. P. Molecular landscape of acute myeloid leukemia in younger adults and its clinical relevance. *Blood* **127**, 29–41 (2016).
 36. Döhner, H. *et al.* Diagnosis and management of AML in adults: 2017 ELN recommendations from an international expert panel. *Blood* **129**, 424–447 (2017).
 37. Cancer, T. & Atlas, G. Genomic and Epigenomic Landscapes of Adult De Novo Acute Myeloid Leukemia The Cancer Genome Atlas Research Network. *N. Engl. J. Med.* **368**, 2059–74 (2013).
 38. Metzeler, K. H. *et al.* Spectrum and prognostic relevance of driver gene mutations in acute myeloid leukemia. *Blood* **128**, 686–698 (2016).
 39. Papaemmanuil, E. *et al.* Genomic classification and prognosis in acute myeloid leukemia. *N Engl J Med* **374**, 2209–2221 (2016).
 40. Tsai, C.-H. *et al.* Genetic alterations and their clinical implications in older patients with acute myeloid leukemia. *Leukemia* **30**, 1485–92 (2016).
 41. Isaacson, P. *et al.* *World Health Organization Classification of Tumours. Pathology and Genetics of Tumours of Haematopoietic and Lymphoid Tissues. World Health Organization Classification of Tu-*

mours: Pathology and Genetics of Tumours of Haematopoietic and Lymphoid Tissues. Lyon, France: IARC Press; 2001. Jaffe ES, Harris NL, Stein H, Vardiman JW, eds. World Health Organization Classification of (2001).

42. Vardiman JW, Thiele J, A. D. E. A. The 2008 revision of the WHO classification of myeloid neoplasms and acute leukemia: rationale and important changes. *Blood* **114**, 937–952 (2008).
43. Döhner, H., Weisdorf, D. J. & Bloomfield, C. D. Acute Myeloid Leukemia. *N. Engl. J. Med.* **373**, 1136–1152 (2015).
44. Appelbaum, F. R. *et al.* Age and acute myeloid leukemia. *Blood* **107**, 3481–3485 (2006).
45. Juliusson, G. *et al.* Age and acute myeloid leukemia: Real world data on decision to treat and outcomes from the Swedish Acute Leukemia Registry. *Blood* **113**, 4179–4187 (2009).
46. Juliusson, G. Older patients with acute myeloid leukemia benefit from intensive chemotherapy: An update from the swedish acute leukemia registry. *Clin. Lymphoma, Myeloma Leuk.* **11**, S54–S59 (2011).
47. Döhner, H. *et al.* Diagnosis and management of acute myeloid leukemia in adults: Recommendations from an international expert panel, on behalf of the European LeukemiaNet. *Blood* **115**, 453–474 (2010).
48. Stone, R. M. *et al.* Phase III open-label randomized study of cytarabine in combination with amonafide L-malate or daunorubicin as induction therapy for patients with secondary acute myeloid leukemia. *J. Clin. Oncol.* **33**, 1252–1257 (2015).
49. Lindsley, R. C. *et al.* Acute myeloid leukemia ontogeny is defined by distinct somatic mutations. *Blood* **125**, 1367–1376 (2015).
50. Patel, J. P. *et al.* Prognostic Relevance of Integrated Genetic Profiling in Acute Myeloid Leukemia. *N. Engl. J. Med.* **366**, 1079–1089 (2012).
51. Bullinger, L., Döhner, K. & Döhner, H. Genomics of acute myeloid leukemia diagnosis and pathways. *J. Clin. Oncol.* **35**, 934–946 (2017).
52. Kantarjian, H. Acute myeloid leukemia-Major progress over four decades and glimpses into the future. *Am. J. Hematol.* **91**, 131–145 (2016).
53. Özpolat, B. Acute promyelocytic leukemia and differentiation therapy: molecular mechanisms of differentiation, retinoic acid resistance and novel treatments. *Turk J Hematol* **26**, 47–61 (2009).
54. Marchwicka, A., Cebrat, M., Sampath, P., Snieżewski, L. & Marcinkowska, E. Perspectives of differentiation therapies of acute myeloid leukemia: the search for the molecular basis of patients' variable responses to 1,25-dihydroxyvitamin d and vitamin d analogs. *Front. Oncol.* **4**, 125 (2014).
55. Nazha, A. *et al.* Clofarabine, idarubicin, and cytarabine (CIA) as frontline therapy for patients ≤60 years with newly diagnosed acute myeloid leukemia. *Am. J. Hematol.* **88**, 961–966 (2013).
56. Hills, R. K. *et al.* Addition of gemtuzumab ozogamicin to induction chemotherapy in adult patients with acute myeloid leukaemia: a meta-analysis of individual patient data from randomised controlled trials. *Lancet Oncol.* **15**, 986–996 (2014).
57. Borthakur, G. *et al.* Treatment of core-binding-factor in acute myelogenous leukemia with fludarabine, cytarabine, and granulocyte colony-stimulating factor results in improved event-free survival. *Cancer* **113**, 3181–3185 (2008).
58. Kottaridis, P. D. *et al.* The presence of a FLT3 internal tandem duplication in patients with acute myeloid leukemia (AML) adds important prognostic information to cytogenetic risk group and response to the first cycle of chemotherapy: Analysis of 854 patients from the United King. *Blood* **98**, 1752–1759 (2001).
59. Stone, R. M. *et al.* Midostaurin plus Chemotherapy for Acute Myeloid Leukemia with a FLT3 Mutation.

- N. Engl. J. Med.* **377**, 454–464 (2017).
60. Benton, C. B. *et al.* Case series of patients with acute myeloid leukemia receiving hypomethylation therapy and retrospectively found to have IDH1 or IDH2 mutations. *Leukemia and Lymphoma* **55**, 1431–1434 (2014).
 61. Diesch, J. *et al.* A clinical-molecular update on azanucleoside-based therapy for the treatment of hematologic cancers. *Clinical Epigenetics* **8**, 71 (2016).
 62. Derissen, E. J. B., Beijnen, J. H. & Schellens, J. H. M. Concise Drug Review: Azacitidine and Decitabine. *Oncologist* **18**, 619–624 (2013).
 63. Agency, E. M. European Medicines Agency. *Prescrire International* **2**, 1–8 (1998).
 64. Nieto, M. *et al.* The European Medicines Agency Review of Decitabine (Dacogen) for the Treatment of Adult Patients With Acute Myeloid Leukemia: Summary of the Scientific Assessment of the Committee for Medicinal Products for Human Use. *Oncologist* **21**, 692–700 (2016).
 65. Niederwieser, C. *et al.* Prognostic and biologic significance of DNMT3B expression in older patients with cytogenetically normal primary acute myeloid leukemia. *Leukemia* **29**, 567–575 (2015).
 66. Qu, Y. *et al.* Differential methylation in CN-AML preferentially targets non-CGI regions and is dictated by DNMT3A mutational status and associated with predominant hypomethylation of HOX genes. *Epigenetics* **9**, 1108–1119 (2014).
 67. Stahl, M., Gore, S. D., Vey, N. & Prebet, T. Lost in translation? Ten years of development of histone deacetylase inhibitors in acute myeloid leukemia and myelodysplastic syndromes. *Expert Opin. Investig. Drugs* **25**, 307–317 (2016).
 68. De Botton S. *et al.* Clinical safety and activity of {AG}-120, a first-in-class, potent inhibitor of the idh1 mutant protein, in a phase 1 study of patients with advanced {IDH}1-mutant hematologic malignancies. *Haematologica* **100**, 214–215 (2015).
 69. Yen, K. *et al.* O11.2 * AG-221 offers a survival advantage in a primary human IDH2 mutant AML xenograft model. *Ann. Oncol.* **26**, ii15–ii15 (2015).
 70. Boddu, P. & Borthakur, G. Therapeutic targeting of isocitrate dehydrogenase mutant AML. *Expert Opin. Investig. Drugs* **26**, 525–530 (2017).
 71. Lu, C. *et al.* IDH mutation impairs histone demethylation and results in a block to cell differentiation. *Nature* **483**, (2012).
 72. Sasaki, M. *et al.* IDH1(R132H) mutation increases murine haematopoietic progenitors and alters epigenetics. *Nature* **488**, 656–659 (2012).
 73. Stein, E. M. *et al.* Enasidenib in mutant IDH2 relapsed or refractory acute myeloid leukemia. *Blood* **130**, (2017).
 74. Kim, E. S. Enasidenib: First Global Approval. *Drugs* **77**, 1705–1711 (2017).
 75. DiNardo, C. D. *et al.* Durable Remissions with Ivosidenib in IDH1 -Mutated Relapsed or Refractory AML. *N. Engl. J. Med.* **378**, 2386–2398 (2018).
 76. Ley, T. J. *et al.* DNA sequencing of a cytogenetically normal acute myeloid leukaemia genome. *Nature* **456**, 66–72 (2008).
 77. Russler-Germain, D. A. *et al.* Cancer Cell The R882H DNMT3A Mutation Associated with AML Dominantly Inhibits Wild-Type DNMT3A by Blocking Its Ability to Form Active Tetramers. *Cancer Cell* **25**, 442–454 (2014).
 78. Pastor, W. A., Aravind, L. & Rao, A. TETonic shift: biological roles of TET proteins in DNA demethylation and transcription. *Nat. Rev. Mol. Cell Biol.* **14**, 341–356 (2013).

79. Figueroa, M. E. *et al.* Leukemic IDH1 and IDH2 Mutations Result in a Hypermethylation Phenotype, Disrupt TET2 Function, and Impair Hematopoietic Differentiation. *Cancer Cell* **18**, 553–567 (2010).
80. Inoue, S. *et al.* Mutant IDH1 Downregulates ATM and Alters DNA Repair and Sensitivity to DNA Damage Independent of TET2. *Cancer Cell* **30**, 337–348 (2016).
81. Schoofs, T. & Müller-Tidow, C. DNA methylation as a pathogenic event and as a therapeutic target in AML. *Cancer Treatment Reviews* **37**, S13–S18 (2011).
82. Turek-Plewa, J. & Jagodzinski, P. P. *The role of mammalian DNA methyltransferases in the regulation of gene expression. Cellular & Molecular Biology Letters* **10**, (2005).
83. Hanahan, D. & Weinberg, R. A. Hallmarks of cancer: The next generation. *Cell* **144**, 646–674 (2011).
84. Hansen, K. D. *et al.* Increased methylation variation in epigenetic domains across cancer types HHS Public Access. *Nat Genet* **43**, 768–775 (2012).
85. Jones, P. A. & Baylin, S. B. The fundamental role of epigenetic events in cancer. *Nat. Rev. Genet.* **3**, 415–428 (2002).
86. Capper, D. *et al.* DNA methylation-based classification of central nervous system tumours. *Nature* **555**, 469–474 (2018).
87. Figueroa, M. E. *et al.* MDS and secondary AML display unique patterns and abundance of aberrant DNA methylation. *Blood* **114**, 3448–3458 (2009).
88. Alvarez, S. *et al.* DNA Methylation Profiles and Their Relationship with Cytogenetic Status in Adult Acute Myeloid Leukemia. *PLoS One* **5**, e12197 (2010).
89. Figueroa, M. E. *et al.* DNA Methylation Signatures Identify Biologically Distinct Subtypes in Acute Myeloid Leukemia. *Cancer Cell* **17**, 13–27 (2010).
90. Akalin, A. *et al.* Base-pair resolution DNA methylation sequencing reveals profoundly divergent epigenetic landscapes in acute myeloid leukemia. *PLoS Genet.* **8**, (2012).
91. Glass, J. L. *et al.* Epigenetic Identity in AML Depends on Disruption of Nonpromoter Regulatory Elements and Is Affected by Antagonistic Effects of Mutations in Epigenetic Modifiers. *Cancer Discov.* **7**, 868–883 (2017).
92. Heintzman, N. D. *et al.* Histone modifications at human enhancers reflect global cell-type-specific gene expression. *Nature* **459**, 108–112 (2009).
93. Li, Y. *et al.* Clinical implications of genome-wide DNA methylation studies in acute myeloid leukemia. *J. Hematol. Oncol.* **10**, 41 (2017).
94. Li, S. *et al.* Distinct evolution and dynamics of epigenetic and genetic heterogeneity in acute myeloid leukemia. *Nat. Med.* **22**, 792–799 (2016).
95. Marcucci, G. *et al.* Epigenetics Meets Genetics in Acute Myeloid Leukemia: Clinical Impact of a Novel Seven-Gene Score. *J. Clin. Oncol.* **32**, 548–556 (2014).
96. Horner, M. J. *et al.* *Seer Cancer Statistics Review, 1975-2006. National Cancer Institute* (2009).
97. Hulegårdh, E. *et al.* Characterization and prognostic features of secondary acute myeloid leukemia in a population-based setting: A report from the Swedish Acute Leukemia Registry. *Am. J. Hematol.* **90**, 208–214 (2015).
98. Juliusson, G. *et al.* Acute myeloid leukemia in the real world: why population-based registries are needed. *Blood* **119**, 3890–9 (2012).
99. Medeiros, B. C. *et al.* Big data analysis of treatment patterns and outcomes among elderly acute myeloid leukemia patients in the United States. *Ann. Hematol.* **94**, 1127–1138 (2015).

100. Fenaux, P. *et al.* Azacitidine prolongs overall survival compared with conventional care regimens in elderly patients with low bone marrow blast count acute myeloid leukemia. *J. Clin. Oncol.* **28**, 562–9 (2010).
101. Dombret, H. *et al.* International phase 3 study of azacitidine vs conventional care regimens in older patients with newly diagnosed AML with >30% blasts. *Blood* **126**, 291–299 (2015).
102. Ziogas, D. C., Voulgarelis, M. & Zintzaras, E. A Network Meta-analysis of Randomized Controlled Trials of Induction Treatments in Acute Myeloid Leukemia in the Elderly. *CLITHE* **33**, 254–279 (2011).
103. Krug, U. *et al.* Therapy of older persons with acute myeloid leukaemia. *Leuk. Res.* **60**, 1–10 (2017).
104. Büchner, T. *et al.* Age, not therapy intensity, determines outcomes of adults with acute myeloid leukemia. *Leukemia* **30**, 1781–1784 (2016).
105. Grimwade, D. *et al.* The predictive value of hierarchical cytogenetic classification in older adults with acute myeloid leukemia (AML): Analysis of 1065 patients entered into the United Kingdom Medical Research Council AML11 trial. *Blood* **98**, 1312–1320 (2001).
106. Lazarevic, V. *et al.* Incidence and prognostic significance of karyotypic subgroups in older patients with acute myeloid leukemia: the Swedish population-based experience. *Blood Cancer J.* **4**, e188 (2014).
107. Büchner, T. *et al.* Age-related risk profile and chemotherapy dose response in acute myeloid leukemia: A study by the german acute myeloid leukemia cooperative group. *J. Clin. Oncol.* **27**, 61–69 (2009).
108. Rao, A. V. *et al.* Age-specific differences in oncogenic pathway dysregulation and anthracycline sensitivity in patients with acute myeloid leukemia. *J. Clin. Oncol.* **27**, 5580–5586 (2009).
109. McLaren, W. *et al.* The Ensembl Variant Effect Predictor. *Genome Biol.* **17**, 122 (2016).
110. Coordinators, N. R., Om-, G. E., Viewer, M. & Read, S. Database resources of the National Center for Biotechnology Information. *Nucleic Acids Res.* **43**, 1–12 (2014).
111. Forbes, S. A. *et al.* COSMIC: Exploring the world's knowledge of somatic mutations in human cancer. *Nucleic Acids Res.* **43**, D805–D811 (2015).
112. National Cancer Institute. The Cancer Genome Atlas data portal. *Nature* **458**, 719–724 (2013).
113. Abecasis, G. R. *et al.* An integrated map of genetic variation from 1,092 human genomes. *Nature* **491**, 56–65 (2012).
114. Robinson, J. T. *et al.* Integrative genomics viewer. *Nat. Biotechnol.* **29**, 24–26 (2011).
115. Thorvaldsdóttir, H., Robinson, J. T. & Mesirov, J. P. Integrative Genomics Viewer (IGV): High-performance genomics data visualization and exploration. *Brief. Bioinform.* **14**, 178–192 (2013).
116. Neumann, M. *et al.* Mutational spectrum of adult T-ALL. *Oncotarget* **6**, 2754–66 (2015).
117. Perez-Llamas, C. & Lopez-Bigas, N. Gitools: Analysis and Visualisation of Genomic Data Using Interactive Heat-Maps. *PLoS One* **6**, e19541 (2011).
118. Shannon, P. *et al.* Cytoscape: A software Environment for integrated models of biomolecular interaction networks. *Genome Res.* **13**, 2498–2504 (2003).
119. Wu, G., Feng, X. & Stein, L. A human functional protein interaction network and its application to cancer data analysis. *Genome Biol* **11**, R53 (2010).
120. Newman, M. E. J. Modularity and community structure in networks. *Proc. Natl. Acad. Sci.* **103**, 8577–8582 (2006).
121. Leiserson, M. D. M., Wu, H.-T., Vandin, F. & Raphael, B. J. Supplementary Information CoMEt: a statistical approach to identify combinations of mutually exclusive alterations in cancer. *Genome Biol.*

- 16**, 160 (2015).
122. Aryee, M. J. *et al.* Minfi: a flexible and comprehensive Bioconductor package for the analysis of Infinium DNA methylation microarrays. *Bioinformatics* **30**, 1363–9 (2014).
 123. Pidsley, R. *et al.* A data-driven approach to preprocessing Illumina 450K methylation array data. *BMC Genomics* **14**, 293 (2013).
 124. Jaffe, A. E. *et al.* Bump hunting to identify differentially methylated regions in epigenetic epidemiology studies. *Int. J. Epidemiol.* **41**, 200–209 (2012).
 125. McLean, C. Y. *et al.* GREAT improves functional interpretation of cis-regulatory regions. *Nat. Biotechnol.* **28**, 495–501 (2010).
 126. Huang, D. W., Lempicki, R. A. & Sherman, B. T. Systematic and integrative analysis of large gene lists using DAVID bioinformatics resources. *Nat. Protoc.* **4**, 44–57 (2009).
 127. Huang, D. W., Sherman, B. T. & Lempicki, R. A. Bioinformatics enrichment tools: Paths toward the comprehensive functional analysis of large gene lists. *Nucleic Acids Res.* **37**, 1–13 (2009).
 128. Halachev, K., Bast, H., Albrecht, F., Lengauer, T. & Bock, C. EpiExplorer: live exploration and global analysis of large epigenomic datasets. *Genome Biol.* **13**, R96 (2012).
 129. Gel, B. & Serra, E. KaryoploteR: An R/Bioconductor package to plot customizable genomes displaying arbitrary data. *Bioinformatics* **33**, 3088–3090 (2017).
 130. Kandoth, C. *et al.* Mutational landscape and significance across 12 major cancer types. *Nature* **502**, 333–339 (2013).
 131. Chou, W. C. *et al.* TET2 mutation is an unfavorable prognostic factor in acute myeloid leukemia patients with intermediate-risk cytogenetics. *Blood* **118**, 3803–3810 (2011).
 132. Paschka, P. *et al.* ASXL1 mutations in younger adult patients with acute myeloid leukemia: A study by the German-Austrian acute myeloid leukemia study group. *Haematologica* **100**, 324–330 (2015).
 133. Yoshida, K. *et al.* Frequent pathway mutations of splicing machinery in myelodysplasia. *Nature* **478**, 64–69 (2011).
 134. Mian, S. A. *et al.* Spliceosome mutations exhibit specific associations with epigenetic modifiers and proto-oncogenes mutated in myelodysplastic syndrome. *Haematologica* **98**, 1058–66 (2013).
 135. Thol, F. *et al.* Frequency and prognostic impact of mutations in SRSF2, U2AF1, and ZRSR2 in patients with myelodysplastic syndromes. *Blood* **119**, 3578–3584 (2012).
 136. Weizmann Institute of Science. GeneCards - Human Genes; Gene Database; Gene Search. *Gene Research* (2017). Available at: <https://www.genecards.org/>. (Accessed: 19th November 2018)
 137. Bullinger, L. *et al.* Quantitative DNA methylation predicts survival in adult acute myeloid leukemia. *Blood* **115**, 636–642 (2010).
 138. Zhang, H. *et al.* Identification of DNA methylation prognostic signature of acute myelocytic leukemia. *PLoS One* **13**, e0199689 (2018).
 139. GenAge. GenAge: The Ageing Gene Database. Available at: <http://genomics.senescence.info/genes/>. (Accessed: 29th June 2018)
 140. Vogelstein, B. *et al.* Cancer Genome Landscapes. *Science* **339**, 1546 (2013).
 141. Tian, R., Basu, M. K. & Capriotti, E. Computational methods and resources for the interpretation of genomic variants in cancer. *BMC Genomics* **16**, S7 (2015).
 142. Metzeler, K. H. *et al.* ASXL1 mutations identify a high-risk subgroup of older patients with primary cytogenetically normal AML within the ELN Favorable genetic category. *Blood* **118**, 6920–9 (2011).

143. Greif, P. A. *et al.* RUNX1 mutations in cytogenetically normal acute myeloid leukemia are associated with a poor prognosis and up-regulation of lymphoid genes. *Haematologica* **97**, 1909–15 (2012).
144. Ribeiro, A. F. T. *et al.* Mutant DNMT3A: A marker of poor prognosis in acute myeloid leukemia. *Blood* **119**, 5824–5831 (2012).
145. Boissel, N. *et al.* Prognostic impact of isocitrate dehydrogenase enzyme isoforms 1 and 2 mutations in acute myeloid leukemia: A Study by the Acute Leukemia French Association Group. *J. Clin. Oncol.* **28**, 3717–3723 (2010).
146. Marcucci, G. *et al.* IDH1 and IDH2 gene mutations identify novel molecular subsets within de novo cytogenetically normal acute myeloid leukemia: A cancer and leukemia group B study. *J. Clin. Oncol.* **28**, 2348–2355 (2010).
147. Green, C. L. *et al.* The prognostic significance of IDH2 mutations in AML depends on the location of the mutation. *Blood* **118**, 409–412 (2011).
148. Chou, W. C. *et al.* Distinct clinical and biological features of de novo acute myeloid leukemia with additional sex comb-like 1 (ASXL1) mutations. *Blood* **116**, 4086–4094 (2010).
149. Au, C. H., Wa, A., Ho, D. N., Chan, T. L. & Ma, E. S. K. Clinical evaluation of panel testing by next-generation sequencing (NGS) for gene mutations in myeloid neoplasms. *Diagn. Pathol.* **11**, 11 (2016).
150. McKerrell, T. *et al.* Development and validation of a comprehensive genomic diagnostic tool for myeloid malignancies. *Blood* **128**, e1-9 (2016).
151. Rapaport, F. *et al.* Genomic Landscapes in Elderly AML. *Blood* **130**, (2017).
152. Guryanova, O. A. *et al.* DNMT3A mutations promote anthracycline resistance in acute myeloid leukemia via impaired nucleosome remodeling. *Nat. Med.* **22**, 1488–1495 (2016).
153. Becker, H. *et al.* Favorable prognostic impact of NPM1 mutations in older patients with cytogenetically normal de novo acute myeloid leukemia and associated gene- and microRNA-expression signatures: a Cancer and Leukemia Group B study. *J. Clin. Oncol.* **28**, 596–604 (2010).
154. Ostronoff, F. *et al.* Prognostic significance of NPM1 mutations in the absence of FLT3-internal tandem duplication in older patients with acute myeloid leukemia: A SWOG and UK national cancer research institute/medical research council report. *J. Clin. Oncol.* **33**, 1157–1164 (2015).
155. Desai, P. *et al.* Somatic mutations precede acute myeloid leukemia years before diagnosis. *Nat. Med.* **24**, 1015–1023 (2018).
156. Stahl, M. *et al.* Epigenetics in Cancer: A Hematological Perspective. *PLoS Genetics* **12**, (2016).
157. Lin, Q. & Wagner, W. Epigenetic Aging Signatures Are Coherently Modified in Cancer. *PLOS Genet.* **11**, e1005334 (2015).
158. Horvath, S. *et al.* Aging effects on DNA methylation modules in human brain and blood tissue. *Genome Biol.* **13**, 1465–6914 (2012).
159. Hannum, G. *et al.* Genome-wide Methylation Profiles Reveal Quantitative Views of Human Aging Rates. *Mol. Cell* **49**, 359–367 (2013).
160. Weidner, C. I. *et al.* Aging of blood can be tracked by DNA methylation changes at just three CpG sites. *Genome Biol.* **15**, (2014).
161. Wang, Y. *et al.* The identification of age-associated cancer markers by an integrative analysis of dynamic DNA methylation changes. *Sci. Rep.* **6**, 22722 (2016).
162. Collinet, C. *et al.* Systems survey of endocytosis by multiparametric image analysis. *Nature* **464**, 243–249 (2010).
163. Vaziri, H. *et al.* Evidence for a mitotic clock in human hematopoietic stem cells: loss of telomeric DNA

- with age. *Proc. Natl. Acad. Sci.* **91**, 9857–9860 (1994).
164. Tashiro, S., Nishihara, Y., Kugou, K., Ohta, K. & Kanoh, J. Subtelomeres constitute a safeguard for gene expression and chromosome homeostasis. *Nucleic Acids Res.* **45**, 10333–10349 (2017).
 165. Ambrosini, A., Paul, S., Hu, S. & Riethman, H. Human subtelomeric duplcon structure and organization. *Genome Biol.* **8**, R151 (2007).
 166. Issa, J. P. J. *et al.* Methylation of the oestrogen receptor CpG island links ageing and neoplasia in human colon. *Nat. Genet.* **7**, 536–540 (1994).
 167. Vitali, C. *et al.* SOCS2 controls proliferation and stemness of hematopoietic cells under stress conditions and its deregulation marks unfavorable acute leukemias. *Cancer Res.* **75**, 2387–2399 (2015).
 168. Schoofs, T., Berdel, W. E. & Müller-Tidow, C. Origins of aberrant DNA methylation in acute myeloid leukemia. *Leukemia* **28**, 1–14 (2014).
 169. Müller-Tidow, C. *et al.* Azacitidine in combination with intensive induction chemotherapy in older patients with acute myeloid leukemia: The AML-AZA trial of the Study Alliance Leukemia. *Leukemia* **30**, 555–61 (2016).
 170. Sekeres, M. A. *et al.* Phase 2 study of the lenalidomide and azacitidine combination in patients with higher-risk myelodysplastic syndromes. *Blood* **120**, 4945–4951 (2012).
 171. Daver, N. *et al.* A phase II study of decitabine and gemtuzumab ozogamicin in newly diagnosed and relapsed acute myeloid leukemia and high-risk myelodysplastic syndrome. *Leukemia* **30**, 268–73 (2016).
 172. Fenaux, P. *et al.* Efficacy of azacitidine compared with that of conventional care regimens in the treatment of higher-risk myelodysplastic syndromes: a randomised, open-label, phase III study. *Lancet Oncol.* **10**, 223–232 (2009).
 173. Xie, M., Jiang, Q. & Xie, Y. Comparison Between Decitabine and Azacitidine for the Treatment of Myelodysplastic Syndrome: A Meta-Analysis With 1392 Participants. *Clin. Lymphoma Myeloma Leuk.* **15**, 22–28 (2015).
 174. Wang, F. *et al.* Targeted Inhibition of Mutant IDH1 in leukemia cells induces cellular differentiation. *Science* **340**, 622–626 (2013).
 175. Fan, B. *et al.* Pharmacokinetic / pharmacodynamic evaluation of AG-120 , a potent inhibitor of the IDH1 mutant protein , in a phase 1 study of IDH1-mutant advanced hematologic malignancies. *Blood* **126**, 1310 (2015).
 176. Boutzen, H. *et al.* Isocitrate dehydrogenase 1 mutations prime the all-trans retinoic acid myeloid differentiation pathway in acute myeloid leukemia. *J. Exp. Med.* **213**, 483–497 (2016).
 177. Gafencu, G. A., Tomuleasa, C. I. & Ghiaur, G. PARP inhibitors in acute myeloid leukaemia therapy: How a synthetic lethality approach can be a valid therapeutic alternative. *Med. Hypotheses* **104**, 30–34 (2017).
 178. Robson, M. *et al.* Olaparib for Metastatic Breast Cancer in Patients with a Germline BRCA Mutation. *N. Engl. J. Med.* **377**, 523–533 (2017).
 179. Faraoni, I. *et al.* BRCA1, PARP1 and γH2AX in acute myeloid leukemia: Role as biomarkers of response to the PARP inhibitor olaparib. *Biochim. Biophys. Acta - Mol. Basis Dis.* **1852**, 462–472 (2015).

APPENDIX A

Table of detailed clinical data for the 93 patients of SAL elderly AML

ID	Material	Age	Sex	Diagnosis	dysplasia	#Blasts	LDH	Leukos	FLT3_ITD	NPM1c_Sanger	NPM1_NGS	NPM1_all	Cytogen.	Int_Chem	Response	Surv_Status	Surv_Time	#Muts_NGS
S15	BM	65	w	deNovo	1	60	309	2	0	0	0	0	Complex	Y	NA	0	1.3	4
35	BM	66	w	sAML	1	50	161	1.1	0	0	0	0	Others	Y	0	1	0.6	11
36	BM	66	m	deNovo	0	95	1794	60	NA	0	0	0	NA	Y	1	0	59.5	8
48	BM	66	m	deNovo	1	70	168	1.8	0	0	0	0	CN	Y	0	1	17.5	10
59	PB	66	w	deNovo	0	90	1210	126	1	1	1	1	Others	Y	1	0	8.7	6
S32	BM	66	w	deNovo	NA	63.5	812	84.1	0	1	1	1	Others	Y	1	1	16.8	7
S47	BM	66	w	deNovo	NA	75.5	272	11	1	1	1	1	CN	Y	1	1	9.9	7
44	BM	67	w	sAML	NA	NA	168	4.1	NA	0	0	0	NA	Y	1	1	28.7	8
63	BM	67	m	deNovo	0	70	390	16.45	0	0	0	0	CN	Y	1	0	15.1	11
S10	BM	67	m	deNovo	0	95	267	42	0	0	0	0	CBF	Y	1	0	7.5	9
S18	BM	67	w	deNovo	NA	70.5	456	41.4	0	0	0	0	Others	Y	1	1	15.4	10
S33	BM	67	w	t-AML	1	30	489	1.47	0	0	0	0	NA	N	0	0	6.5	4
S34	BM	67	m	deNovo	NA	70.5	505	8.8	0	0	0	0	Others	Y	1	1	14.8	8
S46	BM	67	w	deNovo	NA	82	486	14.6	1	0	0	0	CN	Y	1	0	12.4	9
S61	BM	67	m	deNovo	NA	67.5	1254	82.8	0	0	0	0	CN	Y	0	1	1.7	10
S66	BM	67	w	deNovo	NA	96	930	110.8	1	1	1	1	CN	Y	1	1	16.4	6
24	BM	68	m	deNovo	1	80	405	0.86	1	1	0	1	CN	Y	1	1	12.7	10
34	BM	68	w	deNovo	1	75	274	1.4	NA	0	0	0	CN	Y	1	1	54.0	7
42	BM	68	m	deNovo	1	95	369	27.8	NA	NA	1	1	CN	Y	1	0	91.8	9
62	BM	68	m	sAML	1	80	277	2.2	0	0	0	0	CN	Y	0	0	46.2	9
S19	BM	68	m	deNovo	NA	93.5	144	3.8	0	0	0	0	Others	Y	1	1	16.1	7
S53	BM	68	w	deNovo	NA	70	234	1.3	0	0	0	0	CN	Y	1	0	18.1	7
S59	BM	68	m	deNovo	NA	86	4219	114.2	0	0	0	0	Complex	Y	0	1	6.8	9
S65	BM	68	m	deNovo	NA	76.5	407	55.2	1	1	1	1	CN	Y	1	1	23.9	10
S40	BM	69	w	deNovo	NA	91	537	26	0	0	0	0	CBF	Y	1	1	17.8	8
S48	BM	69	w	deNovo	NA	97.5	330	16.2	0	0	0	0	Complex	Y	1	1	5.4	7
S54	BM	69	w	t-AML	NA	68	482	14.7	0	0	0	0	Others	Y	0	1	2.2	13
10	BM	70	m	deNovo	NA	25	223	1.3	0	0	0	0	CN	Y	1	1	29.5	11
32	BM	70	w	sAML	NA	NA	333	1.76	0	0	0	0	Others	N	0	1	8.5	7
33	BM	70	m	deNovo	0	85	464	5.9	NA	1	1	1	NA	Y	0	1	0.7	9
38	BM	70	m	deNovo	1	70	2015	15	0	0	0	0	Others	Y	1	0	63.7	12
64	BM	70	w	sAML	0	60	461	1.38	0	0	0	0	Complex	Y	0	1	7.8	5
S02	BM	70	m	deNovo	1	95	409	80	0	1	1	1	CN	Y	1	0	5.2	5
S05	BM	70	m	sAML	1	30	518	13.32	NA	0	0	0	Complex	N	0	0	2.1	6
S14	BM	70	m	t-AML	1	25	154	0.91	0	1	0	1	Others	N	0	1	1.9	7
S21	BM	70	w	deNovo	1	99	1077	62.71	1	0	0	0	Others	Y	1	0	20.0	6
S22	BM	70	w	t-AML	NA	64	249	4.4	0	0	0	0	Others	Y	1	1	19.2	13
S45	BM	70	w	deNovo	NA	94	744	81.9	1	1	1	1	Others	Y	1	1	12.9	4
22	BM	71	w	deNovo	1	80	931	47.54	NA	0	0	0	Complex	Y	0	1	1.2	3
37	BM	71	m	deNovo	0	90	300	1	NA	0	0	0	Others	Y	1	1	10.1	9
55	BM	71	m	deNovo	1	65	254	4.4	NA	0	0	0	Complex	N	0	0	0.2	9
S26	BM	71	m	deNovo	1	40	138	1.9	0	0	0	0	Others	Y	0	0	11.0	6
S27	BM	71	w	deNovo	0	70	170	1.8	NA	0	0	0	CN	Y	1	1	19.4	5
S37	BM	71	m	deNovo	NA	80	199	1.8	0	0	0	0	CN	Y	1	1	20.0	10
43	BM	72	m	sAML	1	85	346	35.7	NA	0	0	0	NA	Y	1	1	16.9	7
47	BM	72	w	deNovo	0	95	553	20	NA	0	0	0	Complex	Y	0	0	1.3	11
S13	BM	72	m	deNovo	1	30	190	1.49	0	1	0	1	CN	Y	1	0	32.3	1
S16	BM	72	w	sAML	1	50	388	2.53	NA	0	0	0	NA	N	0	0	3.8	3
S35	BM	72	m	deNovo	NA	66	367	6.6	0	0	0	0	Others	Y	1	1	38.6	8
S43	BM	72	w	deNovo	NA	87.5	636	71.9	0	0	0	0	Others	Y	1	1	25.8	9
S58	BM	72	w	sAML	NA	69.5	218	4.7	0	0	0	0	CN	Y	0	1	9.2	7
8	BM	73	w	deNovo	0	80	319	2.15	0	0	0	0	Complex	N	0	1	0.8	6
11	BM	73	w	deNovo	0	99	498	69	1	0	0	0	CN	Y	0	1	3.9	6
S12	BM	73	m	sAML	NA	97	561	47	0	0	0	0	NA	Y	0	1	5.2	6
S39	BM	73	w	deNovo	NA	85.5	1482	10.4	0	0	0	0	CBF	Y	1	0	2.7	4
S57	BM	73	m	sAML	NA	72.5	996	60.7	1	1	1	1	Others	Y	0	1	6.2	5
S64	BM	73	w	sAML	NA	69	276	47	0	0	0	0	Others	Y	0	1	3.0	6
1	BM	74	m	t-AML	1	95	189	1.68	0	0	0	0	Complex	N	0	0	2.2	23
23	BM	74	m	deNovo	0	80	582	56.45	1	1	0	1	CN	Y	1	1	15.5	4
S03	BM	74	m	sAML	1	90	1992	195.76	0	0	0	0	CN	Y	0	1	6.4	9
S17	BM	74	m	deNovo	0	60	333	42.5	0	0	0	0	Others	Y	1	1	27.7	7
S62	BM	74	w	deNovo	NA	88.5	882	160.8	1	0	0	0	Others	Y	0	1	2.6	6
S63	BM	74	m	deNovo	NA	64.5	536	1.4	0	0	0	0	Others	Y	1	1	12.7	4
6	BM	75	m	sAML	0	95	542	91	0	0	0	0	Others	Y	1	1	13.0	10
7	BM	75	m	deNovo	0	99	509	189	0	1	1	1	CN	Y	1	0	15.7	10
S30	BM	75	w	deNovo	NA	70.5	328	10.2	0	0	0	0	Others	Y	1	1	21.9	7
S38	BM	75	w	deNovo	NA	70.5	169	1	0	0	0	0	CN	Y	1	0	6.9	7
S51	BM	75	m	deNovo	NA	95	1184	36	0	0	0	0	Others	Y	0	1	14.8	11
12	BM	76	m	deNovo	1	90	604	149	0	0	0	0	CN	Y	0	1	13.2	12
S06	BM	77	m	deNovo	1	90	431	85	1	1	1	1	NA	N	0	0	5.5	6
S44	BM	77	m	deNovo	NA	63	265	14.9	0	0	0	0	CBF	Y	1	1	20.2	6
20	BM	78	m	deNovo	1	45	363	1.75	0	0	0	0	Others	N	0	1	0.2	4
46	BM	78	m	deNovo	0	95	462	33.8	NA	1	1	1	CN	Y	1	1	63.5	9
S20	BM	78	w	deNovo	NA	64	552	18	0	0	0	0	CBF	Y	1	0	46.9	7
S36	BM	78	w	deNovo	NA	74	714	209.6	1	0	0	0	CN	Y	1	1	7.3	7
S42	BM	78	m	sAML	NA	72.5	516	8.7	1	0	0	0	Others	Y	1	1	43.3	7
58	BM	79	w	deNovo	1	75	647	16	NA	0	0	0	Others	N	0	0	2.1	6
S29	BM	79	m	deNovo	NA	NA	239	18.58	0	0	0	0	NA	N	0	0	0.1	8
S52	BM	79	w	deNovo	NA	64.5	175	1.1	0	1	1	1	Others	Y	1	0	66.0	6
S56	BM	79	m	deNovo	NA	65	392	6.2	0	0	0	0	Others	Y	0	1	3.9	13
30	BM	80	w	deNovo	1	40	251	1.19	0	0	0	0	NA	N	0	0	1.3	6
S23	BM	80	m	deNovo	NA	NA	279	3.7	NA	0	0	0	NA	Y	0	1	1.1	3
S55	BM	80	m	sAML	NA	64.5	454	4.4	0	0	0	0	Complex	Y	0	1	3.1	5
S60	BM	80	w	deNovo	NA	68	1110	45.5	0	0	0	0	Complex	Y	0	1	2.0	3
19	BM	81	m	deNovo	1	95	3340	178.58	NA	1	1	1	NA	NA	NA	1	0.9	12
21	BM	81	w	deNovo	NA	40	1094	82.5	0	0	0	0	CN	N	0	1	2.3	12
31	BM	81	w	deNovo	0	80	398	14.8	NA	1	0	1	CN	N	0	1	9.7	11
26	BM	82	w	deNovo	1	50	235	5	NA	0	0	0	NA	N	0	1	7.6	6
29	BM	83	w	deNovo	NA	NA	NA	NA	NA	0	0	0	NA	NA	NA	NA	NA	3
40	BM	83	m	sAML	0	55	378	4.38	NA	0	0	0	NA	N	0	0	8.0	6
25	BM	86	w	deNovo	0	95	386	63.3	0	0	0	0	NA	N	0	1	0.0	12
28	BM	88	w	deNovo	0	80	263	3.33	NA	0	0	0	NA	N	0	0	0.4	5
S25	BM	90	w	sAML	1	75	1712	127.5	NA	0	0	0	NA	NA	NA	1	0.1	12

APPENDIX B

Table of information from the genetic alterations in the SAL elderly AML

[illegible]

[illegible]

[illegible]

[illegible]

[illegible]

[illegible]

APPENDIX C

Table of DMRs of hierarchical cluster of elderly (vs cluster of young)

DMR Name/tag	chr	start	end	value	area	cluster	IndexStart	IndexEnd	L	clusterL	p-valueArea	fewer	Genes associated (distance, bp)
HyperHer1	chr7	73752935	73753326	3.05	9.14	51887	45260	45262	3	3	3.29E-05	0.00E+00	GTF2IRD1 (-115169), CLIP2 (+49328)
HyperHer2	chr7	73820590	73820652	2.82	8.46	51890	45266	45268	3	3	5.01E-05	0.00E+00	GTF2IRD1 (-47679), CLIP2 (+116816)
HyperHer3	chr12	117042854	117042917	2.70	8.09	14911	71899	71891	3	3	6.22E-05	0.00E+00	MAP1LC3B2 (+45700), C12orf49 (+132980)
HyperHer4	chr17	75096202	75096382	2.53	7.58	26206	91773	91775	3	3	7.92E-05	0.00E+00	SEPT9 (-181200), SEC14L1 (+11461)
HyperHer5	chr11	133928292	133928346	2.45	7.35	12534	67633	67635	3	3	9.20E-05	0.00E+00	IGSF9B (-101439), JAM3 (-10501)
HyperHer6	chr15	100048371	100048500	2.44	7.31	20902	82531	82533	3	3	9.43E-05	0.00E+00	MEF2A (-57469), SYNM (+403150)
HyperHer7	chr5	177913434	177913485	2.41	7.22	46511	33899	33901	3	3	9.79E-05	0.00E+00	PHYKPL (-253674), COL23A1 (+104096)
HyperHer8	chr17	7850478	7850916	2.35	7.04	26472	92226	92228	3	3	1.08E-04	0.00E+00	CHMP6 (-404944), RPTOR (+41629)
HyperHer9	chr17	47296970	47297268	2.34	7.02	28425	90533	90535	3	3	1.10E-04	0.00E+00	ABI3 (+9630), PHOSPHO1 (+11009)
HyperHer10	chr17	1576449	1576724	2.32	6.97	23702	87286	87288	3	3	1.14E-04	0.00E+00	RILP (-23216), PRPF8 (+11544)
HyperHer11	chr4	3365280	3365442	2.32	11.58	41306	23745	23749	5	5	1.11E-05	0.00E+00	HGFAC (-78253), RGS12 (+49487)
HyperHer12	chr11	70253427	70253499	2.31	6.92	11007	65172	65174	3	3	1.17E-04	0.00E+00	CTTN (+8816), SHANK2 (+60490)
HyperHer13	chr7	151442351	151442481	2.28	6.85	53248	47688	47690	3	3	1.19E-04	0.00E+00	RHEB (-225406), PRKAG2 (+131794)
HyperHer14	chr13	114918456	114918702	2.24	6.73	17128	75992	75994	3	3	1.29E-04	0.00E+00	CDC16 (-81783), RASA3 (-20493)
HyperHer15	chr19	4543487	4544574	2.15	12.91	28000	95110	95115	6	6	5.91E-06	0.00E+00	LRG1 (-3545)
HyperHer16	chr11	70265971	70266172	2.15	6.44	11010	65179	65181	3	3	1.51E-04	0.00E+00	CTTN (+21425), SHANK2 (+592300)
HyperHer17	chr10	1505595	1505654	2.14	6.42	5978	55713	55715	3	3	1.58E-04	0.00E+00	ID1 (-410515), ADARB2 (-274045)
HyperHer18	chr16	89023389	89023633	2.14	6.41	23434	86811	86813	3	3	1.59E-04	0.00E+00	PABPN1 (-90485), CBFAT2T3 (+20101)
HyperHer19	chr11	1750302	1750939	2.12	10.62	9060	61431	61435	5	5	1.54E-05	0.00E+00	IFITM10 (+21200), KRTAP5-6 (+32196)
HyperHer20	chr11	69259247	69260271	2.12	16.94	10940	65010	65017	8	8	1.42E-06	0.00E+00	CCND1 (-196096), TPCN2 (+443394)
HyperHer21	chr16	88228257	88228776	2.11	6.34	23345	86661	86663	3	3	1.61E-04	0.00E+00	ZNF469 (-265362), BANP (+224893)
HyperHer22	chr16	89922218	89922539	2.09	6.27	23528	86977	86979	3	3	1.68E-04	0.00E+00	TCF25 (-17641), SPIRE2 (+27463)
HyperHer23	chr17	77901030	77901317	2.06	8.24	28423	92145	92148	4	4	5.79E-05	0.00E+00	CBX4 (-87946), TBC1D16 (+108473)
HyperHer24	chr6	15850753	158508188	2.06	8.23	49866	41339	41342	4	4	5.79E-05	0.00E+00	SERAC1 (+81331), SYNJ2 (+105052)
HyperHer25	chr3	66633255	66633408	2.06	6.17	39935	20146	20148	3	3	1.77E-04	0.00E+00	KBTBD8 (-415399), LRIG1 (-81976)
HyperHer26	chr12	240878313	240878541	2.04	6.13	34886	17577	17579	3	3	1.81E-04	0.00E+00	HDAC4 (-555784), NDUFA10 (+86392)
HyperHer27	chr16	8786696	87866833	2.04	6.12	23322	86624	86626	3	3	1.81E-04	0.00E+00	KLHDC4 (-67210), SLC7A5 (+36329)
HyperHer28	chr22	43166139	43166347	2.04	6.12	37343	104101	104103	3	3	1.82E-04	0.00E+00	AAGALT (-75251), ARFGAP3 (+87165)
HyperHer29	chr17	79434960	79485709	2.03	8.12	28613	92515	92518	4	4	6.10E-05	0.00E+00	FSCN2 (-10223), ACTG1 (-5528)
HyperHer30	chr1	10690443	10690588	2.03	6.08	830	1432	1434	3	3	1.86E-04	0.00E+00	PEX14 (+155572), CASZ1 (+166189)
HyperHer31	chr5	1555791	1555887	2.02	6.07	43502	28229	28231	3	3	1.87E-04	0.00E+00	LPCAT1 (-31747), MRPL36 (+244170)
HyperHer32	chr14	103410516	103411005	2.01	8.02	18778	78903	78906	4	4	6.50E-05	0.00E+00	AMN (+21768), CDC42BPB (+113038)
HyperHer33	chr20	19955436	19955868	1.98	7.91	35105	100026	100029	4	4	6.83E-05	0.00E+00	NAA20 (-42108), RIN2 (+88487)
HyperHer34	chr18	74114570	74114728	1.97	5.90	27366	94034	94036	3	3	2.08E-04	0.00E+00	SMIM21 (-974991), ZNF516 (+92497)
HyperHer35	chr12	1025529	1025755	1.95	5.86	12621	67774	67776	3	3	2.13E-04	0.00E+00	RAD52 (+33246), WNK1 (+163553)
HyperHer36	chr8	21767146	21767310	1.95	5.86	54204	49458	49460	3	3	2.13E-04	0.00E+00	GFR2 (-120906), DOK2 (+4143)
HyperHer37	chr13	114065669	114066074	1.94	7.77	17068	75869	75872	4	4	7.26E-05	0.00E+00	GRTF1 (-47431), ADPRHL1 (+41967)
HyperHer38	chr17	26577563	26577877	1.94	5.81	24432	88633	88635	3	3	2.20E-04	0.00E+00	TMEM97 (-68401), NLK (+208538)
HyperHer39	chr18	60903834	60904418	1.93	7.72	27307	93911	93914	4	4	7.42E-05	0.00E+00	BCL2 (+83235), PHLPP1 (+521443)
HyperHer40	chr1	159046391	159047163	1.92	13.42	4100	7067	7073	7	7	4.97E-06	0.00E+00	AIM2 (-86)
HyperHer41	chr10	131589141	131589189	1.91	5.73	8509	60299	60301	3	3	2.32E-04	0.00E+00	EBF3 (+172940), MGMT (+323717)
HyperHer42	chr18	144260671	144260778	1.90	5.71	56208	52954	52956	3	3	2.38E-04	0.00E+00	GPIHBP1 (-34343), LY6H (-18597)
HyperHer43	chr11	113846918	113846937	1.90	5.69	11788	66461	66463	3	3	2.40E-04	0.00E+00	ZBTB16 (-83387), HTR3A (+11131)
HyperHer44	chr19	16466298	16466636	1.89	7.57	26207	96201	96204	4	4	8.02E-05	0.00E+00	KLF2 (+30839), EPS15L1 (+116356)
HyperHer45	chr17	1373605	1374051	1.89	5.67	23673	87225	87227	3	3	2.42E-04	0.00E+00	CRK (-14276), MYO1C (+22278)
HyperHer46	chr11	330536	331179	1.86	9.31	8861	61042	61046	5	5	2.98E-05	0.00E+00	BAGALNT4 (-36946), IFTM3 (-9808)
HyperHer47	chr19	1975562	1975631	1.84	5.52	6007	55770	55772	3	3	2.64E-04	0.00E+00	ADARB2 (-195927)
HyperHer48	chr11	628318	628677	1.83	7.30	8906	61133	61136	4	4	9.51E-05	0.00E+00	CDHR5 (-2420), SCT (-1355)
HyperHer49	chr16	85262708	85262920	1.82	5.47	23052	86140	86142	3	3	2.72E-04	0.00E+00	GSE1 (-384008), KIAA0513 (+165996)
HyperHer50	chr16	87441441	87441659	1.82	5.46	23279	86568	86560	3	3	2.77E-04	0.00E+00	MAP1LC3B (+16144), ZCCHC14 (+84101)
HyperHer51	chr10	3250774	3251149	1.82	5.46	6031	55808	55810	3	3	2.77E-04	0.00E+00	PITRM1 (-35959), KLF6 (+576605)
HyperHer52	chr5	1494980	1495356	1.82	9.08	43490	28211	28215	5	5	3.52E-05	0.00E+00	SLC6A3 (-49623), LPCAT1 (+28924)
HyperHer53	chr12	133294261	133294835	1.81	5.44	15619	73166	73168	3	3	2.80E-04	0.00E+00	PGAM5 (+7143), ANKLE2 (+43926)
HyperHer54	chr3	196351966	196352142	1.81	5.43	40761	23225	23227	3	3	2.81E-04	0.00E+00	NRROS (-14493), FBXO45 (+56505)
HyperHer55	chr17	79428036	79428750	1.81	7.23	26597	92481	92484	4	4	9.70E-05	0.00E+00	ACTG1 (+51414), ENSG00000171282 (+54853)
HyperHer56	chr17	3704471	3704621	1.80	12.58	23806	87474	87480	7	7	6.88E-06	0.00E+00	ITGAE (-9)
HyperHer57	chr1	152536380	152538888	1.79	7.18	3771	6485	6488	4	4	1.00E-04	0.00E+00	LCE3E (+614)

HyperHler58	chr11	94278324	94279068	1.79	17.94	11514	65988	65997	10	10	1.42E-06	0.00E+00	PIWIL4 (-21778), FUT4 (+1679)
HyperHler59	chr3	184297380	184297522	1.79	5.37	40501	22769	22771	3	3	2.93E-04	0.00E+00	VP58 (-232480), EPHB3 (+17879)
HyperHler60	chr13	113646732	113646889	1.78	5.33	17016	75778	75780	3	3	2.99E-04	0.00E+00	F7 (-113305), MCF2L (+23281)
HyperHler61	chr3	48601117	48602040	1.75	8.74	38443	19247	19251	5	5	4.45E-05	0.00E+00	UCN2 (-373)
HyperHler62	chr17	58499679	58499911	1.74	12.20	25713	91004	91010	7	7	7.80E-06	0.00E+00	USP32 (-30300), APPBP2 (+103785)
HyperHler63	chr12	240196078	240197131	1.74	10.44	34654	17518	17523	6	6	1.73E-05	0.00E+00	HDACA4 (+126038), TWIST2 (+439932)
HyperHler64	chr19	2546844	2547067	1.74	5.22	27834	94845	94847	3	3	3.23E-04	0.00E+00	GADD48B (+70831), GWI7 (+156751)
HyperHler65	chr4	184320416	184320840	1.73	5.18	43128	27570	27572	3	3	3.30E-04	0.00E+00	GADD48B (+70831), CDKN2AIP (-45216)
HyperHler66	chr11	67803951	67804112	1.73	5.18	10872	64895	64897	3	3	3.30E-04	0.00E+00	TCIRG1 (-2451)
HyperHler67	chr16	28943094	28943288	1.71	6.86	21963	84307	84310	4	4	1.19E-04	0.00E+00	CD19 (-69)
HyperHler68	chr16	32049053	32049829	1.71	23.99	47819	37236	37249	14	14	4.73E-07	0.00E+00	TNXB (-35536), ATF6B (+46576)
HyperHler69	chr2	3826610	3826980	1.71	8.55	30520	10362	10366	5	5	4.82E-05	0.00E+00	CDCC2C (+75342)
HyperHler70	chr10	75415704	75415875	1.71	6.84	7122	57713	57716	4	4	1.20E-04	0.00E+00	SYNPO2L (+40)
HyperHler71	chr7	27713782	2774195	1.71	6.84	50650	42815	42818	4	4	1.20E-04	0.00E+00	AMZ1 (+54833), GNA12 (+109869)
HyperHler72	chr19	45449099	45449301	1.71	5.13	29454	97765	97767	3	3	3.44E-04	0.00E+00	APOC2 (-1260)
HyperHler73	chr8	30413794	30413919	1.71	5.12	54499	50011	50013	3	3	3.47E-04	0.00E+00	SMIMT8 (-82260), RBPMS (-171830)
HyperHler74	chr19	33764284	33764550	1.71	6.82	28956	96831	96834	4	4	1.21E-04	0.00E+00	SLC7A10 (-47661), CEBPA (+29053)
HyperHler75	chr16	89163343	89163800	1.71	6.82	23458	86865	86868	4	4	1.22E-04	0.00E+00	CDH15 (-74603), ACSF3 (+3355)
HyperHler76	chr16	85981310	85981947	1.70	10.22	23138	86292	86297	6	6	1.95E-05	0.00E+00	FOXF1 (-562504), IRF8 (+49220)
HyperHler77	chr10	468347	468412	1.70	5.09	5900	55574	55576	3	3	3.54E-04	0.00E+00	DIP2C (+267226), ZMYND11 (+287956)
HyperHler78	chr7	157342543	157342801	1.69	5.06	53471	48180	48182	3	3	3.61E-04	0.00E+00	DNAJB6 (+213012)
HyperHler79	chr12	54866945	54867542	1.68	11.79	13806	69887	69893	7	7	1.02E-05	0.00E+00	GTISF1 (-833)
HyperHler80	chr19	11289349	11289376	1.68	6.73	28349	95722	95725	4	4	1.28E-04	0.00E+00	SPC24 (-22879), KANK2 (+18880)
HyperHler81	chr4	3742095	3742357	1.67	6.70	41077	23827	23830	4	4	1.31E-04	0.00E+00	LIRPAP1 (-207940), ADRA2C (-25899)
HyperHler82	chr8	1847999	1848143	1.67	5.02	53809	48747	48749	3	3	3.75E-04	0.00E+00	MYOM2 (-145084), ARHGEF10 (+75929)
HyperHler83	chr9	13376931	133769184	1.67	5.00	57538	54891	54893	3	3	3.78E-04	0.00E+00	QREP (+167)
HyperHler84	chr15	158263204	158263277	1.67	5.00	52600	48405	48407	3	3	3.78E-04	0.00E+00	PTPRN2 (+117130)
HyperHler85	chr15	79296424	79296585	1.66	4.99	20403	81578	81580	3	3	3.81E-04	0.00E+00	CTSH (-59072), RASGRF1 (+86610)
HyperHler86	chr17	79004850	79006166	1.66	13.28	26516	92319	92320	8	8	5.20E-06	0.00E+00	BAIAP2 (-3454)
HyperHler87	chr5	176734633	176734858	1.66	4.97	46446	33788	33790	3	3	3.87E-04	0.00E+00	RAB24 (-4037), PRELID1 (+3971)
HyperHler88	chr17	1492087	1492206	1.65	4.96	23690	87261	87263	3	3	3.89E-04	0.00E+00	PITPNA (-26037), SLC43A2 (+39983)
HyperHler89	chr17	3600356	3600514	1.65	6.60	23803	87464	87467	4	4	1.37E-04	0.00E+00	P2RX5 (-737)
HyperHler90	chr5	36662804	36662950	1.65	4.94	44043	29215	29217	3	3	3.96E-04	0.00E+00	NIPBL (-213984), SLC1A3 (+56420)
HyperHler91	chr13	114261869	114261986	1.65	4.94	17085	75899	75901	3	3	3.97E-04	0.00E+00	TFDP1 (+22872), ATP4B (+50573)
HyperHler92	chr18	74691269	74691423	1.64	4.93	27383	94084	94066	3	3	3.97E-04	0.00E+00	MBP (+153379), ZNF236 (+155230)
HyperHler93	chr2	239008929	239009118	1.63	8.16	34594	17411	17415	5	5	6.08E-05	0.00E+00	FAM132B (-88625), SCLY (+39494)
HyperHler94	chr21	34774164	34775032	1.62	6.50	36284	102269	102272	4	4	1.45E-04	0.00E+00	IFNGR2 (-804)
HyperHler95	chr1	25291385	25292034	1.62	14.60	1562	2552	2560	9	13	2.60E-06	0.00E+00	RUNX3 (-209)
HyperHler96	chr6	312026	312105	1.62	4.87	48662	34178	34180	3	3	4.23E-04	0.00E+00	IRF4 (-79673), DUSP22 (+19969)
HyperHler97	chr9	139590572	139591234	1.62	6.48	57882	55344	55347	4	4	1.48E-04	0.00E+00	FAM69B (-16119), AGPAT2 (-9028)
HyperHler98	chr7	150548934	150549406	1.62	6.47	53158	47537	47540	4	4	1.48E-04	0.00E+00	AOC1 (+27455), KGNH2 (-126233)
HyperHler99	chr7	2563184	2563909	1.62	8.08	50612	42738	42742	5	5	6.22E-05	0.00E+00	LFNG (+4071), BRAT1 (+31814)
HyperHler100	chr16	46919021	46919194	1.61	6.46	22167	84631	84634	4	4	1.49E-04	0.00E+00	GPT2 (+818)
HyperHler101	chr5	1962311	1962554	1.61	4.84	43571	28402	28404	3	3	4.33E-04	0.00E+00	IRX4 (-75101), IRX2 (+789343)
HyperHler102	chr4	6927183	6927859	1.60	6.41	41247	24187	24190	4	4	1.54E-04	0.00E+00	TADA2B (-117597), TBC1D14 (+15949)
HyperHler103	chr1	24861604	24861919	1.60	8.01	1542	2522	2526	5	5	6.55E-05	0.00E+00	NCNAP (-20840), RCAN3 (+32375)
HyperHler104	chr6	169396683	16939760	1.60	4.80	50215	41951	41953	3	3	4.50E-04	0.00E+00	THBS2 (+254417), SMOC2 (+557891)
HyperHler105	chr7	150139870	150140172	1.60	4.80	53144	47503	47505	3	3	4.50E-04	0.00E+00	GIMAP8 (-7697), ZNF775 (+63597)
HyperHler106	chr5	1807695	1807759	1.60	4.79	43534	28288	28290	3	3	4.50E-04	0.00E+00	NDUFS6 (+6213), IRX4 (+79605)
HyperHler107	chr7	2764209	2764599	1.60	7.98	50646	42800	42804	5	5	6.60E-05	0.00E+00	AMZ1 (+45248), GNA12 (+119554)
HyperHler108	chr20	56630240	56630390	1.59	4.78	35874	101565	101567	3	3	4.53E-04	0.00E+00	CDH26 (+96833)
HyperHler109	chr20	60866007	60866158	1.59	4.77	35919	101629	101631	3	3	4.60E-04	0.00E+00	ADRM1 (+8022), LAMA5 (+56285)
HyperHler110	chr2	105372087	105372865	1.59	4.76	32326	13289	13291	3	3	4.61E-04	0.00E+00	POU3F3 (-98793)
HyperHler111	chr17	78190755	78190983	1.58	4.75	28450	92193	92195	3	3	4.69E-04	0.00E+00	SLC26A11 (-3360), SSGH (+3330)
HyperHler112	chr8	1616381	1616450	1.58	4.74	53781	48699	48701	3	3	4.72E-04	0.00E+00	CLN8 (-95512), DLGAP2 (+166884)
HyperHler113	chr4	3374483	3375144	1.58	7.88	41040	23757	23761	5	5	6.90E-05	0.00E+00	HGFAC (-88800), RGS12 (+58940)
HyperHler114	chr11	971527	972057	1.57	4.71	8955	61246	61248	3	3	4.79E-04	0.00E+00	AP2A2 (+45911), MUC6 (+64914)
HyperHler115	chr17	78753273	78754372	1.56	12.48	26481	92244	92251	8	8	6.86E-06	0.00E+00	CHMP6 (-211818), RPTOR (+234755)

HyperHert116	chr17	38717206	38717275	1.56	4.68	24900	89507	89509	3	3	4.95E-04	0.00E+00	TNS4 (-59392), CCRT (+4483)
HyperHert117	chr7	553412	553693	1.56	4.67	50329	42140	42142	3	3	4.95E-04	0.00E+00	PDGFA (+5478), FAM20C (+360584)
HyperHert118	chr10	1401915	1402293	1.56	4.67	5970	55700	55702	3	3	5.00E-04	0.00E+00	IDIT (-306994), ADARB2 (+377566)
HyperHert119	chr12	131417943	131418217	1.56	4.67	15411	72770	72772	3	3	5.00E-04	0.00E+00	GPR133 (-20372), RAN (+61656)
HyperHert120	chr1	1117473	1117625	1.55	4.65	72	142	144	3	3	5.06E-04	0.00E+00	TTL10 (+8266), TNFRSF18 (+24402)
HyperHert121	chr13	112838611	112838611	1.55	9.29	18940	75626	75631	6	8	3.03E-05	0.00E+00	SPACAT (-192316), SOX1 (+116404)
HyperHert122	chr17	79799358	79799549	1.54	7.72	26637	92565	92569	5	5	7.40E-05	0.00E+00	PPP1R27 (-6545), P4HB (+19116)
HyperHert123	chr7	4754502	4755415	1.54	10.79	5708	42907	42913	7	7	1.49E-05	0.00E+00	AP5Z1 (-60294), FOXK1 (+33019)
HyperHert124	chr1	92952641	92953279	1.54	10.78	3138	5381	5387	7	7	1.49E-05	0.00E+00	GF1 (-3449)
HyperHert125	chr7	601503	601828	1.54	4.61	50337	42153	42155	3	3	5.25E-04	0.00E+00	PDGFA (-42635), PRKAR1B (+151178)
HyperHert126	chr16	88972776	88973054	1.53	4.60	23421	86762	86784	3	3	5.27E-04	0.00E+00	PABPN1L (-39689), CBFATZ3 (+70687)
HyperHert127	chr8	48091424	48091864	1.53	6.11	54778	50485	50488	4	4	1.83E-04	0.00E+00	SPDR (-81523)
HyperHert128	chr3	195849011	195849674	1.52	6.09	40745	23189	23192	4	4	1.85E-04	0.00E+00	TFR (-40283), ZDHHC19 (+88923)
HyperHert129	chr6	7468848	7468973	1.52	4.56	46904	34593	34595	3	3	5.42E-04	0.00E+00	DSP (-72897), R1OK1 (+79182)
HyperHert130	chr7	550508	550640	1.52	4.56	50328	42137	42139	3	3	5.48E-04	0.00E+00	PDGFA (+8457), FAM20C (+357605)
HyperHert131	chr16	89167018	89167481	1.51	6.06	23460	86872	86875	4	4	1.89E-04	0.00E+00	CDH15 (-70925), ACSF3 (+7033)
HyperHert132	chr14	103415458	103416268	1.51	6.05	18780	78909	78912	4	4	1.90E-04	0.00E+00	AMN (+26870), CDC42BPB (+107936)
HyperHert133	chr17	79425877	79426432	1.51	6.04	26596	92477	92480	4	4	1.92E-04	0.00E+00	ENSG00000171282 (+52615), ACTG1 (+53652)
HyperHert134	chr17	998432	998711	1.51	4.52	23637	87167	87169	3	3	5.60E-04	0.00E+00	SP3 (-59693), OLAT1 (+223303)
HyperHert135	chr2	174889675	174890570	1.50	9.01	33372	15128	15133	6	6	3.69E-05	0.00E+00	ABR (-84596), TIMM22 (+98215)
HyperHert136	chr8	1860385	1861136	1.49	8.96	53810	48750	48755	6	6	3.83E-05	0.00E+00	MYOM2 (-132394), ARHGEF10 (+88619)
HyperHert137	chr4	1202509	1203168	1.49	19.41	40901	23483	23495	13	13	9.48E-07	0.00E+00	SPON2 (-36178), CTBP1 (+40086)
HyperHert138	chr19	49577162	49577303	1.49	4.47	29765	98308	98310	3	3	5.80E-04	0.00E+00	KCNA7 (-1035)
HyperHert139	chr9	140683212	140683797	1.49	5.96	58001	55518	55521	4	4	2.00E-04	0.00E+00	CACNA1B (-88736), EHMT1 (+170051)
HyperHert140	chr7	1545385	1545819	1.49	4.47	50510	42535	42537	3	3	5.84E-04	0.00E+00	INTS1 (-1599)
HyperHert141	chr6	31867757	31868144	1.49	8.93	47794	37138	37143	6	6	3.90E-05	0.00E+00	EHMT2 (-2490)
HyperHert142	chr17	78854232	78854418	1.49	4.46	26407	92281	92283	3	3	5.88E-04	0.00E+00	CHMP6 (-113116), RPTOR (+335257)
HyperHert143	chr16	474271	474528	1.49	5.94	21019	82732	82735	4	4	2.02E-04	0.00E+00	RAB17FIP3 (-1219)
HyperHert144	chr7	80346614	80346912	1.48	4.45	26720	92739	92739	3	3	5.92E-04	0.00E+00	HEXDC (-29431), UTS2R (+14610)
HyperHert145	chr6	157931791	157932180	1.48	8.90	49844	41303	41308	6	6	3.97E-05	0.00E+00	SNX9 (-312310), ZDHHC14 (+129821)
HyperHert146	chr6	1410167	1410497	1.48	7.41	46723	34291	34295	5	5	8.84E-05	0.00E+00	FOXG1 (-200349), FOXF2 (+20263)
HyperHert147	chr1	1609982	1601380	1.48	4.44	139	291	293	3	3	5.97E-04	0.00E+00	CDK1T1 (-12246), SLG35E2B (+22902)
HyperHert148	chr14	101908752	101909021	1.48	7.39	18712	78756	78760	5	5	9.03E-05	0.00E+00	DIO3 (-118801), ENSG0000269375 (+549622)
HyperHert149	chr17	81031536	81032067	1.48	4.43	26788	92860	92862	3	3	6.06E-04	0.00E+00	B3GNTL1 (-22116), METRL (-5765)
HyperHert150	chr7	2802374	2802976	1.47	7.37	50653	42824	42828	5	5	9.10E-05	0.00E+00	GNA12 (+81283), AMZ1 (+83519)
HyperHert151	chr16	88111009	88111425	1.47	4.42	23339	86651	86653	3	3	6.08E-04	0.00E+00	ZNF469 (-382662), BANP (+107593)
HyperHert152	chr17	80581701	80581925	1.47	4.41	26738	92776	92778	3	3	6.13E-04	0.00E+00	WDR45B (+24598), FOXK2 (+104222)
HyperHert153	chr2	241585833	241585888	1.47	4.41	34731	17648	17650	3	3	6.13E-04	0.00E+00	AQP12B (+36456), GPR35 (+40999)
HyperHert154	chr14	105154557	105155327	1.47	10.29	18920	79168	79174	7	7	1.92E-05	0.00E+00	INF2 (-1032)
HyperHert155	chr7	119131	119499	1.47	4.40	50308	42111	42113	3	3	6.17E-04	0.00E+00	FAM20C (-73654)
HyperHert156	chr2	11917490	11917787	1.46	4.39	30745	10698	10700	3	3	6.25E-04	0.00E+00	TRIB2 (-999376), LPIN1 (+99918)
HyperHert157	chr16	4714229	4714815	1.46	8.78	21504	83643	83648	6	6	4.35E-05	0.00E+00	NUDT16L1 (-29173), MGRN1 (+39731)
HyperHert158	chr17	77806190	77807201	1.46	7.29	26414	92123	92127	5	5	9.53E-05	0.00E+00	CBX8 (-35781), CBX4 (+6532)
HyperHert159	chr2	209244225	209225123	1.46	7.29	33835	16084	16088	5	5	9.53E-05	0.00E+00	PTH2R (-46882), PIKFYVE (+93883)
HyperHert160	chr16	4103161	4103225	1.46	4.37	21464	83591	83593	3	3	6.37E-04	0.00E+00	CREBBP (-172466), ADCY9 (+62993)
HyperHert161	chr6	31091326	31091608	1.45	4.36	22067	84471	84473	3	3	6.40E-04	0.00E+00	ZNF646 (+5724), PRSS53 (+8817)
HyperHert162	chr11	1107580	1108026	1.45	4.36	8973	61280	61282	3	3	6.42E-04	0.00E+00	MUC5AC (-43777), MUC2 (+32928)
HyperHert163	chr6	155537901	155538055	1.45	8.72	49810	41251	41256	6	6	4.47E-05	0.00E+00	CLDN20 (-47169), T1AM2 (+384147)
HyperHert164	chr1	35250489	35250735	1.45	4.35	1955	3240	3242	3	4	6.48E-04	0.00E+00	GJA4 (-7987), GJB3 (+3822)
HyperHert165	chr2	167507447	167508226	1.44	11.55	50076	41710	41717	8	8	1.14E-05	0.00E+00	CCR6 (-28420), FGFR1OP (+95167)
HyperHert166	chr2	10637974	10638113	1.44	4.32	30688	10608	10610	3	3	6.69E-04	0.00E+00	ODC1 (-49414), NOL10 (+192049)
HyperHert167	chr7	157407820	157408632	1.44	7.19	53489	48218	48222	5	5	1.00E-04	0.00E+00	DNAJB6 (-278566), PTPRN2 (+972145)
HyperHert168	chr1	117529478	117530009	1.44	7.18	3516	6019	6023	5	5	1.00E-04	0.00E+00	CTOT1 (-14638), PTGFRN (+77065)
HyperHert169	chr10	131682386	131682509	1.43	4.29	8513	60308	60310	3	3	6.84E-04	0.00E+00	EBF3 (+79657), MGMT (+47000)
HyperHert170	chr12	132657317	132657669	1.43	5.71	15492	72893	72896	4	4	2.36E-04	0.00E+00	NOC4L (+28500), GALNT9 (+33080)
HyperHert171	chr16	85074868	85075249	1.43	7.13	23025	86099	86103	5	5	1.04E-04	0.00E+00	ZDHHC7 (-29951), KIAA0513 (-21759)
HyperHert172	chr22	17956453	17956641	1.43	7.13	36707	103021	103025	5	5	1.04E-04	0.00E+00	CECR2 (-80)
HyperHert173	chr8	42037170	42037527	1.43	4.28	54731	50408	50410	3	5	6.92E-04	0.00E+00	AP3M2 (+26885), PLAT (+27893)

HyperHler174	chr19	1998801	1999322	1.42	5.88	27776	94729	94732	4	4	2.41E-04	0.00E+00	BTBD2 (+16657), CSNK1G2 (+57874)
HyperHler175	chr12	53490352	53490632	1.42	4.26	13660	69489	69491	3	3	7.02E-04	0.00E+00	IGFBP6 (-737)
HyperHler176	chr2	11673928	11674557	1.42	4.26	30728	10668	10670	3	3	7.03E-04	0.00E+00	GREB1 (+1)
HyperHler177	chr11	66055170	66055683	1.42	5.67	10731	64637	64640	4	4	2.42E-04	0.00E+00	TMEM151A (-3914), YIF1A (+1214)
HyperHler178	chr8	6735472	6735559	1.42	4.25	53908	48925	48927	3	3	7.08E-04	0.00E+00	DEFB1 (+28)
HyperHler179	chr19	1168354	1169138	1.42	5.67	27649	94518	94521	4	4	2.43E-04	0.00E+00	SRNO2 (+5536), GPX4 (+64810)
HyperHler180	chr5	150020212	150020338	1.41	4.24	45856	32773	32775	3	3	7.14E-04	0.00E+00	MYOZ3 (-20169), SYNPO (+39633)
HyperHler181	chr3	52260349	52260671	1.41	5.65	38591	19534	19537	4	4	2.48E-04	0.00E+00	TLR9 (-331)
HyperHler182	chr16	3306524	3307037	1.41	5.64	21423	83515	83518	4	4	2.48E-04	0.00E+00	MEFV (-154)
HyperHler183	chr12	120688557	120688744	1.41	4.23	15017	72084	72086	3	3	7.23E-04	0.00E+00	RPLP0 (-49749), PXN (+14912)
HyperHler184	chr8	19539991	19540396	1.41	5.63	54173	49407	49410	4	5	2.49E-04	0.00E+00	INTS10 (-134457), CSGALNACT1 (-80188)
HyperHler185	chr10	72545053	72545473	1.41	4.22	7053	57606	57608	3	3	7.34E-04	0.00E+00	TBATA (-106)
HyperHler186	chr17	946875	947343	1.40	8.43	33	67	72	6	6	5.11E-05	0.00E+00	ISG15 (-1694)
HyperHler187	chr17	46648525	46648582	1.40	4.21	25341	90257	90259	3	3	7.41E-04	0.00E+00	HOXB3 (-17270), HOXB4 (+8919)
HyperHler188	chr12	133134938	133135463	1.40	5.60	15599	73118	73121	4	4	2.54E-04	0.00E+00	MUC8 (-84475), P2RX2 (-60202)
HyperHler189	chr16	85470485	85470674	1.40	4.20	23079	86184	86186	3	3	7.47E-04	0.00E+00	GSE1 (-176242), KIAA0513 (+373762)
HyperHler190	chr7	151504844	151505116	1.40	4.19	53251	47693	47695	3	3	7.48E-04	0.00E+00	RHEB (-287970), PRKAG2 (+69230)
HyperHler191	chr22	43525330	43525679	1.40	4.19	37353	104126	104128	3	3	7.49E-04	0.00E+00	MCAT (+13895), BIK (+18751)
HyperHler192	chr12	6745171	6745568	1.40	5.59	12849	68157	68160	4	5	2.58E-04	0.00E+00	LPAR5 (+243)
HyperHler193	chr16	71523395	71523912	1.40	8.38	22759	85685	85690	6	6	5.27E-05	0.00E+00	ENSG00000261611 (-440), ZNF19 (-413)
HyperHler194	chr11	67982542	67982703	1.40	4.19	10881	64916	64918	3	4	7.51E-04	0.00E+00	SUV420H1 (-1741)
HyperHler195	chr14	102394274	102394966	1.40	8.38	18739	78838	78843	6	6	5.30E-05	0.00E+00	DYNC1H1 (-36235), PPP2R5C (+166495)
HyperHler196	chr8	142913273	142913350	1.40	4.19	56106	52766	52768	3	3	7.53E-04	0.00E+00	PTP4A3 (+511219), TSNARE1 (+571231)
HyperHler197	chr16	88700622	88700818	1.39	4.17	23384	86717	86719	3	3	7.62E-04	0.00E+00	IL17C (-4281)
HyperHler198	chr7	158324928	158325118	1.39	4.17	53610	48422	48424	3	4	7.63E-04	0.00E+00	PCGF3 (+16520), CPLX1 (+103912)
HyperHler199	chr7	4850075	4850345	1.39	5.56	50717	42946	42949	4	4	2.60E-04	0.00E+00	AP2J1 (+34957), PAPOLB (+51415)
HyperHler200	chr17	70440347	70440395	1.39	4.17	11022	65202	65204	3	3	7.68E-04	0.00E+00	CTTN (+195724), SHANK2 (+418001)
HyperHler201	chr16	88566483	88566748	1.39	4.17	23373	86699	86701	3	3	7.67E-04	0.00E+00	ZC3H18 (-70173), ZFPNM1 (+48891)
HyperHler202	chr4	715865	716282	1.39	5.54	40842	23367	23370	4	4	2.63E-04	0.00E+00	PCGF3 (+16520), CPLX1 (+103912)
HyperHler203	chr2	239432223	239432329	1.38	4.15	34615	17455	17457	3	3	7.75E-04	0.00E+00	TWIST2 (-324397), ASB1 (+96811)
HyperHler204	chr22	29707524	29708028	1.38	5.53	36964	103452	103455	4	4	2.63E-04	0.00E+00	RASL10A (+3989), GAS2L1 (+4745)
HyperHler205	chr4	6890915	6891264	1.38	5.53	41242	24178	24179	4	4	2.64E-04	0.00E+00	TBC1D14 (-20482), KIAA0232 (+106623)
HyperHler206	chr6	170403557	170403962	1.38	4.14	50256	42017	42019	3	3	7.81E-04	0.00E+00	DL1 (+195801), C6orf70 (+252039)
HyperHler207	chr16	86011615	86012468	1.38	6.90	23142	86302	86306	5	5	1.17E-04	0.00E+00	FOXF1 (-532091), IRF8 (+79633)
HyperHler208	chr13	114270609	114270794	1.38	4.13	17086	75902	75904	3	3	7.93E-04	0.00E+00	TEDP1 (+31846), ATP4B (+41799)
HyperHler209	chr14	101512592	101512653	1.37	4.10	18692	78723	78725	3	3	8.19E-04	0.00E+00	DIO3 (-515065), ENSG00000269375 (+153356)
HyperHler210	chr1	2437200	2438037	1.36	4.09	280	549	551	3	3	8.16E-04	0.00E+00	PANK4 (+20420), PLCH2 (+38721)
HyperHler211	chr5	964230	964654	1.36	4.09	43410	28064	28066	3	3	8.23E-04	0.00E+00	BRD9 (-71503), NKD2 (-44502)
HyperHler212	chr21	46929500	46929741	1.36	4.08	36631	102901	102903	3	3	8.25E-04	0.00E+00	SLC19A1 (+32764), COL18A1 (+54218)
HyperHler213	chr2	241807747	241808004	1.36	5.43	34743	17675	17678	4	4	2.87E-04	0.00E+00	AGXT (-20)
HyperHler214	chr1	15127680	15127851	1.36	4.07	1011	1712	1714	3	3	8.32E-04	0.00E+00	TMEM51 (-351262), KAZN (+202566)
HyperHler215	chr9	95820754	95820913	1.36	4.07	56923	54061	54063	3	3	8.34E-04	0.00E+00	SUSD3 (-155)
HyperHler216	chr7	2119340	2119608	1.36	4.07	50576	42671	42673	3	3	8.34E-04	0.00E+00	MAD1L1 (+153404), ELFN1 (+391719)
HyperHler217	chr11	59823993	59824161	1.36	5.42	10371	64040	64043	4	5	2.85E-04	0.00E+00	MSA3 (-79)
HyperHler218	chr6	31560624	31560871	1.35	5.42	47741	36936	36938	4	4	2.84E-04	0.00E+00	NCR3 (+14)
HyperHler219	chr2	113884734	113885277	1.35	4.06	32479	13553	13555	3	3	8.39E-04	0.00E+00	PSD4 (-46542), IL1RN (+8532)
HyperHler220	chr17	79380400	79380706	1.35	6.77	26580	92446	92450	5	5	1.26E-04	0.00E+00	ENSG00000171282 (-7013), ACTG1 (+99254)
HyperHler221	chr2	42566404	42566556	1.35	4.06	31266	11555	11557	3	3	8.45E-04	0.00E+00	COX7A2L (+29670), EML4 (+169980)
HyperHler222	chr17	57915665	57915773	1.35	5.40	25694	90965	90968	4	4	2.60E-06	0.00E+00	GTF2I14 (-15883), DDR1 (+8217)
HyperHler223	chr1	25240865	25240938	1.35	4.05	1554	2538	2540	3	3	8.49E-04	0.00E+00	TUBD1 (+54577), VMP1 (+130893)
HyperHler224	chr7	38356808	38357047	1.35	4.05	51331	44324	44326	3	3	8.51E-04	0.00E+00	RUNX3 (+50599), CLIC4 (+169054)
HyperHler225	chr7	38356808	38357047	1.35	4.05	51331	44324	44326	3	3	8.51E-04	0.00E+00	STARD3NL (+139104), AMPH (+314239)
HyperHler226	chr13	114820966	114821832	1.35	5.39	17102	75936	75939	4	4	2.89E-04	0.00E+00	GAS6 (-254359), RASA3 (+76687)
HyperHler227	chr13	99135543	99135711	1.35	5.39	16593	74921	74924	4	4	2.90E-04	0.00E+00	RNF113B (-306108), STK24 (+38625)
HyperHler228	chr19	3811002	3811194	1.35	4.04	27933	94990	94992	3	3	8.59E-04	0.00E+00	MATK (-9288), ZFR2 (+57928)
HyperHler229	chr19	1155030	1155225	1.35	5.38	27644	94509	94512	4	4	2.90E-04	0.00E+00	SRNO2 (+19154), GPX4 (+51192)
HyperHler230	chr22	46472568	46473721	1.34	6.72	37470	104345	104349	5	5	1.29E-04	0.00E+00	WNIT7B (-100136), PPARA (-73354)
HyperHler231	chr19	55549414	55549842	1.34	9.41	30139	99093	99099	7	7	2.81E-05	0.00E+00	GP6 (+4)

HyperHer232	chr8	1971042	1971471	1.34	4.01	53835	48793	48795	3	3	8.82E-04	0.00E+00	MYOM2 (-21898), ARHGEF10 (+199115)
HyperHer233	chr6	149805995	149806732	1.34	13.38	49698	41058	47067	10	6	5.20E-06	0.00E+00	ZC3H12D (-167)
HyperHer234	chr13	113975974	113976684	1.34	8.02	17054	75846	75851	6	10	6.50E-05	0.00E+00	LAMP1 (+24778), GRT1P1 (+42107)
HyperHer235	chr7	2761640	2761760	1.33	4.00	50645	42797	42799	3	3	8.91E-04	0.00E+00	AMZ1 (+42544), GNA12 (+122258)
HyperHer236	chr20	62084549	62084833	1.33	4.00	36064	101881	101883	3	3	8.93E-04	0.00E+00	CHRNA4 (-91952), KCNQ2 (+19300)
HyperHer237	chr11	15136150	15136505	1.33	9.30	9537	62463	62469	7	7	2.98E-05	0.00E+00	INSC (+2358)
HyperHer238	chr21	44573984	44574022	1.33	3.99	36479	102663	102665	3	3	9.02E-04	0.00E+00	UZAF1 (-46241), CRYAA (-15180)
HyperHer239	chr2	220309434	220309687	1.33	3.98	34092	16524	16526	3	3	9.13E-04	0.00E+00	GMPPA (-54062), SPEG (+9993)
HyperHer240	chr7	1130697	1131133	1.32	5.30	50420	42321	42324	4	4	3.04E-04	0.00E+00	GPER (+4472), ZFAND2A (+68899)
HyperHer241	chr6	31085343	31088434	1.32	3.97	47693	36769	36771	3	3	9.17E-04	0.00E+00	CDSN (-166)
HyperHer242	chr3	11643368	11643630	1.32	3.97	37841	18187	18189	3	3	9.19E-04	0.00E+00	VGLL4 (+41899), ATG7 (+329397)
HyperHer243	chr5	79552427	79553606	1.32	3.97	44622	30338	30340	3	3	9.22E-04	0.00E+00	SERINC5 (-1539)
HyperHer244	chr19	13054427	13054718	1.32	5.27	28443	95921	95924	4	4	3.10E-04	0.00E+00	RAD23A (-2129)
HyperHer245	chr5	957511	957913	1.32	3.95	43407	28059	28061	3	3	9.36E-04	0.00E+00	BRD9 (-64773), NKD2 (-51232)
HyperHer246	chr11	3177622	31778024	1.32	5.26	9218	61892	61895	4	4	3.12E-04	0.00E+00	CARS (-99156), OSBP1L5 (+8761)
HyperHer247	chr11	70477139	70477192	1.32	3.95	11027	65212	65214	3	3	9.39E-04	0.00E+00	CTTN (+232519), SHANK2 (+381206)
HyperHer248	chr10	102046685	102046768	1.31	3.94	7670	58666	58668	3	3	9.41E-04	0.00E+00	BLOC1S2 (-258)
HyperHer249	chr7	102553293	102553457	1.31	5.25	52420	46276	46279	4	4	3.15E-04	0.00E+00	LRRIC17 (-63)
HyperHer250	chr17	39769012	39769213	1.31	3.94	24958	89593	89595	3	3	9.44E-04	0.00E+00	KRT16 (-108)
HyperHer251	chr5	368394	368804	1.31	3.94	43343	27953	27955	3	3	9.45E-04	0.00E+00	AHR (-64308), C5orf55 (+74659)
HyperHer252	chr17	78058774	78058778	1.31	3.94	26442	92177	92179	3	3	9.47E-04	0.00E+00	GAA (-16782), CGDC40 (+48306)
HyperHer253	chr15	41805946	41806234	1.31	5.25	19529	80169	80172	4	4	3.17E-04	0.00E+00	LTK (-86)
HyperHer254	chr17	46651186	46652938	1.31	18.36	25343	90261	90274	14	14	9.46E-07	0.00E+00	HOXB3 (-20778), HOXB4 (+5411)
HyperHer255	chr10	21796152	21796441	1.31	3.93	6336	56312	56314	3	3	9.56E-04	0.00E+00	NEBL (-609766), SKIDA1 (+18314)
HyperHer256	chr17	78755379	78755442	1.31	3.93	26482	92252	92254	3	3	9.58E-04	0.00E+00	CHMP6 (-210230), RPTOR (+236343)
HyperHer257	chr2	8658387	8660087	1.31	3.93	30614	10499	10501	3	3	9.58E-04	0.00E+00	ID2 (-133013)
HyperHer258	chr10	134399880	134400506	1.31	5.23	8683	60637	60640	4	4	3		

HyperHler290	chr7	148801711	148802155	1.23	3.70	53091	47409	47411	3	3	1.19E-03	0.00E+00	ZNF786 (-14136), ZNF425 (+21505)
HyperHler291	chr17	1521312	1521483	1.23	3.70	23695	87270	87272	3	3	1.19E-03	0.00E+00	PITPNA (-55288), SLC43A2 (+10732)
HyperHler292	chr1	45097282	45098125	1.23	6.16	2357	3902	3906	5	5	1.78E-04	0.00E+00	TMEM53 (+42823), RNF220 (+226838)
HyperHler293	chr17	40715222	40715281	1.23	6.15	29301	89706	89710	5	5	1.79E-04	0.00E+00	MLX (-3838)
HyperHler294	chr11	70455140	70455304	1.23	3.69	11025	65208	65210	3	3	1.21E-03	0.00E+00	CITN (+210575), SHANK2 (+403150)
HyperHler295	chr19	54566838	54567279	1.23	3.69	30084	99000	99002	3	3	1.21E-03	0.00E+00	VSTM1 (+1148)
HyperHler296	chr6	32054441	32055046	1.23	12.27	47824	37261	37270	10	24	7.57E-06	0.00E+00	TNXB (-40839), ATF6B (+41273)
HyperHler297	chr2	31543169	31543686	1.23	14.72	47734	36897	36908	12	12	2.60E-06	0.00E+00	TNF (+84)
HyperHler298	chr2	159651559	159692019	1.23	4.90	33137	14704	14707	4	4	4.11E-04	0.00E+00	DAPL1 (-40)
HyperHler299	chr3	195946881	195947062	1.22	3.67	40752	23205	23207	3	3	1.22E-03	0.00E+00	SLC51A (+3582), PCYT1A (+67627)
HyperHler300	chr11	2206073	2206268	1.22	3.66	9139	61666	61668	3	3	1.24E-03	0.00E+00	TH (-13136), ASCL2 (+86011)
HyperHler301	chr18	24283375	24283696	1.22	4.88	27008	93304	93307	4	4	4.18E-04	0.00E+00	KCTD1 (-154137), AQP4 (+162246)
HyperHler302	chr1	3514921	3515194	1.22	3.66	437	821	823	3	3	1.24E-03	0.00E+00	MEGF6 (+13001), ARHGEF16 (+144068)
HyperHler303	chr18	10588980	10589360	1.22	6.09	26886	93055	93059	5	5	1.88E-04	0.00E+00	NAPG (+63139), PIEZO2 (+559417)
HyperHler304	chr4	1804007	1804492	1.22	3.65	40971	23641	23643	3	3	1.28E-03	0.00E+00	FGR3 (+9211), LETM1 (+53724)
HyperHler305	chr8	144631768	144631915	1.22	4.86	56257	53042	53045	4	4	4.29E-04	0.00E+00	GSDMD (-3535)
HyperHler306	chr11	1769289	1769522	1.21	8.49	9063	61439	61445	7	7	5.01E-05	0.00E+00	IFITM10 (+2415), KRTAP5-6 (+50981)
HyperHler307	chr7	149543136	149543177	1.21	3.63	53122	47463	47465	3	3	1.28E-03	0.00E+00	ATP6V0E2 (-26900), ZNF862 (+7701)
HyperHler308	chr6	32026556	32027379	1.21	6.05	47810	37211	37215	5	5	1.91E-04	0.00E+00	TNXB (-13113), ATF6B (+88999)
HyperHler309	chr19	14591203	14591345	1.21	3.63	28530	96064	96066	3	3	1.29E-03	0.00E+00	PTGERT (-5100), GIPC1 (+15670)
HyperHler310	chr11	2555406	2555576	1.21	3.63	9174	61755	61757	3	3	1.29E-03	0.00E+00	KCNQ1 (+89270), CDKN1C (+351620)
HyperHler311	chr11	70416238	70416309	1.21	3.62	11020	65198	65200	3	3	1.29E-03	0.00E+00	CITN (+171627), SHANK2 (+442098)
HyperHler312	chr16	84840283	84840564	1.21	3.62	23011	86078	86080	3	3	1.30E-03	0.00E+00	CRISPLD2 (-13166), USP10 (+106840)
HyperHler313	chr5	169593	170081	1.21	3.62	43327	27920	27922	3	3	1.30E-03	0.00E+00	SDHA (-48519), PLEKHG4B (+29464)
HyperHler314	chr17	2886250	2886453	1.20	3.61	23774	87411	87413	3	3	1.30E-03	0.00E+00	ORD5 (+80549), RAP1GAP2 (+186620)
HyperHler315	chr1	36615845	36616030	1.20	3.61	1994	3309	3311	3	3	1.30E-03	0.00E+00	TRAPPC3 (-868)
HyperHler316	chr17	6921295	6921465	1.20	3.61	23946	87748	87750	3	3	1.31E-03	0.00E+00	BCLB (-4959)
HyperHler317	chr1	12655992	12656315	1.20	4.81	946	1613	1616	4	4	4.43E-04	0.00E+00	DHR33 (+21583), TNFRSF-1B (+429094)
HyperHler318	chr6	31544694	31544960	1.20	4.81	47763	36909	36912	4	4	4.44E-04	0.00E+00	TNF (+1483), LTβ (+5375)
HyperHler319	chr8	144654887	144655447	1.20	6.01	56263	53056	53060	5	6	1.95E-04	0.00E+00	NAPRT1 (+5616), GSDMD (+19790)
HyperHler320	chr8	143279443	143279882	1.20	4.80	56132	52807	52810	4	4	4.47E-04	0.00E+00	TSNARE1 (+204880), PTP4A3 (+877570)
HyperHler321	chr2	242710824	242711046	1.20	3.60	34802	17782	17784	3	3	1.32E-03	0.00E+00	GAL3S12 (-5305), D2HGHDH (+36941)
HyperHler322	chr8	37731969	37732224	1.20	3.60	54617	50192	50194	3	3	1.32E-03	0.00E+00	BRF2 (-24675), RAB11FIP1 (+24875)
HyperHler323	chr13	107132340	107132458	1.20	3.60	16733	75220	75222	3	3	1.32E-03	0.00E+00	EFNB2 (+55063)
HyperHler324	chr3	127473609	127473936	1.20	3.59	39619	21149	21151	3	3	1.34E-03	0.00E+00	MGLL (+67928), APTB1 (+81990)
HyperHler325	chr14	95837801	95837929	1.20	3.59	19486	78374	78376	3	3	1.34E-03	0.00E+00	CLMN (-51622), SYNE3 (+104308)
HyperHler326	chr10	134260981	134261655	1.19	4.77	8671	60615	60618	4	4	4.58E-04	0.00E+00	STK32C (-139874), INPP5A (-90006)
HyperHler327	chr1	1149192	1149661	1.19	4.77	79	156	159	4	4	4.60E-04	0.00E+00	TNFRSF4 (+85)
HyperHler328	chr17	77128445	77128623	1.19	3.56	26354	92013	92015	3	3	1.38E-03	1.00E-03	ENGASE (+57507), RBFOX3 (+350029)
HyperHler329	chr7	101361395	101361745	1.18	3.55	52381	46219	46221	3	3	1.39E-03	1.00E-03	CUX1 (-97721), MYL10 (-88994)
HyperHler330	chr18	74692116	74692235	1.18	3.55	27384	94067	94069	3	3	1.40E-03	1.00E-03	MBP (+152549), ZNF236 (+156060)
HyperHler331	chr19	51225848	51226849	1.18	8.27	29891	98590	98596	7	7	5.72E-05	0.00E+00	GLEC11A (-237)
HyperHler332	chr17	38350921	38351468	1.18	7.08	51329	44317	44322	6	6	1.07E-04	0.00E+00	STARO3NL (+133371), AMPH (+319872)
HyperHler333	chr12	27396706	27396937	1.18	4.72	13202	68711	68714	4	4	4.78E-04	0.00E+00	STK38L (-286)
HyperHler334	chr8	143694070	143694305	1.18	3.53	56164	52861	52863	3	3	1.41E-03	1.00E-03	ARC (+2675), BAI1 (+163367)
HyperHler335	chr1	3806715	3807312	1.18	3.53	472	913	915	3	3	1.41E-03	1.00E-03	C1orf74 (+9835), DFEB (+33169)
HyperHler336	chr19	4531638	4531961	1.18	4.71	27996	95091	95094	4	4	4.82E-04	0.00E+00	PLIN4 (-14084), PLIN5 (+3436)
HyperHler337	chr7	99970448	99971016	1.18	4.70	52275	46033	46036	4	4	4.88E-04	0.00E+00	PIRA (-336)
HyperHler338	chr11	1475775	1475899	1.18	3.53	9027	61383	61385	3	3	1.42E-03	1.00E-03	MOB2 (+32139), BRSK2 (+43455)
HyperHler339	chr22	19710880	19711327	1.17	8.22	36752	103105	103111	7	7	5.79E-05	0.00E+00	GP1BB (+636)
HyperHler340	chr8	144824625	144824658	1.17	4.69	56283	53107	53110	4	4	4.88E-04	0.00E+00	FAM83H (-8671), SCRIB (+72907)
HyperHler341	chr17	7107939	7108792	1.17	5.87	29683	87793	87787	5	5	2.13E-04	0.00E+00	ASGR1 (-25483), ACADVL (-12078)
HyperHler342	chr19	6482011	6482169	1.17	3.51	28110	95290	95292	3	3	1.45E-03	1.00E-03	DENND1C (-271)
HyperHler343	chr20	642436	642894	1.17	4.68	34859	99540	99545	4	4	4.93E-04	0.00E+00	SRXN1 (-8651), SCRT2 (+14158)
HyperHler344	chr6	52171973	52172083	1.17	3.51	48571	38892	38894	3	3	1.45E-03	1.00E-03	PAQR8 (-54898), MCM3 (-22393)
HyperHler345	chr10	31422942	31423550	1.17	3.51	6525	56693	56695	3	3	1.45E-03	1.00E-03	ZEB1 (-184855), ZNF438 (-102380)
HyperHler346	chr7	157451243	157451906	1.17	7.01	53494	48228	48233	6	6	1.11E-04	0.00E+00	DNAJB6 (+321915), PTPRN2 (+928796)
HyperHler347	chr6	6900945	6901065	1.17	3.50	46883	34566	34568	3	3	1.46E-03	1.00E-03	RREB1 (-207036), LY86 (+312664)

HyperHler348	chr7	2518188	2518824	1.17	4.67	50604	42723	42726	4	4	4.98E-04	0.00E+00	LFNG (-40970), CHST12 (+75283)
HyperHler349	chr1	1067099	1067223	1.17	3.50	59	116	118	3	3	1.48E-03	1.00E-03	TTL10 (-42122), C1orf159 (-15683)
HyperHler350	chr17	75318655	75318682	1.17	3.50	26221	91801	91803	3	3	1.48E-03	1.00E-03	TNRC6C (-682368), SEPT9 (+41277)
HyperHler351	chr17	71361857	71361901	1.17	3.50	25995	91422	91424	3	3	1.47E-03	1.00E-03	CDCA2EP4 (-53565), SDK2 (+278349)
HyperHler352	chr15	93580022	93580327	1.16	5.82	20749	82200	82204	5	5	2.17E-04	0.00E+00	RGMA (-36917), CHD2 (+137117)
HyperHler353	chr19	728040	728385	1.16	3.49	27575	94392	94394	3	3	1.48E-03	1.00E-03	MISP (-22913), PALM (+19112)
HyperHler354	chr6	32053100	32053748	1.16	6.98	47823	37255	37260	6	6	1.12E-04	0.00E+00	TNXB (-39519), ATF6B (+42593)
HyperHler355	chr6	30860866	30860905	1.16	3.48	47664	36680	36682	3	3	1.49E-03	1.00E-03	GTF2I4 (-15075), DDR1 (+9025)
HyperHler356	chr22	18042550	18042722	1.16	3.48	36708	103026	103028	3	3	1.49E-03	1.00E-03	SLC25A18 (-503)
HyperHler357	chr12	14413090	14413690	1.16	4.63	13056	68469	68472	4	4	5.15E-04	0.00E+00	GRIN2B (-280337), ATF7IP (-105226)
HyperHler358	chr6	170531180	170531847	1.16	5.79	50272	42045	42049	5	5	2.24E-04	0.00E+00	DLL1 (+68047), C6orf70 (+379793)
HyperHler359	chr6	41254433	41254885	1.16	4.63	48285	38395	38396	4	4	5.15E-04	0.00E+00	TREM1 (-202)
HyperHler360	chr1	246952118	246952508	1.16	5.78	5839	9964	9968	5	8	2.24E-04	0.00E+00	SCCPDH (+64964), AHCTF1 (+142413)
HyperHler361	chr12	133120548	133120760	1.16	3.47	15596	73112	73114	3	3	1.51E-03	1.00E-03	P2RX2 (-74749), MUC8 (-69928)
HyperHler362	chr8	42823718	42823946	1.16	4.62	54751	50439	50442	4	4	5.18E-04	0.00E+00	CHRNA8 (+97)
HyperHler363	chr20	44574271	44575021	1.16	4.62	35591	101029	101032	4	4	5.19E-04	0.00E+00	PCIFT (-11379), ZNF335 (+26165)
HyperHler364	chr1	203155737	203156625	1.15	5.77	4798	8250	8254	5	5	2.25E-04	0.00E+00	CH13.1 (-304)
HyperHler365	chr6	160241105	160241556	1.15	4.61	49905	41412	41415	4	4	5.22E-04	0.00E+00	MAS1 (-86643), PNLDG1 (+20030)
HyperHler366	chr17	43324322	43325791	1.15	12.69	25212	90033	90043	11	11	6.62E-06	0.00E+00	SPATA32 (+14422), FMNL1 (+25901)
HyperHler367	chr17	56355331	56355431	1.15	3.46	25668	90912	90914	3	3	1.53E-03	1.00E-03	MPO (+2915), LPO (+39594)
HyperHler368	chr10	3138418	3138534	1.15	3.45	6025	55799	55801	3	3	1.54E-03	1.00E-03	PFKP (+28764), PITRM1 (+76527)
HyperHler369	chr1	1851439	1852604	1.15	6.90	157	324	329	6	10	1.17E-04	0.00E+00	TMEM52 (-1310)
HyperHler370	chr2	74208590	74208655	1.15	3.44	31881	12550	12552	3	3	1.57E-03	1.00E-03	TET3 (-64827), DGUOK (+54670)
HyperHler371	chr1	26880547	26881009	1.14	5.72	1629	2691	2695	5	5	2.33E-04	0.00E+00	ARID1A (-141746), RPS8KA1 (+8435)
HyperHler372	chr17	78735268	78735596	1.14	5.72	28479	92236	92240	5	5	2.34E-04	0.00E+00	CHMP6 (-230209), RPTOR (+216364)
HyperHler373	chr4	1294566	1295078	1.14	5.72	40909	23517	23517	5	5	2.34E-04	0.00E+00	UNSSA (-46282), MAEA (+11183)
HyperHler374	chr12	25707564	25707667	1.14	3.43	13182	68687	68689	3	3	1.58E-03	1.00E-03	IFLTD1 (-1399)
HyperHler375	chr16	85433309	85433718	1.14	4.58	23074	86173	86176	4	4	5.38E-04	0.00E+00	GSET (-213308), KIAA0513 (+336696)
HyperHler376	chr3	9944183	9944537	1.14	3.43	37772	18057	18059	3	3	1.58E-03	1.00E-03	IL17RE (+57)
HyperHler377	chr16	28888747	28888925	1.14	3.42	21956	84300	84302	3	3	1.59E-03	1.00E-03	ATP2A1 (-890)
HyperHler378	chr6	35108605	35109298	1.14	6.84	48094	38123	38128	6	6	1.20E-04	0.00E+00	TCP11 (+472)
HyperHler379	chr19	35981347	35981549	1.14	4.56	29033	96993	96996	4	4	5.44E-04	0.00E+00	KRTDAP (-15)
HyperHler380	chr16	15596053	15596423	1.14	4.56	21721	83973	83976	4	4	5.44E-04	0.00E+00	MPV17L (+1066602), KIAA0430 (+140785)
HyperHler381	chr10	126308381	126308562	1.14	3.41	8364	60048	60050	3	3	1.60E-03	1.00E-03	FAM53B (+124152), LHPP (+180663)
HyperHler382	chr19	50921745	50922484	1.14	6.82	29861	98513	98518	6	6	1.22E-04	0.00E+00	SPIB (-83), SPIB (-80)
HyperHler383	chr2	242702553	242702881	1.14	3.41	34801	17779	17781	3	3	1.61E-03	1.00E-03	GAL3ST2 (-13523), D2HGDH (+28723)
HyperHler384	chr2	25527266	25527366	1.13	3.40	30977	11089	11091	3	3	1.62E-03	1.00E-03	POMC (-135544), DNMT3A (+38143)
HyperHler385	chr4	681086	681440	1.13	3.40	40837	23355	23357	3	3	1.62E-03	1.00E-03	MFSD7 (+1967), MYL5 (+9552)
HyperHler386	chr10	375248	375830	1.13	3.40	5888	55555	55557	3	3	1.63E-03	1.00E-03	ZMYND11 (+195115), DIP2C (+360067)
HyperHler387	chr20	62168463	62168878	1.13	9.06	36086	101908	101915	8	8	3.62E-05	0.00E+00	PTK6 (+24)
HyperHler388	chr1	231156632	231156359	1.13	1.132	5554	9504	9513	10	10	1.21E-05	0.00E+00	TRIM67 (-142720), ARV1 (+41201)
HyperHler389	chr2	238495793	238500081	1.13	3.39	34566	17363	17365	3	3	1.64E-03	1.00E-03	RAB17 (-201)
HyperHler390	chr6	4890079	4890278	1.13	3.39	46841	34477	34479	3	3	1.64E-03	1.00E-03	CDYL (+113510), RPP40 (+141102)
HyperHler391	chr10	323260	323809	1.13	3.39	5885	55550	55552	3	3	1.64E-03	1.00E-03	ZMYND11 (+143111), DIP2C (+412071)
HyperHler392	chr2	3496921	3497214	1.13	3.38	30499	10322	10324	3	3	1.65E-03	1.00E-03	AD11 (+26489), TRAPPC12 (+113561)
HyperHler393	chr12	58210661	58210878	1.12	3.37	13956	70140	70142	3	3	1.66E-03	1.00E-03	AVIL (-516)
HyperHler394	chr4	3516065	3516758	1.12	5.62	41059	23796	23800	5	5	2.51E-04	0.00E+00	LRPAP1 (+17874), DOK7 (+51374)
HyperHler395	chr12	110252616	110252831	1.12	3.37	14675	71332	71334	3	3	1.67E-03	1.00E-03	TRPV4 (-28)
HyperHler396	chr14	23623480	23624377	1.12	8.99	17262	76181	76188	8	8	3.74E-05	0.00E+00	CEBPE (-35104), SLC7A8 (+28920)
HyperHler397	chr9	35563534	35564052	1.12	3.36	56636	53686	53688	3	3	1.69E-03	1.00E-03	TESK1 (-41574), RUSC2 (+25164)
HyperHler398	chr2	98377791	98377939	1.12	3.36	32197	13089	13091	3	3	1.69E-03	1.00E-03	ZAP70 (+47842), TMEM131 (+234489)
HyperHler399	chr10	94448532	94448728	1.12	3.36	7493	58285	58287	3	3	1.69E-03	1.00E-03	HHEX (+685)
HyperHler400	chr6	167571324	167571630	1.12	3.36	50079	41728	41730	3	3	1.70E-03	1.00E-03	GPR31 (+340)
HyperHler401	chr12	132687617	132687729	1.12	3.36	15505	72923	72925	3	3	1.70E-03	1.00E-03	GALNT9 (+2900), NOC4L (+58680)
HyperHler402	chr6	166140451	166140706	1.12	3.36	50001	41573	41575	3	3	1.70E-03	1.00E-03	PDE10A (-65022), SDIM1 (+169146)
HyperHler403	chr17	32690127	32690569	1.12	4.48	24615	88945	88948	4	4	5.79E-04	0.00E+00	CCL1 (-98)
HyperHler404	chr20	47896448	47897451	1.12	7.81	35675	101174	101180	7	7	7.07E-05	0.00E+00	ZNF1 (-2194)
HyperHler405	chr12	56323639	56323816	1.12	3.35	13841	69945	69947	3	3	1.72E-03	1.00E-03	WIBG (-2031), DGKA (-1028)

HypertHler406	chr10	11936672	11937255	1.11	3.34	6198	56103	56105	3	3	1.72E-03	1.00E-03	UPF2 (+140932), ECHDC3 (+152599)
HypertHler407	chr15	93591750	93591806	1.11	3.34	20750	82205	82207	3	3	1.73E-03	1.00E-03	RGMA (+25314), CHD2 (+148720)
HypertHler408	chr11	62573844	62574403	1.11	3.34	10502	64255	64257	3	3	1.73E-03	1.00E-03	NXF1 (-350)
HypertHler409	chr22	50968250	50968343	1.11	5.57	37643	104611	104613	5	5	2.59E-04	0.00E+00	SCO2 (-3429), TYMP (+147)
HypertHler410	chr17	79442037	79442206	1.11	3.33	26602	92500	92502	3	3	1.74E-03	1.00E-03	ACTG1 (+37685), ENSG00000171282 (+68582)
HypertHler411	chr20	62200091	62200854	1.11	7.78	36091	101925	101931	7	7	1.72E-05	0.00E+00	SRMS (-21616), HELZ2 (+3335)
HypertHler412	chr13	187453973	187454477	1.11	3.33	40574	22887	22889	3	3	1.74E-03	1.00E-03	RTP2 (-33880), BCL6 (+9290)
HypertHler413	chr17	80266884	80267030	1.11	3.33	26700	92687	92689	3	3	1.70E-03	1.00E-03	CSNK1D (-35350), CD7 (+8521)
HypertHler414	chr1	147737016	147737207	1.11	4.43	3620	6243	6246	4	4	6.03E-04	0.00E+00	NBPF24 (-137563), PPIAL4A (+218307)
HypertHler415	chr22	50173996	50174297	1.11	7.75	37571	104498	104504	7	7	7.35E-05	0.00E+00	BRD1 (+44305)
HypertHler416	chr17	9431108	943342	1.11	3.32	23633	87160	87162	3	3	1.77E-03	1.00E-03	TMM22 (+42868), ABR (+139943)
HypertHler417	chr10	45495677	45495971	1.10	4.40	6719	56992	56995	4	4	6.18E-04	0.00E+00	ZNF22 (-99), C10orf25 (+512)
HypertHler418	chr17	7082724	7083064	1.10	3.29	23962	87780	87782	3	3	1.82E-03	1.00E-03	ASGR1 (-11)
HypertHler419	chr8	143596671	143596947	1.10	4.38	56156	52850	52853	4	4	6.29E-04	0.00E+00	BAL1 (+66018), ARC (+100024)
HypertHler420	chr11	45115390	45115819	1.10	3.29	10082	63595	63597	3	3	1.85E-03	1.00E-03	TP53I11 (-143894), PRDM11 (-53289)
HypertHler421	chr4	3387281	3387341	1.10	3.29	41041	23762	23764	3	3	1.83E-03	1.00E-03	HGFAC (-56303), RGST2 (+71437)
HypertHler422	chr16	2082689	2083393	1.09	5.47	21296	83275	83279	5	5	2.73E-04	0.00E+00	TSC2 (-14425), SLC9A3R2 (+6172)
HypertHler423	chr17	46653615	46654330	1.09	4.37	25344	90275	90278	4	4	6.34E-04	0.00E+00	HOXB3 (-22689), HOXB4 (+3500)
HypertHler424	chr17	34207332	34207663	1.09	4.37	24675	89056	89059	4	4	6.37E-04	0.00E+00	CCL5 (+14)
HypertHler425	chr10	743286	743761	1.09	4.37	5933	55650	55653	4	4	6.37E-04	0.00E+00	DIP2C (-7918), LARP4B (+188178)
HypertHler426	chr17	79128918	79129078	1.09	4.37	26536	92356	92359	4	4	6.38E-04	0.00E+00	AATK (+10819), BAIAP2 (+120036)
HypertHler427	chr15	23810843	23811369	1.09	4.36	19054	79389	79392	4	9	6.39E-04	0.00E+00	MKRN3 (+652)
HypertHler428	chr21	45575559	45575832	1.09	3.27	36527	102737	102739	3	4	1.85E-03	1.00E-03	C21orf33 (+22209), ICOSLG (+85132)
HypertHler429	chr11	76858729	76859387	1.09	5.45	11269	65603	65607	5	5	2.78E-04	0.00E+00	MYO7A (+19748), GPPD4 (+139405)
HypertHler430	chr15	41914122	41914454	1.09	3.26	19534	80177	80179	3	3	1.89E-03	1.00E-03	MGA (-38322), TYRO3 (+63056)
HypertHler431	chr12	8068600	8068706	1.08	3.25	12917	68277	68279	3	3	1.89E-03	1.00E-03	SLC2A14 (-43233), SLC2A3 (+20218)
HypertHler432	chr11	2919689	2921176	1.08	13.01	9196	61847	61858	12	12	5.91E-06	0.00E+00	SLC22A18 (-3217)
HypertHler433	chr8	145008110	145008397	1.08	3.25	59301	53149	53151	3	3	1.90E-03	1.00E-03	EPHK1 (-56622), PLEC (+16790)
HypertHler434	chr20	35169380	35169884	1.08	7.57	35374	100570	100576	7	7	8.06E-05	0.00E+00	MYL9 (-254)
HypertHler435	chr10	22725309	22725587	1.08	3.23	6361	56378	56380	3	3	1.93E-03	1.00E-03	SPAG6 (+91049), PIP4K2A (+278036)
HypertHler436	chr12	57569768	57569940	1.08	4.31	13892	70019	70022	4	4	6.72E-04	0.00E+00	NXPH4 (-40724), LRP1 (+47572)
HypertHler437	chr7	100167198	100167564	1.08	3.23	52288	46050	46052	3	3	1.94E-03	1.00E-03	SAP25 (+3869), AGFG2 (+30533)
HypertHler438	chr7	20256996	20257178	1.08	3.23	50900	43360	43362	3	3	1.94E-03	2.00E-03	MACC1 (-74)
HypertHler439	chr12	123469284	123469669	1.08	3.23	15113	72251	72253	3	3	1.95E-03	2.00E-03	ABCB9 (-3281)
HypertHler440	chr1	27961563	27962037	1.07	7.52	1695	2815	2821	7	7	8.29E-05	0.00E+00	FGR (-12)
HypertHler441	chr12	3697378	3697542	1.07	3.22	30508	10340	10342	3	3	1.96E-03	2.00E-03	ALIC (-8325), COLEC11 (+47964)
HypertHler442	chr13	31309032	31309799	1.07	3.22	15934	73759	73761	3	3	1.96E-03	2.00E-03	ALOX5AP (-229)
HypertHler443	chr1	203144862	203145364	1.07	3.22	4795	8245	8247	3	3	1.96E-03	2.00E-03	MYBPH (-172)
HypertHler444	chr18	45458021	45458698	1.07	4.28	27153	93627	93630	4	4	6.91E-04	0.00E+00	SMAD2 (-848)
HypertHler445	chr16	44044325	44044507	1.07	3.21	48431	38638	38640	3	3	1.99E-03	2.00E-03	TMEM63B (-50235), VEGFA (+305972)
HypertHler446	chr11	68747554	68747636	1.07	3.20	10911	64957	64959	3	3	2.00E-03	2.00E-03	MRGPRD (+860)
HypertHler447	chr17	1686627	1686737	1.07	3.20	23714	87311	87313	3	3	2.00E-03	2.00E-03	SERPINF1 (+21429), SMYD4 (+46493)
HypertHler448	chr15	31515984	31515984	1.07	4.27	19296	79797	79800	4	9	6.99E-04	0.00E+00	KLF13 (-103191), TRPM1 (-62391)
HypertHler449	chr17	2059150	2060130	1.07	8.53	50568	42648	42655	8	9	4.89E-05	0.00E+00	MAD1L1 (-213238), ELFN1 (+331885)
HypertHler450	chr16	2733388	2733801	1.07	3.20	21304	83292	83294	3	3	2.01E-03	2.00E-03	NTHL1 (-35728), PKD1 (+52304)
HypertHler451	chr1	109204168	109204325	1.07	5.33	3280	5629	5633	5	5	2.98E-04	0.00E+00	HEMNT1 (-99)
HypertHler452	chr4	1600072	1600531	1.06	3.19	40951	23609	23611	3	3	2.02E-03	2.00E-03	NKX1-1 (-200183), FAM53A (+85686)
HypertHler453	chr4	1221838	1222037	1.06	3.19	40904	23499	23501	3	3	2.05E-03	2.00E-03	SPON2 (-56277), CTBP1 (+20887)
HypertHler454	chr11	692963	693032	1.06	3.19	8912	61159	61161	3	3	2.03E-03	2.00E-03	TMEM80 (-2818), DEAF1 (+2534)
HypertHler455	chr1	32708234	32708485	1.06	4.25	1855	3054	3057	4	4	7.09E-04	0.00E+00	LOK (-8480), EIF31 (+20389)
HypertHler456	chr12	53297547	53298027	1.06	3.19	13651	69473	69475	3	3	2.03E-03	2.00E-03	KRT78 (-55009), KRT18 (+22466)
HypertHler457	chr19	1280841	1281113	1.06	3.18	27688	94554	94556	3	3	2.05E-03	2.00E-03	MUM1 (-4913)
HypertHler458	chr7	128579876	128579964	1.06	3.18	52782	46888	46890	3	3	2.04E-03	2.00E-03	IRF5 (+1926), TNPO3 (-115048)
HypertHler459	chr17	46641504	46642104	1.06	5.30	25338	90247	90251	5	5	3.01E-04	0.00E+00	HOXB3 (-10520), HOXB4 (+15669)
HypertHler460	chr13	44989900	44990174	1.06	3.18	16128	74110	74112	3	3	2.04E-03	2.00E-03	SERP2 (+42059), TSC22D1 (+160664)
HypertHler461	chr17	80190129	80190154	1.06	3.17	26687	92653	92655	3	3	2.08E-03	2.00E-03	SLC16A3 (-1421)
HypertHler462	chr11	67418045	67418365	1.06	11.61	10861	64866	64868	11	11	1.11E-05	0.00E+00	ACY3 (-75)
HypertHler463	chr2	24233923	24234017	1.06	3.17	30939	11011	11013	3	3	2.08E-03	2.00E-03	FKBP1B (-38614), MFSD2B (+1019)

HyperHler464	chr6	167536521	167536526	167536521	1.05	6.33	50077	41718	41723	6	6	1.62E-04	0.00E+00	CCR6 (+32)
HyperHler465	chr12	132663428	132663383	132663383	1.05	8.44	15495	72899	72906	8	8	5.08E-05	0.00E+00	GALNT9 (+28917), NOC4L (+34663)
HyperHler466	chr19	840737	841082	841082	1.05	5.27	27593	94426	94430	5	6	3.09E-04	0.00E+00	PTN3 (+53)
HyperHler467	chr6	31026287	31026287	31026287	1.05	4.21	47688	36756	36759	4	4	7.36E-04	0.00E+00	MUC22 (+47859), C6orf15 (+54226)
HyperHler468	chr20	62367372	62368256	62368256	1.05	9.48	36110	101959	101967	9	9	2.70E-05	0.00E+00	SLC2A4RG (-3400), LIME1 (-181)
HyperHler469	chr13	123813383	123813465	123813465	1.05	3.15	39512	20974	20976	3	5	2.11E-03	0.00E+00	KALRN (-104)
HyperHler470	chr12	84517474	84517950	84517950	1.05	8.41	32012	12793	12800	8	8	5.18E-05	0.00E+00	SUCLG1 (+168892)
HyperHler471	chr12	52585695	52586127	52586127	1.05	6.29	13602	69388	69393	6	6	1.69E-04	0.00E+00	RT80 (-127)
HyperHler472	chr8	10493118	10489270	10489270	1.05	3.14	53982	49040	49042	3	3	2.14E-03	0.00E+00	KP1L1 (+23418), PRSS55 (+106138)
HyperHler473	chr6	44528765	44528865	44528865	1.05	3.14	48464	38677	38679	3	3	2.14E-03	0.00E+00	RUNX2 (-767291), CDC5L (+173553)
HyperHler474	chr8	144896176	144896307	144896307	1.04	3.13	52990	53126	53128	3	4	2.18E-03	0.00E+00	FAM83H (-80271), SCRIB (+1307)
HyperHler475	chr5	148810061	148810203	148810203	1.04	6.26	45806	32687	32692	6	6	1.69E-04	0.00E+00	IL17B (-17293), CSNK1A1 (+120395)
HyperHler476	chr18	133772742	133773115	133773115	1.04	3.13	55918	52473	52475	3	3	2.17E-03	0.00E+00	TMEV1 (-101)
HyperHler477	chr13	112616931	112617294	112617294	1.04	3.12	16896	75494	75496	3	3	2.18E-03	0.00E+00	SOX1 (-104800), TEX29 (+644098)
HyperHler478	chr6	792658	792778	792778	1.04	4.16	46680	34205	34208	4	4	7.68E-04	1.00E+00	FOXO1 (-519957), EXOC2 (-96607)
HyperHler479	chr1	156211409	156211896	156211896	1.04	10.39	3979	6839	6848	10	10	1.84E-05	0.00E+00	BGLAP (-100)
HyperHler480	chr12	322214	323242	323242	1.04	12.45	12597	67727	67738	12	12	7.09E-06	0.00E+00	SLC6A12 (+961)
HyperHler481	chr10	1559112	1559249	1559249	1.04	3.11	5985	55733	55735	3	3	2.21E-03	0.00E+00	ID1 (-464071), ADARB2 (+220489)
HyperHler482	chr17	80159399	80159595	80159595	1.04	3.11	26678	92639	92641	3	3	2.21E-03	0.00E+00	FASN (-103289), SLC16A3 (-32066)
HyperHler483	chr17	76875678	76876239	76876239	1.04	4.14	26322	91958	91961	4	4	7.80E-04	1.00E+00	USP36 (-38990), ENSG00000178404 (+23324)
HyperHler484	chr12	64834106	64834430	64834430	1.04	3.11	31614	12127	12129	3	3	2.21E-03	0.00E+00	SERTAD2 (+46779), AFTPH (+82803)
HyperHler485	chr17	79432709	79433150	79433150	1.03	4.14	26600	92494	92497	4	4	7.86E-04	1.00E+00	ACTG1 (+46877), ENSG00000171282 (+59390)
HyperHler486	chr5	66461884	66462662	66462662	1.03	4.13	44374	29833	29836	4	4	7.90E-04	1.00E+00	CD180 (+30354), MAST4 (+570084)
HyperHler487	chr12	103352296	103352711	103352711	1.03	3.10	32308	13262	13264	3	3	2.23E-03	0.00E+00	MFSD9 (+809)
HyperHler488	chr12	133000497	133000830	133000830	1.03	3.10	15568	73068	73070	3	5	2.24E-03	0.00E+00	GALNT9 (-310091), MUC8 (+50062)
HyperHler489	chr14	95786621	95786801	95786801	1.03	3.09	18481	78363	78365	3	3	2.24E-03	0.00E+00	GLMN (-468)
HyperHler490	chr5	1503595	1503979	1503979	1.03	3.09	43491	28216	28218	3	3	2.28E-03	0.00E+00	SLC5A3 (-58242), LPCAT1 (+20305)
HyperHler491	chr6	6588737	6589075	6589075	1.03	4.12	46870	34548	34551	4	4	8.00E-04	1.00E+00	LY86 (+565)
HyperHler492	chr7	2653651	2654420	2654420	1.03	7.20	50626	42762	42768	7	7	9.96E-05	0.00E+00	TTYH3 (-17549), IQCE (+55404)
HyperHler493	chr5	176937350	176937527	176937527	1.03	4.11	48475	33839	33842	4	4	8.06E-04	1.00E+00	DOK3 (-581)
HyperHler494	chr19	55417436	55417647	55417647	1.03	4.11	30133	99084	99087	4	4	8.07E-04	1.00E+00	NCRI (+34)
HyperHler495	chr16	4732262	4732406	4732406	1.03	3.08	27508	83654	83656	3	3	2.28E-03	0.00E+00	NUDT16L1 (-11361), MGRN1 (+57543)
HyperHler496	chr6	106583161	106583218	106583218	1.02	3.07	49084	39958	39960	3	3	2.30E-03	0.00E+00	PRDM1 (+48995), ATG5 (+190476)
HyperHler497	chr19	1854549	1854819	1854819	1.02	4.09	27762	94710	94713	4	4	8.17E-04	2.00E+00	REXO1 (-6232), KLF16 (+8883)
HyperHler498	chr6	31894990	31895598	31895598	1.02	7.15	47797	37151	37157	7	7	1.02E-04	0.00E+00	ENSG00000244255 (-181), C2 (+40)
HyperHler499	chr12	108991777	108992148	108992148	1.02	4.09	14634	71254	71257	4	4	8.24E-04	0.00E+00	TMEM119 (-63)
HyperHler500	chr21	46341006	46341380	46341380	1.02	4.07	36583	102829	102832	4	5	8.31E-04	0.00E+00	PTTG1P (-47441), ITGB2 (+7595)
HyperHler501	chr7	151547969	151548111	151548111	1.02	3.05	53254	47698	47700	3	3	2.34E-03	0.00E+00	RHEB (-331030), PRKAG2 (+26170)
HyperHler502	chr12	112203795	112204327	112204327	1.02	3.05	47429	71413	71415	3	3	2.34E-03	0.00E+00	ALDH2 (-665)
HyperHler503	chr6	32043739	32044869	32044869	1.02	7.12	47816	37226	37232	7	7	1.08E-04	0.00E+00	TNXB (-30399), ATF6B (+51713)
HyperHler504	chr6	170418412	170418678	170418678	1.02	3.05	50259	42024	42026	3	3	2.34E-03	0.00E+00	DL1 (+181016), C6orf70 (+266824)
HyperHler505	chr22	49765054	49765229	49765229	1.02	3.05	37551	104466	104468	3	3	2.34E-03	0.00E+00	BRD1 (+463310), FAM19A5 (+879870)
HyperHler506	chr2	105924245	105924659	105924659	1.02	3.05	32352	13342	13344	3	3	2.38E-03	0.00E+00	TGFBRAP1 (+22039), GPR45 (+66252)
HyperHler507	chr9	136566991	136567339	136567339	1.02	3.05	57668	55059	55061	3	4	2.38E-03	0.00E+00	SARDH (+37877), DBH (+65863)
HyperHler508	chr7	155276169	155276880	155276880	1.02	6.10	53336	47898	47903	6	10	1.84E-04	0.00E+00	BNM33 (-160848), EN2 (+25701)
HyperHler509	chr11	64627528	64627776	64627776	1.02	3.05	10625	64451	64453	3	3	2.35E-03	0.00E+00	CD42BPG (-15611), EHD1 (+18539)
HyperHler510	chr19	35629603	35630474	35630474	1.02	9.14	29018	96963	96961	9	9	3.28E-05	0.00E+00	FXYD7 (-4115), LGI4 (-3935), FXYP1 (-887)
HyperHler511	chr1	1533632927	153364020	153364020	1.02	6.09	3816	6552	6557	6	6	1.85E-04	0.00E+00	S100A8 (+190)
HyperHler512	chr6	32181764	32182013	32182013	1.01	3.04	47859	37498	37500	3	3	2.38E-03	0.00E+00	GPSM3 (-21206), NOTOH4 (+9955)
HyperHler513	chr17	74868604	74869001	74869001	1.01	3.04	26198	91759	91761	3	4	2.36E-03	0.00E+00	MGA15B (+74)
HyperHler514	chr7	630473	630914	630914	1.01	5.07	50340	42160	42164	5	5	3.60E-04	0.00E+00	PDGFA (-71663), PRKAR1B (+122150)
HyperHler515	chr11	1891872	1892608	1892608	1.01	11.14	9084	61485	61495	11	11	1.25E-05	0.00E+00	TNNT3 (-48552), LSP1 (+5845)
HyperHler516	chr5	143191565	143192067	143192067	1.01	4.04	45711	32511	32514	4	4	8.58E-04	0.00E+00	NN3 (-408562), YIPF5 (+358407)
HyperHler517	chr8	81599484	81599569	81599569	1.01	3.03	55265	51441	51443	3	3	2.39E-03	0.00E+00	ZNF704 (+187489), ZBTB10 (+201625)
HyperHler518	chr11	67350153	67350326	67350326	1.01	3.03	10852	64847	64849	3	3	2.39E-03	0.00E+00	GSTP1 (-826)
HyperHler519	chr12	6308758	6309025	6309025	1.01	3.03	12812	6804	6806	3	3	2.39E-03	0.00E+00	CD9 (+11)
HyperHler520	chr6	15504844	15506085	15506085	1.01	8.07	47090	34953	34960	8	8	6.24E-05	0.00E+00	DTNBP1 (+157808), JARID2 (+258938)
HyperHler521	chr10	135202522	135203200	135203200	1.01	7.06	8827	60964	60970	7	7	1.08E-04	0.00E+00	MITG1 (-4814), ENSG00000254536 (-1477)

HyperHler522	chr14	24801073	24801794	1.01	4.03	17309	76285	76288	4	6	8.65E-04	5.00E-03	ADCY4 (+2843), LTB4R (+18917)
HyperHler523	chr5	965717	966019	1.01	3.02	43411	28067	28069	3	3	2.42E-03	9.00E-03	BRD9 (-72929), NKD2 (-43076)
HyperHler524	chr8	145086659	145086882	1.00	3.01	53118	53196	53198	3	3	2.44E-03	1.10E-02	SPATC1 (+169)
HyperHler525	chr13	114880761	114881103	1.00	5.01	75968	75972	75972	5	5	3.77E-04	1.00E-03	GAS6 (-313892), RASA3 (+17154)
HyperHler526	chr20	62509164	62509309	1.00	3.01	36124	101989	101991	3	3	2.48E-03	1.10E-02	DNAJC5 (-17298), TPD52L2 (+12590)
HyperHler527	chr2	102608155	102608233	1.00	3.00	32283	13224	13226	3	3	2.47E-03	1.10E-02	IL1R2 (-112)
HyperHler528	chr14	23284518	23284968	1.00	3.00	17235	76133	76135	3	3	2.47E-03	1.10E-02	SLC7A7 (+269)
HyperHler529	chr8	141220177	141220490	1.00	3.00	56002	52602	52604	3	3	2.47E-03	1.10E-02	TRAPPC9 (+248344), C8orf17 (+276918)
HyperHler530	chr11	9346719	93467095	1.00	3.00	11494	65948	65950	3	3	2.48E-03	1.10E-02	C11orf54 (-7850), KIAA1731 (+72102)
HyperHler531	chr16	89573312	89573955	1.00	4.00	23501	86934	86937	4	4	8.92E-04	6.00E-03	SPG7 (-1177)
HyperHler532	chr6	161796785	161796884	1.00	3.00	49940	41473	41475	3	3	2.48E-03	1.10E-02	AGPAT4 (-101727)
HyperHler533	chr22	22901145	22902047	1.00	9.97	36839	103253	103262	10	11	2.22E-05	0.00E+00	PRAME (+100)
HyperHler534	chr11	64980819	64981297	1.00	3.99	10652	64493	64493	4	4	9.02E-04	6.00E-03	POLA2 (-48175), CAPN1 (+31125)
HyperHler535	chr10	90611782	90611911	1.00	2.99	7435	58186	58188	3	3	2.51E-03	1.20E-02	STAMBP1 (-27644), LIPM (+49360)
HyperHler536	chr19	17918795	17919173	1.00	2.99	28689	96332	96334	3	3	2.51E-03	1.20E-02	BGN73 (+13065), INSL3 (+13399)
HyperHler537	chr12	107711489	107711648	1.00	2.99	14600	71202	71204	3	3	2.51E-03	1.20E-02	BTBD11 (-621)
HyperHler538	chr20	62318426	62318588	0.99	3.97	36105	101947	101950	4	4	9.18E-04	6.00E-03	TNFRSF6B (-9514), RTE11-TNFRSF6B (+27751)
HyperHler539	chr19	50936038	50936172	0.99	3.97	29863	98525	98528	4	4	9.18E-04	6.00E-03	MYBP2C (-55)
HyperHler540	chr20	20036853	20037150	0.99	4.96	35108	100032	100036	5	5	3.88E-04	1.00E-03	CRNKL1 (-212)
HyperHler541	chr7	999994	1000336	0.99	2.97	50384	42240	42242	3	3	2.55E-03	1.20E-02	ADAP1 (-5832), COX19 (+15070)
HyperHler542	chr11	43290958	43291043	0.99	2.97	10004	63415	63417	3	3	2.55E-03	1.20E-02	AP15 (-42538)
HyperHler543	chr1	118157	1118391	0.99	2.97	73	145	147	3	3	2.55E-03	1.20E-02	TLL10 (+48991), TNFRSF18 (+23677)
HyperHler544	chr17	79282893	79283959	0.99	7.93	26557	92395	92402	8	8	6.74E-05	0.00E+00	SLC38A10 (-14321), TMEM105 (+21048)
HyperHler545	chr6	168106055	168106222	0.99	2.97	50098	41764	41766	3	4	2.58E-03	1.20E-02	TC10 (-308185), C6orf123 (+91400)
HyperHler546	chr1	50574507	50574591	0.99	2.97	2504	4198	4200	3	4	2.58E-03	1.20E-02	ELAVL4 (+2585), DMR1A2 (+314623)
HyperHler547	chr1	203273571	203274134	0.99	2.97	4805	8264	8266	3	3	2.57E-03	1.20E-02	BTG2 (-811)
HyperHler548	chr6	167189213	167189544	0.99	2.96	50072	41704	41706	3	3	2.58E-03	1.20E-02	MPC1 (-392892), RPS6KA2 (+86661)
HyperHler549	chr7	99769432	99769602	0.99	2.96	52270	46020	46022	3	3	2.59E-03	1.20E-02	GAL3S14 (-3144)
HyperHler550	chr19	11689715	11689987	0.99	6.90	28382	95788	95794	7	7	1.17E-04	0.00E+00	ACP5 (-62)
HyperHler551	chr10	45958759	45958885	0.99	2.96	6726	57002	57004	3	3	2.60E-03	1.20E-02	ALOX5 (+89147), MARCH8 (+131532)
HyperHler552	chr12	96389483	96390059	0.99	4.93	14404	70840	70844	5	5	3.99E-04	1.00E-03	HAL (-372)
HyperHler553	chr15	69754609	69754714	0.99	2.96	20103	81069	81071	3	3	2.60E-03	1.20E-02	RPLP1 (+9539), TLE3 (+635853)
HyperHler554	chr16	66612955	66613407	0.98	10.83	22578	85358	85368	11	11	1.49E-05	0.00E+00	CMTM2 (-179)
HyperHler555	chr11	67142001	67142268	0.98	2.95	10825	64795	64797	3	3	2.61E-03	1.20E-02	CLOF1 (-927)
HyperHler556	chr12	132854818	132855224	0.98	2.95	15522	72962	72964	3	6	2.61E-03	1.20E-02	GALNT9 (-164448), MUC8 (+195705)
HyperHler557	chr17	79419796	79420424	0.98	5.90	26592	92467	92472	6	6	2.08E-04	0.00E+00	ENSG00000171282 (+46570), ACTG1 (+59897)
HyperHler558	chr10	134211620	134211908	0.98	3.92	8664	60596	60599	4	4	9.59E-04	6.00E-03	INPP5A (-139560), STK32C (-90320)
HyperHler559	chr17	80398117	80398854	0.98	2.94	26725	92748	92750	3	3	2.68E-03	1.20E-02	OGFOD3 (-22034), C17orf62 (+10099)
HyperHler560	chr19	827429	828170	0.98	7.83	27588	94410	94417	8	8	7.02E-05	0.00E+00	AZU1 (-26)
HyperHler561	chr11	381709	381875	0.98	2.94	8872	61066	61068	3	3	2.68E-03	1.20E-02	PKP3 (-12425), B4GALNT4 (+1988)
HyperHler562	chr6	32076079	32076592	0.98	6.85	47834	37349	37355	7	8	1.20E-04	0.00E+00	TNKB (-62431), ATF6B (+19681)
HyperHler563	chr4	6695464	6695614	0.98	2.93	41232	24162	24164	3	3	2.67E-03	1.20E-02	STOOP (+743)
HyperHler564	chr12	8834114	8834151	0.98	2.93	12932	68294	68296	3	3	2.67E-03	1.20E-02	MFAP5 (-18725), RIMKL (-16385)
HyperHler565	chr16	85659946	85660534	0.98	2.93	23107	86235	86237	3	3	2.67E-03	1.20E-02	GSE11 (+13418), GINS2 (+62365)
HyperHler566	chr1	151030968	151031295	0.98	2.93	3698	6368	6370	3	3	2.67E-03	1.20E-02	MLLT11 (+898)
HyperHler567	chr20	43882990	43883746	0.98	5.86	35545	100929	100934	6	6	2.13E-04	0.00E+00	SLPI (-163)
HyperHler568	chr16	28518200	28518385	0.98	2.93	21946	84286	84288	3	3	2.68E-03	1.20E-02	IL27 (-138)
HyperHler569	chr12	240291068	240291657	0.98	3.90	34663	17559	17542	4	4	9.79E-04	6.00E-03	HDAC4 (+31280), TWIST2 (-534680)
HyperHler570	chr16	556039	556350	0.98	2.93	21014	82740	82742	3	3	2.69E-03	1.20E-02	CAPN15 (-21661), RAB11FIP3 (+80576)
HyperHler571	chr17	5137692	5138696	0.98	4.88	23896	67636	67640	5	5	4.19E-04	1.00E-03	SCIMP (-139)
HyperHler572	chr11	503807	504937	0.97	7.79	8890	61101	61108	8	8	7.14E-05	0.00E+00	RNH1 (-802)
HyperHler573	chr12	1609245	1609537	0.97	6.81	12826	67782	67788	7	7	1.22E-04	0.00E+00	FBXL14 (+93940), ERC1 (+508987)
HyperHler574	chr4	2943901	2944692	0.97	4.86	47018	23717	23721	5	5	4.24E-04	1.00E-03	MFSD10 (-8112), NOP14 (+20815)
HyperHler575	chr8	144416327	144416485	0.97	2.92	56229	52975	52997	3	3	2.72E-03	1.20E-02	TOP1MT (+660)
HyperHler576	chr6	33282885	33282971	0.97	3.89	47988	37928	37931	4	13	9.92E-04	6.00E-03	TAPBP (-939)
HyperHler577	chr17	75315837	75316784	0.97	5.83	26220	91795	91800	6	6	2.17E-04	0.00E+00	TNRC6C (-684826), SEPT9 (+38819)
HyperHler578	chr11	68779817	68780136	0.97	3.88	10919	64970	64973	4	4	9.97E-04	6.00E-03	MGRPRF (+900)
HyperHler579	chr12	124864528	124865130	0.97	4.86	15155	72310	72314	5	5	4.28E-04	1.00E-03	NCOR2 (+114969), ZNF664 (+407159)

HyperHler580	chr1	22141170	22141400	0.97	3.88	1418	2342	2345	4	4	9.98E-04	6.00E-03	LDLRAD2 (+2527), HSPG2 (+122505)
HyperHler581	chr12	52404134	52404422	0.97	3.88	13591	69374	69377	4	4	1.00E-03	6.00E-03	NR4A1 (-12338), GRASP (+3554)
HyperHler582	chr1	16163479	16164122	0.97	6.78	1056	1775	1781	7	7	1.25E-04	0.00E+00	SPEN (-10558), FBLIM1 (+72807)
HyperHler583	chr7	28998195	28998595	0.97	5.80	51133	44001	44006	6	14	2.21E-04	0.00E+00	CHN2 (-235633), CREB5 (+546251)
HyperHler584	chr11	102826565	102826680	0.97	2.90	11627	66165	66167	3	3	2.77E-03	1.20E-02	MMP13 (-160)
HyperHler585	chr17	129845574	129845832	0.97	2.90	52811	46931	46933	3	3	2.78E-03	1.20E-02	SSMEM1 (-1997), TMEM209 (-365)
HyperHler586	chr13	520995622	520995661	0.96	2.89	38584	19524	19526	3	3	2.79E-03	1.30E-02	DUSP7 (-8976), POC1A (+88886)
HyperHler587	chr17	83011118	83011192	0.96	2.89	2470	88017	88019	3	3	2.80E-03	1.30E-02	RNF222 (-11)
HyperHler588	chr1	203733971	203734559	0.96	2.87	4829	8295	8300	6	6	2.24E-04	0.00E+00	LAX1 (-39)
HyperHler589	chr17	615111683	61511829	0.96	2.89	25768	91111	91113	3	3	2.80E-03	1.30E-02	CYB5B1 (+11789), TANC2 (+424839)
HyperHler590	chr6	30130458	30132226	0.96	17.35	47589	36390	36407	18	19	1.42E-06	0.00E+00	TRIM10 (-2631), TRIM15 (+349)
HyperHler591	chr22	21986960	21987190	0.96	7.70	36820	103217	103224	8	8	7.50E-05	1.00E-03	YDJC (-2722)
HyperHler592	chr17	46645972	46646444	0.96	3.85	25339	90252	90255	4	4	1.03E-03	7.00E-03	HOXB3 (-14924), HOXB4 (+11265)
HyperHler593	chr6	64261439	64261846	0.96	6.73	48659	39031	39037	7	7	1.29E-04	1.00E-03	PTP4A1 (-274)
HyperHler594	chr17	78748077	78748494	0.96	2.87	28480	92241	92243	3	3	2.88E-03	1.50E-02	CHMP6 (-217355), RPTOR (+229218)
HyperHler595	chr19	14224992	14225172	0.96	3.83	28511	96031	96034	4	4	1.04E-03	7.00E-03	SAMD1 (-23562), PRKACA (+3474)
HyperHler596	chr22	50986511	50986962	0.96	2.87	37649	104627	104629	3	7	2.88E-03	1.50E-02	TYMP (-18293), SYCE3 (+14597)
HyperHler597	chr8	143085750	143086459	0.96	5.75	56116	52780	52785	6	6	2.31E-04	1.00E-03	TSNARE1 (+398438), PTP4A3 (+684012)
HyperHler598	chr1	95006322	95006729	0.96	3.83	3172	5430	5433	4	4	1.04E-03	7.00E-03	F3 (+830)
HyperHler599	chr11	71259341	71259581	0.96	2.87	11074	65309	65311	3	3	2.87E-03	1.50E-02	KRTAP5-9 (-5)
HyperHler600	chr16	32077744	32078624	0.96	8.61	47835	37356	37364	9	9	4.75E-05	1.00E-03	TNXB (-64279), ATF6B (+17833)
HyperHler601	chr19	42502731	42503412	0.95	4.77	29353	97599	97603	5	5	4.58E-04	2.00E-03	ATP1A3 (-4690)
HyperHler602	chr12	132670344	132671672	0.95	6.68	15497	72908	72914	7	7	1.32E-04	1.00E-03	GALNT9 (+19565), NOC4L (+42015)
HyperHler603	chr6	30698984	30698987	0.95	8.59	47648	36612	36620	9	9	4.75E-05	1.00E-03	TUBB (+10808), FLOT1 (+11724)
HyperHler604	chr10	88024529	88024673	0.95	5.72	7373	58073	58078	6	6	2.34E-04	1.00E-03	GRID1 (+101634)
HyperHler605	chr2	2401531103	240153778	0.95	2.86	34648	17502	17504	3	5	2.90E-04	1.60E-02	HDAC4 (+169202), TWIST2 (+396766)
HyperHler606	chr12	6881590	6882083	0.95	5.71	12867	68184	68189	6	6	2.38E-04	1.00E-03	LAG3 (+151)
HyperHler607	chr16	875988559	87598893	0.95	2.85	23289	88574	88576	3	3	2.92E-03	1.60E-02	ZCCHC14 (-63075), JPH3 (-47785)
HyperHler608	chr2	219246468	219247055	0.95	3.80	33989	16307	16310	4	4	1.07E-03	7.00E-03	SLC11A1 (+10)
HyperHler609	chr1	109849854	109850562	0.95	3.80	3309	5668	5671	4	4	1.08E-03	7.00E-03	MYBPHL (-545)
HyperHler610	chr1	161171211	161171819	0.95	4.74	4180	7187	7191	5	5	4.70E-04	2.00E-03	ADAMTS4 (-2689), NDUFS2 (+2410)
HyperHler611	chr3	52812033	52812520	0.95	4.74	38612	19577	19581	5	5	4.70E-04	2.00E-03	ITIH1 (+669)
HyperHler612	chr13	114831142	114831705	0.95	2.85	17107	75952	75954	3	3	2.95E-03	1.60E-02	GAS6 (-264384), RASA3 (+66662)
HyperHler613	chr17	75315081	75315244	0.95	2.85	26219	91792	91794	3	3	2.95E-03	1.60E-02	TNRC6C (-685974), SEPT9 (+37671)
HyperHler614	chr12	174877357	174877566	0.95	2.84	33368	15122	15124	3	3	2.95E-03	1.60E-02	SP3 (-47032), OLA1 (+235964)
HyperHler615	chr13	111128054	111128102	0.95	2.84	16822	75371	75373	3	3	2.95E-03	1.60E-02	RAB20 (+86002), COL4A2 (+168464)
HyperHler616	chr6	906060913	90661242	0.95	3.79	48897	39491	39494	4	4	1.08E-03	7.00E-03	GJA10 (+56890), BACH2 (+345383)
HyperHler617	chr19	2302401	2303032	0.95	5.68	27803	94792	94797	6	6	2.41E-04	1.00E-03	LINGO3 (-10694), LSM7 (+25898)
HyperHler618	chr11	74178114	74178883	0.95	6.83	11176	65466	65472	7	7	1.38E-04	1.00E-03	KCNE3 (+174)
HyperHler619	chr11	68856817	68869906	0.95	2.84	10925	64986	64988	3	3	2.98E-03	1.60E-02	CCND1 (-598993), TPCN2 (+40497)
HyperHler620	chr16	1587684	1587842	0.94	2.83	21242	83184	83186	3	3	2.98E-03	1.60E-02	TMEM204 (+4189), IFT140 (+74346)
HyperHler621	chr20	31261784	31261994	0.94	2.83	35279	100420	100422	3	3	2.98E-03	1.60E-02	COMMD7 (+69914), ASXL1 (+315734)
HyperHler622	chr12	22590017	22590199	0.94	2.83	13142	68628	68630	3	3	2.98E-03	1.60E-02	ST8SIA1 (-102460), C2CD5 (+107372)
HyperHler623	chr17	78865263	78866235	0.94	6.61	26502	92291	92297	7	8	1.37E-04	1.00E-03	CHMP6 (-99892), RPTOR (+346681)
HyperHler624	chr2	241905733	241906367	0.94	4.71	34756	17700	17704	5	5	4.79E-04	2.00E-03	SNED1 (-32210), ENSG00000226321 (+44059)
HyperHler625	chr13	113707471	113707579	0.94	2.83	17034	75814	75817	3	3	3.01E-03	1.70E-02	F7 (-52596), MCF2L (+83990)
HyperHler626	chr7	157620445	157620943	0.94	3.77	53534	48300	48303	4	4	1.10E-03	7.00E-03	DNAJB6 (+491034), PTPRN2 (+759677)
HyperHler627	chr17	155584080	155584274	0.94	2.83	53359	47946	47948	3	3	3.01E-03	1.70E-02	SHH (+20790), RBM33 (+146804)
HyperHler628	chr8	145051491	145051795	0.94	2.82	56373	53188	53190	3	3	3.02E-03	1.70E-02	PLEC (-26599), PARP10 (+8979)
HyperHler629	chr8	21916635	21916853	0.94	3.76	54223	49496	49499	4	4	1.11E-03	7.00E-03	DMTN (+27)
HyperHler630	chr20	19866974	19867145	0.94	4.70	35100	100012	100016	5	5	4.84E-04	2.00E-03	RIN2 (-105)
HyperHler631	chr19	35940425	35940483	0.94	2.82	29032	96990	96992	3	3	3.03E-03	1.70E-02	FFAR2 (+1251), KRTDAP (+40979)
HyperHler632	chr1	223317364	223317548	0.94	3.76	5285	9041	9044	4	5	1.12E-03	7.00E-03	HLR5 (-6827), UNC54 (+675945)
HyperHler633	chr5	176304988	176305077	0.94	2.82	46431	33761	33763	3	3	3.04E-03	1.70E-02	TKS3 (+21300), SUG5A (+67555)
HyperHler634	chr10	72254314	72254335	0.94	2.82	7042	57584	57586	3	3	3.04E-03	1.70E-02	PALD1 (+15748), PRF1 (+108206)
HyperHler635	chr16	67516162	67516546	0.94	2.81	22640	85473	85475	3	3	3.08E-03	1.70E-02	ATP6V0D1 (-1214)
HyperHler636	chr17	33787402	33787739	0.94	2.81	24652	89020	89022	3	4	3.07E-03	1.70E-02	SLFN13 (-11715), SLFN12L (+27305)
HyperHler637	chr21	44863611	44864600	0.94	4.68	36495	102686	102690	5	5	4.94E-04	3.00E-03	SIK1 (-17098), HSF2BP (+215268)

HyperHic638	chr20	62328427	62328427	0.93	3.74	36106	101951	101954	4	4	1.15E-03	8.00E-03	TNFRSF6B (+177)
HyperHic639	chr14	104621467	104622128	0.93	4.67	18859	79057	79061	5	5	4.98E-04	4.00E-03	C14orf144 (-38743), KIF26A (+16738)
HyperHic640	chr12	6485537	6485916	0.93	2.80	12824	68113	68115	3	9	3.10E-03	1.80E-02	SCNN1A (-1337)
HyperHic641	chr6	89927233	89927651	0.93	2.80	48892	39480	39482	3	3	3.12E-03	1.80E-02	GABRR1 (-290)
HyperHic642	chr5	149887461	149887787	0.93	3.73	45847	32759	32762	4	4	1.16E-03	8.00E-03	NDST1 (-50)
HyperHic643	chr10	95326033	95326248	0.93	3.72	7512	58332	58335	4	4	1.16E-03	8.00E-03	FEAR4 (-281)
HyperHic644	chr10	11246612	11246763	0.93	2.79	6186	58066	58068	3	3	3.13E-03	1.80E-02	CELF2 (+186795), USP6NL (+327586)
HyperHic645	chr7	72362292	72362809	0.93	6.51	7047	57591	57597	7	7	1.44E-04	2.00E-03	PRF1 (-20)
HyperHic646	chr17	1633714	1634018	0.93	2.79	32708	87299	87301	3	3	3.14E-03	1.80E-02	SERPINF2 (-12264), WDR81 (+5612)
HyperHic647	chr4	2933715	2934188	0.93	3.72	41017	23713	23716	4	5	1.16E-03	8.00E-03	MFSD10 (+2233), ADD1 (+88368)
HyperHic648	chr6	170535724	170536124	0.93	3.71	50275	42054	42057	4	4	1.17E-03	8.00E-03	DLT1 (+63637), C6orf70 (+384203)
HyperHic649	chr11	4415193	4415245	0.93	2.79	9241	61935	61937	3	3	3.15E-03	1.80E-02	TRIM21 (-293)
HyperHic650	chr22	44568387	44568812	0.93	4.64	37383	104180	104184	5	5	5.10E-04	4.00E-03	PARVG (-236)
HyperHic651	chr1	156215418	156215951	0.93	3.71	3980	6849	6852	4	4	1.17E-03	8.00E-03	PAQR6 (+2158), BGLAP (+3932)
HyperHic652	chr15	45028083	45028270	0.93	3.71	19606	80277	80280	4	5	1.17E-03	8.00E-03	SORD (-287125), TRIM69 (+6891)
HyperHic653	chr11	14927004	14927549	0.93	3.71	9529	62410	62413	4	4	1.17E-03	8.00E-03	CYP2R1 (-13479), CALCA (+66623)
HyperHic654	chr13	20762982	20763457	0.93	2.78	15671	73259	73261	3	3	3.16E-03	1.80E-02	GJB2 (+699)
HyperHic655	chr16	1537775	1538803	0.93	5.56	21233	83155	83160	6	6	2.60E-04	3.00E-03	PTX4 (+179)
HyperHic656	chr2	102866879	102867466	0.93	3.70	32293	13240	13243	4	4	1.18E-03	8.00E-03	IL1RL1 (-60789), IL1RL2 (+63740)
HyperHic657	chr16	832828	833250	0.93	7.41	21064	82832	82839	8	9	8.84E-05	2.00E-03	MSLN (-113)
HyperHic658	chr4	159131324	159131516	0.92	3.69	42892	27125	27128	4	4	1.20E-03	8.00E-03	TMEM144 (+19)
HyperHic659	chr1	41156730	41156980	0.92	2.77	2203	3677	3679	3	3	3.20E-03	1.80E-02	NEFG (-533)
HyperHic660	chr3	189349003	189349323	0.92	4.82	40596	22926	22930	5	5	5.21E-04	4.00E-03	TP63 (-53)
HyperHic661	chr17	37123767	37123949	0.92	4.61	24791	89276	89280	5	9	5.23E-04	4.00E-03	LASPI (+97746), PLXDC1 (+184044)
HyperHic662	chr19	51220286	51220537	0.92	2.77	29889	98586	98588	3	3	3.22E-03	1.80E-02	SHANK1 (-217)
HyperHic663	chr11	69482043	69482597	0.92	3.69	10951	65062	65065	4	5	1.21E-03	8.00E-03	ORAOV1 (+7795), CCND1 (+26465)
HyperHic664	chr7	1428806	1428900	0.92	2.77	50491	42507	42509	3	3	3.22E-03	1.80E-02	MICALL2 (+70285), UNCX (+156310)
HyperHic665	chr3	107810361	107810791	0.92	5.53	39251	20585	20590	6	6	2.64E-04	3.00E-03	CD47 (-715)
HyperHic666	chr1	2193187	2193293	0.92	2.76	9138	61662	61664	3	4	3.23E-03	1.80E-02	TH (-205)
HyperHic667	chr1	9224003	9224376	0.92	2.76	760	1314	1316	3	3	3.24E-03	1.80E-02	H6PD (-70644), GPR157 (-34961)
HyperHic668	chr2	157291262	157292127	0.92	5.52	33123	14672	14677	6	6	2.65E-04	3.00E-03	GP2 (-258)
HyperHic669	chr19	8372814	8373608	0.92	6.44	28211	95466	95472	7	7	1.52E-04	2.00E-03	CD320 (+28)
HyperHic670	chr11	67052509	67052992	0.92	3.67	10815	64780	64781	4	4	1.22E-03	8.00E-03	ANKRD13D (-4011)
HyperHic671	chr1	156046344	156046832	0.92	2.75	3960	6816	6818	3	3	3.27E-03	1.90E-02	MEX3A (+5201), RAB25 (+15637)
HyperHic672	chr3	10326540	10326774	0.92	2.75	37790	18087	18089	3	3	3.27E-03	2.00E-02	GHRL (+7974), ENSG00000272410 (+35601)
HyperHic673	chr10	131669406	131669630	0.92	2.75	8512	60305	60307	3	3	3.28E-03	2.00E-02	EBF3 (+92587), MGMT (+404070)
HyperHic674	chr4	3432342	3432546	0.92	2.75	41046	23771	23773	3	3	3.28E-03	2.00E-02	HGFAC (-11170), RGS12 (+116570)
HyperHic675	chr21	4523232	45232595	0.92	3.67	36510	102713	102716	4	4	1.23E-03	9.00E-03	AGPAT3 (-112475), RRP1 (+23020)
HyperHic676	chr8	144371537	144371779	0.92	2.75	56224	52980	52982	3	3	3.29E-03	2.00E-02	ZNF696 (-1901)
HyperHic677	chr2	65066822	65067288	0.91	2.74	31629	12144	12146	3	3	3.30E-03	2.00E-02	SERTAD2 (-206008), SLC1A4 (-129480)
HyperHic678	chr8	21905599	21905960	0.91	2.74	54215	49482	49484	3	4	3.30E-03	2.00E-02	DMTN (-10937), FGF17 (+5843)
HyperHic679	chr3	196065289	196065569	0.91	8.23	40756	23211	23219	9	9	5.79E-05	2.00E-03	TMSF19 (-170)
HyperHic680	chr16	14403004	14403425	0.91	4.56	21704	83952	83956	5	5	5.48E-04	4.00E-03	MKL2 (+230070), PARN (+320909)
HyperHic681	chr11	1506936	1507347	0.91	3.65	9030	61369	61392	4	4	1.26E-03	9.00E-03	MOB2 (+834)
HyperHic682	chr17	3907349	3907994	0.91	3.84	23821	87500	87503	4	4	1.26E-03	9.00E-03	ATP2A3 (-40087), ZZZEF1 (+138642)
HyperHic683	chr3	194408516	194409431	0.91	5.46	40708	23119	23124	6	9	2.75E-04	3.00E-03	LSG1 (-15768), XXYL1 (+582922)
HyperHic684	chr8	22456092	22456421	0.91	3.64	54266	49566	49569	4	5	1.26E-03	9.00E-03	C8orf68 (-903)
HyperHic685	chr16	83171068	83171299	0.91	2.73	22947	85963	85985	3	3	3.35E-03	2.00E-02	HSBP1 (-670264), CDH13 (+510614)
HyperHic686	chr20	45947025	45947226	0.91	2.73	35657	101146	101148	3	3	3.35E-03	2.00E-02	ZMYND8 (+38288), EYA2 (+423863)
HyperHic687	chr6	161860203	161860359	0.91	2.73	41943	41480	41482	3	3	3.36E-03	2.10E-02	AGPAT4 (-165188)
HyperHic688	chr7	73720808	73721031	0.91	2.73	51884	45255	45257	3	3	3.37E-03	2.10E-02	GTF2IRD1 (-147380), CLIP2 (+17115)
HyperHic689	chr19	36004632	36004716	0.91	2.73	29036	97000	97002	3	4	3.37E-03	2.10E-02	DMKN (-120)
HyperHic690	chr3	64008007	64008387	0.91	4.54	38855	20020	20024	5	5	5.51E-04	4.00E-03	PSMD6 (+1039), ATXN7 (+157964)
HyperHic691	chr14	105619511	105619701	0.91	2.73	13965	79247	79249	3	3	3.37E-03	2.10E-02	GPR132 (-87839), JAG2 (+15555)
HyperHic692	chr16	764420	7644794	0.91	2.72	21051	82809	82811	3	3	3.37E-03	2.10E-02	METRN (-508)
HyperHic693	chr10	134045514	134045913	0.91	3.63	8649	60566	60569	4	4	1.26E-03	1.00E-02	DPSYL4 (-45310), STK32C (+75730)
HyperHic694	chr19	5074616	5074758	0.91	2.72	28038	95176	95178	3	4	3.40E-03	2.10E-02	KDM4B (+105555), PTPRS (+266127)
HyperHic695	chr8	145018816	145018928	0.91	2.72	56306	53157	53159	3	3	3.41E-03	2.10E-02	EPPK1 (-66240), PLEC (+6172)

HyperHler696	chr2	234359654	234359783	0.90	2.71	34389	17072	17074	3	3	3	3.41E-03	2.10E-02	DGKD (+96566), USP40 (+114517)
HyperHler697	chr17	79228937	79229385	0.90	2.71	26546	92377	92379	3	3	3	3.42E-03	2.10E-02	C17orf89 (+16122), SLC38A10 (+39944)
HyperHler698	chr19	55566493	55567039	0.90	2.71	30146	99106	99108	3	4	4	3.42E-03	2.10E-02	EP58L1 (-860)
HyperHler699	chr10	73533891	73534338	0.90	3.62	7083	57649	57652	4	4	4	1.30E-03	2.10E-02	C10orf54 (-503)
HyperHler700	chr13	113356724	113357112	0.90	2.71	16987	75722	75724	3	3	3	3.43E-03	2.10E-02	MCF2L (-266617), ATP11A (+12275)
HyperHler701	chr16	85465589	85465657	0.90	2.71	23078	86181	86183	3	3	3	3.44E-03	2.10E-02	GSE1 (-181179), KIAA0513 (+368805)
HyperHler702	chr14	24779793	24780926	0.90	11.74	17307	76271	76283	13	13	13	1.06E-05	1.00E-03	LTB4R (-2157), CIDEB (+241)
HyperHler703	chr12	49688844	49689212	0.90	2.71	13473	69190	69192	3	5	5	3.44E-03	2.10E-02	TROAP (-28034), PRPH (+1543)
HyperHler704	chr1	246728663	246728727	0.90	2.71	5837	9960	9962	3	3	3	3.44E-03	2.10E-02	CNST (-1053), TFB2M (+931)
HyperHler705	chr17	7341436	7341936	0.90	4.51	23994	87863	87867	5	8	8	5.65E-04	4.00E-03	FGF11 (-660)
HyperHler706	chr17	79374327	79374741	0.90	3.61	28575	92434	92437	4	4	4	1.31E-03	1.00E-02	ENSG00000171282 (+984)
HyperHler707	chr1	11795746	11796079	0.90	8.11	894	1531	1539	9	9	9	6.15E-05	2.00E-03	AGTRAP (-299)
HyperHler708	chr12	127413363	127413369	0.90	2.70	32700	13991	13993	3	3	3	3.48E-03	2.10E-02	GYPC (-143)
HyperHler709	chr21	34185927	34186122	0.90	2.69	36269	102227	102229	3	3	3	3.51E-03	2.20E-02	OLIG2 (-212218), C21orf62 (-5997)
HyperHler710	chr17	76975944	76976357	0.90	5.38	26331	91972	91977	6	6	6	2.90E-04	3.00E-03	LGALS3BP (+40)
HyperHler711	chr10	134362126	134362170	0.90	2.69	8681	60632	60634	3	3	3	3.51E-03	2.20E-02	INPP5A (+10824), NKX6-2 (+237408)
HyperHler712	chr17	77810509	77810912	0.90	2.69	28415	92128	92130	3	3	3	3.51E-03	2.20E-02	CBX8 (-39796), CBX4 (+2517)
HyperHler713	chr8	48648813	48649457	0.90	4.48	54790	50506	50510	5	5	5	5.78E-04	4.00E-03	CEBPD (+2513), SPIDR (+475968)
HyperHler714	chr13	50070550	50070766	0.90	2.69	18212	74245	74247	3	3	3	3.52E-03	2.20E-02	PHF11 (+561)
HyperHler715	chr11	130271767	130271903	0.90	2.69	12399	67414	67416	3	3	3	3.52E-03	2.20E-02	ZBTB44 (-37254), ADAMTS8 (+27053)
HyperHler716	chr14	104741786	104742172	0.90	2.69	18873	79088	79090	3	3	3	3.53E-03	2.20E-02	C14orf180 (-304042), C14orf144 (+31438)
HyperHler717	chr1	28843736	28844028	0.89	2.68	1723	2853	2855	3	3	3	3.54E-03	2.30E-02	RCC1 (-887)
HyperHler718	chr11	2241249	2241568	0.89	2.68	9146	61681	61683	3	3	3	3.54E-03	2.30E-02	TH (-48374), ASCL2 (+50773)
HyperHler719	chr12	133022677	133022965	0.89	3.58	15577	73086	73089	4	6	6	1.35E-03	1.00E-02	GALNT9 (-332243), KLC8 (+27910)
HyperHler720	chr10	3823758	3824687	0.89	6.25	6056	55841	55847	7	7	7	1.70E-04	2.00E-03	PITRM1 (-609220), MUF6 (+3244)
HyperHler721	chr20	57267176	57267680	0.89	3.57	35828	101448	101451	4	4	4	1.36E-03	1.00E-02	NPEPL1 (-241)
HyperHler722	chr17	80988390	80988709	0.89	2.88	26782	92851	92853	3	3	3	3.58E-03	2.40E-02	ZNF750 (-190096), B3GNTL1 (+21136)
HyperHler723	chr2	231090329	231090745	0.89	4.48	34268	18873	18877	5	5	5	5.89E-04	4.00E-03	SP140 (+91)
HyperHler724	chr19	39360313	39361447	0.89	4.45	29183	97301	97305	5	5	5	5.92E-04	4.00E-03	HNRNPL (-19907), RINL (+8039)
HyperHler725	chr9	137772544	137772580	0.89	2.67	57731	55136	55138	3	4	4	3.61E-03	2.50E-02	FCN2 (-96)
HyperHler726	chr6	30686922	30687221	0.89	3.55	47644	36599	36602	4	4	4	1.39E-03	1.10E-02	MDC1 (-1406), TUBB (-906)
HyperHler727	chr22	32026779	32026975	0.89	4.44	37037	103586	103590	5	5	5	5.99E-04	4.00E-03	PISD (-2670)
HyperHler728	chr22	219233446	219233650	0.89	2.66	33987	16303	16305	3	3	3	3.62E-03	2.50E-02	TMBIM1 (-81976), SLC11A1 (-13204)
HyperHler729	chr8	22735111	22735478	0.89	4.44	54283	49599	49603	5	5	5	5.99E-04	4.00E-03	EGR3 (-184480), PEBP4 (+50126)
HyperHler730	chr6	11111894	11112117	0.89	2.66	48997	34839	34841	3	3	3	3.62E-03	2.50E-02	ERVFRD-1 (-41)
HyperHler731	chr9	139871955	139872395	0.89	3.55	57912	55387	55390	4	6	6	1.40E-03	1.10E-02	PTGDS (+218)
HyperHler732	chr5	149867577	149868855	0.89	3.54	45844	32753	32756	4	4	4	1.40E-03	1.10E-02	RPS14 (-38906), NDST1 (-19458)
HyperHler733	chr6	10555808	10556326	0.89	3.54	46983	34784	34787	4	5	5	1.40E-03	1.10E-02	GCNT6 (-77926), GCNT2 (+27478)
HyperHler734	chr11	1948933	1949113	0.89	4.43	9095	61514	61518	5	5	5	6.05E-04	4.00E-03	MRPL23 (-19485), TNNT3 (+8231)
HyperHler735	chr13	4794020	4794082	0.88	2.65	37706	17930	17932	3	3	3	3.68E-03	2.90E-02	BHLHE40 (-228760), ITPR1 (+259019)
HyperHler736	chr10	131843597	131844047	0.88	3.52	8529	60361	60364	4	5	5	1.43E-03	1.30E-02	GLRX3 (-90841), EBF3 (-81717)
HyperHler737	chr1	155043883	155044345	0.88	5.29	3909	6729	6734	6	6	6	3.05E-04	3.00E-03	EFNA3 (-7234), EFNA4 (+7877)
HyperHler738	chr1	247681242	247681439	0.88	2.64	5861	10012	10014	3	6	6	3.71E-03	3.10E-02	OR2B11 (-66033), OR2C3 (+15800)
HyperHler739	chr6	170559721	170559869	0.88	2.64	50280	42062	42064	3	3	3	3.71E-03	3.10E-02	DL1 (+39786), C6orf70 (+408074)
HyperHler740	chr18	61604237	61604367	0.88	2.64	27317	93927	93929	3	4	4	3.72E-03	3.10E-02	HMSD (-12233), SERPINB10 (+29077)
HyperHler741	chr6	30029929	30030069	0.88	3.52	47563	36242	36245	4	4	4	1.44E-03	1.40E-02	PPP1R11 (-4866), ZNRD1 (+968)
HyperHler742	chr10	6185502	6186015	0.88	2.64	6107	55931	55933	3	3	3	3.73E-03	3.20E-02	PFKFB3 (-59135), RBM17 (+54450)
HyperHler743	chr17	78829626	78829930	0.88	2.63	26494	92272	92274	3	3	3	3.75E-03	3.20E-02	CHMP6 (-135863), RPTOR (+310710)
HyperHler744	chr6	42883504	42883762	0.88	3.51	48364	38514	38517	4	4	4	1.45E-03	1.40E-02	PTORA (-94)
HyperHler745	chr16	88844415	88845204	0.88	2.63	23494	86925	86927	3	3	3	3.20E-03	3.20E-02	ANKRD11 (+87276), ZNF778 (+185575)
HyperHler747	chr19	43856594	43857074	0.88	2.63	29391	97650	97652	3	3	3	3.11E-04	3.00E-03	PIEZO1 (+6809), GTU2 (+71939)
HyperHler748	chr20	60456296	60466503	0.88	2.63	35887	101581	101583	3	3	3	3.78E-03	3.20E-02	PSG9 (-83154), TEX101 (-48814)
HyperHler749	chr13	49107693	49108353	0.87	2.62	16194	74220	74222	3	3	3	3.78E-03	3.40E-02	TCF4 (+184466), CDH4 (+628918)
HyperHler750	chr6	25027586	25027714	0.87	2.62	47221	35186	35188	3	5	5	3.78E-03	3.50E-02	RC3TB2 (-654)
HyperHler751	chr1	26527870	26527928	0.87	2.62	1609	2636	2638	3	3	3	3.78E-03	3.50E-02	LRRIC16 (-252006), FAM65B (-116455)
HyperHler752	chr1	197745025	197745238	0.87	2.62	4652	7979	7981	3	3	3	3.80E-03	3.50E-02	CEP85 (-32794), CATSPER4 (+10847)
HyperHler753	chr8	143407432	143408047	0.87	2.62	56136	52814	52816	3	3	3	3.80E-03	3.50E-02	DENND1B (-677)

HyperHler754	chr3	193987426	193987757	0.87	3.49	40684	23074	23077	4	4	1.48E-03	1.50E-02	CPN2 (+84465), HES1 (+133658)
HyperHler755	chr20	52199520	52199778	0.87	4.36	35736	101266	101270	5	5	6.42E-04	6.00E-03	ZNF217 (+10729), TSHZ2 (+610703)
HyperHler756	chr12	54778312	54779175	0.87	3.49	13797	69875	69878	4	4	1.48E-03	1.50E-02	GPR84 (+20473), ZNF385A (+6338)
HyperHler757	chr10	12979760	129797840	0.87	2.61	83762	60213	60214	3	3	3.82E-03	3.60E-02	PTPRE (+92475), MKI67 (+126849)
HyperHler758	chr17	79109729	79109910	0.87	3.48	26534	92349	92352	4	5	1.49E-03	1.50E-02	AATK (+29937), BAIAP2 (+100858)
HyperHler759	chr1	1897585	1897785	0.87	2.61	168	343	345	3	3	3.83E-03	3.60E-02	GABRD (+53095), TMEM52 (+46973)
HyperHler760	chr13	114810631	114810794	0.87	2.61	17099	75923	75925	3	3	3.84E-03	3.60E-02	GAS6 (+243673), RASA3 (+87373)
HyperHler761	chr9	139237366	139237503	0.87	2.61	57841	55289	55291	3	3	3.84E-03	3.60E-02	GPSM1 (+15503), DNIZ (+20806)
HyperHler762	chr19	55219519	55219964	0.87	2.61	30129	99077	99079	3	3	3.84E-03	3.60E-02	KIR3DL3 (-16242), LILRB4 (+46163)
HyperHler763	chr16	89168508	89168963	0.87	2.61	23461	86877	86879	3	4	3.84E-03	3.60E-02	CDH15 (+69439), ACSF3 (+8519)
HyperHler764	chr8	145024929	145025760	0.87	7.83	53308	53161	53169	9	9	7.02E-05	2.00E-02	PLEC (-301)
HyperHler765	chr20	61508481	61508590	0.87	2.61	35969	101723	101725	3	3	3.85E-03	3.60E-02	TGFL5 (-15421), DIDO1 (+60738)
HyperHler766	chr7	4778839	4779342	0.87	5.22	50710	42921	42926	6	6	3.23E-04	4.00E-03	AP5Z1 (-36162), FOXK1 (+57151)
HyperHler767	chr20	896876	897050	0.87	2.61	34873	99588	99590	3	3	3.85E-03	3.60E-02	ANGPT4 (-3)
HyperHler768	chr1	1058077	1058658	0.87	2.61	58	113	115	3	3	3.85E-03	3.60E-02	TLL10 (-50915), C1orf159 (-6890)
HyperHler769	chr12	56040025	560400336	0.87	4.34	13826	69921	69925	5	5	6.53E-04	6.00E-03	METTL7B (-35149), OR10PT (+9537)
HyperHler770	chr3	183543680	183543962	0.87	2.60	40463	22707	22709	3	3	3.88E-03	3.60E-02	MAP6D1 (-405)
HyperHler771	chr2	85637673	85637851	0.87	3.47	32042	12839	12842	4	4	1.51E-03	1.50E-02	CAPG (-86)
HyperHler772	chr1	54619445	54619895	0.87	2.60	2604	4391	4393	3	3	3.87E-03	3.60E-02	CDCP2 (-227)
HyperHler773	chr11	57232331	57232556	0.87	3.47	10299	63900	63903	4	4	1.52E-03	1.50E-02	RTN4RL2 (+4422), SLC43A1 (+50815)
HyperHler774	chr11	67646654	6765204	0.86	3.46	9187	61779	61782	4	4	1.53E-03	1.70E-02	CDKN1C (+60261), KCNQ1 (+380629)
HyperHler775	chr11	67646654	6765204	0.86	4.32	10864	64879	64883	5	5	6.68E-04	6.00E-03	ALDH3B2 (-322827), UNC93B1 (+6664)
HyperHler776	chr2	242813634	242814898	0.86	4.32	34822	17822	17826	5	5	6.68E-04	6.00E-03	CXXC11 (+2385)
HyperHler777	chr5	145236139	145236262	0.86	2.59	45728	32535	32537	3	3	3.96E-03	4.20E-02	PRELID2 (-21334), GRXCR2 (+16330)
HyperHler778	chr1	9884565	9885517	0.86	8.62	808	1387	1396	10	10	4.75E-05	2.00E-03	CLSTN1 (-457)
HyperHler779	chr1	243645911	243646787	0.86	6.03	5780	9878	9884	7	7	1.93E-04	3.00E-03	SDCCAG8 (+226991), AKT3 (+367081)
HyperHler780	chr16	69966815	69967212	0.86	5.16	22718	85618	85623	6	6	3.35E-04	4.00E-03	CLEC18A (-18069), WWP2 (+170805)
HyperHler781	chr20	30073209	30073576	0.86	5.16	35241	100359	100364	6	6	3.35E-04	4.00E-03	HMT3 (-28838), REM1 (+10297)
HyperHler782	chr6	30124214	30124299	0.86	3.44	47587	36383	36386	4	4	1.57E-03	1.90E-02	TRIM10 (+4454), TRIM40 (+19470)
HyperHler783	chr2	240259002	240259213	0.86	2.57	34662	17536	17538	3	3	4.01E-03	4.30E-02	HDAC4 (+63535), TWIST2 (+502435)
HyperHler784	chr22	46508454	46508604	0.86	4.29	3474	104359	104363	5	5	6.86E-04	8.00E-03	WN7B (-135520), PPARA (-37970)
HyperHler785	chr16	891263	891605	0.86	3.43	21081	82873	82876	4	4	1.58E-03	2.00E-02	GNG13 (-40711), LMF1 (+129555)
HyperHler786	chr14	104668772	104668921	0.86	3.43	18865	79069	79072	4	4	1.58E-03	2.00E-02	C14orf144 (-41694), KIF26A (+63787)
HyperHler787	chr12	122444450	122444621	0.86	2.57	15083	72196	72198	3	3	4.02E-03	4.30E-02	BCL7A (-12792), WDR66 (+88768)
HyperHler788	chr1	248902767	248903325	0.86	4.28	5873	10049	10053	5	5	6.91E-04	8.00E-03	ZNF672 (-229433), OR141 (-57417)
HyperHler789	chr17	81039747	81039990	0.86	2.57	26790	92866	92868	3	5	4.04E-03	4.40E-02	METRNL (+2302)
HyperHler790	chr2	10470961	10471388	0.85	2.56	30681	10596	10598	3	3	4.06E-03	4.40E-02	HPCAL1 (-27349), ODC1 (+117455)
HyperHler791	chr3	13060741	13060974	0.85	3.42	37885	18256	18259	4	4	1.59E-03	2.00E-02	IQSEC1 (-51690), NUP210 (+400951)
HyperHler792	chr19	836606	836716	0.85	2.56	27591	94420	94422	3	3	4.07E-03	4.40E-02	PRTN3 (-4302)
HyperHler793	chr16	85607562	85608058	0.85	2.56	23100	86223	86225	3	3	4.08E-03	4.40E-02	GSE1 (-39012), KIAA0513 (+510992)
HyperHler794	chr11	61159687	61159739	0.85	2.56	10413	64114	64116	3	5	4.09E-03	4.40E-02	TMEM216 (+554)
HyperHler795	chr17	6358363	6358599	0.85	3.41	23922	87677	87680	4	5	1.61E-03	2.00E-02	FAM64A (+10720), ACKR6 (+101333)
HyperHler796	chr7	27141388	27142100	0.85	2.55	51035	43632	43634	3	28	4.11E-03	4.40E-02	HOXA2 (+686)
HyperHler797	chr11	6273431	6273507	0.85	2.55	10844	64836	64838	3	3	4.11E-03	4.40E-02	PITPNM1 (-626)
HyperHler798	chr8	142297121	142297256	0.85	2.55	52698	52696	52698	3	3	4.14E-03	4.40E-02	SLC45A4 (-58516), GPR20 (+80178)
HyperHler799	chr12	6756377	6756678	0.85	3.39	12851	68164	68167	4	7	1.64E-03	2.10E-02	ACRBP (+98)
HyperHler800	chr2	238578376	238578491	0.85	2.54	34574	17374	17376	3	3	4.17E-03	4.70E-02	RAB17 (-78698), LRRFIP1 (-22548)
HyperHler801	chr6	28829631	28830041	0.85	3.38	47454	35840	35843	4	4	1.65E-03	2.10E-02	SCAND3 (-274874), TRIM27 (+61780)
HyperHler802	chr5	96078430	96078834	0.85	2.54	44819	30730	30732	3	3	4.19E-03	4.80E-02	ERAP1 (+65171), CAST (-80691)
HyperHler803	chr4	24901695	24981807	0.85	2.54	41584	24760	24762	3	5	4.19E-03	4.80E-02	LG2 (+50750), SOD3 (+184666)
HyperHler804	chr3	46448084	46449313	0.85	7.61	38378	19110	19118	9	9	7.90E-05	2.00E-03	ACKR5 (-350)
HyperHler805	chr8	144255650	144255688	0.84	2.53	52027	52951	52953	3	3	4.20E-03	4.80E-02	GPIHBP1 (-39399), LY6H (-13541)
HyperHler806	chr7	48473757	48474021	0.84	2.53	25509	90659	90661	3	3	4.21E-03	4.80E-02	LRRCS9 (+1025), EMET (-23308)
HyperHler807	chr5	141062313	141062571	0.84	2.53	45629	32407	32409	3	3	4.22E-03	4.90E-02	ARAP3 (-654)
HyperHler808	chr2	242754333	242754514	0.84	2.53	34806	17789	17791	3	3	4.23E-03	4.90E-02	NEU4 (+2329), PDGCD1 (+46636)
HyperHler809	chr1	1173264	1173622	0.84	2.53	83	163	165	3	4	4.24E-03	4.90E-02	B3GALT6 (+5814), FAM132A (+8659)
HyperHler810	chr18	74845154	74845829	0.84	3.37	27390	94078	94081	4	4	1.67E-03	2.10E-02	MBP (-767)
HyperHler811	chr4	183795763	183795822	0.84	2.53	43112	27547	27549	3	3	4.25E-03	4.90E-02	DCTD (+42739), TENM3 (+631211)

HyperHer812	chr22	25595589	25595840	0.84	4.20	36908	103373	103377	5	5	7.42E-04	9.00E-03	CRYBB3 (-102)
HyperHer813	chr19	4539943	4540333	0.84	2.52	27988	95106	95108	3	3	4.28E-03	5.00E-02	PLIN5 (-4902), LRG1 (+348)
HyperHer814	chr12	7070562	7070732	0.84	2.52	12887	68225	68227	3	3	4.28E-03	5.00E-02	PHB2 (+9341), PTPN6 (+10213)
HyperHer815	chr12	109203581	109203758	0.84	2.52	14642	71270	71272	3	3	4.28E-03	5.00E-02	CORO1C (-78299), SSH1 (+47696)
HyperHer816	chr11	66103386	66104485	0.84	9.23	10742	64658	64668	11	11	3.13E-05	2.00E-03	RIN1 (+64)
HyperHer817	chr17	79429330	79429729	0.84	2.51	26598	92485	92487	3	3	4.30E-03	5.10E-02	ACTG1 (+50277), ENSG00000171282 (+55990)
HyperHer818	chr19	8521114	852311	0.84	2.51	27599	94442	94444	3	4	4.31E-03	5.10E-02	CFD (-7240), ELANE (+1199)
HyperHer819	chr17	3824384	3824497	0.84	2.51	23814	87490	87492	3	3	4.31E-03	5.10E-02	PRX1 (-4647)
HyperHer820	chr18	77545028	77545223	0.84	2.51	27471	94225	94227	3	3	4.33E-03	5.10E-02	KCNG2 (-78542), CTDP1 (+105325)
HyperHer821	chr14	104171259	104172109	0.84	5.02	18827	78998	79003	6	6	3.76E-04	5.00E-03	RCCC3 (+6757), KLC1 (+76106)
HyperHer822	chr20	748992	749620	0.84	5.85	34865	99558	99564	7	7	2.14E-04	3.00E-02	SLC52A3 (-175)
HyperHer823	chr17	78851149	78851262	0.84	2.51	28496	92277	92279	3	4	4.35E-03	5.20E-02	CHMP6 (-114435), RPTOR (+332138)
HyperHer824	chr1	153513810	153514482	0.84	3.34	3825	6570	6573	4	4	1.73E-03	2.20E-02	S100A5 (+95)
HyperHer825	chr1	3394709	3395258	0.83	3.34	427	805	808	4	4	1.74E-03	2.20E-02	ARHGEF16 (+23994), MEGF6 (+133075)
HyperHer826	chr16	89151047	89151343	0.83	2.50	23455	86859	86861	3	3	4.37E-03	5.30E-02	CBFA2T3 (-107583), ACSF3 (-9022)
HyperHer827	chr10	58823004	5882576	0.83	2.50	6095	55909	55911	3	3	4.37E-03	5.30E-02	FBXO18 (-53909), GDI2 (-26928)
HyperHer828	chr6	30070074	30070738	0.83	7.50	47571	36310	36318	9	9	8.35E-05	2.00E-03	RNF39 (-26742), TRIM31 (+10477)
HyperHer829	chr7	157695747	157695878	0.83	2.50	53546	48326	48328	3	3	4.39E-03	5.40E-02	DNAJB6 (+566153), PTPRN2 (+684558)
HyperHer830	chr7	2773010	2773127	0.83	2.50	50649	42812	42814	3	4	4.40E-03	5.40E-02	AMZ1 (+55913), GNA12 (+110889)
HyperHer831	chr5	134735544	134735914	0.83	4.99	45265	31479	31484	6	6	3.80E-04	5.00E-03	H2AFY (-417)
HyperHer832	chr2	27719501	27720122	0.83	3.32	31077	11256	11259	4	4	1.76E-03	2.50E-02	FNDCA (-1700), GCKR (+103)
HyperHer833	chr11	63448356	63448455	0.83	2.49	10536	64311	64313	3	3	4.42E-03	5.40E-02	RTN3 (-549)
HyperHer834	chr5	128564606	128564742	0.83	2.49	45126	31220	31222	3	3	4.42E-03	5.40E-02	C5orf63 (-155490), MEGF10 (-61877)
HyperHer835	chr7	155640537	155640784	0.83	2.49	53374	47975	47977	3	3	4.43E-03	5.70E-02	SHH (-35694), C7orf13 (+782687)
HyperHer836	chr6	15501652	15502099	0.83	2.49	47089	34950	34952	3	3	4.45E-03	5.70E-02	DTNBP1 (+161397), JARID2 (+255349)
HyperHer837	chr13	113622539	113622750	0.83	4.97	17009	75762	75767	6	6	3.87E-04	6.00E-03	MCF2L (-890)
HyperHer838	chr12	4397947	4398508	0.83	2.48	12751	67976	67978	3	3	4.48E-03	5.80E-02	C12orf5 (-32143), CCND2 (+152800)
HyperHer839	chr3	129024601	129024712	0.83	2.48	39700	21286	21288	3	3	4.48E-03	5.80E-02	H1FX (+10463), CPOGT (+56208)
HyperHer840	chr12	54942853	54943009	0.83	2.48	53206	47627	47629	3	6	4.47E-03	5.80E-02	ASB10 (-1029)
HyperHer841	chr7	150885084	150885458	0.83	2.48	13810	69897	69899	3	3	4.47E-03	5.80E-02	PDE1B (-203)
HyperHer842	chr13	113689422	113689955	0.83	3.31	17028	75802	75805	4	5	1.79E-03	3.00E-02	F7 (-70432), MCF2L (+66154)
HyperHer843	chr17	80345221	80345367	0.83	2.48	26719	92734	92736	3	3	4.48E-03	5.90E-02	HEXDC (-30900), UTS2R (+13141)
HyperHer844	chr7	130125756	130125836	0.83	3.31	52822	46946	46949	4	14	1.79E-03	3.00E-02	CEP41 (-44718), MEST (-6138)
HyperHer845	chr11	70563131	70563792	0.83	3.30	11039	65244	65247	4	8	1.79E-03	3.00E-02	SHANK2 (+294910), CITN (+318815)
HyperHer846	chr5	176543901	176544135	0.83	3.30	46443	33776	33779	4	5	1.80E-03	3.00E-02	NSD1 (-16908), FGFR4 (+30131)
HyperHer847	chr14	105125984	105126372	0.83	2.48	18914	79158	79160	3	3	4.50E-03	5.90E-02	TMEM179 (-54194), INF2 (-29796)
HyperHer848	chr3	50376000	50376216	0.83	3.30	38523	19434	19437	4	4	1.80E-03	3.00E-02	TUSC2 (-10434), RASSF1 (+2164)
HyperHer849	chr12	4488893	4489155	0.83	2.48	12755	67986	67988	3	6	4.51E-03	5.90E-02	FGF23 (-130)
HyperHer850	chr10	134664471	134664800	0.82	2.47	8712	60711	60713	3	3	4.54E-03	6.20E-02	GPR123 (-236773), NKX6-2 (-65080)
HyperHer851	chr17	80292079	80292252	0.82	2.47	26710	92706	92708	3	3	4.55E-03	6.20E-02	SECTM1 (-292)
HyperHer852	chr3	13678918	13679636	0.82	5.76	37913	18325	18331	7	7	2.28E-04	6.00E-03	FLN2 (+88646), WNT17A (+242341)
HyperHer853	chr13	31019673	31020218	0.82	3.29	15927	73748	73751	4	5	1.82E-03	3.30E-02	KATNAL1 (-138325), HMGB1 (+171788)
HyperHer854	chr16	31548640	31549141	0.82	2.47	22102	84542	84544	3	3	4.55E-03	6.20E-02	ZNF720 (-175664), AHSP (+9706)
HyperHer855	chr8	144408128	144408900	0.82	3.29	56227	52969	52992	4	4	1.85E-03	3.30E-02	TOP1MT (+8553), ZNF696 (+34954)
HyperHer856	chr13	113296192	113296447	0.82	3.29	16981	75713	75716	4	4	1.83E-03	3.30E-02	TUBGCP3 (-53839), ATP11A (-48323)
HyperHer857	chr1	152595322	152596177	0.82	5.74	3772	6489	6495	7	7	2.31E-04	6.00E-03	LCE3A (-171)
HyperHer858	chr21	47456315	47456446	0.82	2.46	36656	102941	102943	3	3	4.60E-03	6.20E-02	COL6A2 (-61630), COL6A1 (+54730)
HyperHer859	chr17	196280012	19628421	0.82	3.28	24356	88510	88513	4	4	1.84E-03	3.40E-02	SLC47A2 (-8288), ALDH3A1 (+20555)
HyperHer860	chr1	16091100	16091599	0.82	2.45	1054	1773	1773	3	4	4.62E-03	6.30E-02	FLN1M1 (+356)
HyperHer861	chr10	6214016	6214079	0.82	2.45	6111	55937	55939	3	3	4.63E-03	6.30E-02	PKFMB3 (-30846), RBM17 (+82739)
HyperHer862	chr13	24269867	24270321	0.82	2.45	15747	73410	73413	3	3	4.63E-03	6.30E-02	INFRSF19 (+116595), MIPPEP (+193464)
HyperHer863	chr21	46077715	46077731	0.82	2.45	35561	102792	102794	3	5	4.64E-03	6.30E-02	KRTAP12.4 (-3147), KRTAP12-3 (-126)
HyperHer864	chr10	88717364	88717926	0.82	2.45	7402	58130	58132	3	6	4.65E-03	6.40E-02	SNCG (-768), MMRN2 (-273)
HyperHer865	chr9	126101872	126102244	0.81	2.44	57291	54574	54576	3	3	4.69E-03	6.70E-02	STRBP (-71203), CRB2 (-16481)
HyperHer866	chr12	133161835	133162043	0.81	2.44	15601	73123	73125	3	3	4.71E-03	6.80E-02	MUC8 (-111213), P2RX2 (-33464)
HyperHer867	chr2	55450737	55450874	0.81	2.44	15251	11964	11966	3	3	4.71E-03	6.80E-02	RTN4 (-173126), RPS27A (-8732)
HyperHer868	chr6	30168645	30169069	0.81	2.44	47594	36436	36438	3	3	4.72E-03	7.00E-02	TRIM26 (+12286), TRIM15 (-37864)
HyperHer869	chr5	1911127	191486	0.81	3.25	43330	27925	27928	4	10	1.91E-03	3.80E-02	SDHA (-27049), PLEKHG4B (+50934)

HyperHer870	chr8	127568650	1275686163	0.81	2.43	55823	52345	52347	3	7	4.76E-03	7.30E-02	FAM84B (+1731)
HyperHer871	chr1	2838805	2839247	0.81	4.05	319	610	614	5	5	8.49E-04	1.80E-02	MMEL1 (-274587), ACTRT2 (-99020)
HyperHer872	chr19	56004925	56005437	0.81	2.43	30199	99203	99205	3	3	4.77E-03	7.50E-02	SSC5D (+5247), SBK2 (+43275)
HyperHer873	chr3	3151795	3152038	0.81	2.43	37692	17908	17910	3	3	4.77E-03	7.50E-02	IL5RA (+141)
HyperHer874	chr19	10213271	10213722	0.81	2.43	28281	95597	95599	3	3	4.77E-03	7.50E-02	PPAN-P2RY11 (-3574), PPAN (-3547), ANGPTL6 (-25)
HyperHer875	chr1	230849801	230850299	0.81	2.43	5545	9493	9495	3	3	4.78E-03	7.50E-02	AGT (-7)
HyperHer876	chr1	1957073	1957805	0.81	4.04	180	370	374	5	5	8.54E-04	1.80E-02	PRKZ (-24470), GABRD (+6659)
HyperHer877	chr16	89118603	89119709	0.81	6.46	23452	86849	86856	8	8	1.49E-04	8.00E-03	CRFA2T3 (-75544), ACSF3 (-41061)
HyperHer878	chr16	29195900	29196472	0.81	2.42	21973	84325	84327	3	3	4.81E-03	7.70E-02	LAT (+200039), NPIPB11 (+219164)
HyperHer879	chr16	32101066	32103577	0.81	2.42	21402	83469	83471	3	3	4.84E-03	8.00E-02	OR1F1 (-44035), CASP16 (+15968)
HyperHer880	chr14	105147537	105147781	0.80	2.41	18918	79166	79168	3	3	4.88E-03	8.50E-02	TMEM179 (-75675), INF2 (-8315)
HyperHer881	chr17	79377272	79378207	0.80	4.01	26578	92444	92446	5	5	8.83E-04	2.60E-02	ENSG00000171282 (+4200), ACTG1 (+102067)
HyperHer882	chr2	98852865	98852938	0.80	2.40	32208	13111	13113	3	3	4.91E-03	8.70E-02	TMEM131 (-240563), CNGA3 (-109701)
HyperHer883	chr15	89153687	89154196	0.80	3.20	20573	81883	81886	4	4	2.00E-03	4.70E-02	DET1 (-64048), AEN (-10595)
HyperHer884	chr7	1025760	1026310	0.80	3.20	50390	42258	42261	4	5	2.01E-03	4.70E-02	GPR146 (-68886), CYP2W1 (+3200)
HyperHer885	chr19	10405595	10406364	0.80	2.39	28299	95628	95630	3	3	4.97E-03	8.80E-02	ICAM5 (+5503), ZGLP1 (+14396)
HyperHer886	chr8	10530053	10530148	0.80	2.39	53985	49046	49048	3	3	4.97E-03	8.80E-02	C6orf74 (-46)
HyperHer887	chr16	15931778	15933557	0.80	3.19	21243	83187	83190	4	4	2.02E-03	4.70E-02	TMEM204 (+9794), IFT140 (+68743)
HyperHer888	chr5	179588840	1795888673	0.80	2.39	46593	34047	34049	3	4	4.98E-03	8.80E-02	RASGEF1C (-23208), MAPK9 (+130542)
HyperHer889	chr16	4732911	4733181	0.80	2.39	21509	83657	83659	3	3	5.02E-03	9.10E-02	NUDT16L1 (-10649), MGRN1 (+58255)
HyperHer890	chr1	1132665679	113266753	0.79	2.38	3427	5867	5869	3	3	5.02E-03	9.10E-02	FAM19A3 (+2675), SLC16A1 (+232969)
HyperHer891	chr17	17255427	17255771	0.79	2.38	24272	88389	88391	3	3	5.07E-03	9.40E-02	MED9 (-124701), NT5M (+48950)
HyperHer892	chr1	27894985	27895490	0.79	2.38	1686	2798	2800	3	3	5.08E-03	9.40E-02	WASF2 (-78554), AHDCT1 (+34920)
HyperHer893	chr16	34178713	34188238	0.79	2.38	22094	84529	84531	3	3	5.08E-03	9.40E-02	SLC5A2 (-6413), TGFBI1 (+14646)
HyperHer894	chr17	48354476	4835627	0.79	2.37	23875	87598	87600	3	3	5.09E-03	9.40E-02	GP1BA (-40)
HyperHer895	chr1	29950301	29956004	0.79	2.37	353	668	670	3	3	5.11E-03	9.40E-02	ARHGEF16 (-375537), PROM116 (+9678)
HyperHer896	chr16	29599012	29599390	0.79	7.90	47518	36039	36048	10	11	6.88E-05	6.00E-03	GABBR1 (+1761), OR2H2 (+43518)
HyperHer897	chr2	12863394	1286641	0.79	3.16	30418	10193	10193	4	4	2.09E-03	4.90E-02	TPO (-130715), SNTG2 (-339964)
HyperHer898	chr8	884647	884842	0.79	2.37	53710	48598	48600	3	3	5.12E-03	9.50E-02	DLGAP2 (-564787), TDRP (-388964)
HyperHer899	chr10	135171713	135171746	0.79	2.37	8822	60952	60954	3	4	5.12E-03	9.50E-02	FUOM (-201)
HyperHer900	chr12	16499963	16500185	0.79	2.37	13090	68533	68535	3	4	5.15E-03	9.60E-02	MGST1 (-638)
HyperHer901	chr7	138720989	138721085	0.79	2.36	52957	47197	47199	3	3	5.16E-03	9.60E-02	KIAA1549 (-54963), ZC3HAV1 (+73367)
HyperHer902	chr7	157348161	157348266	0.79	2.36	53473	48189	48191	3	3	5.17E-03	9.60E-02	DNAJB6 (+218554)
HyperHer903	chr7	4746131	4746462	0.79	2.36	50703	42900	42902	3	3	5.19E-03	9.60E-02	AP521 (-68956), FOXK1 (+24357)
HyperHer904	chr17	46676099	46676375	0.79	2.36	25360	90335	90337	3	4	5.19E-03	9.60E-02	HOXB5 (-4914)
HyperHer905	chr16	87388240	87388531	0.79	3.15	21595	83776	83779	4	4	2.13E-03	5.10E-02	ABAT (-68440), METT122 (+22841)
HyperHer906	chr3	100712322	100712345	0.79	2.36	39206	20534	20536	3	3	5.20E-03	9.60E-02	AB13BP (+25)
HyperHer907	chr17	80372493	80372912	0.79	3.14	26722	92741	92744	4	4	2.13E-03	5.10E-02	HEXDC (-3491)
HyperHer908	chr1	36785859	36788416	0.79	7.86	1998	3316	3325	10	10	6.95E-05	6.00E-03	EVA1B (-2617), THRAP3 (+97121)
HyperHer909	chr14	62035431	62035585	0.79	2.36	17804	77322	77323	3	3	5.21E-03	9.70E-02	HIF-1A (-128832), PRKGH (+247073)
HyperHer910	chr9	141016791	141017457	0.79	2.36	55543	55541	55543	3	3	5.22E-03	9.80E-02	CACNA1B (+244883)
HyperHer911	chr17	1133546	1133706	0.79	2.36	23652	87192	87194	3	3	5.22E-03	9.80E-02	ABR (-50458), BHLHA9 (-40227)
HyperHer912	chr15	40802888	40803416	0.78	2.35	19496	80109	80111	3	3	5.24E-03	9.90E-02	RPUSD2 (-58347), CHST14 (+39992)
HyperHer913	chr1	180922636	180923569	0.78	3.92	4516	7765	7769	5	6	9.65E-04	3.50E-02	STX6 (+68944), XPR1 (+321963)
HyperHer914	chr6	31804078	31804883	0.78	3.13	4784	37107	37110	4	4	2.16E-03	5.30E-02	HSPA1B (+8969), NEU1 (+26202)
HyperHer915	chr16	13935684	13940689	0.78	3.13	21210	83106	83109	4	4	2.17E-03	5.30E-02	TSR3 (+8075), BAIAP3 (+9332)
HyperHer916	chr13	20797356	20797693	0.78	3.13	15676	73276	73278	4	4	2.17E-03	5.30E-02	GJB2 (-33606), GJB6 (+9009)
HyperHer917	chr2	25499619	25500416	0.78	3.91	30974	11082	11086	5	5	9.73E-04	3.00E-02	POMC (-108246), DNMT3A (+65441)
HyperHer918	chr10	81002480	81003657	0.78	3.91	7265	57903	57907	5	5	9.73E-04	3.00E-02	PP1F (-104165), ZMI21 (+174277)
HyperHer919	chr11	65314454	65315625	0.78	6.25	10683	64543	64550	8	11	1.70E-04	1.10E-02	LTPB3 (+106559), SCYL1 (+22492)
HyperHer920	chr11	62621178	62621791	0.78	3.90	10504	64259	64263	5	5	9.78E-04	3.00E-02	SLC3A2 (-2098)
HyperHer921	chr7	150147553	150148073	0.78	6.21	53145	47507	47514	8	9	1.75E-04	1.10E-02	GMAP8 (+95)
HyperHer922	chr1	153762201	153762564	0.77	4.65	3841	6612	6617	6	6	5.07E-04	1.70E-02	SLC27A3 (+14615), GATAD2B (+133068)
HyperHer923	chr21	43823809	43824109	0.77	3.87	36457	102628	102632	5	6	1.01E-03	3.50E-02	UBASH3A (-65)
HyperHer924	chr16	1148030	1148520	0.77	3.09	21144	82990	82993	4	5	2.27E-03	5.90E-02	CIQTNF8 (-2031)
HyperHer925	chr17	80273242	80273685	0.77	3.08	26702	92691	92694	4	4	2.28E-03	5.90E-02	CSNK1D (-41857), CD7 (+2014)
HyperHer926	chr6	106433792	106434169	0.77	3.08	49070	39928	39928	4	9	2.28E-03	5.90E-02	PREP (-583022), PRDM1 (-100214)
HyperHer927	chr2	242953754	242953754	0.77	3.08	34832	17840	17843	4	4	2.29E-03	5.90E-02	CXXC11 (+142211)

HyperHler928	chr17	40489513	40489785	0.77	3.84	25014	89673	89677	5	5	1.04E-03	3.20E-02	STAT5A (+50084), STAT3 (+50937)
HyperHler929	chr11	2292677	2292787	0.76	3.05	9149	61697	61700	4	24	2.33E-03	6.20E-02	ASCL2 (-550)
HyperHler930	chr17	45949677	45949878	0.76	3.81	25299	90175	90179	5	5	1.00E-03	3.50E-02	SP2 (-23738), SP6 (-21219)
HyperHler931	chr10	73848817	73849167	0.76	5.33	7090	57665	57671	7	9	2.98E-04	1.50E-02	SPOCK2 (-461)
HyperHler932	chr7	50132653	50133000	0.76	3.80	51550	44688	44692	5	7	1.07E-03	3.60E-02	CtcfT2 (-2805), ZFPBP (+33)
HyperHler933	chr7	139256124	139256620	0.76	4.56	52973	47221	47226	6	6	5.43E-04	2.40E-02	CLEC2L (+47770), HIPK2 (+221145)
HyperHler934	chr7	2138722	2139216	0.76	3.03	50581	42681	42684	4	4	2.38E-03	7.00E-02	MAD1L1 (+133909), ELFN1 (+411214)
HyperHler935	chr13	114814024	114814706	0.76	6.07	71100	75926	75933	8	8	1.88E-04	1.60E-02	GAS6 (-247329), RASA3 (+83721)
HyperHler936	chr2	241721504	241722113	0.76	3.03	34738	17664	17667	4	5	2.40E-03	7.10E-02	KIF1A (+37916), AQP12A (+90547)
HyperHler937	chr10	135090098	135090565	0.75	3.77	8806	60919	60923	5	5	1.10E-03	4.10E-02	ADAM8 (+40)
HyperHler938	chr19	51231557	51232007	0.75	3.77	29894	98601	98605	5	5	1.10E-03	4.10E-02	GPR32 (+41939), CLEC11A (+5196)
HyperHler939	chr17	62075103	62075409	0.75	3.01	25802	91156	91159	4	4	2.44E-03	7.40E-02	SCN4A (-24978), ICAM2 (+22738)
HyperHler940	chr7	1894209	1895060	0.75	3.76	50550	42614	42618	5	5	1.12E-03	4.40E-02	ELFN1 (+166880), MAD1L1 (+378243)
HyperHler941	chr11	1082797	1083509	0.75	4.48	8969	61269	61274	6	6	5.78E-04	3.20E-02	MUC5AC (-68427), MUC2 (+8278)
HyperHler942	chr12	54763081	54763433	0.75	2.99	13793	69865	69868	4	4	2.51E-03	8.00E-02	GPR84 (-4986)
HyperHler943	chr6	146919932	146920295	0.75	6.72	49657	40986	40994	9	9	1.29E-04	1.40E-02	ADGB (+13)
HyperHler944	chr10	135342560	135343248	0.75	2.98	8836	60987	60990	4	8	2.52E-03	8.20E-02	CYP2E1 (+8994), SYCE1 (+36234)
HyperHler945	chr19	5492717	54928185	0.74	2.97	30112	99049	99052	4	6	2.58E-03	8.30E-02	LENG8 (-32114), TTYH1 (+1251)
HyperHler946	chr12	53183930	53184086	0.74	2.97	13641	69458	69461	4	5	2.58E-03	8.30E-02	KRT78 (-12879), KRT3 (+5893)
HyperHler947	chr7	27143398	27143788	0.74	2.97	51035	43656	43659	4	28	2.57E-03	8.30E-02	HOXA2 (-1203)
HyperHler948	chr6	34203153	34203887	0.74	2.96	48066	38081	38084	4	4	2.58E-03	8.40E-02	HMGAI (-1130)
HyperHler949	chr1	45189875	45190912	0.74	3.71	2364	3916	3920	5	6	1.18E-03	4.70E-02	TMEM53 (-50167), KIF2C (-15098)
HyperHler950	chr16	85932383	85932853	0.74	2.96	23130	86274	86277	4	8	2.58E-03	8.50E-02	IRF8 (+209)
HyperHler951	chr22	24823110	24823554	0.74	4.44	36882	103326	103331	6	6	5.96E-04	3.40E-02	ADORA2A (-198)
HyperHler952	chr16	89005932	89006877	0.74	3.70	23430	86802	86806	5	5	1.18E-03	4.80E-02	PABPNIL (-73379), CBFA2T3 (+37207)
HyperHler953	chr15	68497992	68498857	0.74	2.94	20058	81004	81007	4	4	2.63E-03	9.60E-02	CALML4 (-526)
HyperHler954	chr17	72357092	72358370	0.74	3.88	28026	91471	91475	5	5	1.21E-03	5.50E-02	BTBD17 (-96)
HyperHler955	chr13	128779277	128779601	0.73	5.13	39691	21270	21276	7	7	3.44E-04	3.10E-02	GP9 (-171)
HyperHler956	chr13	107028903	107029443	0.73	3.66	16731	75213	75217	5	5	1.24E-03	5.70E-02	EFNB2 (+158289), DAOA (+910581)
HyperHler957	chr6	32014300	32016247	0.73	10.94	47806	37187	37201	15	21	1.42E-05	1.00E-03	TNKB (-1369)
HyperHler958	chr2	37571677	37571901	0.73	3.64	31203	11424	11428	5	5	1.28E-03	6.10E-02	OPCT (+72)
HyperHler959	chr13	52528955	52529524	0.73	6.54	38603	19559	19567	9	10	1.41E-04	1.80E-02	STAB1 (-114)
HyperHler960	chr4	1304836	1305425	0.73	3.63	40911	23522	23526	5	5	1.29E-03	6.30E-02	UVSSA (-35973), MAEA (+21492)
HyperHler961	chr13	52813652	52813920	0.72	3.59	38613	19582	19586	5	5	1.33E-03	7.70E-02	ITIH3 (-15028), ITIH1 (+2178)
HyperHler962	chr10	3281803	3282650	0.71	3.57	6034	55813	55817	5	5	1.38E-03	7.90E-02	PITRM1 (-67224), KLIF6 (+545240)
HyperHler963	chr17	43922122	43922356	0.71	3.56	25238	90075	90079	5	6	1.38E-03	8.50E-02	SPPL2C (-17)
HyperHler964	chr5	154026371	154027256	0.71	4.27	45942	32928	32933	6	6	6.99E-04	5.90E-02	HAND1 (-168990), LARP1 (-65648)
HyperHler965	chr10	135123006	135123764	0.71	4.26	8811	60929	60934	6	6	7.03E-04	6.00E-02	ZNF511 (+1406), CALY (+27026)
HyperHler966	chr17	65471303	65471507	0.71	3.54	25886	91276	91280	5	5	1.41E-03	9.30E-02	NOL1 (-242544), PITPNC1 (+97134)
HyperHler967	chr6	31590513	31590870	0.71	3.53	47745	36947	36951	5	5	1.41E-03	9.40E-02	PRRC2A (+2190), BAG6 (+29785)
HyperHler968	chr1	156357871	156358408	0.71	4.23	3987	6870	6875	6	7	7.23E-04	6.70E-02	RHBG (-19137), Ctorf61 (+41044)
HyperHler969	chr8	38757532	38757859	0.70	3.52	54653	50250	50254	5	5	1.43E-03	9.50E-02	PLEKHA2 (-1057)
HyperHler970	chr17	1477843	1479213	0.70	5.63	23688	87252	87259	8	8	2.49E-04	4.20E-02	PITPNA (-12418), SLC43A2 (+53602)
HyperHler971	chr12	123380870	123381003	0.70	3.52	15108	72241	72245	5	5	1.43E-03	9.70E-02	VP-S37B (+54)
HyperHler972	chr6	31627617	31627714	0.70	4.21	47750	36961	36966	6	6	7.37E-04	7.00E-02	Ctorf47 (+883)
HyperHler973	chr6	32121433	32121566	0.69	4.16	47845	37453	37458	6	18	7.68E-04	8.00E-02	PRRT1 (-171), PPT2-EGFL8 (-499), PPT2 (+200)
HyperHler974	chr13	80054976	80055241	0.69	4.84	16456	74659	74665	7	7	4.32E-04	6.20E-02	NDFIP2 (-178)
HyperHler975	chr16	875257	876216	0.69	4.84	21077	82862	82868	7	7	4.32E-04	6.20E-02	GNGL3 (-25004), LMF1 (+145262)
HyperHler976	chr6	3848790	3849190	0.69	4.80	48826	34456	34462	7	7	4.47E-04	7.10E-02	FAM50B (-630)
HyperHler977	chr11	70516627	70517411	0.67	4.72	11034	65231	65237	7	7	4.77E-04	9.10E-02	CTTN (+272372), SHANK2 (+341353)
HyperHler978	chr11	30881658	30881842	0.63	6.34	47669	36698	36707	10	19	1.61E-04	6.50E-02	VARF2 (-358)
HyperHler979	chr6	30039130	30039801	0.53	11.06	47565	36250	36270	21	24	1.32E-05	2.00E-02	RNF39 (+4198), PPPIR11 (+4601)
HypoHler662	chr6	101848767	101847706	-0.50	8.01	49034	39840	39855	16	19	6.53E-05	7.20E-02	GRIK2 (+573)
HypoHler661	chr1	3566950	3568243	-0.50	11.54	440	827	849	23	24	1.14E-05	7.00E-03	TP73 (-1487), WRAP73 (-960)
HypoHler660	chr2	176971820	176974060	-0.50	8.06	33427	15295	15310	16	16	6.34E-05	6.70E-02	HOXD10 (-8367), HOXD11 (+926)
HypoHler659	chr5	122429178	122431419	-0.52	7.76	45061	31112	31126	15	15	7.31E-05	6.30E-02	PRDM6 (+5483), CEP120 (+328698)
HypoHler658	chr7	27280914	27282444	-0.53	11.62	51091	43893	43914	22	23	1.11E-05	1.20E-02	EVX1 (-485)
HypoHler657	chr12	114845868	114847641	-0.54	8.66	14822	71620	71635	16	16	4.61E-05	4.00E-02	TBX5 (-508)

HypoHic656	chr3	62354546	62357176	-0.54	7.59	38813	19908	19921	14	14	7.92E-05	8.00E-02	FEZF2 (+3329), PTPRG (+808276)
HypoHic655	chr6	28557080	28558006	-0.55	9.34	47419	35683	35699	17	20	2.88E-05	3.10E-02	SCAND3 (-2431)
HypoHic654	chr5	63255045	63257710	-0.55	7.15	44350	29760	29772	13	19	1.02E-04	9.70E-02	HTR1A (+1402)
HypoHic653	chr4	174450016	174451964	-0.55	7.15	44350	27360	27372	13	25	1.02E-04	9.70E-02	HAND2 (+395)
HypoHic652	chr5	50678451	50679681	-0.56	7.28	44208	29525	29537	13	15	9.55E-05	8.30E-02	ISL1 (+145)
HypoHic651	chr7	45960367	45961778	-0.56	9.54	51481	44559	44575	17	22	2.67E-05	5.40E-02	IGFBP3 (-223)
HypoHic650	chr13	112720171	112721950	-0.56	7.87	16919	75548	75561	14	14	6.93E-05	5.40E-02	SOK1 (+552)
HypoHic649	chr3	62363842	62365402	-0.57	7.34	38816	19945	19957	13	18	9.20E-05	7.70E-02	FEZF2 (-5332), CADPS (+496532)
HypoHic648	chr1	91190005	91192803	-0.57	13.04	3101	5281	5303	23	23	5.44E-06	2.00E-03	BARHL2 (-8610), ZNF644 (+295626)
HypoHic647	chr1	217307696	217311511	-0.57	11.36	5193	8873	8892	20	27	1.21E-05	1.90E-02	ESRRG (-412809), GPATCH2 (+494820)
HypoHic646	chr8	55370407	55372569	-0.57	7.97	54896	50721	50734	14	18	6.62E-05	4.80E-02	SOX17 (+993)
HypoHic645	chr8	50822168	50823541	-0.57	6.84	54836	50597	50608	12	12	1.20E-04	9.30E-02	SNTG1 (-1378)
HypoHic644	chr5	170734856	170736572	-0.57	8.58	46183	33318	33332	15	15	4.75E-05	2.50E-02	TLX3 (-574)
HypoHic643	chr6	117197952	117199067	-0.57	6.88	49278	40276	40287	12	12	1.18E-04	9.10E-02	RFX6 (+87)
HypoHic642	chr2	176986659	176988284	-0.58	6.91	33435	15346	15357	12	24	1.17E-04	8.90E-02	HOXD9 (+384)
HypoHic641	chr6	50817793	50819236	-0.58	6.91	48554	38863	38874	12	13	1.17E-04	8.90E-02	TFAP2B (-31779)
HypoHic640	chr4	183062004	183065224	-0.58	8.64	43089	27502	27516	15	18	4.68E-05	2.20E-02	TENM3 (-100968)
HypoHic639	chr4	185939458	185941601	-0.58	7.52	43170	27640	27652	13	13	8.28E-05	6.20E-02	HELT (+447)
HypoHic638	chr2	154333568	154335698	-0.58	6.96	33097	14582	14593	12	18	1.14E-04	8.30E-02	RPRM (+689)
HypoHic637	chr12	45443808	45445385	-0.58	8.15	13370	69012	69025	14	15	6.10E-05	3.60E-02	DBX2 (+285)
HypoHic636	chr6	56111812	56112696	-0.58	7.59	48628	38978	38990	13	13	7.90E-05	6.00E-02	COL21A1 (+290)
HypoHic635	chr6	100895050	100897445	-0.59	8.24	49022	39749	39762	14	16	5.79E-05	3.40E-02	MCHR2 (-454149), SIM1 (+16557)
HypoHic634	chr5	11903145	11904912	-0.59	8.24	43826	28866	28879	14	14	5.79E-05	3.40E-02	CTNND2 (+126)
HypoHic633	chr17	32483771	32484259	-0.59	6.50	24606	88922	88932	11	13	1.44E-04	9.90E-02	ASIC2 (-863979), CCL2 (-98319)
HypoHic632	chr10	134597884	134600357	-0.59	12.43	8696	60655	60675	21	35	7.09E-06	1.00E-02	NKX6-2 (+435)
HypoHic631	chr6	29974083	29975427	-0.60	17.28	47558	36207	36235	29	31	1.42E-06	0.00E+00	ZNRD1 (-54276), HLA-A (+65718)
HypoHic630	chr4	111531926	111533517	-0.60	6.01	42382	28203	28212	10	14	1.95E-04	9.10E-02	PITYX2 (+11537), ENPEP (+135493)
HypoHic629	chr5	63801834	63802993	-0.60	7.84	44355	28793	28805	13	13	7.02E-05	4.60E-02	RGS7BP (+286)
HypoHic628	chr2	45170322	45172265	-0.60	6.64	31356	11703	11713	11	11	1.36E-04	7.90E-02	SIX3 (+2392), SIX2 (+65275)
HypoHic627	chr4	147560126	147562073	-0.60	6.04	42738	26824	26833	10	10	1.92E-04	8.60E-02	EDNRA (-840984), POU4F2 (+1055)
HypoHic626	chr2	228028601	228029790	-0.61	7.26	34240	18804	18815	12	13	9.67E-05	5.30E-02	COL4A4 (-367), COL4A3 (-85)
HypoHic625	chr6	74218468	74219307	-0.61	6.07	20221	81239	81248	10	10	1.89E-04	8.60E-02	LOXL1 (+89)
HypoHic624	chr4	155663225	155664311	-0.61	6.06	42858	27041	27041	10	14	1.87E-04	8.50E-02	LRAT (-1355)
HypoHic623	chr3	147125287	147126703	-0.61	12.16	39980	21834	21853	20	39	8.04E-06	1.00E-02	ZIC4 (-3924), ZIC1 (-1176)
HypoHic622	chr11	12029738	12031099	-0.61	6.10	9449	62282	62291	10	13	1.85E-04	8.30E-02	DKK3 (+210)
HypoHic621	chr6	85433055	85484863	-0.61	6.10	48849	39395	39404	10	13	1.84E-04	8.30E-02	NT5E (-675850), TBX18 (-9722)
HypoHic620	chr2	107502354	107504169	-0.61	7.33	32386	13389	13400	12	12	9.36E-05	5.00E-02	ST6GAL2 (-160)
HypoHic619	chr1	27709634	27709928	-0.61	7.35	1670	2764	2775	12	13	9.20E-05	5.00E-02	CD164L2 (+12)
HypoHic618	chr14	57275967	57279275	-0.61	11.04	17702	77094	77111	18	20	1.35E-05	1.10E-02	OTX2 (-434)
HypoHic617	chr6	100911526	100912168	-0.61	6.76	49026	39791	39801	11	12	1.27E-04	7.10E-02	SIM1 (+958)
HypoHic616	chr5	5139866	5140935	-0.62	5.54	43704	28690	28698	9	18	2.63E-04	9.50E-02	ADAMTS16 (-42)
HypoHic615	chr6	10415597	10416090	-0.62	6.77	46970	34721	34731	11	18	1.28E-04	7.10E-02	TFAP2A (-374)
HypoHic614	chr10	118896012	118898082	-0.62	8.63	8099	59513	59526	14	14	4.71E-05	2.20E-02	VAX1 (+520)
HypoHic613	chr5	113698683	113699683	-0.62	11.10	44967	30940	30957	18	19	1.25E-05	1.10E-02	KCNN2 (+1631), TRIM36 (+817583)
HypoHic612	chr7	156795356	156797833	-0.62	8.03	53418	48063	48075	13	15	6.50E-05	4.00E-02	MXN1 (+6750), NOM1 (+54178)
HypoHic611	chr1	165323692	165326345	-0.62	10.51	4272	7326	7342	17	17	1.68E-05	1.10E-02	LMX1A (+933)
HypoHic610	chr4	93224895	93227270	-0.62	8.03	42227	25927	25939	13	13	6.48E-05	4.00E-02	GRID2 (+533)
HypoHic609	chr12	106978920	106980319	-0.62	6.21	14587	71173	71182	10	10	1.75E-04	7.30E-02	RFX4 (-15295), POLR3B (+228184)
HypoHic608	chr4	104640489	104641548	-0.62	5.60	42321	26090	26098	9	10	2.55E-04	8.90E-02	TACR3 (-46)
HypoHic607	chr3	147140118	147141614	-0.62	7.47	39988	21895	21906	12	13	8.47E-05	4.30E-02	ZIC1 (+3695)
HypoHic606	chr19	50193437	50194662	-0.62	5.61	29819	98423	98431	9	13	2.52E-04	8.70E-02	CPT1C (-323)
HypoHic605	chr5	131592974	131593413	-0.63	5.65	45173	31312	31320	9	10	2.48E-04	8.40E-02	PDLIM4 (-170)
HypoHic604	chr8	65289751	65292321	-0.63	11.33	55023	50970	50987	18	19	1.21E-05	1.10E-02	BHLHE22 (-201778)
HypoHic603	chr12	47224649	47226255	-0.63	6.30	13395	69067	69076	10	10	1.63E-04	6.70E-02	PCED1B (-247934), SLC38A4 (-5672)
HypoHic602	chr6	30227800	30228083	-0.63	5.67	47600	36449	36457	9	12	2.42E-04	8.20E-02	TRIM39 (-66679), TRIM26 (-46799)
HypoHic601	chr2	63275509	63276565	-0.63	5.67	31593	12084	12092	9	27	2.42E-04	8.20E-02	OTX1 (-1900)
HypoHic600	chr8	25901335	25902611	-0.63	5.68	54374	49792	49800	9	10	2.41E-04	8.20E-02	EBF2 (+940)
HypoHic599	chr16	77468277	77469540	-0.63	5.69	22868	85845	85853	9	12	2.40E-04	8.20E-02	ADAMTS18 (+102)

HypoHic598	chr5	1874703	1876719	-0.63	8.24	43552	28338	28350	13	13	5.79E-05	3.30E-02	IRX4 (+11621), NDUF56 (+74197)
HypoHic597	chr6	123317124	123318023	-0.64	6.35	49338	40395	40404	10	10	1.60E-04	6.30E-02	CLVS2 (+458)
HypoHic596	chr2	176963948	176964720	-0.64	6.36	33423	15274	15283	10	13	1.59E-04	6.30E-02	HOXD10 (-16973), HOXD11 (-7680), HOXD12 (-124)
HypoHic595	chr19	9608637	9609704	-0.64	6.36	28248	95539	95548	10	10	1.59E-04	6.30E-02	ZNF560 (+112)
HypoHic594	chr3	147110322	147113092	-0.64	12.11	39974	21789	21807	19	25	8.75E-06	9.00E-03	PLSCR1 (-849056), ZIC4 (+10364)
HypoHic593	chr14	38052740	38052525	-0.64	6.38	17481	76711	76720	10	10	1.56E-04	6.10E-02	FOXA1 (+10243), MIPOL1 (+386841)
HypoHic592	chr11	20181456	20182122	-0.64	5.76	9687	62734	62742	9	16	2.27E-04	6.90E-02	DBX1 (+81)
HypoHic591	chr5	150326069	150326642	-0.64	5.77	45869	32795	32803	9	10	2.25E-04	6.90E-02	GPX3 (-73768), ZNF300 (-41811)
HypoHic590	chr2	14772312	14773457	-0.64	7.08	30771	10731	10741	11	11	1.07E-04	5.10E-02	NBAS (+928569)
HypoHic589	chr13	108518419	108519880	-0.64	5.79	16758	75255	75263	9	12	2.23E-04	6.70E-02	FAM155A (-67)
HypoHic588	chr6	28457210	28458328	-0.64	5.15	47395	35607	35614	8	8	3.38E-04	9.80E-02	ZSCAN23 (-46525), GPX6 (+25801)
HypoHic587	chr14	102025815	102027797	-0.64	12.89	18723	78784	78803	20	20	6.38E-06	6.00E-03	DIO3 (-882)
HypoHic586	chr6	100916916	100917871	-0.64	5.16	49028	39818	39825	8	8	3.37E-04	9.80E-02	SIM1 (-4589)
HypoHic585	chr12	128750971	128752586	-0.65	5.82	15267	72498	72506	9	9	2.17E-04	6.70E-02	TMEM132C (-169)
HypoHic584	chr7	121939827	121940992	-0.65	5.18	52642	46622	46629	8	8	3.30E-04	9.70E-02	AASS (-166534), FEZF1 (+4149)
HypoHic583	chr11	65816463	65816985	-0.65	5.83	10724	64619	64627	9	9	2.18E-04	6.70E-02	SF3B2 (-3083), GAL3ST3 (-73)
HypoHic582	chr6	84417933	84419360	-0.65	9.08	49830	39331	39344	14	15	3.52E-05	1.60E-02	SNAP91 (+480)
HypoHic581	chr6	32119616	32120203	-0.65	6.50	47844	37431	37440	10	10	1.45E-04	5.50E-02	PPT2-EGFL8 (-2089), PPT2 (-1390), PRR11 (-181)
HypoHic580	chr7	93519220	93520527	-0.65	8.45	52116	45629	45641	13	14	5.08E-05	2.60E-02	TFP2 (+429)
HypoHic579	chr8	17270347	17271322	-0.65	6.50	54135	49344	49353	10	10	1.45E-04	5.50E-02	MTMR7 (+1)
HypoHic578	chr4	66535145	66535655	-0.65	5.22	41933	25461	25468	8	8	3.23E-04	9.20E-02	EPHA5 (+661)
HypoHic577	chr6	133561649	133562776	-0.65	22.84	49475	40615	40649	35	39	4.73E-07	0.00E+00	EYA4 (-276)
HypoHic576	chr4	111541965	111543401	-0.65	5.22	42387	26238	26245	8	8	3.22E-04	9.20E-02	PITX2 (+1576), ENPEP (+145454)
HypoHic575	chr6	28174875	28176230	-0.65	5.88	47381	35567	35575	9	9	2.11E-04	6.20E-02	ZSCAN9 (-17500), ZKSCAN8 (+65837)
HypoHic574	chr2	183730940	183732062	-0.65	5.24	33551	15645	15652	8	8	3.20E-04	9.20E-02	FRZB (+389)
HypoHic573	chr4	122301573	122302268	-0.66	5.90	42512	26488	26496	9	11	2.09E-04	6.10E-02	QREPR (+293)
HypoHic572	chr1	91182128	91183051	-0.66	7.21	3098	5254	5264	11	11	9.89E-05	4.40E-02	BARHL2 (+204)
HypoHic571	chr11	91957448	91958799	-0.66	5.25	11456	65863	65890	8	8	3.17E-04	9.00E-02	FAT3 (-127138)
HypoHic570	chr14	37051417	37051495	-0.66	5.26	17454	76610	76617	8	8	3.15E-04	8.70E-02	NKX2-8 (+129)
HypoHic569	chr3	192441985	192445594	-0.66	7.89	40641	23002	23013	12	12	6.88E-05	2.80E-02	HRASL5 (-513624), FGF12 (-318452)
HypoHic568	chr11	71954082	71955599	-0.66	6.58	11093	65332	65341	10	10	1.40E-04	4.90E-02	PHOX2A (-71)
HypoHic567	chr1	107682302	107684425	-0.66	5.27	3261	5599	5606	8	9	3.10E-04	8.40E-02	NTNG1 (-78)
HypoHic566	chr6	29943188	29944093	-0.66	7.90	47555	36190	36201	12	13	6.83E-05	2.80E-02	ZNRD1 (-85390), HLA-A (+34604)
HypoHic565	chr2	124782117	124783254	-0.66	6.59	32686	13967	13976	10	11	1.39E-04	4.90E-02	CNTNAP5 (-178)
HypoHic564	chr5	168727752	168729267	-0.66	7.91	48152	33260	33271	12	12	6.81E-05	2.80E-02	SLIT3 (-377)
HypoHic563	chr8	145925258	145926089	-0.66	5.28	56389	53325	53332	8	9	3.06E-04	8.20E-02	ARHGAP39 (-94590), ZNF251 (+55316)
HypoHic562	chr8	85096868	85097429	-0.66	5.28	55290	51489	51496	8	9	3.06E-04	8.20E-02	RALYL (+39)
HypoHic561	chr7	116962516	116963502	-0.66	5.29	52588	46515	46522	8	9	3.05E-04	8.20E-02	WNT2 (+334)
HypoHic560	chr1	57837655	57889604	-0.66	7.27	2697	4515	4525	11	11	9.62E-05	4.20E-02	C8B (-456942), DAB1 (+1099)
HypoHic559	chr17	47209660	47210599	-0.66	7.94	25423	90515	90526	12	12	6.69E-05	2.70E-02	B4GALNT2 (-199)
HypoHic558	chr10	50887212	50887632	-0.66	5.30	6796	57159	57166	8	15	3.04E-04	8.10E-02	CHAT (+65339), OGDHL (+82947)
HypoHic557	chr3	192231892	192233698	-0.66	5.30	40637	22989	22996	8	8	3.03E-04	8.10E-02	HRASL5 (-726119), FGF12 (-105967)
HypoHic556	chr10	106399877	106401517	-0.66	8.63	7901	59156	59168	13	13	4.75E-05	2.40E-02	SORCS3 (-162)
HypoHic555	chr12	22093960	22095530	-0.66	9.29	13136	68605	68618	14	15	3.03E-05	1.20E-02	CMAS (-104463), ABCG9 (-5037)
HypoHic554	chr11	7694814	7695528	-0.66	5.32	9339	62119	62126	8	8	2.99E-04	7.70E-02	CYB5R2 (+268)
HypoHic553	chr10	42862876	42863550	-0.67	5.32	6624	56827	56834	8	9	2.99E-04	7.60E-02	ZNF33B (+270779)
HypoHic552	chr6	29759047	29760909	-0.67	7.99	47544	36131	36142	12	13	6.57E-05	2.70E-02	HLA-G (-34328), HLA-F (+69243)
HypoHic551	chr2	189156549	189157566	-0.67	6.00	33576	15694	15702	9	9	1.96E-04	5.00E-02	GULP1 (-501)
HypoHic550	chr6	30094980	30095802	-0.67	15.99	47578	36345	36368	24	24	1.69E-06	0.00E+00	TRIM31 (-14508), TRIM40 (-9396)
HypoHic549	chr1	241520286	241520924	-0.67	4.68	5747	9827	9833	7	8	4.94E-04	9.50E-02	RG57 (-76)
HypoHic548	chr2	98703324	98703698	-0.67	5.36	32203	13098	13105	8	10	2.94E-04	7.10E-02	CNGA3 (-259107), TMEM131 (-91157)
HypoHic547	chr4	46390832	46392657	-0.67	12.74	41784	25130	25148	19	19	6.62E-06	5.00E-03	GABRG1 (-265647), GABRA2 (+85502)
HypoHic546	chr8	31496363	31498345	-0.67	7.37	54511	50029	50039	11	11	9.08E-05	3.70E-02	NRG1 (-908379), WRN (+606032)
HypoHic545	chr6	28554680	28555653	-0.67	12.07	47418	35662	35679	18	22	8.75E-06	5.00E-03	SCAND3 (-55)
HypoHic544	chr7	94537805	94538408	-0.67	8.05	52132	45698	45709	12	12	6.36E-05	2.50E-02	PPP1R9A (+1158), PON1 (+415912)
HypoHic543	chr6	72130432	72130799	-0.67	6.04	48692	39022	39100	9	10	1.92E-04	4.70E-02	RIMS1 (-466111), OGFRL1 (+132110)
HypoHic542	chr11	101918140	101918575	-0.67	5.38	11596	66117	66124	8	11	2.92E-04	7.00E-02	ANGPTL5 (-131105), YAP1 (-62834)
HypoHic541	chr4	155664941	155665832	-0.67	6.06	42859	27042	27050	9	9	1.89E-04	4.50E-02	LRAT (+264)

HypoHie540	chr4	76555547	76556042	-0.67	7.41	42041	25626	25636	11	11	8.80E-05	3.50E-02	CDKL2 (+105)
HypoHie539	chr6	10384975	10386160	-0.67	6.07	48955	34672	34680	9	9	1.87E-04	4.50E-02	OFC1 (-448016), TFAP2A (+29902)
HypoHie538	chr19	51177036	51177144	-0.67	6.07	29882	98566	98574	9	9	1.87E-04	4.50E-02	SYT3 (-29948), SHANK1 (+48945)
HypoHie537	chr20	36148320	36150061	-0.67	22.95	33405	100624	100657	34	36	4.73E-07	0.00E+00	NNAT (-426)
HypoHie536	chr7	8480779	8483710	-0.68	10.13	50811	43142	43156	15	16	2.08E-05	6.00E-03	NXPH1 (+8660)
HypoHie535	chr2	176946790	176949017	-0.68	11.48	33416	15234	15250	17	17	1.18E-05	5.00E-03	HOXD10 (-33403), HOXD11 (-24110), HOXD12 (-16554), HOXD13 (-9715), EVX2 (+737)
HypoHie534	chr3	145878431	145879710	-0.68	6.77	39950	21712	21721	10	10	1.28E-04	4.00E-02	PLOD2 (-117)
HypoHie533	chr3	170746029	170746586	-0.68	4.74	40285	22411	22417	7	7	2.81E-04	8.50E-02	SLC2A2 (-1769)
HypoHie532	chr10	99739825	99790910	-0.68	5.43	7620	58535	58542	8	10	2.81E-04	6.30E-02	CRFAC1 (+217)
HypoHie531	chr7	95025611	95025924	-0.68	5.44	52138	45721	45728	8	20	2.80E-04	6.20E-02	PON3 (-95)
HypoHie530	chr7	121955502	121957254	-0.68	4.76	52649	46670	46676	7	7	4.65E-04	8.20E-02	FEZF1 (-12319), RNF133 (+382332)
HypoHie529	chr14	60973462	60974461	-0.68	6.12	17762	77209	77217	9	11	1.82E-04	4.10E-02	SIX6 (-1707)
HypoHie528	chr15	68120393	68122574	-0.68	6.13	20043	80979	80987	9	9	1.80E-04	4.00E-02	PIAS1 (-225033), SKOR1 (+9442)
HypoHie527	chr2	237086398	237087777	-0.68	4.77	34518	17280	17286	7	7	4.57E-04	7.90E-02	GBX2 (-10076), ASB18 (+85900)
HypoHie526	chr1	190447232	190448126	-0.68	4.10	4624	7939	7944	6	7	8.14E-04	9.80E-02	FAM5C (-920)
HypoHie525	chr14	63511872	63512760	-0.68	4.10	17826	77353	77358	6	6	8.12E-04	9.70E-02	KCNH5 (-143)
HypoHie524	chr2	45155201	45156207	-0.68	5.47	31346	11659	11666	8	12	2.74E-04	5.80E-02	SIX3 (-13198), CAMKMT (+566601)
HypoHie523	chr10	8095797	8097331	-0.69	9.59	6153	56023	56036	14	18	2.62E-05	1.10E-02	GATA3 (-92)
HypoHie522	chr4	48987791	48988321	-0.69	5.48	41815	25213	25220	8	9	2.71E-04	5.40E-02	CWF43 (-208)
HypoHie521	chr1	228651848	228652581	-0.69	4.12	5468	9355	9360	6	9	8.01E-04	9.00E-02	RNF187 (-22547), HIST3H2BB (+6407)
HypoHie520	chr14	29242823	29244278	-0.69	6.18	17359	76411	76419	9	9	1.76E-04	3.30E-02	FOXP1 (+8501)
HypoHie519	chr3	6903921	6905031	-0.69	4.12	37724	17963	17968	6	6	8.00E-04	9.00E-02	GRM7 (+1674)
HypoHie518	chr6	31691506	31692375	-0.69	13.75	47765	37029	37048	20	28	4.28E-06	3.00E-03	LY6G6 (-2319), C6orf25 (+780)
HypoHie517	chr16	68771035	68772225	-0.69	4.13	22693	85576	85581	6	10	7.92E-04	8.60E-02	CDH1 (+502)
HypoHie516	chr4	186456009	186457012	-0.69	6.20	43190	27685	27693	9	9	1.75E-04	3.20E-02	PDLM3 (+151)
HypoHie515	chr4	122685675	122686564	-0.69	6.20	42518	26510	26518	9	15	7.85E-04	3.20E-02	TMEM155 (+220)
HypoHie514	chr6	168719954	168720679	-0.69	4.13	50162	41869	41874	6	7	7.89E-04	8.50E-02	DACT2 (+85)
HypoHie513	chr6	27512849	27513479	-0.69	4.13	47338	35467	35472	6	6	7.88E-04	8.50E-02	ZNF184 (-72267), HIST1H2BL (+262545)
HypoHie512	chr3	62860802	62861311	-0.69	5.53	39830	19973	19980	8	12	2.64E-04	4.90E-02	CADPS (-3)
HypoHie511	chr2	14773973	14775494	-0.69	6.91	30772	10742	10751	10	10	1.17E-04	2.90E-02	NBAS (+926720)
HypoHie510	chr6	70576168	70576871	-0.69	4.84	48672	39054	39060	7	7	4.33E-04	6.20E-02	COL19A1 (+57)
HypoHie509	chr2	108602860	108603466	-0.69	6.92	32391	13406	13415	10	11	1.17E-04	2.90E-02	SLC5A7 (+168)
HypoHie508	chr6	19691654	19692418	-0.69	4.16	47156	35066	35071	6	6	7.69E-04	8.00E-02	ID4 (-145581)
HypoHie507	chr1	54821910	54822503	-0.69	4.16	2613	4403	4408	6	7	7.69E-04	8.00E-02	SSBP3 (+49885), C1orf191 (+118497)
HypoHie506	chr3	147126763	147128157	-0.69	9.03	39980	21855	21867	13	39	3.69E-05	1.70E-02	ZIC1 (+289)
HypoHie505	chr2	177052486	177053568	-0.70	9.05	33463	15491	15503	13	13	3.67E-05	1.50E-02	HOXD1 (-280)
HypoHie504	chr1	47489195	47489776	-0.70	4.18	2444	4047	4052	6	6	7.55E-04	7.60E-02	CYP4X1 (+246)
HypoHie503	chr6	125283969	125284659	-0.70	5.58	49354	40421	40428	8	8	2.58E-04	4.70E-02	RNF217 (-20200)
HypoHie502	chr7	96631384	96633530	-0.70	8.38	52172	45791	45802	12	13	5.27E-05	1.60E-02	DLX6 (-2403)
HypoHie501	chr6	78172192	78174065	-0.70	7.68	48782	39237	39247	11	11	7.54E-05	2.20E-02	HTR1B (+361)
HypoHie500	chr5	54516372	54516879	-0.70	4.90	44250	29610	29616	7	7	4.12E-04	5.60E-02	MCIDAS (+6517), GPX8 (+60680)
HypoHie499	chr6	28641622	28642394	-0.70	7.70	47426	35766	35776	11	11	7.50E-05	2.20E-02	SCAND3 (-86896), TRIM27 (+249758)
HypoHie498	chr6	42927940	42928920	-0.70	18.90	48368	38521	38547	27	27	9.48E-07	0.00E+00	GNMT (-66)
HypoHie497	chr10	71389696	71390385	-0.70	4.91	7008	57520	57526	7	8	4.04E-04	5.40E-02	C10orf35 (+27)
HypoHie496	chr14	54413371	54413931	-0.70	3.51	17627	76958	76962	5	6	1.44E-03	9.80E-02	DDHD1 (-793835), BMP4 (+9878)
HypoHie495	chr12	103350170	103351443	-0.70	5.62	14515	71021	71028	8	9	2.50E-04	4.20E-02	ASCL1 (-657)
HypoHie494	chr18	67067721	67068730	-0.70	4.22	27330	93965	93969	6	7	7.32E-04	6.80E-02	DOK6 (-65)
HypoHie493	chr12	54320564	54322092	-0.70	5.63	13707	69563	69570	8	10	2.50E-04	4.20E-02	CACOCO1 (-200104), HOXC13 (-11207)
HypoHie492	chr14	31803067	31803836	-0.70	4.93	27043	93478	93484	7	7	3.99E-04	5.20E-02	NOL4 (+63)
HypoHie491	chr19	29234671	29236898	-0.70	18.30	17354	76381	76406	26	26	3.98E-04	0.00E+00	FOXP1 (+735)
HypoHie490	chr19	58629719	58630089	-0.70	4.93	30317	99449	99455	7	10	3.98E-04	5.20E-02	ZSCAN18 (-111)
HypoHie489	chr8	98299880	98299510	-0.70	5.84	55477	51768	51775	8	8	2.49E-04	4.20E-02	TSPYL5 (-19)
HypoHie488	chr19	39465969	39466757	-0.70	4.93	29193	97320	97326	7	8	3.97E-04	5.00E-02	FBXO17 (-187)
HypoHie487	chr14	121992261	121993098	-0.70	3.52	42507	26478	26482	5	6	1.43E-03	9.50E-02	NDNF (+993)
HypoHie486	chr18	12254452	12254566	-0.71	4.24	26908	93098	93103	6	8	7.19E-04	6.70E-02	CIDEA (+191)
HypoHie485	chr17	9682752	9683061	-0.71	5.65	24120	88114	88121	8	8	2.45E-04	3.90E-02	PCVRN (-53669), GAST (+238961)
HypoHie484	chr6	32116591	32117079	-0.71	11.32	47842	37398	37413	16	30	1.21E-05	2.00E-03	PRT2 (-4465), PRRT1 (-2894)
HypoHie483	chr7	1276617	1278508	-0.71	8.50	50446	42401	42412	12	12	5.01E-05	1.50E-02	UNCX (+5020), MICALL2 (+221575)

HypoHic482	chr14	62583787	62584600	-0.71	4.96	17819	77340	77346	7	8	3.89E-04	4.60E-02	SYT16 (+121653), KCN15 (+927979)
HypoHic481	chr12	72668976	72667707	-0.71	5.89	14147	70409	70416	8	8	2.40E-04	3.70E-02	TRHDE (+879)
HypoHic480	chr8	69242921	69244734	-0.71	7.12	55084	51102	51111	10	10	1.08E-04	2.10E-02	PREX2 (+379475)
HypoHic479	chr17	27313033	27313499	-0.71	3.56	2475	88710	88714	5	5	1.37E-03	8.20E-02	PHF12 (-34477), SEZ6 (+20050)
HypoHic478	chr2	80529621	80530948	-0.71	4.99	31998	12763	12769	7	8	3.81E-04	4.20E-02	LRRTM1 (+1589)
HypoHic477	chr8	24813853	24814393	-0.71	3.56	54346	49736	49740	5	5	1.37E-03	8.10E-02	DOCK5 (-228357), NEFM (+43498)
HypoHic476	chr8	93113829	93114437	-0.71	3.57	55370	51620	51624	5	5	1.35E-03	7.70E-02	RUNX1T1 (-6427), TRIK1 (+864240)
HypoHic475	chr7	121942915	121947425	-0.72	17.90	52645	46633	46657	25	25	1.42E-06	4.00E+00	FEZF1 (-611)
HypoHic474	chr6	29893605	29894248	-0.72	5.01	47552	36174	36180	7	7	3.78E-04	0.00E-02	HLA-A (-15110), HLA-G (+99171)
HypoHic473	chr15	65689058	65689433	-0.72	4.30	19975	80865	80870	6	6	6.79E-04	5.40E-02	IGDCC3 (-18868), IGDCC4 (+26164)
HypoHic472	chr11	105480347	105481863	-0.72	10.75	11646	66186	66200	15	15	1.49E-05	2.00E-03	GRIA4 (+305)
HypoHic471	chr12	39299326	39299726	-0.72	3.58	13319	68894	68898	5	5	1.34E-03	7.70E-02	KIF21A (+537262), ALG10B (+589146)
HypoHic470	chr14	105944604	105945885	-0.72	4.30	19003	79304	79309	6	7	6.77E-04	5.40E-02	CRIP1 (-7509), CRIP2 (+5846)
HypoHic469	chr1	67772896	67773044	-0.72	3.59	2868	4827	4831	5	5	1.34E-03	7.70E-02	IL12RB2 (-77)
HypoHic468	chr6	96462814	96464135	-0.72	5.02	49934	39541	39547	7	7	3.75E-04	4.00E-02	FUT9 (-385)
HypoHic467	chr2	48699637	48700498	-0.72	3.59	33109	14624	14628	5	5	1.33E-03	7.70E-02	CCLN3 (+240)
HypoHic466	chr3	155554688	155555414	-0.72	7.19	38452	19272	19281	10	10	1.00E-04	2.00E-02	CCLSR3 (+280)
HypoHic465	chr13	39261165	39262298	-0.72	5.76	16058	74001	74008	8	8	2.28E-04	3.30E-02	FREM2 (+466)
HypoHic464	chr10	57398976	57391271	-0.72	5.05	6856	57269	57275	7	8	3.68E-04	3.70E-02	MTMR2L5 (+31724), ZWINT (+730562)
HypoHic463	chr3	119421604	119422359	-0.72	5.77	39423	20832	20839	8	8	2.28E-04	3.10E-02	MAATSI (+113)
HypoHic462	chr14	38068873	38068853	-0.72	5.06	17488	76733	76739	7	14	3.64E-04	3.70E-02	FOXA1 (-3474)
HypoHic461	chr10	133109867	133110731	-0.72	3.62	8573	60422	60426	5	5	1.30E-03	7.20E-02	PPP2R2D (-637656)
HypoHic460	chr13	112722719	112723581	-0.72	4.34	18920	75562	75567	6	6	6.53E-04	4.80E-02	SPACA7 (-307483), SOX1 (+1237)
HypoHic459	chr3	46607965	46608139	-0.72	3.62	38386	19136	19140	5	5	1.29E-03	6.50E-02	TGDF1 (-10675), RTP3 (+69071)
HypoHic458	chr5	72598865	72599503	-0.72	3.62	44452	30009	30013	5	6	1.29E-03	6.40E-02	TMEM174 (+130162), FOXD1 (+145168)
HypoHic457	chr18	5629371	5630428	-0.72	5.07	26843	92974	92980	7	7	3.58E-04	3.30E-02	EPB41L3 (-85659), TMEM200C (+266054)
HypoHic456	chr5	3596996	3597760	-0.73	3.63	43674	28623	28627	5	9	1.29E-03	6.30E-02	IRX1 (+1210)
HypoHic455	chr5	140261653	140262304	-0.73	5.08	45485	31935	31941	7	7	3.57E-04	3.30E-02	PCDHAT3 (+126)
HypoHic454	chr11	216896852	216897284	-0.73	3.63	5183	8850	8854	5	5	1.28E-03	6.30E-02	ESRRG (-273)
HypoHic453	chr11	128693961	128694388	-0.73	4.36	12344	67323	67328	6	6	6.42E-04	4.40E-02	KCNJ1 (+18254), FLI1 (+130285)
HypoHic452	chr10	94179972	94180753	-0.73	4.36	7489	58276	58281	6	6	6.39E-04	4.30E-02	MARCH5 (+129443), IDE (+153470)
HypoHic451	chr6	39901897	39902348	-0.73	4.36	48253	38344	38349	6	8	6.39E-04	4.30E-02	MOGSI (-6668), LRFN2 (+653081)
HypoHic450	chr3	6902337	6903327	-0.73	5.10	37723	17956	17962	7	7	3.53E-04	3.20E-02	GRM7 (+30)
HypoHic449	chr6	30652771	30653732	-0.73	8.74	47640	36575	36586	12	16	4.45E-05	7.00E-03	DHX16 (-12438), PPP1R18 (+2420)
HypoHic448	chr12	45268999	45270896	-0.73	18.20	13365	68983	69007	25	26	1.18E-06	0.00E+00	NELL2 (+932)
HypoHic447	chr6	28510281	28510532	-0.73	5.83	47409	35637	35644	8	9	2.17E-04	2.70E-02	GPX5 (+16705), SCAND3 (+44705)
HypoHic446	chr1	75590483	75591353	-0.73	3.65	2922	4923	4927	5	5	1.26E-03	6.10E-02	LHX8 (-3201)
HypoHic445	chr4	154711304	154711563	-0.73	4.38	42843	26988	26993	6	32	6.32E-04	4.20E-02	SFRP2 (-1162)
HypoHic444	chr5	95295740	95296502	-0.73	3.65	44802	30695	30699	5	5	1.25E-03	6.10E-02	GLRX (-137703), ELL2 (+1654)
HypoHic443	chr3	132756780	132757973	-0.73	8.04	39739	21356	21366	11	12	6.48E-05	1.20E-02	TMEM108 (+142)
HypoHic442	chr2	105483826	105484823	-0.73	4.40	32344	13323	13328	6	6	6.24E-04	4.00E-02	MRPS9 (-170116), POU3F3 (+12356)
HypoHic441	chr4	164253006	164253656	-0.73	3.66	42921	27162	27166	5	5	1.24E-03	5.70E-02	NPY1R (+683)
HypoHic440	chr5	80529067	80529340	-0.73	4.40	44634	30363	30368	6	6	6.17E-04	3.90E-02	GKMT2 (+61)
HypoHic439	chr12	85305829	85307152	-0.73	9.55	14271	70603	70615	13	18	2.67E-05	4.00E-03	SLC6A15 (+164)
HypoHic438	chr1	1475143	1475742	-0.74	5.15	128	256	262	7	7	3.40E-04	3.00E-02	TMEM240 (+294)
HypoHic437	chr13	112759355	112760313	-0.74	4.41	16930	75600	75605	6	16	6.13E-04	3.90E-02	SPACA7 (-270799), SOX1 (+37921)
HypoHic436	chr17	11501503	11502254	-0.74	8.83	24159	88181	88192	12	12	4.23E-05	6.00E-03	DNAH9 (+131)
HypoHic435	chr3	85008587	85008828	-0.74	2.95	39121	20423	20426	4	4	2.62E-05	9.30E-02	CADM2 (-766924)
HypoHic434	chr17	53342740	53343561	-0.74	4.43	23579	90785	90790	6	6	6.05E-04	3.60E-02	HLF (-778)
HypoHic433	chr2	52626814	52627438	-0.74	6.64	13606	69398	69406	9	10	1.38E-04	1.50E-02	KRT17 (+228)
HypoHic432	chr7	1279790	1280491	-0.74	3.69	50448	42415	42419	5	5	1.20E-03	4.90E-02	UNCX (+7598), MICALL2 (+218997)
HypoHic431	chr6	31760233	31760629	-0.74	4.44	47775	37075	37080	6	11	5.99E-04	3.50E-02	VWAT7 (-15360), VARS (+3299)
HypoHic430	chr12	125002007	125003064	-0.74	4.44	15171	72344	72349	6	11	5.97E-04	3.40E-02	NCOR2 (-22738), SCARB1 (+345857)
HypoHic429	chr8	15397637	15398333	-0.74	3.70	54114	49310	49314	5	6	1.19E-03	4.80E-02	TUSC3 (+193)
HypoHic428	chr11	89867679	89867976	-0.74	4.44	11443	65865	65870	6	10	5.98E-04	3.40E-02	NAALAD2 (+131)
HypoHic427	chr2	468179	468105	-0.74	5.19	30368	10113	10119	7	10	3.30E-04	2.60E-02	FAM150B (-180346), TMEM18 (+208797)
HypoHic426	chr13	108520391	108520945	-0.74	3.71	16759	75264	75268	5	5	1.18E-03	4.70E-02	FAM155A (-1585)
HypoHic425	chr16	49316845	49317262	-0.74	3.71	22211	84700	84704	5	5	1.18E-03	4.70E-02	CBLN1 (-1312)

HypoHic424	chr14	27067372	-0.74	4.45	17343	76356	76361	6	6	5.92E-04	3.30E-02	NOVA1 (-903)
HypoHic423	chr6	166074870	-0.74	4.45	49994	41568	41563	6	6	5.92E-04	3.30E-02	PDE10A (+244)
HypoHic422	chr6	12758466	-0.74	3.71	47320	35423	35427	5	10	1.17E-03	4.70E-02	ZNF391 (-97880), PRSS16 (+43115)
HypoHic421	chr10	135050326	-0.74	14.85	8800	60890	60899	20	31	2.60E-06	1.00E-03	VENTX (-234)
HypoHic420	chr8	101661767	-0.74	5.94	55525	51875	51882	8	11	2.02E-04	2.20E-02	SNX31 (-17)
HypoHic419	chr2	42067938	-0.74	4.46	31268	11527	11532	6	6	5.89E-04	3.30E-02	RKDC (-208867)
HypoHic418	chr15	31621629	-0.74	2.98	19300	79811	79814	4	4	2.55E-03	8.30E-02	KLF13 (+2678), OTUD7A (+325806)
HypoHic417	chr7	1265635	-0.74	4.47	50400	42369	42374	6	6	5.86E-04	3.30E-02	ZFAND2A (-66818), UNCX (-6111)
HypoHic416	chr11	43568922	-0.75	2.98	10009	63425	63428	4	4	2.53E-03	8.20E-02	HSO17B12 (-133020), API5 (+235700)
HypoHic415	chr1	58715499	-0.75	7.46	2712	4545	4554	10	10	8.49E-05	1.30E-02	DAB1 (-826209), OMA1 (+296534)
HypoHic414	chr6	27342438	-0.75	5.23	47328	35443	35449	7	7	3.21E-04	2.50E-02	ZNF391 (-13442), PRSS16 (+127553)
HypoHic413	chr2	115919785	-0.75	2.99	32515	13620	13620	4	8	2.52E-03	8.20E-02	DPP10 (+824)
HypoHic412	chr6	117584596	-0.75	2.99	49281	40290	40293	4	4	2.51E-03	8.00E-02	GLL2 (-2031)
HypoHic411	chr3	26663551	-0.75	4.48	38072	18551	18556	6	13	5.75E-04	3.20E-02	LRRIC3B (-579)
HypoHic410	chr1	6208717	-0.75	2.99	561	1033	1036	4	4	2.51E-03	8.00E-02	CHD5 (+31191), KONAB2 (+103011)
HypoHic409	chr5	140305713	-0.75	8.23	45487	31943	31953	11	11	5.79E-05	1.10E-02	PCDHAC1 (-392)
HypoHic408	chr4	90757139	-0.75	4.49	42218	25913	25918	6	6	5.71E-04	3.10E-02	SNCA (+954)
HypoHic407	chr4	206232	-0.75	4.50	40806	23291	23296	6	6	5.70E-04	3.10E-02	ZNF732 (+92555), ZNF595 (+153345)
HypoHic406	chr8	110987530	-0.75	6.00	55646	52092	52099	8	9	1.98E-04	2.00E-02	KCNV1 (+183)
HypoHic405	chr11	30037696	-0.75	12.77	9815	63012	63028	17	17	6.62E-06	0.00E+00	KCNAA4 (+165)
HypoHic404	chr6	29691981	-0.75	5.26	47538	36110	36116	7	7	3.13E-04	2.30E-02	HLA-F (+861)
HypoHic403	chr2	1747700	-0.75	6.01	30447	10243	10250	8	8	1.95E-04	2.00E-02	PXDN (-110)
HypoHic402	chr4	111549880	-0.75	6.02	42392	26280	26267	8	8	1.93E-04	1.80E-02	PITX2 (-6251)
HypoHic401	chr7	70597058	-0.75	8.29	51802	45129	45139	11	11	5.70E-05	1.00E-02	WBSR17 (+515)
HypoHic400	chr4	81106414	-0.76	5.30	42105	25718	25724	7	7	3.03E-04	2.00E-02	PRDM8 (+376)
HypoHic399	chr20	26188639	-0.76	5.30	35220	100321	100327	7	7	3.01E-04	1.90E-02	ZNF337 (-521347)
HypoHic398	chr6	31650735	-0.76	12.89	47759	36995	37011	17	17	6.39E-06	0.00E+00	LY6G5G (-2855)
HypoHic397	chr1	32930375	-0.76	7.61	1874	3097	3106	10	10	7.90E-05	8.00E-03	ZBTB88 (+107)
HypoHic396	chr8	1771973	-0.76	3.81	53795	48725	48729	5	5	1.07E-03	3.60E-02	ARHGEF10 (+41)
HypoHic395	chr3	170302890	-0.76	7.62	40271	22384	22393	10	12	7.87E-05	8.00E-03	SLC7A14 (+402)
HypoHic394	chr16	49499006	-0.76	3.05	22216	84709	84712	4	4	2.34E-03	6.50E-02	CBLN1 (-183454), ZNF423 (+357454)
HypoHic393	chr10	63422630	-0.76	4.57	6906	57353	57358	6	6	5.39E-04	2.40E-02	ARID9B (-238204), TMEM26 (-209647)
HypoHic392	chr5	3605783	-0.76	9.15	43681	28641	28651	12	12	3.24E-05	2.00E-03	IRX1 (+10291)
HypoHic391	chr1	237205098	-0.76	3.05	5691	9743	9746	4	4	2.33E-03	6.20E-02	RYR2 (-251)
HypoHic390	chr4	41875193	-0.77	3.06	41749	25047	25050	4	5	2.32E-03	6.10E-02	PHOX2B (-124502), TMEM33 (-61648)
HypoHic389	chr7	44185323	-0.77	3.06	51440	44490	44493	4	4	2.32E-03	6.10E-02	MYL7 (-4822)
HypoHic388	chr1	183154981	-0.77	6.13	4567	7852	7859	8	9	1.81E-04	1.30E-02	LAMC2 (-110)
HypoHic387	chr12	59313279	-0.77	7.67	13980	70169	70178	10	10	7.73E-05	8.00E-03	LRIG3 (+463)
HypoHic386	chr13	58203618	-0.77	5.37	16328	74422	74428	7	7	2.93E-04	1.50E-02	PCDH17 (-2656)
HypoHic385	chr8	22089400	-0.77	3.84	54246	49529	49533	5	6	1.04E-03	3.20E-02	POLR3D (-13159), BMP1 (+67340)
HypoHic384	chr8	27348650	-0.77	3.84	54414	49895	49899	5	8	1.04E-03	3.20E-02	EPHX2 (+499)
HypoHic383	chr4	188916496	-0.77	9.99	43279	27843	27855	13	13	2.22E-05	2.00E-03	ZFP42 (-51)
HypoHic382	chr6	33041343	-0.77	6.15	47938	37701	37708	8	10	1.79E-04	1.30E-02	HLA-DPB1 (-2764)
HypoHic381	chr18	55103353	-0.77	3.08	27234	93776	93779	4	4	2.28E-03	5.90E-02	ONECUT2 (+652)
HypoHic380	chr3	40428383	-0.77	6.16	38245	18862	18869	8	8	1.78E-04	1.20E-02	ENTPD3 (+52)
HypoHic379	chr2	237076164	-0.77	13.87	334513	17245	17262	18	26	3.78E-06	0.00E+00	GBX2 (-631)
HypoHic378	chr2	200468445	-0.77	3.86	33684	15865	15869	5	5	1.02E-03	3.10E-02	SATB2 (-145917), FTCDNL1 (+247130)
HypoHic377	chr3	55520834	-0.77	5.40	36684	19710	19716	7	7	2.85E-04	1.30E-02	LRTM1 (-559081), WNT5A (-2791)
HypoHic376	chr1	62660556	-0.77	3.09	2777	4663	4666	4	6	2.28E-03	5.90E-02	GNPTG (+28059), UNKL (+34709)
HypoHic375	chr16	1429863	-0.77	3.09	21216	83119	83119	4	4	2.28E-05	1.00E-02	PRICKLE2 (-460403), ADAMTS9 (+2142)
HypoHic374	chr3	64670459	-0.77	10.05	38882	20069	20081	13	13	2.18E-05	1.00E-02	KANK4 (+124376), INADL (+452560)
HypoHic373	chr2	121412005	-0.77	3.09	32642	13902	13905	4	4	2.25E-03	5.80E-02	GLI2 (-137766), INHBB (+308500)
HypoHic372	chr19	20278013	-0.77	4.64	28826	96600	96605	6	6	5.10E-04	1.70E-02	ZNF486 (+135)
HypoHic371	chr1	228075423	-0.77	3.10	5428	9241	9244	4	4	2.23E-03	5.80E-02	WNT9A (+60013), PRSS38 (+72192)
HypoHic370	chr6	126079089	-0.78	3.10	49371	40454	40457	4	4	2.23E-03	5.70E-02	HEY2 (-1136)
HypoHic369	chr19	3887751	-0.78	4.66	27921	94988	94973	6	6	5.01E-04	1.70E-02	CACTIN (-61301), PIP5K1C (+12363)
HypoHic368	chr18	28621490	-0.78	13.21	27015	93332	93348	17	17	5.44E-06	0.00E+00	DSC3 (+382)
HypoHic367	chr19	44952417	-0.78	5.44	29431	97729	97735	7	7	2.80E-04	1.20E-02	ZNF229 (+52)

HypoHic366	chr19	23945472	23945903	-0.78	3.89	28869	96691	96695	5	5	9.97E-04	3.00E-02	ZNF681 (-3995), RPSAP58 (-128)
HypoHic365	chr3	154145810	154146871	-0.78	6.22	40087	22043	22050	8	8	1.74E-04	1.10E-02	DHX36 (-104055), GPR149 (+1163)
HypoHic364	chr4	187644620	187647690	-0.78	15.56	43246	27787	27806	20	20	1.60E-06	0.00E+00	FAT1 (-1146)
HypoHic363	chr14	334030660	33403226	-0.78	3.11	17396	76481	76484	4	4	2.20E-03	5.70E-02	NPAS3 (-5380), AKAP6 (+604664)
HypoHic362	chr5	178986131	178986906	-0.78	7.01	46568	34011	34019	9	9	1.10E-04	7.00E-03	RUFY1 (+8960), HNRNP11 (+65151)
HypoHic361	chr2	5831147	5831722	-0.78	3.12	30547	10399	10402	4	4	2.10E-03	5.60E-02	SOX11 (-1364)
HypoHic360	chr3	185000208	185001026	-0.78	5.46	40517	22790	22796	7	7	2.77E-04	1.20E-02	MAP3K13 (-80291), EHHADH (-28731)
HypoHic359	chr6	32976805	32977708	-0.78	6.24	47936	37698	37695	8	8	1.72E-04	1.10E-02	HLA-DOA (+132)
HypoHic358	chr6	28602643	28603779	-0.78	25.78	47424	37582	37564	33	33	2.32E-07	0.00E+00	SCAND3 (-48049), TRIM27 (+288605)
HypoHic357	chr10	125034002	125034818	-0.78	5.47	8302	59934	59940	7	8	2.73E-04	1.20E-02	GPR26 (-39461), BUB3 (+120617)
HypoHic356	chr6	26271193	26271827	-0.78	3.91	47262	35291	35295	5	5	9.73E-04	3.00E-02	HIST1H2BT (-1634), HIST1H3G (+102)
HypoHic355	chr13	28553501	28553805	-0.78	3.91	15876	73675	73679	5	5	9.72E-04	3.00E-02	CDX2 (-8377), URAD (+9121)
HypoHic354	chr11	170630070	170630734	-0.78	4.69	4360	7483	7488	6	6	4.89E-04	1.70E-02	PRRX1 (-2645)
HypoHic353	chr10	26222922	26223310	-0.78	3.13	6434	56539	56542	4	6	2.17E-03	5.30E-02	MYO3A (-80)
HypoHic352	chr10	128593624	128594417	-0.78	5.48	8428	60137	60143	7	7	2.72E-04	1.20E-02	DOK1 (+43)
HypoHic351	chr12	110156245	110156459	-0.78	3.92	14669	71316	71320	5	5	9.64E-04	3.00E-02	MMAB (-144673), TRPV4 (+96344)
HypoHic350	chr3	12045449	12046420	-0.78	4.71	37849	18201	18206	6	8	4.83E-04	1.70E-02	TAMM41 (-157642), TIMP4 (+154916)
HypoHic349	chr19	12758716	12759156	-0.78	3.92	28405	95844	95848	5	5	9.61E-04	3.00E-02	MAN2B1 (+18620), ZNF791 (+37204)
HypoHic348	chr16	30907560	30908233	-0.78	3.14	22051	84446	84449	4	4	2.15E-03	5.20E-02	BC17C (-1616), CTFF1 (-31)
HypoHic347	chr4	82135607	82135987	-0.79	2.36	42122	25763	25765	3	3	5.22E-03	9.80E-02	PRKG2 (+391)
HypoHic346	chr19	58520847	58521273	-0.79	3.14	30308	99411	99414	4	4	2.14E-03	5.10E-02	ZSCAN1 (-24374), ZNF606 (-6343)
HypoHic345	chr7	12443529	12443926	-0.79	3.93	50830	43183	43187	5	7	9.58E-04	2.90E-02	VWDE (-197)
HypoHic344	chr22	36806001	36806580	-0.79	3.93	37100	103688	103692	5	5	9.58E-04	2.90E-02	MYH9 (-22228), TXN2 (+71786)
HypoHic343	chr5	1882775	1883473	-0.79	6.29	43557	28364	28371	8	8	1.65E-04	1.10E-02	IRX4 (+4238), NDUFS6 (+81580)
HypoHic342	chr14	103739856	103740597	-0.79	3.93	18807	78968	78972	5	5	9.55E-04	2.90E-02	EIF5 (-60112), TNFAIP2 (+150429)
HypoHic341	chr7	1282630	1283255	-0.79	2.36	50450	42422	42424	3	7	5.19E-03	9.60E-02	UNCX (+10400), MICALL2 (+216195)
HypoHic340	chr2	214148958	214149735	-0.79	2.36	33883	16167	16169	3	3	5.19E-03	9.60E-02	SPAG16 (+234)
HypoHic339	chr13	51471469	51471929	-0.79	3.15	16241	74292	74295	4	4	2.13E-03	5.00E-02	RNASEH2B (-66115), DLEU1 (+761392)
HypoHic338	chr6	115519436	115520072	-0.79	7.09	42454	26393	26401	9	10	1.06E-04	7.00E-03	UGT8 (+143)
HypoHic337	chr4	114177329	114177535	-0.79	3.15	49223	40199	40202	4	4	2.11E-03	5.00E-02	MARGKS (-1109)
HypoHic336	chr12	47219626	47219958	-0.79	8.68	13394	69056	69066	11	11	4.58E-05	5.00E-03	SLC38A4 (-12)
HypoHic335	chr13	43566633	43566902	-0.79	2.37	16106	74076	74078	3	3	5.13E-03	9.50E-02	DNAJC15 (-30571), TNFSF11 (+418479)
HypoHic334	chr6	24910562	24911615	-0.79	11.06	47219	35171	35174	14	14	1.35E-05	0.00E+00	FAM65B (+106)
HypoHic333	chr6	46138699	46139019	-0.79	6.32	48486	38705	38712	8	8	1.62E-04	1.00E-02	ENPP5 (-151)
HypoHic332	chr12	54426670	54428592	-0.79	11.86	13757	69775	69789	15	15	9.93E-06	0.00E+00	HOXC5 (+994)
HypoHic331	chr5	16179210	16180419	-0.79	12.66	43888	28955	28970	16	19	6.62E-06	0.00E+00	MARCH11 (+69)
HypoHic330	chr1	911194674	91195504	-0.79	3.96	3102	5304	5308	5	10	9.30E-04	2.70E-02	BARHL2 (-12295), ZNF644 (+291941)
HypoHic329	chr4	148402128	148402869	-0.79	4.75	42755	26854	26859	6	8	4.68E-04	1.50E-02	EDNRA (+430)
HypoHic328	chr7	94284258	94285911	-0.79	22.97	52128	45662	45690	29	32	4.73E-07	0.00E+00	PEG10 (-552), SGCE (+351)
HypoHic327	chr2	172972681	172973241	-0.79	3.17	33329	15068	15071	4	4	2.07E-03	4.90E-02	ITGA6 (-319556), DLX2 (-5333)
HypoHic326	chr3	64253534	64253818	-0.79	4.76	38867	20042	20047	6	6	4.65E-04	1.40E-02	PRICKLE2 (-42545), ADAMTS9 (+420000)
HypoHic325	chr18	35145353	35147826	-0.79	18.24	27092	93500	93522	23	23	1.18E-06	0.00E+00	CELF4 (-590)
HypoHic324	chr14	188953092	188953969	-0.79	6.35	43282	27880	27867	8	8	1.59E-04	9.00E-03	ZFP42 (+36606), TRIML2 (+73216)
HypoHic323	chr11	111169284	111169473	-0.79	3.18	17174	66304	66307	4	4	2.05E-03	4.80E-02	ARHGAP20 (-589328), C11orf92 (+6391)
HypoHic322	chr12	85673200	85673347	-0.80	3.18	14275	70630	70633	4	4	2.04E-03	4.80E-02	ALX1 (-611)
HypoHic321	chr19	52956622	52957180	-0.80	7.96	30010	98838	98847	10	11	6.64E-05	6.00E-03	ZNF578 (+72)
HypoHic320	chr13	53422381	53422871	-0.80	6.37	16279	74352	74359	8	12	1.58E-04	9.00E-03	PCDH8 (+149)
HypoHic319	chr6	134638742	134639355	-0.80	5.58	49507	40725	40731	7	9	2.58E-04	1.00E-02	SGK1 (+147)
HypoHic318	chr3	21399977	21417150	-0.80	7.17	37683	17887	17895	9	11	1.01E-04	7.00E-03	CTNN4 (-138649)
HypoHic317	chr17	18956647	18957232	-0.80	4.80	24284	88414	88414	6	6	4.47E-04	1.40E-02	RAI1 (+9071), SREBF1 (+136443)
HypoHic316	chr1	18965931	18967232	-0.80	3.20	1220	2002	2005	4	22	1.99E-03	4.70E-02	PAX7 (+410)
HypoHic315	chr19	11704344	11785248	-0.80	10.42	23383	95796	95808	13	14	1.75E-05	1.00E-03	ZNF823 (+64982), ZNF627 (+76561)
HypoHic314	chr13	93879303	93879769	-0.80	4.01	16504	74751	74755	5	5	8.83E-04	2.60E-02	GPO6 (+441)
HypoHic313	chr14	33402027	33402512	-0.80	3.21	17395	76480	76480	4	5	1.98E-03	4.60E-02	NPAS3 (-6253), AKAP6 (+603791)
HypoHic312	chr11	7272667	7274234	-0.80	8.03	9321	62088	62097	10	10	6.50E-05	6.00E-03	SYT9 (+370)
HypoHic311	chr6	152128535	152129400	-0.80	4.82	49761	41175	41175	6	10	4.40E-04	1.40E-02	ESR1 (+17337), SYNE1 (+829566)
HypoHic310	chr7	158110405	158110685	-0.80	2.41	53585	48384	48386	3	4	4.80E-03	8.30E-02	PTPRN2 (+269826), DNAJB6 (+980885)
HypoHic309	chr3	62304470	62305213	-0.80	6.44	38810	19893	19900	8	11	1.52E-04	8.00E-03	FEZF2 (+54348), PTPRG (+757257)

[illegible]

HypoHier250	chr19	38307803	38308263	-0.84	3.35	29135	97206	97209	4	4	1.71E-03	2.20E-02	SIPA1L3 (-89835), ZNF573 (-43642)
HypoHier249	chr8	35092887	35092876	-0.84	3.35	54553	50100	50103	4	4	1.71E-03	2.20E-02	UNC5D (-193)
HypoHier248	chr2	206550819	206551466	-0.84	2.51	33783	15993	15995	3	4	4.30E-03	5.10E-02	NRP2 (+3919), INO80D (+399763)
HypoHier247	chr5	15499895	15500913	-0.84	5.87	43870	28928	28928	7	7	2.13E-04	3.00E-03	FBXL7 (+89)
HypoHier246	chr19	4474970	4475136	-0.84	2.52	27990	95083	95085	3	3	4.29E-03	5.10E-02	ENSG00000167674 (+2769), PLIN4 (+42663)
HypoHier245	chr11	126286370	126286828	-0.84	3.35	12276	67216	67219	4	4	1.70E-03	2.20E-02	ST3GAL4 (+10922), KIRREL3 (+584056)
HypoHier244	chr19	49249932	49250561	-0.84	5.87	29736	98258	98264	7	7	2.13E-04	3.00E-03	IZUMO1 (-81)
HypoHier243	chr1	228464049	228464232	-0.84	2.52	5456	9309	9311	3	7	4.29E-03	5.10E-02	OBSCN (+68310), TRIM11 (+130400)
HypoHier242	chr10	129535138	129535968	-0.84	9.25	8452	60187	60197	11	11	3.17E-05	2.00E-03	FOXJ2 (+54)
HypoHier241	chr14	38091400	38092175	-0.84	5.89	17492	76759	76765	7	7	2.11E-04	3.00E-03	SSTR1 (-585416), FOXA1 (-27549)
HypoHier240	chr8	145910546	145911897	-0.84	6.73	59387	53315	53322	8	9	1.28E-04	3.00E-03	ARHGAP39 (-80138), ZNF251 (+69768)
HypoHier239	chr11	24518149	24518448	-0.84	7.58	9744	62899	62899	9	9	7.99E-05	2.00E-03	LUZP2 (-425)
HypoHier238	chr18	74961196	74962794	-0.84	16.84	27391	94090	94109	20	28	1.42E-06	0.00E+00	GALR1 (-510)
HypoHier237	chr1	88928168	88928467	-0.84	2.53	3072	5216	5218	3	6	4.24E-03	4.90E-02	PKNX (-221587)
HypoHier236	chr7	4832112	4832535	-0.84	4.22	50712	42936	42940	5	5	7.32E-04	9.00E-03	AP5Z1 (+17071), PAPOLB (+69301)
HypoHier235	chr10	60935663	60937257	-0.85	11.84	6879	57299	57312	14	14	9.93E-06	0.00E+00	PHYHPL (+110)
HypoHier234	chr1	6947541	6947773	-0.85	4.23	9309	62053	62057	5	7	7.21E-04	9.00E-03	ZNF215 (+3)
HypoHier233	chr11	73894730	73895278	-0.85	5.09	51894	45272	45277	6	6	3.55E-04	5.00E-03	GF2F1 (-177007), GTF2IRD1 (+28704)
HypoHier232	chr7	164290179	164290833	-0.85	6.78	4238	7265	7272	8	8	1.25E-04	3.00E-03	PBX1 (-238366), NUF2 (+998762)
HypoHier230	chr4	101439954	101440278	-0.85	2.54	42296	26058	26060	3	3	4.18E-03	4.70E-02	CLDN15 (-5062), FIS1 (+1203)
HypoHier229	chr10	95653378	95654134	-0.85	5.93	7521	58359	58365	7	7	2.03E-04	3.00E-03	SLC35G1 (+26)
HypoHier228	chr6	105388668	105388731	-0.85	2.55	49052	39879	39881	3	5	4.15E-03	4.40E-02	HACE1 (-80906), LIN28B (-16223)
HypoHier227	chr11	69286145	69286352	-0.85	3.40	10944	65024	65027	4	4	1.63E-03	2.00E-02	CND1 (-169606), TPCN2 (+469884)
HypoHier226	chr3	16216094	16216215	-0.85	3.41	37989	18420	18423	4	4	1.61E-03	2.00E-02	GALNT15 (-1)
HypoHier225	chr19	46318439	46319398	-0.85	7.66	29532	97906	97914	9	9	7.78E-05	2.00E-03	RSPH6A (-342)
HypoHier224	chr6	27635558	27635849	-0.85	3.41	47352	35502	35505	4	4	1.60E-03	2.00E-02	ZNF184 (-194807), HIST1H2BL (+140005)
HypoHier223	chr3	181444131	181444131	-0.85	10.25	40425	22654	22665	12	14	1.94E-05	1.00E-03	SOX2 (+15167)
HypoHier222	chr13	97646639	97647084	-0.86	6.85	16562	74878	74885	8	9	1.19E-04	3.00E-03	OXGR1 (-258)
HypoHier221	chr4	126237986	126238929	-0.86	5.14	42555	26572	26577	6	6	3.41E-04	4.00E-03	FAT4 (+904)
HypoHier220	chr2	5835853	5837348	-0.86	8.57	30551	10410	10419	10	10	4.80E-05	2.00E-03	SOX1 (+3802)
HypoHier219	chr3	164914150	164915196	-0.86	11.14	40210	22282	22294	13	16	1.25E-05	1.00E-03	SLITRK3 (-883)
HypoHier218	chr13	50706583	50707586	-0.86	6.86	16233	74277	74284	8	8	1.19E-04	3.00E-03	RNASEH2B (-776729), DLEU1 (+50778)
HypoHier217	chr8	79578116	79578360	-0.86	4.30	55236	51396	51400	5	6	6.79E-04	8.00E-03	ZC2HC1A (-44)
HypoHier216	chr8	38831148	38832728	-0.86	7.74	54657	50258	50266	9	9	7.35E-05	2.00E-03	HTRA4 (+255)
HypoHier215	chr1	95392925	95393429	-0.86	4.30	3185	5452	5456	5	5	6.77E-04	8.00E-03	CNN3 (-343)
HypoHier214	chr11	121971092	121971247	-0.86	3.45	12115	66951	66954	4	8	1.55E-03	1.90E-02	BLID (+15753), SORL1 (+648258)
HypoHier213	chr10	1651238	1651391	-0.86	2.59	5993	55747	55749	3	3	3.94E-03	4.10E-02	ID1 (-566205), ADARB2 (+128355)
HypoHier212	chr7	26897182	26897714	-0.86	6.05	51025	43602	43608	7	7	1.91E-04	3.00E-03	SKAP2 (+6914), SNX10 (+565905)
HypoHier211	chr7	121512781	121513944	-0.87	6.06	52630	46597	46603	7	7	1.89E-04	3.00E-03	PTPRZ1 (+220)
HypoHier210	chr12	97379628	97379917	-0.87	2.60	14417	70861	70863	3	3	3.88E-03	3.60E-02	NEDD1 (+78529)
HypoHier209	chr1	1108820	1109832	-0.87	5.21	70	135	140	6	6	3.28E-04	4.00E-03	TTL10 (+43)
HypoHier208	chr12	4918169	4919591	-0.87	7.81	12766	68003	68011	9	9	7.07E-05	2.00E-03	KCNA6 (+538)
HypoHier207	chr13	70681804	70682324	-0.87	3.48	16389	74512	74515	4	11	1.49E-03	1.50E-02	KLHL1 (+527)
HypoHier206	chr7	49812836	49813763	-0.87	7.83	51544	44664	44672	9	9	7.02E-05	2.00E-03	VWC2 (+43)
HypoHier205	chr4	6202091	6202609	-0.87	6.11	41188	24086	24092	7	7	1.84E-04	3.00E-03	JAKMIP1 (-68)
HypoHier204	chr6	161188322	161188638	-0.87	3.49	49935	41463	41466	4	4	1.48E-03	1.50E-02	MAP3K4 (-224336), PLG (+65206)
HypoHier203	chr2	241496830	241497599	-0.87	6.11	34725	17636	17642	7	7	1.83E-04	3.00E-03	DUSP28 (-2504), ANKMY1 (+165)
HypoHier202	chr2	45240373	45241008	-0.87	2.62	31780	11764	11766	3	6	3.79E-03	3.50E-02	SIX2 (-4122)
HypoHier201	chr2	154729059	154730157	-0.87	7.01	33102	14608	14615	8	9	1.11E-04	3.00E-03	KCNJ3 (-825203), GALNT13 (+1182)
HypoHier200	chr17	79140481	79140589	-0.88	2.63	26539	92363	92365	3	3	3.78E-03	3.40E-02	ATK (-718)
HypoHier199	chr20	37352612	37353158	-0.88	6.14	35445	100732	100738	7	7	1.80E-04	2.00E-03	SLC32A1 (-220)
HypoHier198	chr3	38422202	3842717	-0.88	4.38	37700	17918	17922	5	5	6.29E-04	5.00E-03	SETMAR (-502528), LRRN1 (+1339)
HypoHier197	chr2	46043	46558	-0.88	2.63	30345	10062	10064	3	3	3.75E-03	3.20E-02	FAM110C (+84)
HypoHier196	chr1	26644234	26645161	-0.88	5.27	1614	2646	2651	6	7	3.10E-04	3.00E-03	UBXN11 (+156), CD52 (+250)
HypoHier195	chr7	134576049	134576386	-0.88	5.28	52892	47096	47101	6	6	3.07E-04	3.00E-03	AGBL3 (-9504), CALD1 (+11817)
HypoHier194	chr17	17625521	17626127	-0.88	2.64	24286	88416	88418	3	3	3.72E-03	3.10E-02	RAT1 (+41037), SREBF1 (+114477)
HypoHier193	chr1	3663164	3663705	-0.88	4.41	461	894	898	5	5	6.13E-04	4.00E-03	SMIM1 (-25917), TP73 (+94351)

HypoHert192	chr7	153584416	153585368	-0.88	7.07	53274	47734	47741	8	8	1.08E-04	2.00E-03	DPP6 (-164873)
HypoHert191	chr8	110986371	110987019	-0.88	4.42	55645	52087	52091	5	5	6.07E-04	4.00E-03	SYBU (-282675), KCNV1 (+1381)
HypoHert190	chr11	118402280	118402540	-0.89	2.66	11964	66736	66738	3	3	3.69E-03	2.60E-02	TMEM25 (+486)
HypoHert189	chr12	236578808	236579780	-0.89	3.54	34470	17183	17186	4	6	1.40E-02	1.20E-02	AGAP1 (+176543), GBX2 (+497718)
HypoHert188	chr1	145714010	145714143	-0.89	2.67	3598	6202	6204	3	3	3.61E-03	2.50E-02	PDZK1 (-29186), CD160 (-7216)
HypoHert187	chr9	13278512	13278977	-0.89	2.67	56481	53484	53486	3	3	3.50E-03	2.40E-02	MPDZ (+818)
HypoHert186	chr12	179184854	179184866	-0.89	2.67	33497	15541	15543	3	3	3.59E-03	2.40E-02	OSBPL6 (+125852), PRKRA (+131098)
HypoHert185	chr16	19837015	19838211	-0.89	7.15	47165	35080	35087	8	8	1.02E-04	2.00E-03	ID4 (-4)
HypoHert184	chr13	75149833	75149974	-0.89	2.68	16410	74547	74549	3	3	3.54E-03	2.20E-02	KLF12 (-580718), TBC1D4 (+906346)
HypoHert183	chr16	1585644	1586043	-0.89	2.68	21241	83181	83183	3	3	3.54E-03	2.20E-02	TMEM204 (+2270), IFT140 (+76267)
HypoHert182	chr16	238048	238618	-0.90	7.16	37664	17849	17856	8	8	1.01E-04	2.00E-03	CHL1 (+54)
HypoHert181	chr16	54966471	54967786	-0.90	5.38	22349	84962	84967	6	6	2.91E-04	3.00E-03	IRX8 (-390543), IRX5 (+2355)
HypoHert180	chr1	155146302	155146785	-0.90	3.59	3917	6744	6747	4	4	1.33E-03	1.00E-02	KRTCAP2 (-735), TRIM46 (+101)
HypoHert179	chr2	106362547	106362832	-0.90	2.69	32366	13364	13366	3	3	3.50E-03	2.20E-02	C2orf40 (-319422), NCK2 (+1336)
HypoHert178	chr13	46425508	46426026	-0.90	8.08	16156	74148	74156	9	9	6.22E-05	2.00E-03	SIAH3 (+104)
HypoHert177	chr14	27065974	27066771	-0.90	4.49	17342	76351	76355	5	5	5.71E-04	4.00E-03	NOVA1 (+587)
HypoHert176	chr7	79081666	79084078	-0.90	20.73	51985	45392	45414	23	26	4.73E-07	4.00E+00	MAGI2 (+18)
HypoHert175	chr12	133195061	133195520	-0.90	3.61	15611	73148	73151	4	4	1.31E-03	1.00E-02	P2RX2 (-112)
HypoHert174	chr11	101453871	101454823	-0.90	8.12	11586	68087	68095	9	11	6.12E-05	2.00E-03	TRPC6 (+312)
HypoHert173	chr8	121137734	121138133	-0.90	2.71	55734	52234	52236	3	5	3.43E-03	2.10E-02	COL14A1 (+587)
HypoHert172	chr6	5851031	5851840	-0.91	3.63	48857	34497	34500	4	4	1.29E-03	1.00E-02	NRN1 (+155764), FARS2 (+590159)
HypoHert171	chr7	2756996	2758014	-0.91	3.63	50643	42788	42791	4	7	1.28E-03	1.00E-02	AMZ1 (+36349), GNA12 (+126453)
HypoHert170	chr8	57069888	57070013	-0.91	2.73	54929	50788	50790	3	4	3.37E-03	2.10E-02	MOS (-43310), PLAG1 (+53987)
HypoHert169	chr15	48489952	48470794	-0.91	6.37	19652	80363	80369	7	7	1.58E-04	2.00E-03	MYEF2 (+341)
HypoHert168	chr6	1601229	1601802	-0.91	4.55	46734	34317	34321	5	5	5.49E-04	4.00E-03	FOXC1 (-9165), FOXF2 (+211447)
HypoHert167	chr4	174421377	174422308	-0.91	7.28	42966	27293	27300	8	8	9.60E-05	2.00E-03	SCRG1 (-101456), HAND2 (+29237)
HypoHert166	chr9	125796809	125797284	-0.91	2.73	57287	54567	54569	3	3	3.35E-03	2.00E-02	GPR21 (+241)
HypoHert165	chr7	142494148	142494492	-0.91	5.47	53038	47320	47325	6	9	2.74E-04	3.00E-03	EPHB6 (-58472), PRSS1 (+36990)
HypoHert164	chr17	16171702	1617465	-0.91	4.57	23705	87292	87296	5	6	5.40E-04	4.00E-03	TLCD2 (-3552)
HypoHert163	chr1	24645802	24646392	-0.91	10.97	1531	2499	2510	12	12	1.37E-05	1.00E-03	GRHL3 (+182)
HypoHert162	chr15	41803428	41804283	-0.92	4.58	19527	80162	80166	5	5	5.38E-04	4.00E-03	LTK (+2148), ITPKA (+17783)
HypoHert161	chr5	74162621	74162924	-0.92	6.41	44494	30091	30097	7	7	1.54E-04	2.00E-03	FAM169A (-110)
HypoHert160	chr2	45159894	45160554	-0.92	7.33	31348	11672	11679	8	8	9.34E-05	2.00E-03	SIX3 (-8678), CAMKMT (+571121)
HypoHert159	chr12	96252066	96252245	-0.92	2.76	14398	70830	70832	3	6	3.25E-03	1.80E-02	SNRPF (-550)
HypoHert158	chr16	8768031	8768425	-0.92	2.76	21596	83780	83782	3	4	3.24E-03	1.80E-02	ABAT (-38598), METTL22 (+52683)
HypoHert157	chr5	178367621	178368620	-0.92	10.12	46533	33940	33950	11	12	2.08E-05	2.00E-03	ZNF454 (-71)
HypoHert156	chr4	165877875	165878219	-0.92	6.45	42933	27197	27203	7	7	1.51E-04	2.00E-03	MARCH1 (-572845), TRIM61 (+20773)
HypoHert155	chr6	33039396	33039500	-0.92	4.61	47937	37696	37700	5	5	5.24E-04	4.00E-03	HLA-DPB1 (-4255)
HypoHert154	chr4	81118188	81119473	-0.92	8.30	42106	25727	25735	9	11	5.68E-05	2.00E-03	FGF5 (-68922), PRDM8 (+12407)
HypoHert153	chr11	32454718	32455192	-0.92	7.40	9878	63212	63219	8	11	8.87E-05	2.00E-03	WTT1 (+2221), RCNT1 (+342505)
HypoHert152	chr12	66122804	66123496	-0.93	4.63	14043	70267	70271	5	6	5.17E-04	4.00E-03	HMG2A (-94761), MSRB3 (+450727)
HypoHert151	chr16	54321848	54323498	-0.93	7.43	22334	84924	84931	8	8	8.63E-05	2.00E-03	IRX3 (-198)
HypoHert150	chr4	187476326	187476953	-0.93	9.30	43229	27758	27767	10	13	2.98E-05	2.00E-03	MTNR1A (+81)
HypoHert149	chr3	42947263	42947385	-0.93	2.79	36285	18950	18952	3	7	3.12E-03	1.80E-02	ZNF662 (-334)
HypoHert148	chr19	53758289	53758609	-0.93	4.66	30029	98883	98887	5	5	5.01E-04	4.00E-03	VNTR2 (-3096), ZNF677 (-323)
HypoHert147	chr21	34405553	34405997	-0.93	3.73	36277	102259	102262	4	4	1.15E-03	8.00E-03	OLIG1 (-36675), OLIG2 (+7532)
HypoHert146	chr19	57617602	57618436	-0.93	3.73	30269	99326	99329	4	4	1.15E-03	8.00E-03	ZM2 (-265922), USP29 (-13392)
HypoHert145	chr10	96162066	96162189	-0.94	5.61	7535	58385	58390	6	7	2.52E-04	3.00E-03	TBC1D12 (-133)
HypoHert144	chr6	31430641	31431969	-0.94	7.49	47715	36852	36859	8	8	8.37E-05	1.00E-03	MICB (-34587), MICA (+59949)
HypoHert143	chr7	751331	752456	-0.94	9.37	50352	42180	42189	10	13	2.84E-05	1.00E-03	PRKAR1B (+950)
HypoHert142	chr5	166405485	166406845	-0.94	5.63	46094	33181	33186	6	6	2.49E-04	1.00E-03	TENM2 (-305639)
HypoHert141	chr16	54315551	54316049	-0.94	3.75	22330	84911	84914	4	4	1.12E-03	7.00E-03	IRX3 (+4875), FTO (+577925)
HypoHert140	chr17	14028690	14029701	-0.94	12.22	50838	43208	43220	13	13	7.80E-06	0.00E+00	ETV1 (+375)
HypoHert139	chr17	9479910	9480428	-0.94	8.46	24107	88076	88084	9	9	5.01E-05	1.00E-03	STX8 (-616), WDR16 (+225)
HypoHert138	chr2	74875227	74875548	-0.94	7.55	31926	12652	12659	8	8	8.11E-05	1.00E-03	M1AP (-224)
HypoHert137	chr12	63327142	63327207	-0.94	2.83	14003	70204	70206	3	3	3.00E-03	1.60E-02	PPM1H (+1642), MON2 (+466578)
HypoHert136	chr1	60280088	60281077	-0.94	8.50	2747	4603	4611	9	9	5.01E-05	1.00E-03	HOOK1 (+50)
HypoHert135	chr2	241459638	241460002	-0.94	2.83	34724	17633	17635	3	3	2.99E-03	1.60E-02	ANKMY1 (+37560), GPC1 (+84732)

HypoH134	chr11	65194933	65195039	-0.95	3.78	10672	64518	64521	4	4	1.09E-03	7.00E-03	SCYL1 (-97562), FRMD8 (+40916)
HypoH133	chr12	71833017	71833193	-0.95	3.79	14133	70386	70389	4	4	1.09E-03	7.00E-03	LGR5 (-445)
HypoH132	chr8	688018	688417	-0.95	2.84	53689	48568	48570	3	3	2.99E-03	1.60E-02	DLGAP2 (-761314), TDRP (-192437)
HypoH131	chr9	115818857	115819364	-0.95	3.80	57158	54384	54387	4	5	1.07E-03	7.00E-03	ZFP37 (-115)
HypoH130	chr6	30458158	30458730	-0.95	6.65	47620	36515	36521	7	7	1.35E-04	1.00E-03	PRR3 (-66219), HLA-E (+1200)
HypoH129	chr19	863054	863244	-0.95	3.81	27604	94453	94456	4	4	1.08E-03	7.00E-03	CFD (+3696), MED16 (+30069)
HypoH128	chr18	674434	674560	-0.95	2.86	53687	48561	48563	3	3	2.90E-03	1.60E-02	DLGAP2 (-775035), TDRP (-178716)
HypoH127	chr11	125774082	125774447	-0.96	5.75	12258	67189	67194	6	6	2.31E-04	1.00E-03	PUS3 (-1149), DDX23 (+7)
HypoH126	chr11	209404846	209405064	-0.97	2.91	5023	8562	8584	3	3	2.75E-03	1.20E-02	PLXNA2 (-987290), CAMK1G (-352107)
HypoH125	chr11	40314618	40315404	-0.97	4.85	9900	63393	63397	5	5	4.28E-04	1.00E-03	LRRCA4 (+653)
HypoH124	chr8	54163622	54164442	-0.98	9.76	54868	50654	50663	10	11	2.48E-05	0.00E+00	OPRK1 (+225)
HypoH123	chr5	140345643	140346403	-0.98	10.75	45491	31960	31970	11	12	1.49E-05	0.00E+00	PCDHAC2 (+203)
HypoH122	chr2	240302585	240302855	-0.98	3.91	34665	17544	17547	4	4	9.71E-04	6.00E-03	HDAC4 (+19923), TWIST2 (+546047)
HypoH121	chr1	228644750	228646224	-0.98	18.60	5466	9333	9351	19	19	9.48E-07	0.00E+00	HIST3H2BB (-321), HIST3H2A (+73)
HypoH120	chr5	150284416	150284796	-0.98	6.86	45867	32787	32793	7	7	1.19E-04	0.00E+00	ZNF300 (-61)
HypoH119	chr2	154727925	154728468	-0.98	5.89	33101	14602	14607	6	7	2.10E-04	0.00E+00	GALNTT3 (+229)
HypoH118	chr7	95990265	95990837	-0.98	2.94	52235	45974	45976	3	3	2.64E-03	1.20E-02	BUD31 (-15713), ARPC1B (+18198)
HypoH117	chr7	155599026	155599780	-0.98	3.94	53364	47956	47959	4	4	9.45E-04	6.00E-03	SHH (+5564), RBM33 (+162030)
HypoH116	chr6	33091357	33091841	-0.98	5.91	47947	37760	37765	6	6	2.08E-04	0.00E+00	HLA-DPA1 (-43112), COL11A2 (+68677)
HypoH115	chr4	110223040	110224247	-0.99	15.76	42371	26170	26185	16	16	1.68E-06	0.00E+00	COL25A1 (+155)
HypoH114	chr3	128204047	128205496	-0.99	8.88	39646	21186	21194	9	9	4.04E-05	0.00E+00	DNAJB8 (-18961), GATA2 (+7256)
HypoH113	chr6	41605343	41605784	-0.99	2.96	48317	38450	38452	3	3	2.59E-03	1.20E-02	MDFI (-621)
HypoH112	chr18	20713759	20714332	-0.99	2.96	26971	93224	93226	3	6	2.58E-03	1.20E-02	CABLES1 (-1681)
HypoH111	chr4	467983	468201	-0.99	5.93	40811	23307	23312	6	6	2.04E-04	0.00E+00	ZNF721 (+24853), ZNF141 (+136468)
HypoH110	chr7	1067302	1067459	-0.99	2.97	50402	42278	42280	3	3	2.57E-03	1.20E-02	GPR146 (-27540), CYP2W1 (+44546)
HypoH109	chr6	10529935	10530035	-0.99	2.97	46982	34781	34783	3	3	2.57E-03	1.20E-02	GCNT6 (-104008), GCNT2 (+1396)
HypoH108	chr9	90113813	90114156	-0.99	3.97	58854	53976	53979	4	4	9.23E-04	6.00E-03	CTSL (-228449), DAPK1 (+1189)
HypoH107	chr15	35046760	35047411	-0.99	5.96	19363	79897	79902	6	8	2.01E-04	0.00E+00	GJD2 (+80)
HypoH106	chr1	144930572	144931379	-0.99	2.98	3573	6170	6172	3	3	2.54E-03	1.20E-02	PDE4DIP (+64046), NBPFG9 (+119228)
HypoH105	chr9	136149908	136150823	-0.99	4.97	57639	55017	55021	5	5	3.86E-04	1.00E-03	OBP2B (-65738), SURF6 (+52869)
HypoH104	chr3	16974160	16974681	-1.00	2.99	38001	18436	18438	3	3	2.50E-03	1.20E-02	PLCL2 (+47969), TBC1D5 (+767091)
HypoH103	chr1	228646970	228646970	-1.00	2.99	5467	9352	9354	3	3	2.50E-03	1.20E-02	HIST3H2A (-1383), HIST3H2BB (+1135)
HypoH102	chr4	103998289	103998497	-1.00	5.01	42314	26078	26082	5	5	3.77E-04	1.00E-03	SIC982 (-463)
HypoH101	chr16	175623960	17563300	-1.00	3.01	21749	84007	84009	3	3	2.44E-03	1.10E-02	XYLT1 (+1608)
HypoH100	chr7	29923339	29924165	-1.01	7.07	51152	44037	44043	7	7	1.08E-04	0.00E+00	WIPF3 (+49411), SCRNI1 (+106153)
HypoH99	chr5	178322737	178322924	-1.01	6.09	46531	33932	33937	6	6	1.85E-04	0.00E+00	ZFP2 (-64)
HypoH98	chr19	56988398	56989543	-1.02	7.16	30244	99262	99268	7	7	1.01E-04	0.00E+00	ZNF667 (-272)
HypoH97	chr19	19221316	19221574	-1.02	4.09	28785	96511	96514	4	4	8.19E-04	2.00E-03	TMEM161A (+27857), SLIC25A42 (+46637)
HypoH96	chr11	124747075	124747263	-1.02	4.10	12220	67126	67129	4	4	8.14E-04	2.00E-03	ROBO3 (+11887), ROBO4 (+21008)
HypoH95	chr19	11199851	11199965	-1.02	6.15	28345	95712	95717	6	6	1.79E-04	0.00E+00	LDLR (-130)
HypoH94	chr12	51786038	51786547	-1.03	3.09	13558	69316	69318	3	3	2.28E-03	4.00E-03	SLC4A8 (-32282), GALNT6 (-8946)
HypoH93	chr2	164592561	164593498	-1.04	9.33	33209	14847	14855	9	11	2.93E-05	0.00E+00	FIGN (-513)
HypoH92	chr12	62583974	62584454	-1.04	3.12	13993	70191	70193	3	3	2.19E-03	3.00E-03	FAM19A2 (+2409)
HypoH91	chr19	51196754	51197463	-1.04	3.12	29885	98560	98582	3	3	2.19E-03	3.00E-03	SYT3 (-55807), SHANK1 (+23086)
HypoH90	chr11	8190152	8190837	-1.05	6.27	9372	62167	62172	6	6	1.67E-04	0.00E+00	RIC3 (+41)
HypoH89	chr17	75955921	75956222	-1.05	3.14	26263	91865	91867	3	3	2.13E-03	3.00E-03	TNRC6C (-45065), SEPT9 (+678580)
HypoH88	chr14	24640047	24642317	-1.05	14.72	17300	76260	76263	14	14	2.60E-06	0.00E+00	REC8 (+570)
HypoH87	chr6	152011103	152011666	-1.05	5.26	49757	41156	41160	5	5	3.11E-04	0.00E+00	ESR1 (-246)
HypoH86	chr14	91866325	91866751	-1.06	4.25	18350	78136	78139	4	4	7.10E-04	0.00E+00	GPR68 (-146289), CDC88C (+17583)
HypoH85	chr2	241936844	241937034	-1.06	3.19	34762	17711	17713	3	3	2.03E-03	2.00E-03	SNED1 (-1316)
HypoH84	chr3	44753946	44754587	-1.07	11.76	38325	19014	19024	11	11	1.04E-05	0.00E+00	ZNF502 (+129)
HypoH83	chr14	106329158	106329652	-1.07	4.29	19024	79341	79344	4	4	6.88E-04	0.00E+00	TMEM121 (+336465)
HypoH82	chr19	58570419	58570995	-1.08	8.61	30313	99434	99441	8	8	4.79E-05	0.00E+00	ZNF135 (+100)
HypoH81	chr2	216946201	216946429	-1.08	3.23	33908	16202	16204	3	3	1.93E-03	1.00E-03	TMEM169 (-274), PECR (+224)
HypoH80	chr4	6201080	6201536	-1.08	3.24	41187	24083	24085	3	5	1.92E-03	1.00E-03	JAKMIP1 (+974)
HypoH79	chr7	37024020	37024760	-1.08	6.48	24785	89260	89265	6	6	1.47E-04	0.00E+00	LASPI (-1722)
HypoH78	chr3	128209772	128210541	-1.08	4.33	39649	21199	21202	4	4	6.61E-04	0.00E+00	DNAJB8 (-24346), GATA2 (+1871)
HypoH77	chr3	185911316	185912486	-1.09	8.71	40543	22826	22833	8	8	4.47E-05	0.00E+00	ETV5 (-85000), DGKG (+168125)

HypoHler76	chr6	32908466	32909003	-1.09	8.73	47925	37655	37662	8	13	4.47E-05	0.00E+00	HLA-DMB (+112)
HypoHler75	chr19	51189671	51190179	-1.09	4.37	29884	98576	98579	4	4	6.38E-04	0.00E+00	SYT3 (-48623), SHANK1 (+30270)
HypoHler74	chr11	32448293	32450692	-1.10	15.39	9875	63190	63203	14	14	1.68E-06	0.00E+00	WTT1 (+7683), RCNT1 (+337043)
HypoHler73	chr10	121300857	121301343	-1.10	3.31	8177	59708	59710	3	3	1.79E-03	0.00E-03	GRS10 (+1120), GRS5 (+333999)
HypoHler72	chr17	38084119	38084459	-1.11	4.43	24849	89423	89426	4	4	6.03E-04	0.00E+00	ORMDL3 (-1195)
HypoHler71	chr4	89978251	89978566	-1.11	3.34	42214	25906	25908	3	3	1.74E-03	1.00E-03	FAM13A (-36)
HypoHler70	chr1	3309864	3310911	-1.11	5.57	409	774	778	5	5	2.59E-04	0.00E+00	ARHGFE16 (-60802), PRDM16 (+324613)
HypoHler69	chr16	54324187	54325929	-1.11	10.03	22335	84932	84940	9	9	2.20E-05	0.00E+00	IRX3 (-4383)
HypoHler68	chr6	21667333	21668049	-1.12	4.46	47181	35112	35115	4	4	5.88E-04	0.00E+00	SOX4 (+73719), PRL (+630039)
HypoHler67	chr4	114681314	114681880	-1.13	5.63	42444	26372	26376	5	5	2.49E-04	0.00E+00	CAMK2D (+627)
HypoHler66	chr11	65324768	65325249	-1.13	3.39	10685	64555	64557	3	3	1.69E-03	1.00E-03	LTP3 (+690)
HypoHler65	chr1	47696212	47696701	-1.13	4.52	2451	4069	4072	4	4	5.62E-04	0.00E+00	TAL1 (-1014)
HypoHler64	chr7	810958	811390	-1.13	3.40	50356	42198	42200	3	3	1.62E-03	1.00E-03	SUN1 (-60964), HEATR2 (+44836)
HypoHler63	chr6	97265662	97265776	-1.14	3.41	48944	39558	39560	3	4	1.61E-03	1.00E-03	GPR63 (-380)
HypoHler62	chr21	27944586	27945708	-1.14	5.68	36186	102103	102107	5	5	2.41E-04	0.00E+00	CYR1 (+456)
HypoHler61	chr10	128993810	128995192	-1.15	12.52	8439	60157	60167	11	11	6.86E-06	0.00E+00	NPS (-353112), DOCK1 (+400523)
HypoHler60	chr7	121784249	121784596	-1.15	5.74	52638	46614	46618	5	5	2.31E-04	0.00E+00	AASS (-10547), FEZF1 (+160136)
HypoHler59	chr17	5000803	5001281	-1.16	4.62	23892	87621	87624	4	4	5.19E-04	0.00E+00	USP6 (-18691), ZFP3 (+19499)
HypoHler58	chr3	239188	240139	-1.16	8.10	37665	17857	17863	7	7	6.18E-05	0.00E+00	CNTN6 (-894586), CHL1 (+1385)
HypoHler57	chr7	8011594	8012104	-1.17	3.50	50800	43115	43117	3	3	1.47E-03	1.00E-03	GLCC1 (+3424), ICA1 (+290062)
HypoHler56	chr19	57183016	57183268	-1.17	3.50	30253	99287	99289	3	3	1.47E-03	1.00E-03	ZNF835 (-14)
HypoHler55	chr11	32451777	32452839	-1.17	8.22	9876	63204	63210	7	7	5.79E-05	0.00E+00	WT1 (+4868), RCN1 (+339858)
HypoHler54	chr16	10912331	10912718	-1.18	5.88	21640	83855	83859	5	5	2.12E-04	0.00E+00	TVP23A (+117)
HypoHler53	chr11	101785507	101785806	-1.18	10.62	11592	66103	66111	9	9	1.54E-05	0.00E+00	KIAA1377 (-89)
HypoHler52	chr20	44035850	44036136	-1.19	3.57	35556	100965	100967	3	3	1.38E-03	0.00E+00	DBNDD2 (-654)
HypoHler51	chr3	151176727	151178904	-1.20	3.61	40060	22002	22004	3	3	1.30E-03	0.00E+00	IGSF10 (-2319)
HypoHler50	chr8	11057947	11059303	-1.21	13.27	54015	49102	49112	11	11	5.02E-06	0.00E+00	XKR6 (+250)
HypoHler49	chr19	12911875	12912252	-1.21	3.62	28421	95872	95874	3	3	1.29E-03	0.00E+00	PRDX2 (+609)
HypoHler48	chr2	37551024	37551108	-1.21	3.62	31201	11420	11422	3	3	1.29E-03	0.00E+00	QPCT (-20651), PRKD3 (-6029)
HypoHler47	chr19	58545001	58545837	-1.22	13.38	30309	99415	99425	11	11	5.20E-06	0.00E+00	ZSCAN1 (-15)
HypoHler46	chr8	116679763	116680127	-1.22	4.88	55672	52137	52140	4	4	4.17E-04	0.00E+00	TRPS1 (+1283)
HypoHler45	chr11	6439806	6440065	-1.23	3.69	9295	62029	62031	3	3	1.21E-03	0.00E+00	APBB1 (+364)
HypoHler44	chr12	48592635	48592818	-1.24	3.71	13430	69123	69125	3	3	1.18E-03	0.00E+00	ORT0AD1 (+4443), C12orf68 (+15361)
HypoHler43	chr1	208084640	208085455	-1.24	6.19	5004	8555	8559	5	5	1.76E-04	0.00E+00	CD34 (-301)
HypoHler42	chr5	137071523	137071799	-1.24	4.98	45331	31663	31666	4	4	3.84E-04	0.00E+00	KLHL3 (+118)
HypoHler41	chr1	205781722	205782099	-1.25	3.74	4923	8431	8433	3	3	1.14E-03	0.00E+00	SLC41A1 (+393)
HypoHler40	chr1	110254709	110254886	-1.25	6.24	3333	5706	5710	5	5	1.72E-04	0.00E+00	GSTM5 (-74)
HypoHler39	chr15	89920348	89922071	-1.25	17.53	20616	81963	81976	14	18	1.42E-06	0.00E+00	POLG (-43132), RHOG (+118634)
HypoHler38	chr20	3051954	3052692	-1.26	13.82	34941	99696	99706	11	11	4.28E-06	0.00E+00	OXT (+57)
HypoHler37	chr12	93966060	93967711	-1.27	10.13	14357	70752	70759	8	8	2.08E-05	0.00E+00	CRADD (-104607), SOCS2 (+3296)
HypoHler36	chr10	74034644	74034667	-1.27	3.82	7095	57676	57678	3	3	1.08E-03	0.00E+00	DDIT4 (-978)
HypoHler35	chr5	178487310	178487826	-1.28	10.23	46541	33967	33974	8	8	1.94E-05	0.00E+00	ZNF354C (+152)
HypoHler34	chr5	178003633	178004685	-1.30	6.48	48520	33913	33917	5	5	1.47E-04	0.00E+00	PHYKPL (-344373), COL23A1 (+13397)
HypoHler33	chr19	38747174	38747378	-1.32	6.62	29146	97228	97232	5	8	1.38E-04	0.00E+00	PPP1R14A (-45)
HypoHler32	chr1	208083913	208084071	-1.33	4.00	5003	8552	8554	3	3	8.94E-04	0.00E+00	CD34 (+755)
HypoHler31	chr19	12305553	12306497	-1.34	6.71	28396	95824	95828	5	5	1.30E-04	0.00E+00	ZNF136 (+32146), ZNF44 (+99603)
HypoHler30	chr1	47694517	47695475	-1.36	8.15	2450	4063	4068	6	6	6.08E-05	0.00E+00	TAL1 (+447)
HypoHler29	chr10	124133785	124133822	-1.36	4.08	8253	59823	59825	3	3	8.27E-04	0.00E+00	PLEKHA1 (-408)
HypoHler28	chr3	100053070	100053188	-1.39	4.17	39197	20521	20523	3	3	7.60E-04	0.00E+00	NIT2 (-416)
HypoHler27	chr5	76248637	76248923	-1.39	4.18	44537	30163	30165	3	3	7.59E-04	0.00E+00	CRHBP (+242)
HypoHler26	chr7	143582146	143582630	-1.39	5.57	53062	47365	47368	4	4	2.58E-04	0.00E+00	CTAGE6 (-127599), OR2F2 (-49871)
HypoHler25	chr3	57994941	57995180	-1.40	4.21	38748	19815	19817	3	3	7.40E-04	0.00E+00	FLNB (+934)
HypoHler24	chr7	65196614	65196881	-1.44	4.33	51761	45073	45075	3	3	6.57E-04	0.00E+00	VKORC1L1 (-141506), ZNF92 (+358036)
HypoHler23	chr19	58220080	58220837	-1.46	16.09	30299	99376	99386	11	11	1.68E-06	0.00E+00	ZNF154 (+77)
HypoHler22	chr2	85810844	85812023	-1.50	10.47	32052	12858	12864	7	8	1.70E-05	0.00E+00	VAMP5 (-97)
HypoHler21	chr11	32458566	32461230	-1.50	24.08	9880	63224	63239	16	16	4.73E-07	0.00E+00	WT1 (-2772)
HypoHler20	chr5	67583598	67584380	-1.52	16.72	44386	29849	29859	11	11	1.42E-06	0.00E+00	SLC30A5 (-805484), PIK3R1 (-72441)
HypoHler19	chr12	122018770	122019525	-1.54	13.83	15064	72156	72164	9	9	4.02E-06	0.00E+00	KDM2B (-259)

HypoHier18	chr8	42356637	42356871	-1.54	4.61	54742	50427	50429	3	3	5.23E-04	0.00E+00	SMIM19 (-39544), VDAC3 (+107333)
HypoHier17	chr7	2847517	2847575	-1.54	4.62	50654	42829	42831	3	3	5.19E-04	0.00E+00	GNA12 (+36412), AMZ1 (+128390)
HypoHier16	chr1	42363598	42384647	-1.55	13.97	2260	3796	3764	9	9	3.07E-06	0.00E+00	HIVEP3 (+46)
HypoHier15	chr20	11898478	11899258	-1.57	7.86	35043	99896	99900	5	5	6.93E-05	0.00E+00	NONE
HypoHier14	chr9	135039836	135040296	-1.65	4.95	57583	54943	54945	3	3	3.91E-04	0.00E+00	NTNG2 (+2732), SETX (+190306)
HypoHier13	chr7	150211761	150211939	-1.66	8.29	53146	47515	47519	5	5	5.68E-05	0.00E+00	GIMAP7 (-68)
HypoHier12	chr6	10521452	10521715	-1.68	6.72	46980	34776	34779	4	5	1.29E-04	0.00E+00	TFAP2A (-106114), GCNT2 (-7005)
HypoHier11	chr22	38201496	38201848	-1.72	6.87	37166	103806	103809	4	4	1.19E-04	0.00E+00	GCAT (-2240), HIF0 (+558)
HypoHier10	chr16	1583810	1584516	-1.72	13.79	21240	83173	83180	8	8	4.28E-06	0.00E+00	TMEM204 (+589)
HypoHier9	chr10	114712695	114713187	-1.80	7.21	8007	59325	59328	4	6	9.86E-05	0.00E+00	HABP2 (-599844), TCF7L2 (+2932)
HypoHier8	chr19	58399865	58400559	-1.83	10.96	30303	99390	99395	6	6	1.37E-05	0.00E+00	ZNF814 (+193)
HypoHier7	chr5	76249502	76250527	-1.85	9.26	44538	30166	30170	5	5	3.10E-05	0.00E+00	AGGF1 (-76195), CRHBP (+1477)
HypoHier6	chr13	76334583	76334866	-1.89	7.57	16421	74560	74563	4	4	8.02E-05	0.00E+00	LMO7 (-72)
HypoHier5	chr14	74179674	74180217	-1.90	5.69	18029	77643	77645	3	3	2.40E-04	0.00E+00	PNMA1 (+1182), ACO16 (+96398)
HypoHier4	chr7	143579665	143580147	-1.92	7.69	53061	47361	47364	4	4	7.50E-05	0.00E+00	CTAGE6 (-125117), OR2F2 (-52353)
HypoHier3	chr11	128391271	128391494	-2.03	6.09	12325	67281	67283	3	3	1.89E-04	0.00E+00	ETS1 (+66054)
HypoHier2	chr5	76115672	76116535	-2.15	15.08	44534	30154	30160	7	7	1.89E-06	0.00E+00	S100Z (-29820), F2RL1 (+1302)
HypoHier1	chr3	194866750	194868843	-2.16	6.49	40719	23140	23142	3	4	1.48E-04	0.00E+00	LSG1 (-47559), XXYL1 (+123099)